Take a walk on the wild side: characterizing 17D immunity using wild-type yellow fever viruses and vaccinees with diverse orthoflavivirus infection history

Felicity J. Coulter, M.Sc.

A DISSERTATION

Thesis submitted to the Department of Molecular Microbiology and Immunology
Oregon Health & Science University
School of Medicine

In Partial Fulfillment of the Requirements for the Degree of Doctor of Philosophy

August 2024

Messer, W.B, M.D., Ph.D.

Haigwood, N. L., Ph.D.

Moses, A.V., Ph.D.

Hanley, K. A., Ph.D.

Burwitz, B. J., Ph.D.

I. Table of Contents

II. Common Abbreviations

A	Angola		**YF**	Yellow fever
Ab	Antibody		**YFV**	Yellow fever virus
ACIP	Advisory Committee on Immunization Practices		**ypv**	Years post-vaccination
C	Capsid		**ZIKV**	Zika virus
DENV	Dengue virus			
E	Envelope			
E/CA	East/Central Africa			
EA	East Africa			
FRNT	Focus reduction neutralization test			
JEV	Japanese encephalitis virus			
M	Membrane			
NAb	Neutralizing antibody			
NHP	Non-human primate			
NS	Nonstructural			
NT	Neutralization titer			
PCR	Polymerase chain reaction			
prM	Pre-membrane			
PRNT	Plaque reduction neutralization test			
RT-PCR	Reverse-transcription polymerase chain reaction			
SA-I	South America I			
SA-II	South America II			
WA-I	West Africa I			
WA-II	West Africa II			

III. Dedication

I would like to dedicate this work to those who have supported me throughout this journey. First, I would like to express my deep gratitude to my mentor, Bill, whose scientific guidance, supervision, and endless support has in equal parts made this work possible. Thank you for inspiring me, for investing in my goals, and for our many candid conversations, which I hope to continue. You have taught me so much.

I would like to sincerely thank my committee for their mentorship and scientific guidance that significantly shaped this work and the scientist I am today. Every single one of you inspire me. Thank you for your unwavering support during wavering times, and for pushing me out of my comfort zone. Thank you to Nancy for believing in me and investing in my success and happiness from beginning to end. The opportunity to work directly with you is a privilege. Thank you to Ashlee for your profound kindness and wisdom, and for sharing your journey so openly. Thank you also for asking hard questions. Thank you to Kathy, for making stats fun(!) and accessible. Your work and the energy you bring to every conversation inspires me. Thank you to Bella and Ben who supported me through very different halves of this journey.

I would like to acknowledge previous Messer lab members Zoe Lyski, Bettie Kareko, Chad Nix, Jana Mooster, Zhengchun Lu, David Xthona Lee, and Shannon Young, and current Messer lab members Courtney Micheletti, Sam Osman, Abram Estrada, Shuhua Luo, and Sarah Sampouw who have significantly supported to this work at the bench and through conversations. You have been an absolute delight to work alongside. Chad and Courtney, I am especially grateful for your friendship.

I would like to thank my family who continue to support my dreams, even as they took me 5,000 miles away from home and also my dear friends back in the UK who have done the same. To my equally dear US friends, thank you for sharing laughs and tears, holidays, and celebrations, and so much more. To Whitney, my fellow jungle girl, thank you for unforgettable adventures. To Ros, I am especially grateful for everything. And finally, to my partner Devin, thank you for your love and support, and for always believing in me.

IV: Abstract

The highly successful 17D vaccine has been the keystone of yellow fever virus (YFV) control since its development in the 1930s. Consequently, the 17D vaccine is considered a gold standard live-attenuated vaccine and has been touted as providing "lifelong" immunity. Within the field, neutralizing antibodies (NAbs) against the 17D vaccine strain are widely accepted as the primary correlate of protection. Despite its demonstrable success, many studies dispute the longevity 17D-elicited NAbs, as one-in-five vaccinees become seronegative by 10 years post-vaccination. Nevertheless, the United States Advisory Committee on Immunization Practices (ACIP) rescinded the booter dose recommendation in 2015, and do not currently recommend a booster dose for most travelers, which deviates from historical practices. Today the need for a booster dose remains controversial. While the need for booster dose receives a lot of attention, other knowledge gaps of lesser prominence are equally important.

First, the occurrence of breakthrough infection is understudied. Breakthrough infection has been reviewed once before, but the "lack of evidence" contributed to ACIP's decision to rescind the booster recommendation. However, there are significant limitations within this body of work, and despite the value of breakthrough infection as a measure of vaccine efficacy, breakthrough cases are incompletely understood, in part because of dismissal of the possibility of such cases. Second, very few studies have quantified the ability of 17D-elicited NAbs to neutralize wild-type YFV viruses with clinical relevance, representing a significant knowledge regarding the efficacy of the 17D vaccine against currently circulating wild-type strains, and an unknown risk of breakthrough infection resulting from vaccine failure.

Chapter 1 introduces these topics and provides detailed background and context for the research described here that address these critical unanswered questions in the field. Chapter 2 addresses the first knowledge gap regarding vaccine breakthrough and provides a comprehensive review of breakthrough infection since the last major review which was conducted ACIP in 2015. This analysis spans eight decades and highlights the diversity of cases and reporting, including cases from the recent outbreak in Brazil between 2016 and 2019. Importantly, we identify both the

limitations in the quality of data, and factors contributing to underreporting that limit our understanding of breakthrough infection.

Chapter 3 updates the methods used to quantify infectious wild-type YFV *in vitro.* Using a panel of wild-type fever strains belonging to each of the seven YFV genotypes, isolated between 1927 and 2018. Historically, these isolates have been quantified using the traditional plaque assay, the long-standing gold standard for YFV quantification. The plaque assay is both time- and resource-intensive, and we set out to optimize a more efficient method. In this chapter we summarize the process of optimizing the higher-throughput immunofocus assay to quantify our panel of wild-type YFV strains. In addition to facilitating the subsequent research described here, this higher-throughput, cheaper, and more accessible method advances the field.

Chapter 4 addresses the second knowledge gap of the potency of 17D-elicited serum NAbs against wild-type YFV and represents the major findings of this project. We selected a subset of previously recruited 17D vaccinees up to 11-years post-vaccination, where ≥10 years is the historical interval at which a booster dose was historically recommended. Using this cohort, we performed focus reduction neutralization tests (FRNT) to determine 50% neutralization test (NT_{50}) titers against our panel of 12 wild-type YFVs. Strikingly, NT_{50} titers against viruses belonging to the South America-I (SA-I) genotype were particularly low, and below the limit of detection of 1:10 for several participants, but not all. In order to better understand these differences, we stratified out participants based on evidence of heterologous infection with orthoflaviviruses dengue- and Zika virus. In doing so, we observed a significantly reduced proportion of seropositive vaccinees against SA-I strains that was specific to individuals *without* heterologous infection. Meanwhile, the proportion of seropositive vaccinees amongst vaccinees *with* heterologous infection was not significantly reduced, suggesting a boosting effect. Finally, we constructed the first antigenic map of 17D immune sera against wild-type yellow fever viruses, establishing the antigenic landscape of an important human pathogen. These data reshape our understanding of 17D-elicited NAbs, and have implications for future vaccination strategies.

Chapter 1: Introduction

Section 1.1: Preface

Viral diseases such as yellow fever (YF) cause untold global suffering. With no current antiviral therapies, control of YF virus (YFV) relies upon prevention of disease primarily by vaccination with the live attenuated vaccine, 17D. While the 17D vaccine has been in use, practically unchanged, for almost 90 years, ongoing outbreaks and reemergence in Africa and South America in recent years highlight the critical need to increase our understanding of this important vaccine. This work strives to facilitate the improvement of vaccination strategies including vaccination regimens and vaccine design that are crucial in reducing the global burden of disease.

Section 1.2: Yellow fever disease

1.3.1 A brief historical introduction

Yellow fever (YF) has plagued human populations for centuries. YF was previously known as "yellow Jack", a term used as early as the 17th century by British and French sailors[1, 2] and "bronze John" by the people of New Orleans during the 19th Century[3] in reference to yellow appearance of the skin suffered by some infected individuals.[4] Though not strictly characteristic of YF, black vomit was encountered frequently enough that Spanish and Portuguese speakers referred to YF colloquially as "*vomito negro*" and was a symptom captured by a 19th century illustration of the disease by Mexican artist Gaudalupe Posada.[5]

During the 1793 YF outbreak in Philadelphia, the physician Benjamin Rush controversially treated YF patients with aggressive methods. These included bleeding, known as venesection, and purging using purgatives such as calomel containing mercury, which were thought to ease symptoms by redirecting the fever away from the vital organs. While these treatments were controversial relative to the cold baths used to reduce fever and milder purging techniques utilized by other physicians,

they were adopted by a small number of medical professionals,[6] and likely caused much more harm than good.

Since these early accounts, our understanding of YF disease and approaches to have fortunately evolved and advanced.

1.3.2 Current day understandings

1.3.2a Clinical presentation

Fifty-five percent of YFV infected individuals are asymptomatic, 33% experience mild symptoms, and an unfortunate 12% will progress to severe disease, of which there is a 30-60% mortality rate.[7] Symptoms begin three to six days following the bite of an infected mosquito and typically last between three and four days. After this initial period, most recover fully, however, some will experience a 24-hour period of remission before entering the "intoxication phase" where they will begin to exhibit life-threatening severe symptoms.[8] Severe symptoms include jaundice caused by significant viral replication within the liver, resulting in impaired liver function and failure.[9] Pathological alterations to the kidneys can ultimately result in renal failure. Involvement of the gastrointestinal tract can cause mixing of gastric acid with blood which is the underlying cause of black vomit.[9] Involvement of the central nervous system include cerebral edema, hemorrhage, and encephalopathy.[9] Notably, hemorrhagic symptoms occur with a much higher incidence amongst fatal cases compared to non-fatal.[10] The spectrum of mild and severe symptoms of YF are summarized in Table 1.1.

Mild symptoms	Sudden onset of fever
	Chills
	Headache
	Backache

	Myalgia (general muscle pain)
	Prostration (fatigue)
	Nausea
	Vomiting
Severe symptoms	Jaundice
	Hemorrhaging
	Organ failure
Clinical signs	Faget sign – an unusual pairing of bradycardia (slow pulse) with a fever.
	Leukopenia, which peaks around five days following symptom onset followed by leukocytosis during the second week of illness.
	Thrombocytopenia – low platelet count.
	Elevated liver enzymes – bilirubin, serum aspartate, aminotransferase, alanine aminotransferase.
	Elevate blood urea nitrogen (BUN) and creatinine.
	Albuminuria – presence of albumin in the urine, observed by 4 days following symptom onset.
	Anuria – reduced urine output.

Table[1.1]

[Tab1.1]

Table 1.1 Yellow fever symptoms and clinical features.

Mild symptoms, severe symptoms, and clinical features of YF summarized from the Control of Communicable Diseases Manual 2024[11, 12]

While recovery from acute disease typically occurs within 1 weeks of symptom onset,[13] some individuals suffer fatigue and weakness for many months.[8] More recently, reports from Brazil have documented late-relapsing hepatitis in around 16% of YF patients, which presents as reoccurrence of jaundice and elevated liver transaminases and bilirubin 46-90 days following symptom onset and following complete recovery from acute disease.[14-19] At this point in time, it is unclear if these reports of late-relapsing hepatitis represent a new sequala of YF, or new detection of an already existing sequala made possible by the sheer magnitude of the Brazilian outbreak that was accompanied by an abundance of high quality reporting.

1.3.2b Case definitions

The Centers for Disease Control and Prevention (CDC) provides a set of "uniform criteria" to define diseases including YF (Table 1.2). These terms provide a standardized way to count cases of YF across different reporting regions with consistency for the purpose of conducting disease surveillance and making informed public health decisions, such as initiating vaccination campaigns and mosquito control efforts. While these definitions offer a standardized method for counting cases, multiple factors may introduce biases, such as the type of case definition used, and the accessibility to resources, including healthcare and trained physicians, and the laboratory reagents required to conduct diagnostic testing. Importantly, bias introduced by any means may impede surveillance efforts, representing a huge challenge for disease control. The limitations of specific case definitions introduced in this section are discussed in detail in Chapter 2.5.2.

Table[1.2]

Term	**Definition**
Probable case	"A case that meets the above clinical and epidemiologic linkage criteria, and meets the following: - Yellow fever virus-specific IgM antibodies in CSF or serum, **AND** negative IgM results for other arboviruses endemic to the region where exposure occurred, **AND** no history of yellow fever vaccination."

Confirmed case	"A case that meets the above clinical criteria and meets one or more of the following: - Isolation of yellow fever virus from, or demonstration of yellow fever viral antigen or nucleic acid in, tissue, blood, CSF, or other body fluid, **AND** no history of yellow fever vaccination within 30 days before onset of illness unless there is molecular evidence of infection with wild-type yellow fever virus. - Four-fold or greater rise or fall in yellow fever virus-specific neutralizing antibody titers in paired sera, **AND** no history of yellow fever vaccination within 30 days before onset of illness. - Yellow fever virus-specific IgM antibodies in CSF or serum with confirmatory virus-specific neutralizing antibodies in the same or a later specimen, **AND** no history of yellow fever vaccination."
Clinical criteria	- "Acute illness with at least one of the following: fever, jaundice, or elevated total bilirubin ≥ 3 mg/dl, **AND** absence of a more likely clinical explanation."
Confirmatory laboratory evidence	- "Isolation of yellow fever virus from, or demonstration of yellow fever viral antigen or nucleic acid in, tissue, blood, CSF, or other body fluid. - Four-fold or greater rise or fall in yellow fever virus-specific neutralizing antibody titers in paired sera. - Yellow fever virus-specific IgM antibodies in CSF or serum with confirmatory virus-specific neutralizing antibodies in the same or a later specimen."
Presumptive laboratory evidence	- "Yellow fever virus-specific IgM antibodies in CSF or serum, and negative IgM results for other arboviruses endemic to the region where exposure occurred."
Epidemiological link	- "Epidemiologically linked to a confirmed yellow fever case, or visited or resided in an area with a risk of yellow fever in the 2 weeks before onset of illness."

[Tab1.2]

Table 1.2 CDC surveillance case definitions.

Surveillance cases definition are used for public health surveillance of disease, and are not intended for use by healthcare providers as guidance for diagnosis.[20]

1.3.2c Diagnosis

YF may be diagnosed using virological techniques, including real-time reverse transcription polymerase chain reaction (qRT-PCR), RT-PCR, viral isolation, and immunohistochemistry (IHC), and serological techniques, including enzyme-linked immunosorbent assay (ELISA) and plaque reduction neutralization assay (PRNT). Details of these assays are provided in a technical report co-published by the Pan American Health Organization (PAHO) and the World Health Organization (WHO)[21] and summarized in Table 1.3.

An important consideration for appropriate diagnostic selection is interval since symptom onset. RT-PCR may be used 0-10 days post symptom onset, and serological diagnostic testing may be used 6-15 days post symptom onset. Each method has advantages and disadvantages. Both are susceptible to false positives if an individual has recently received the 17D vaccine; as such, a history of vaccination must be taken. Additionally, cross-reactivity between orthoflaviviruses means that a positive IgM-ELISA may be interpreted as "recent orthoflavivirus infection" and a PRNT may be considered to confirm YF diagnosis.[21] The implications of using specific diagnostic methods to confirm cases and report incidence are discussed in Chapter 2.5.4.

Table[1.3]

Assay	Sample type(s)	Description	Considerations
Virological methods			
qRT-PCR	Serum	Detects viral RNA present in the circulating blood.	Limited to the acute viremic phase of infection, 0-10 days post symptom onset.

			Cannot distinguish between wild-type YFV infection and vaccine induced viremia. Positive RT-PCR confirms diagnosis.
Viral isolation	Serum or tissue	Isolation of virus may be done by infecting cells *in vitro,* or animals typically using serum samples, or sometimes tissue samples taken post-mortem.	This method is useful when further characterization of the virus is desired but is resource intensive and rarely used as a diagnostic.
IHC	Tissue	Sections of post-mortem live sections are stained for the presence of viral antigens.	"Gold-standard" for diagnosis of fatal YF cases. Positive IHC confirms diagnosis.
Serological methods			
IgM-ELISA	Serum	Detection of YFV-specific IgM using purified YFV antigens.	Predominantly in-house assays, as no standardized commercial ELISA kit exists. Susceptible to cross-reactivity to other flaviviruses, especially with DENV and ZIKV. Positive result indicates presumptive YF only. Confirmation requires evidence of seroconversion using paired samples (acute and convalescent ≥1 week interval).

IgG-ELISA	Serum	Detection of YFV-specific IgG using purified YFV antigens.	May be performed on convalescent samples, typically used during a serosurvey to demonstrate immunity to YFV as a proxy for prior infection. Does not discriminate against vaccine-acquire immunity. Susceptible to cross-reactivity to other flaviviruses, especially with DENV and ZIKV.
PRNT	Serum	Detection of YFV-specific neutralizing antibodies (NAbs).	Higher sensitivity than ELISA, but still susceptible to cross-reactivity and must be performed using a panel of flaviviruses. Does not discriminate against vaccine-acquire NAbs. Positive result indicates presumptive YF only. Confirmation requires evidence of seroconversion using paired samples (acute and convalescent ≥1 week interval).

[Tab1.3]

Table 1.3 PAHO and WHO diagnostic testing.

Summary of virological and serological diagnostic testing guidelines provided by PAHO and the WHO.[21]

RT-PCR: reverse transcription polymerase chain reaction, IgM: immunoglobulin M, ELISA: enzyme-linked immunosorbent assay, PRNT: plaque reduction neutralization test, IHC: immunohistochemistry; DENV: dengue virus; ZIKV: Zika virus; PRNT: plaque reduction neutralization test.

Following diagnosis, International Classification of Disease (ICD) codes may be assigned. The ICD-10 code for YF is A95.9,[22] and the ICD-11 code is 1D47[11]. While these codes are predominantly used within the United States for insurance and reimbursement, they may also be used to query regional or national databases for the purpose of surveillance. In the United States, YF is a regionally reportable and nationally notifiable disease.[8]

1.3.2d Treatment

According to the CDC[23] current treatment of YF relies on management of symptoms and supportive care, including rest, hydration, maintenance of nutrition, and the use of analgesics and antipyretics to manage pain and fever. Importantly, because of the risk of hemorrhaging, non-steroidal anti-inflammatory drugs (NSAIDs) may increase the risk of bleeding and should be avoided. Care of patients with severe YF is describe by Simon *et al.*, 2024.[9] Cases of severe YF should be admitted to the intensive care unit (ICU) and monitored closely for disseminated intravascular coagulation, hemorrhage, kidney, and liver dysfunction. Treatment plans include transfusion of plasma to manage coagulopathy, and dialysis to manage renal failure.

Section 1.3: Epidemiology

Reservoirs of YFV are maintained within paleotropical- and neotropical- non-human primate (NHP) hosts in Africa and South America, respectively. The distribution of YFV and the risk of outbreaks are therefore dictated by the geographical range, proximity, and interactions of NHPs, humans, and mosquito vectors. The transmission of YFV between hosts and vectors is discussed in more detail in Section 1.5: *Transmission of YF virus in diverse hosts*. According to the WHO, as of 2023 YF is endemic in 47 countries, with 34 located in Africa and 13 in Central and South America.[24]

1.3.1 Africa

In 2013, 130,000 (95% CI 51,000–380,000) cases of YF were estimated to occur resulting in 78,000 (95% CI 19,000–180,000) deaths.[25] While the confidence intervals around these figures suggest a high level of uncertainty, these data align with previous estimates of 200,000 global cases and 30,000 deaths annually, of which 90% of cases are believed to occur in Africa.[26] Cases of YF are severely underreported in Africa,[27] due to clinical misdiagnosis of diseases which present with similar symptoms, such as dengue, malaria, and typhoid,[28] undiagnosed cases due to inaccessibility to diagnostic reagents and resources,[29, 30] and challenges with maintaining high quality data collection and routine surveillance.[31]

Historically, children have been most affected by YF, with fewer cases reported amongst adults who would acquire immunity following natural infection or vaccination.[32] Since 2013, the 17D vaccine was incorporated into the Expanded Immunization Program which aimed to routinely vaccinate children against YF between nine and 12 months of age.[33] Also in 2013, vaccination campaigns were estimated to reduce cases by 27%,[25] however, in 2021, only 47% of infants in Africa were estimated to have been vaccinated.[34] Additionally, up to 50% of infants who receive vaccination before the age of two years are reported to be seronegative 5-10 years post-vaccination (ypv).[35] Despite gallant and improved vaccination efforts, these figures suggest that over half of infants in Africa are living with significant risk of contracting YF disease.

In the past decade notable outbreaks have occurred in Angola[36] and neighboring Democratic Republic of the Congo (DRC). Manuel *et al.*, 2024[37] retrospectively reported 4,618 suspected- and 884 confirmed cases of YF during the 2016 outbreak in Angola, with 384 deaths and a case fatality rate of 13.6% among confirmed cases. Incidence of disease was 2.5X higher in males (4.62 per 100,000) compared to females (1.89 per 100,000), with the highest incidence (10.88 per 100,000), reported amongst males aged 20-29 years. The authors speculate that higher incidence in young males is the result of increased work outdoors compared to females but note increased incidence in males in multiple age groups, suggesting that other factors such as reporting bias may be at play. In 2016, the DRC reported 2,269 suspected and 78 confirmed cases, 57 of which had been imported from Angola, and 88% occurring in men with a median age of 31 years.[38]

During the same year, 11 cases of YF were reported amongst Chinese workers travelling home from Angola, two of which were fatal.[39-41] This marked the first ever documented importation of YFV from Africa into Asia.[42] YFV has otherwise appeared absent from Asia, but with millions of immunologically naïve and susceptible human hosts living in close proximity with competent vectors *Aedes aegypti*, the Angola to China importation event represented a significant risk of potential emergence.[43]

A 2024 report by the WHO provides recent data on YF in Africa.[31] Between 2023 and 2024, suspected and confirmed cases of YF were documented by 13 African countries: Burkina Faso, Cameroon, the Central African Republic, Chad, Republic of the Congo, Côte d'Ivoire, the DRC, Guinea, Niger, Nigeria, South Sudan, Togo and Uganda. Cases were reported more often in males (sex ratio M:F of 1.7), 69% of cases were in individuals over the age of 15 years, with a median age of 25 years, and the case fatality for this period was reported as 11%. The countries where YF vaccination is recommended are shown in Figure 1.1.[8]

Figure[1.1]

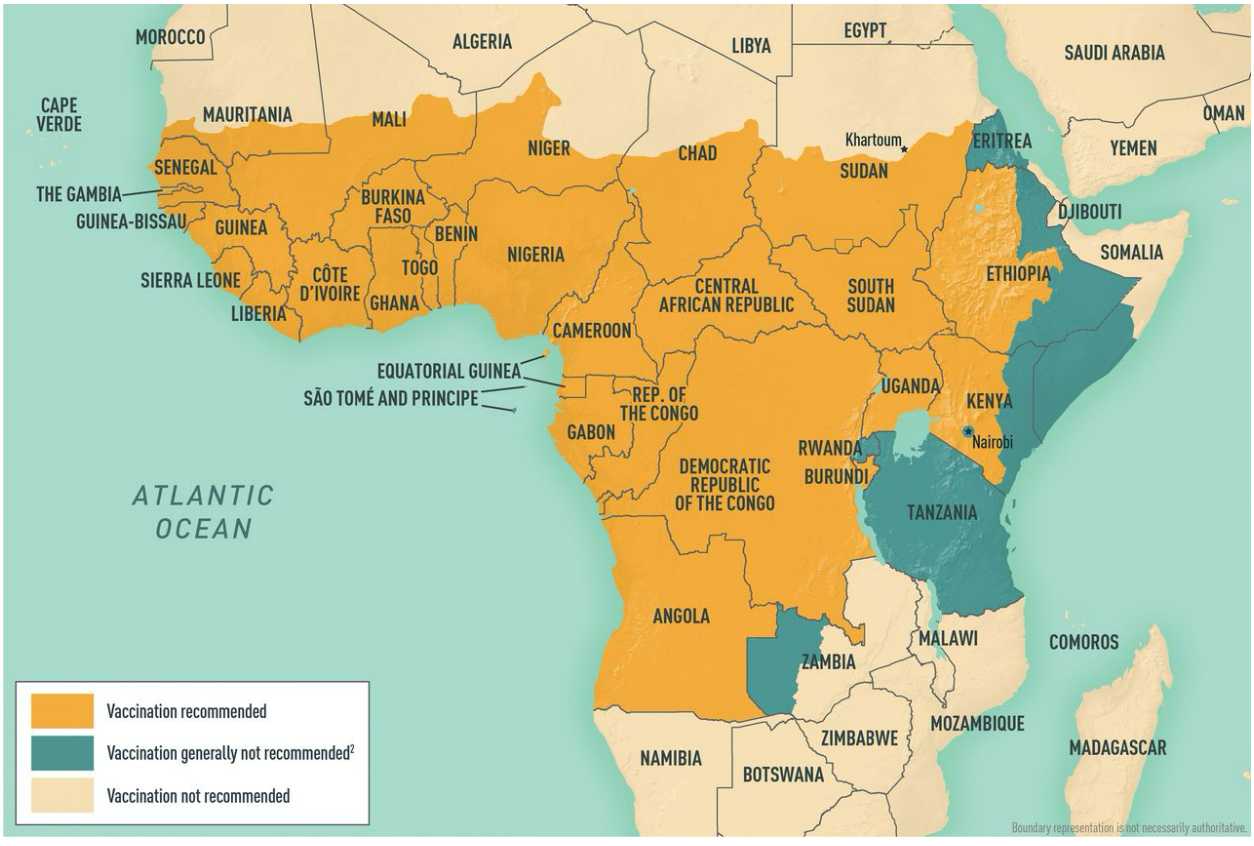

[Figure 1.1]

Figure 1.1. ***Map showing regions where vaccination is recommended in Africa, 2022***

This image is in the public domain. Source: CDC Yellow Book 2024.[8] Use of this image does not constitute its endorsement or recommendation by the U.S. Government, Department of Health and Human Services, or Centers for Disease Control and Prevention.

1.3.2 The Americas

The first recorded epidemic of YF in the Americas was reported in Yucatán, Mexico in 1648.[44] In 1685, YF was first reported in Brazil in the Northeast region,[45] an outbreak that preceded many other outbreaks which were countered with efforts to control disease by vector control and vaccination. Following such efforts, the last documented urban case of YF was in 1942,[46] and in 1958 the PAHO declared that the *Aedes aegypti* mosquito responsible for unban transmission had been eradicated from Argentina, Belize, Bermuda, Bolivia, Chile, Equator, the Panama Canal zone, Paraguay, Peru, and Uruguay.[47] Unfortunately, failure to eradicate *Aedes aegypti* from neighboring countries resulted in reinfestation, and by 1977 the vector had reestablished in the Brazilian states of Salvador and Bahia.[47]

Despite reintroduction of *Aedes aegypti,* cases of YF in Brazil attributable to spillover transmission from non-human primates (NHP) have persisted in sylvatic areas , until the 2016-2019 outbreak,[48] which intruded upon urban areas in eastern Brazil, causing 2,205 confirmed cases and 734 deaths.[49] Still, as YF spilled into urban areas after emerging in Minas Gerais in 2016 and spreading into the states of São Paulo, Espírito Santo, Rio de Janeiro, and Bahia in 2017,[50] data show that human cases of YF during this outbreak were the result of spillover transmission.[51] In the state of Minas Gerais which was the epicenter of the outbreak, 905 cases were confirmed; 85% were male, 69% were between 30 and 59 years old, and 12% were reported amongst individuals who had received vaccination.[52]

Outside of Brazil, urban transmission of YFV was reported in Santa Cruz, Bolivia between 1997 and 1998.[53] Between 2023 and 2024, cases of YF were reported in 5 countries: Bolivia, Brazil, Columbia, Guyana and Peru.[54] The countries and regions of South America where vaccination is

currently recommended are shown in Figure 1.2, including expanded areas incorporated following the outbreak that began in Brazil in 2016.

Figure[1.2]

[Figure 1.2]

Figure 1.2 ***Map showing regions where vaccination is recommended in South America, 2022***

This image is in the public domain. Source: CDC Yellow Book 2024.[8] Use of this image does not constitute its endorsement or recommendation by the U.S. Government, Department of Health and Human Services, or Centers for Disease Control and Prevention.

Section 1.4: Yellow fever virus virology

1.4.1 Classification

Yellow fever virus (YFV) (*orthoflavivirus flavi*), named for the yellow – *flavus (Latin)* – jaundice it causes in some YFV infected individuals, is the prototype virus in the *orthoflavivirus* genus, of the *Flaviviridae* family (Table 1).[55, 56] There are currently 89 species described within the *Flaviviridae* family, which are divided amongst the *hepacivirus*, *pegivirus, pestivirus,* and *orthoflavivirus* genera, and YFV is one of 53 species of *orthoflaviruses*, including dengue virus, Japanese encephalitis virus, Powassan virus, Saint Louis encephalitis virus, tick-borne encephalitis virus, West Nile Virus, and Zika virus.

Table[1.4]

Taxon rank	**Taxon name**
Realm	*Riboviria*
Kingdom	*Orthornavirae*
Phylum	*Kitrinoviricota*
Class	*Flasuviricetes*
Order	*Amarillovirales*
Family	*Flaviviridae*
Genus	*Orthoflavivirus*
Species	*Orthoflavivirus flavi*

[Tab1.4]

[1.4] Taxonomic classification of yellow fever virus.

Taxonomic classification of YF virus following renaming of the previously named "*Flavivirus"* genus to *Orthoflavivirus" by the International Committee on Taxonomy of Viruses in 2023.*[55, 56]

1.4.2 Genomic organization and structure

YFV has a single stranded positive-sense RNA genome which is 10,760 – 11,008 nucleotides long including 5' and 3' untranslated regions, and a single open reading frame encoding a single polypeptide which is cleaved into three structural proteins, capsid, pre-membrane (prM), and envelope (E), and seven non-structural (NS) proteins, NS1, NS2A, NS2B, NS3, NS4A, NS4B and NS5. The genomic organization and translated protein topology of YFV is shown in Figure 1.3.[57] The YFV virion is 40-60nm (400-600 angstroms) in diameter[58, 59] and the genome is contained within a nucleocapsid encoded by C, which is enveloped by a lipid bilayer originating from host membranes. The mature YFV virion is smooth and spherical and is decorated with viral proteins prM/M and E which play key roles during the cellular attachment and fusion events involving interactions with cellular membranes.

Figure[1.3]

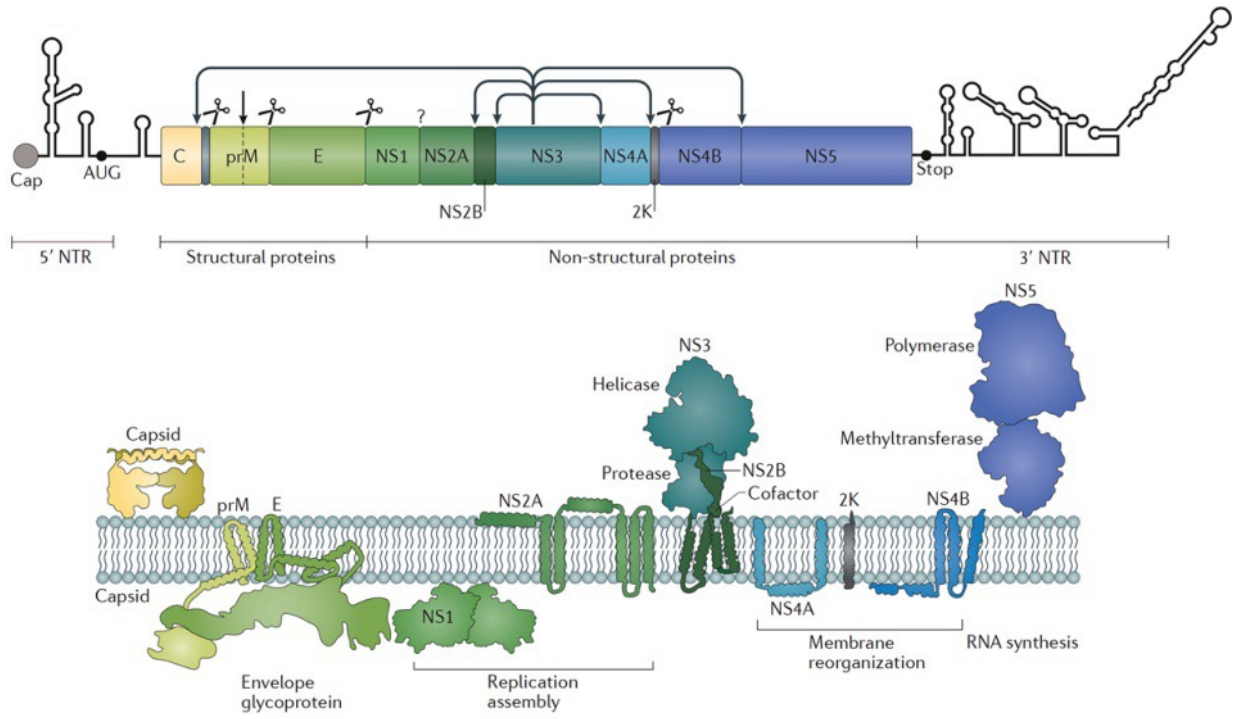

[Figure 1.3]

Figure 1.3 ***Orthoflavivirus*** **genome organization and translated protein topology.**

Reprinted from Neufeldt *et al.*, 2018[57] which is licensed under Creative Commons.
In the top panel, scissor indicate cleavage sites within the polypeptide conducted by cellular peptidase, arrows show cleave sites of viral protease, black vertical arrow indicates furin cleavage site, conducted in the Golgi by host protease furin. Question mark indicates cleavage site by unknown protease. In the bottom panel, topology of viral proteins is shown, with prM, E, and NS1 residing in the endoplasmic reticulum (ER) lumen, C, NS3, and NS5 residing on the cytoplasmic side of the ER membrane, and NS2A, NS2B, NS4A, and NS4A residing within the membrane. The 2K peptide also resides within the membrane.

1.4.2a Structural proteins

The C, prM and E proteins are structural components of the virion.[57] The E glycoprotein, which is the primary target of neutralizing antibodies, is 493 amino acid residues long[60] and ~53kDa with two transmembrane helices and an ectodomain consisting of three distinct β-barrel domains, E-domain (ED)-I, ED-II, and ED-III.[59] ED-I links together ED-II—containing a dimerization domain and the 13 amino acid highly conserved fusion loop—with ED-III, an immunoglobulin (Ig)-like domain that is thought to interact with cellular receptors.[61] On the surface of mature orthoflavivirus virions, two E monomers dimerize via ED-II in a "head-to-toe" formation, forming 90 homodimers and 30 antiparallel rafts in an icosahedral "herringbone" pattern.[62, 63]

1.4.2b Non-structural proteins

NS1 is a ~355 amino acid glycoprotein which is highly conserved amongst the orthoflaviviruses and plays multiple roles. After translation into the luminal side of the ER, NS1 monomers rapidly dimerize. Each dimer consists of three distinct domains: a small β-roll containing the hydrophobic dimerization domain which is connected to a wing-domain comprised of an α/β subdomain via a discontinuous connector, and a β-ladder which is formed by 18 β-strands, nine from each monomer creating a continuous β-sheet.[64] Intracellularly, NS1 dimers remain associated with cell membranes and studies on DENV NS1 have demonstrated co-localization with assembled virus particles suggesting that NS1 may play a role in viral budding or assembly.[64] In greatest abundance, NS1 dimer trimerize to form hexamers that are processed through the trans-golgi

network and secreted from the cell. Extracellularly, hexameric NS1 is thought to play a role in immune evasion and pathogenesis through interactions with and modulation of the extracellular glycocalyx of endothelial cells. *In vitro,* YFV NS1 degrades the extracellular glycocalyx via upregulation of heparanase and cathepsin L in human liver sinusoidal microvascular endothelial cells, and *in vivo,* systemic treatment of mice with DENV2 NS1 results in vascular permeability.[65] While a great body of research exists exploring this phenomenon with regard to DENV NS1, research linking these finding to YF disease in human populations is relatively new and limited.[66]

The remaining NS proteins play various roles in viral replication which are reviewed by Neufeldt et al., 2018.[57] NS2A is required for viral replication and NS2B serves as cofactor that recruits NS3 to the ER membrane. NS3 has multiple enzymatic functions and serves as a protease that cleaves the viral polypeptide, a nucleotide 5' triphosphatase (NTPase) and RNA 5′ triphosphatase that both play a role in 5' cap formation, and as a helicase. NS4A which is integrated within the ER membrane is responsible for membrane curvature, and NS4B, which becomes integrated within the membrane because of co-translation with signal peptide 2K, interacts with NS3 and is required for viral replication but has no independent enzymatic activity. Like NS3, NS5 also has multiple enzymatic activities involved in 5′-RNA capping and viral genome methylation, and a RNA-dependent RNA polymerase located at the C-terminal domain for viral RNA synthesis.

1.4.3 Replication cycle

YFV replication begins with cell entry. Following viral attachment to cell surface receptors (Fig.1.4, step 1) via epitopes within the ED-III of the E glycoprotein, internalization of the virion occurs via clathrin-mediated endocytosis (Fig.1.4, step 2). During endosomal maturation (Fig.1.4, step 3), a decrease in pH causes a conformational change of the E glycoprotein which reveals a fusion loop located within ED-II which imbeds within the endosomal membrane resulting in fusion and release of the viral genome into the cytoplasm (Fig.1.4, step 4). Host-mediated translation of the positive sense RNA genome (Fig.1.4, step 5) initiates several rounds of viral replication at the endoplasmic reticulum (ER) membrane, followed by assembly of new immature virions which then bud into the ER lumen (Fig.1.4, step 6). As newly synthesized virions become encapsulated with ER-derived membranes, they are decorated with newly translated full-length prM and E

which form 60 trimers of prM-E heterodimers resembling spikes, where the fusion loop of ED-II is effectively capped by prM,[59] preventing premature fusion which would otherwise occur because of the low pH environment as virions bud from the golgi towards the cell membrane. Virus maturation occurs as virions are processed through the trans-golgi network, where low-pH conditions of 5-6 expose a cleavage site within prM which is cleaved by host enzyme furin (Fig.1.4, step 7).[67] Following cleavage, the pr peptide remains associated with E through interactions with ED-I and ED-II of dimerized E monomers, within which the fusion loop is buried, providing stabilization and preventing premature fusion.[67] Following secretion from the cell, virions are exposed to neutral pH and the 91 amino acid pr peptide is released (Fig.1.4, step 8),[61] resulting in mature virions with an exposed fusion loop, ready to begin the next replication cycle. Extracellularly, the E glycoprotein is exposed to the host immune system, representing the primary antigenic target of NAbs, which have been widely accepted as a correlate of protection since the earliest vaccination studies in humans.[68]

Figure[1.4]

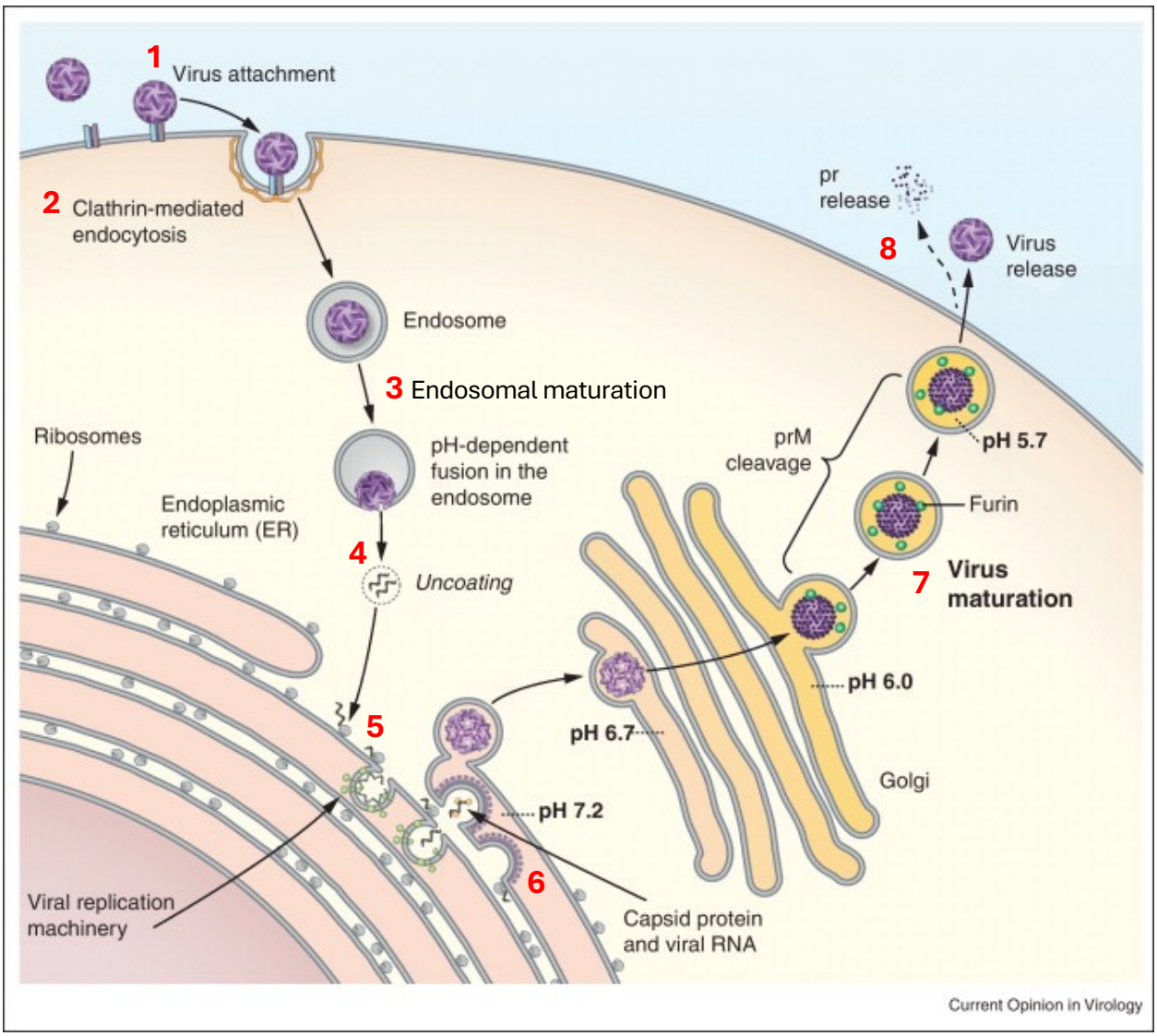

[Figure 1.4]

Figure 1.4 Orthoflavivirus **replication cycle**

Reprinted and adapted from Pierson & Diamond, 2012, Copyright (2012), with permission from Elsevier.[61]

1.4.4 Host target cells

In humans, YFV is viscerotropic with significant viral replication occurring in the liver. Following the bite of an infected mosquito, dermal dendritic cells (DCs) are the first cells to become infected with YFV before being trafficked to the lymph nodes.[69] Following establishment of cellular entry of DENV via the DC-specific ICAM-grabbing non-integrin (DC-SIGN) receptor, Barba-Spaeth *et*

al., 2005 investigated this molecule as a possible route of DC cell entry for YFV, using the 17D vaccine strain.[70] However, both immature DCs (iDCs) and mature DCs (mDCs) were shown to be permissive to 17D and that infection occurred in the presence of anti-DC-SIGN antibodies, indicating that cell entry occurs in a DC-SIGN-independent manner.

A viscerotropic infection model using a wild-type Asibi strain in rhesus macaques has demonstrated amplification of YFV in the lymph nodes that precedes significant viral replication in up to 80% of hepatocytes[71] resulting in necrosis, where amplification within the liver plays a central role in establishing disease and causing pathogenesis such as acute liver damage and jaundice.[72] Infection of hepatocytes has also been demonstrated *in vitro* using the 17D vaccine strain.[71]

Pathological studies of YFV in humans are sparse and are biased towards fatal cases, and therefore severe disease. The involvement of the liver has been demonstrated by post-mortem histopathology of liver sections showing the presence of Councilman bodies which are areas of acidophilic hepatocellular necrosis with midzonal distribution,[73] and a characteristic pathological finding of YFV infection. The same study demonstrated the involvement of hepatocytes and Kupffer cells was indicated by the presence of ceroid pigment in these altered cell types in amounts that were proportional to the extent of liver damage.

More recently, data generated during the outbreak in Brail has shed light on pathological findings that are less well documented. The occurrence of late-relapsing hepatitis in 16% of YF patients has been well-documented,[14-19] and is discussed in *Section 1.3.2a*. Outside of the liver, Giugni et all., 2023 investigated cardiac pathology amongst fatalities received at a morgue in São Paulo, Brazil found myocardial fibrosis and myocardial hypertrophy in 93% of patients, with endothelial alterations in 92% of patients, in addition to detection of YFV RNA in 96% of cardiac samples.[74] These findings clearly demonstrate the involvement of myocardial injury in severe YF.

Section 1.5: Yellow fever virus strains

1.5.1 Wild-type strains

YFV strains are phylogenetically classified into seven genotypes, with five circulating in West Africa: West Africa I (WA-I), West Africa II (WA-II), East Africa (EA), and East/Central Africa (E/CA), Angola (A); and two which circulate in South America: South America I (SA-I) and South America II (SA-II), shown in Figure 1.5. Phylogenetic analyses estimate that current circulating African strains emerged within the last 1,500 years with South American strains emerging 300-400 years ago on the east coast and spreading westward,[75] which aligns with hypotheses that YFV was brought to the America's upon ships during the slave trade during the 16th century.

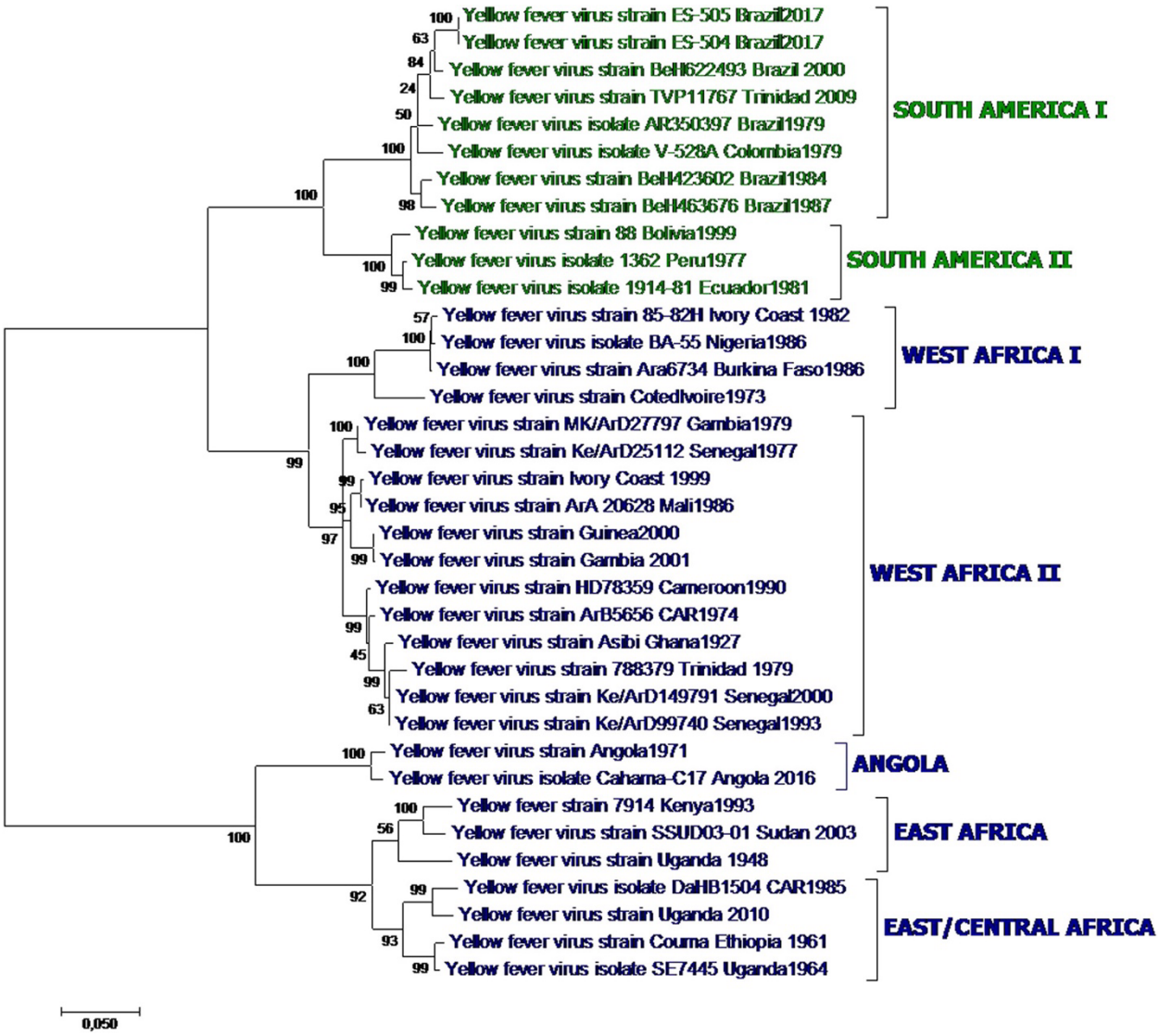

Figure[1.5]

[Figure 1.5]

Figure 1.5 ***Phylogenetic tree of YFV strains***

Reprinted from Domingo *et al.*, 2018[76] licensed under Creative Commons.

Phylogenetic tree of 36 YFV strains constructed using 1428 nucleotide sequence the bridges the prM-E junction.

Compared to more recent phylogenetic analysis of utilizes whole YFV genome sequences,[77] prior phylogenetic analysis of YFV that established the genotypes recognized today utilized a 670-bp fragment that crosses the prM-E junction, including the entire 225 nucleotides of M, and 337 nucleotides of the genome encoding the 5' end of the E glycoprotein.[75, 78, 79] In 2001 Mutebi *et*

al.[78] sequenced 38 spatially and temporally distinct African YFV strains. Phylogenetic analysis divided these strains into two major lineages—West African and East/Central African—between which, there are five total clades. WA-I and WA-II, which had been previously identified, belonging to the West African lineage, and EA, E/CA and A, belonging to the East/Central African lineage. Importantly, genotypes were defined as distinct by a >9% difference in the nucleotide sequence, and all virus strains shared 74.8 to 100% identity by nucleotide sequence, and 91.9 to 100% identity by amino acid sequence across all five genotypes.

Mutebi *et al.*, also characterized nucleotide and amino acid diversity within genotypes, finding that strains belonging to the E/CA (n=11) genotype were the most diverse, with up to 8.3% nucleotide- and up to 4.2% amino acid-variation between strains, followed by the EA (n=3) with up to 7.7% nucleotide- and 1.4% amino acid-variation between strains. Strains belonging to the WA-I (n=12) genotype varied up to 6.8% by nucleotide sequence and 1.8% by amino acid sequence, and WA-II (n=10) had up to 2.8% nucleotide- and 1.8% amino acid-variation between strains.

In 2017 Mir *et al.*[80] conducted phylogenetic analysis of South American strains (n=137) isolated from nine countries between 1954 and 2017. These data showed SA-I and SA-II genotypes as reciprocally monophyletic and geographically distinct. While SA-I strain isolates originated from multiple countries including Brazil, Colombia, Venezuela, and Trinidad and Tobago, while all isolates belonging to the SA-II genotype originated in Peru. Regarding the evolution and dissemination of strains, the authors note that "lineage replacement" likely played a critical role in shaping the SA-I genotype, with simultaneous emergence of a new strain and reduction in the diversity of SA-I strains across multiple countries occurring in the mid-1990s, likely originating from a strain which emerged in Trinidad and Tobago in 1977. Contrastingly, the authors found evidence of co-circulation of multiple strains belonging to the SA-II genotype with no evidence of lineage replacement. Interestingly, SA-II genotype strains are rarely isolated outside of Peru.[81]

1.5.2 Laboratory strains

According to United States biosafety guidelines provided by the Biosafety in Microbiological and Biomedical Laboratories manual,[82] wild-type YFV strains are classified as biosafety level (BSL)-3 pathogens, based on recommendations provided by the American Committee on Arthropod-Borne Viruses (ACAV) Subcommittee on Arbovirus Laboratory Safety (SALS). Meanwhile, the 17D vaccine strain, for which "attenuation has been firmly established", may be handled at BSL-2 due to few reports of laboratory-associated infections in combination with the low probability of infection resulting from aerosolized droplets. The requirement for BSL-3 containment and additional training for handling wild-type YFV strains poses substantial barriers to research, which can only occur at institutes equipped with appropriate facilities. Consequently, 17D is the predominant laboratory strain, for both research and diagnostic purposes. Outside of the 17D vaccine strains, the Asibi strain has been historically used as the reference wild-type strain.[83, 84]

In addition to native viruses, attenuated or not, infectious clones[85-87] have been engineered, in addition to reporter viruses,[88, 89] and pseudoviruses[90] which bypass the need for a BSL-3 facility and increases the accessibility of YFV research.

Section 1.6: Transmission of YFV in diverse hosts

YFV is an arbovirus (arthropod-borne virus) and is thus able—and obligated—to replicate within and successively between vertebrate and invertebrate hosts. Although "host" accurately describes any infected organism, the standard convention within the YF field is that YFV is transmitted between "primate hosts" by "mosquito vectors". Compared to other orthoflaviviruses such as West Nile Virus, which includes birds and mosquitos, and humans as dead-end hosts,[91] YFV has a relative narrow range of vertebrate and arthropod host species. Transmission of YFV occurs in three distinct transmission cycles: (i) the urban cycle, (ii) the sylvatic, jungle or enzootic cycle, and (iii) the intermediate, rural, or Savannah cycle.[92] While all three transmission cycles are observed in Africa (Figure 1.6), only the urban and sylvatic transmission cycles are observed in South America to date (Figure 1.7).

Figure[1.6]

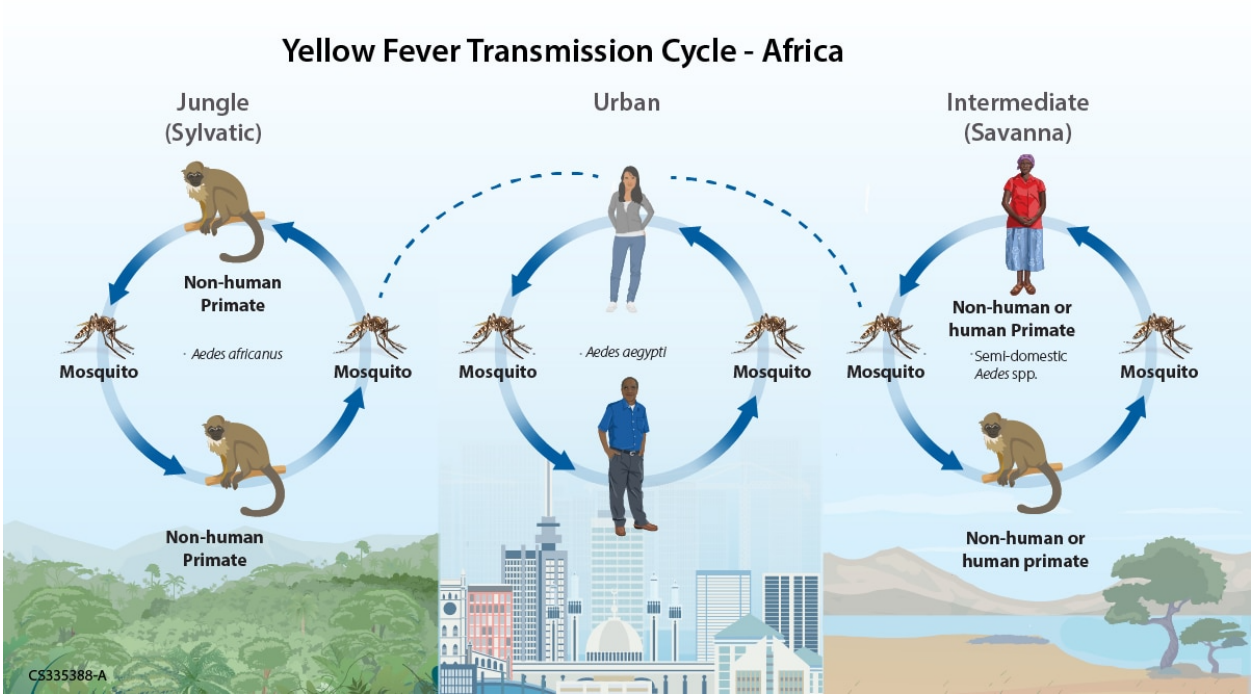

[Figure 1.6]

Figure 1.6 ***Transmission cycles of YFV in Africa.***

This image is in the public domain. Source: CDC Yellow Book 2024.[93] Use of this image does not constitute its endorsement or recommendation by the U.S. Government, Department of Health and Human Services, or Centers for Disease Control and Prevention.

Figure[1.7]

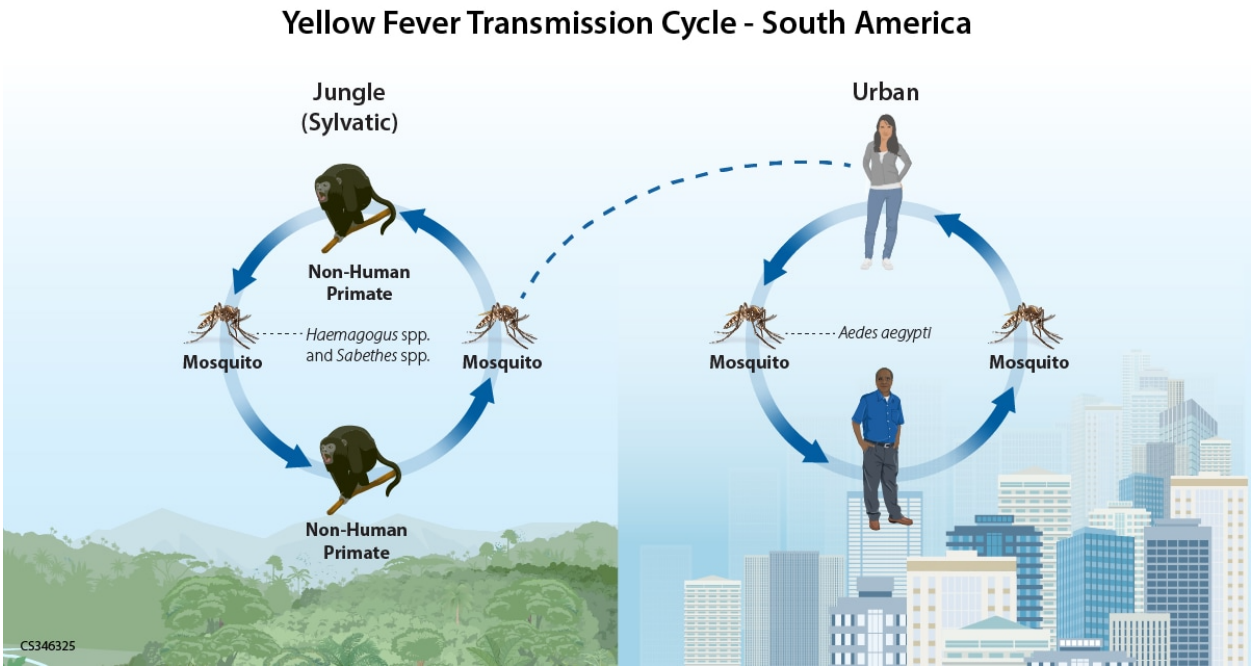

[Figure 1.7]

[1.7] ***Transmission cycles of YFV in South America.***

This image is in the public domain. Source: CDC Yellow Book 2024.[93] Use of this image does not constitute its endorsement or recommendation by the U.S. Government, Department of Health and Human Services, or Centers for Disease Control and Prevention.

1.6.1 Primate hosts

1.6.1a Humans

Humans (*Homo sapiens)* are considered amplifying hosts of urban YFV, meaning that YFV can replicate to sufficiently high concentrations to sustain transmission. Humans become infected following the bite of an infected mosquito and will be infectious during the viremic phase of infection when the virus is present at high enough levels in the blood to be transmitted to a susceptible biting mosquito, and so the transmission cycle continues. By qRT-PCR, one study found between 372 and 2.75E+6 copies of YFV RNA genome per mL of blood (2.57-6.44 $\log_{10}$

copies/mL) amongst hospitalized YF patients in São Paolo, Brazil (n=76), with significantly higher viral loads observed amongst individuals with fatal outcomes compared to survivors. [94, 95]

1.6.1b Non-human primates

Non-human primates (NHP) are key amplifying hosts for sylvatic and savannah cycles of YFV. In Africa, the predominant NHP belong to the genus's *Cerecopithecus*, Colobus, and *Erythrocheus*, and in South America, YFV has been isolated from *Alouatta* spp. (howler monkeys), *Callithrix* (marmosets), and *Sapajus*.[96] NHP host species and geographical locations are summarized in Table 1.5.

Table[1.5]

Non-human primate host	**Common name**	**Geographical location**
Cerecopithecus spp.	Vervets	Africa
Colobus spp.	Colobus monkey	Africa
Erythrocebus spp.	Hussar	Africa
Alouatta spp.	Howler monkey	South America
Callithrix spp.	Marmosets	South America
Sapajus spp,	Capuchin monkey	South America
Ateles spp.	Spider monkey	South America
Aotus spp.	Owl monkeys	South America

[Tab1.5]

Table 1.5 Non-human primate hosts of YFV.

NHP hosts of YFV by scientific name, common name, and geographical location.[97]

Notably, paleotropical NHPs of Africa typically suffer milder disease following infection as compared to their neotropical counterparts. Amongst neotropical NHPs of South America, Howler monkeys (*Alouatta* spp.) are considered reliable sentinels for YFV based on their high susceptibility to infection and high mortality rates.[98] A recent paper by de Azevedo Fernandes *et*

al.,2021,[99] who performed immunohistochemistry on post-mortem NHP samples collected through local surveillance programs in São Paulo Brazil during the most recent outbreak, described differences in mortality and infection rates among NHP species, with the highest rates of infection (63%) and mortality (62%) reported amongst *Alouatta* spp. (n=708), and lower rates amongst *Callicebus* spp. (32% infection, 29% mortality), *Callithrix* spp. (3% infection, 1% mortality), and *Sapajus* spp. (14% infection, 14% mortality). However, a recent paper from Garcia-Oliveira *et al.*, 2024[51] who sampled carcasses collected under a passive surveillance program in the bordering state of Minas Gerais between 2021 and 2023, when there was no longer an outbreak, collected only four *Alouatta* spp. out of 166 total carcasses, none of which were infected. Instead, *Callithrix* spp. represented 89% of collected samples (148/166), of which 11% (16/148) were positive for YFV by RT-PCR conducted on liver tissue. The authors note low genomic loads observed amongst *Callithrix* spp. which may suggest low susceptibility for YFV. They also note that most (72%) *Callithrix* spp. samples come from urban areas, suggesting the likelihood of sampling bias due to their proximity with human populations. Overall, these articles emphasize differences in findings due to both sample technique and the type of area being sampled. While *Alouatta* spp. represent a robust sentinel during outbreaks, the tendency of *Callithrix* spp. to inhabit urban areas points to their potential value in surveillance when active outbreaks are not occurring.

1.6.2 Mosquito vector

1.6.2a Establishing Aedes aegypti *as the vector of YF*

While Carlos Finlay, a Cuban physician and epidemiologist, is often credited as the first to suggest mosquitoes as the vector of YFV, Kuno 2024[100] presents earlier scientific contributions on the discovery of mosquito transmission, including contributions made by John Crawford, Josiah Notts, and Louis Beauperthuy. Following time in Dutch Guiana, Baltimore-based Irish physician Crawford published his theory on the "involvement of insects in causation of yellow fever" in 1811, although his theory was ill-received by both the medical community and public.

Thirty-seven years later, in 1848, Nott, an Alabama-based physician, published his opinion that insects were involved in causing YF. Nott had previously lost four children to YF within a single

week. The first documented theory of mosquito involvement came in 1854 from Beauperthuy, a French physician who collected "striped-legged" mosquito specimens in Venezuela, believing that they transmitted poisons to humans from putrefying soil. While Finlay's awareness of these other contributions is debated, he remains the most credited for discovering the role of mosquitoes in YFV transmission.[100]

In 1881, Finlay theorized that the *Aedes aegypti* mosquito (previously named *Culex cubenisis* and then *Stegomyia fasciata*) was the vector of YFV.[101] Originally written and delivered in Spanish and later translated into English,[102] Finlay's theory was initially ill-received after he failed to demonstrate mosquito-transmission from infected people – a failure postulated to have resulted from a limited understanding of incubation times.[101] Nonetheless, Finlay's theory laid the groundwork for further ethically questionable yet important experiments conducted by Walter Reed and colleagues at the turn of the 20th century.[103] Reed experimentally allowed mosquitoes to feed on 11 infected individuals, before allowing those same mosquitoes to feed on "non-immune" individuals. In the absence of informed consent and study guidelines, these individuals comprised of soldiers, Cuban "volunteers", and volunteer physicians who were members of Reed's research group.[104] Infection resulted from mosquitoes that had taken a bloodmeal from two of the 11 original cases, causing mild disease in six individuals, severe disease in six, and death in two. Importantly, he noted successful infection resulting from mosquitoes that were 10-13 days post-infectious bloodmeal, versus unsuccessful infection in the non-immune individuals bitten with mosquitoes that were 2-8 days post infectious bloodmeal, a critical period that would later be coined the extrinsic incubation period. A crucial outcome of Reed's transmission experiments was a successful public health campaign led by General William Gorgas to control *Aedes aegypti*, resulting in elimination of YF in Cuba in 1902,[105, 106] 25 years before isolation of the virus.

1.6.2b Mosquito species

Aedes aegypti, colloquially known as the "yellow fever mosquito"[100] was the first YFV mosquito vector to be identified due to its role in transmitting human disease within urban transmission cycles. However, there are many other mosquito species responsible for transmitting the virus within intermediate and sylvatic cycles, which are summarized in Table 1.6.

Table[1.6]

Vector	**Geographical location(s)**	**Transmission cycle**
Aedes aegypti	South American Africa	Urban
Aedes albopictus	Africa South American	Urban
Aedes africanus	Africa	Intermediate Sylvatic
Aedes furcifer	Africa	Intermediate
Aedes luteocephalus	Africa South America	Intermediate Sylvatic
Aedes metallicus	Africa	Intermediate
Aedes vittatus	Africa	Intermediate
Aedes simpsoni complex	Africa	Intermediate
Haemagogus janthinomys	South America	Sylvatic
Haemagogus leucocelaenus	South America	Sylvatic
Haemagogus spegazzinii	South America	Sylvatic
Sabethes chloropterus	South America	Sylvatic

[Tab1.6]

Table 1.6 Mosquito vectors of YFV.

Summarized from Kuno 2024.[100]

Section 1.7: Experimental animal models

1.7.1 *Rhesus macaque*

After failed attempts by Stokes et al, 1928[107] to inoculate guinea pigs, chimpanzees, and baboons with YFV, successful inoculation of toque macaques (*Macaca sinica*) was achieved. However, not all animals were susceptible to infection, and the "pathological picture of human YF [was] not reproduced." With the goal of establishing a better model of human disease, successful infection in rhesus macaques (*Macaca mulatta*) that caused disease manifestations similar to those observed in humans was achieved, representing a significant advance in the field that ultimately permitted development of a life-saving vaccine. While similar to disease in humans, YFV infection in rhesus macaques is typically more severe, as demonstrated by infection with the virulent wild-type DakH1279 strain which results in ~72% fatality.[72, 108]

1.7.2 Syrian golden hamster

An experimental infection model using the Syrian golden hamster (*Mesocricetus auratus)* was established by Robert Tesh and colleagues in 2001.[109, 110] With an intact immune system, the Syrian golden hamster tolerates infection with the 17D vaccine strain well which has application in vaccinology studies.[97] Compared to rhesus macaques, the Syrian golden hamster exhibits less severe disease[97] and a fatality rate of ~23%,[109] which has allowed the study of disease progression. Development of a YFV infection model using the Jiminez strain results in disease with similar kinetics of viremia and rates of mortality as is observed in humans.[109] However, this model does not fully replicate disease observed in humans, with notable differences in liver pathology.[97]

1.7.3 AG129 mouse

Because mice are naturally resistant to infection with orthoflavivirus, disruption of the interferon (IFN) pathway is required to model disease. The AG129 mouse is a double knock-out mouse lacking both the alpha/beta and gamma IFN receptors (IFN α,β,γ $R^{-/-}$) which is permissive to YFV infection.[111] Due to impaired anti-viral responses, infection with the attenuated 17D strain is lethal and does not recapitulate disease in humans well; nonetheless, this model has application in antiviral studies.[97]

Section 1.8: 17D vaccine

1.8.1 17D vaccine development

1.8.1a Historical context

In the spring of 1925, the Rockefeller Foundation formed the West African Yellow Fever Commission and set up an outpost in Lagos, Nigeria, where Western scientists were sent to study "the yellow fever problem" with the goal of understanding "the way in which yellow fever spreads" in an effort to control disease.[112] Before identification of YFV, *Leptospira icteroides,* a bacterium responsible for causing leptospirosis, was proposed as the potential infectious agent responsible for causing YF.[113] However, failed attempts to isolated the bacterium from patients' blood called for reexamination of YF cases in order to accurately identify the causative agent.[107] In 1927, these efforts resulted in the isolation of YFV, and YFV became the first human pathogenic virus to be isolated.

1.8.1b Virus isolation

The specific events that led to the isolation of YFV are described in a 1928 paper published in the American Journal of Tropical Medicine, authored by Adrian Stokes, Johannes Bauer, and Paul Hudson. The findings were published shortly following the death of Stokes who suffered fatal YF which likely occurred following a laboratory-acquired infection.[107]

At 4pm on June 29, 1927, amid a YF outbreak in the capital of Ghana, Accra, and surrounding villages, a 28-year-old Ghanaian man named Asibi presented with fever, chills, and a severe headache. Under the care of Dr. Alexander Mahaffy, Asibi was noted to have an elevated temperature of 103°F, a pulse of 96, and fatigue, and was complaining of headache and back pain. While Dr. Mahaffy described Asibi as "very ill," Asibi's fever broke the following day before he made a "rapid recovery" and returned to work just five days following symptom onset. By modern day standards, Asibi's symptoms were relatively mild.

Blood taken from Asibi 33 hours following symptom onset was used to inoculate "rhesus 253-A" by intraperitoneal injection. Fever was observed four days post infection and necropsy was performed, revealing evidence of hemorrhaging within the stomach and the lungs, in addition to moderate amounts of necrosis in the liver. At the time of necropsy—four-days post infection and the day of symptom onset—blood and "liver and kidney emulsions" were prepared from rhesus 253-A, and intraperitoneally injected into rhesus 253-B, which also developed a fever and died six days following infection. The "Asibi" strain was passaged monkey-to-monkey in this manner a total of 53 times, with fatal outcomes in all but one.[114]

In addition to virus isolation, this study's findings included establishing rhesus macaques as a model host for human disease, establishing experimental conditions to successful model transmission between macaques and *Aedes aegypti* mosquitoes, and a preliminary attempt to characterize the virus through filtration, which were later expanded upon to demonstrate that the virus was able to pass through very small filters and maintain infectivity.[115]

1.8.1c Attenuation by serial passage

In the laboratories of the International Health Division of the Rockefeller Foundation in New York, a South African scientist named Max Theiler, among others, began the process of viral attenuation by serially passaging the Asibi strain through various tissues. First, a cultivation method for maintaining the virus without passage through animals was established, using minced chicken embryos and liquid media that contained small amounts of either human-derived, or rhesus-derived

YFV-naïve serum, which was believed to prolong survival of extracellular virus.[105, 114, 116] Following 18 passages in embryonic mouse tissue, the Asibi strain was passaged 58 times in minced whole chick tissue, and then minced whole chick tissue that had had the brain and spinal cord removed by dissection, for over 160 times.[114] The events of virus isolation and passage through animals and various tissues are summarized in Figure. 1.8 (black text, boxes, left).

Throughout the attenuation process, aliquots of virus stocks were reserved, and virulence was assessed. In 1937, Max Theiler and colleagues reported their observations of key events of attenuation using the 89th, 114th, and 176th virus subcultures in a paper published in the Journal of Experimental Medicine, which are summarized in Figure 1.8 (blue and orange boxes).[84] While rhesus macaques (n=6) exhibited 100% mortality due to encephalitis following intraspinal and intraperitoneal infection with the 89th subculture, macaques that were infected intracerebrally with the 114th subculture—which had undergone serial passage through minced whole chick tissues lacking the brain and spinal cord—survived (n=4), indicating an important loss of neurotropism.

To test for circulating virus, groups of suckling mice (n=3-8)—which possess immature immune systems which render them suspectable to YFV infection[117]—were infected with blood taken one to 10 days post-infection from each NHP infected with the 114th subculture, where high mortality within a group of mice indicated high levels of circulating virus. Low mortality was observed across all groups, with death of only a single mouse per group which was observed following blood taken from NHPs 2-4 days post-infection, compared to high levels of mortality in groups of mice infected with blood taken 4-6 days post-infection from NHPs infected with the 89th subculture, indicating loss of viscerotropism in the 114th subculture.

Next, the immunity of NHPs that had survived intracerebral infection with subculture 114 was investigated two-fold. First, the authors conducted "protection tests" by mixing
serial dilutions of serum with a standard concentration of virus and incubating for 1 hour at 37°C to allow binding of any neutralizing antibodies to the surface of virions. Groups of mice were then inoculated intracerebrally with each serum-virus mixture, and the serum dilution at which 50% of the mice survived a lethal challenge was interpolated. These protection test demonstrated the presence of neutralizing antibodies, albeit at relatively low titers of 1:10 – 1:45, at four weeks post

infection. Second, animals were subjected to a challenge experiment 41-day post-infection using the French neurotropic strain which was delivered intracerebrally. All animals survived, indicating immunity had indeed been acquired following initial inoculation with the 114th (later named 17D), although febrile illness was noted in all four NHP, and encephalitis in one. Further loss of virulence was observed between passages 114 and 176, as indicated by an increase in the average interval time observed between infection and death in mice following intracerebral inoculation.

In 1951, Theiler was awarded the Nobel Prize in Physiology or Medicine, "for his discoveries concerning yellow fever and how to combat it,"[118] becoming the first Nobel laureate to be recognized for the development of a vaccine.[119] It would be another 72 years before the Nobel Prize was awarded for development of an antiviral vaccine, to Katalin Karikó and Drew Weissman, "for their discoveries concerning nucleoside base modifications that enabled the development of effective mRNA vaccines against COVID-19."[120]

Figure[1.8]

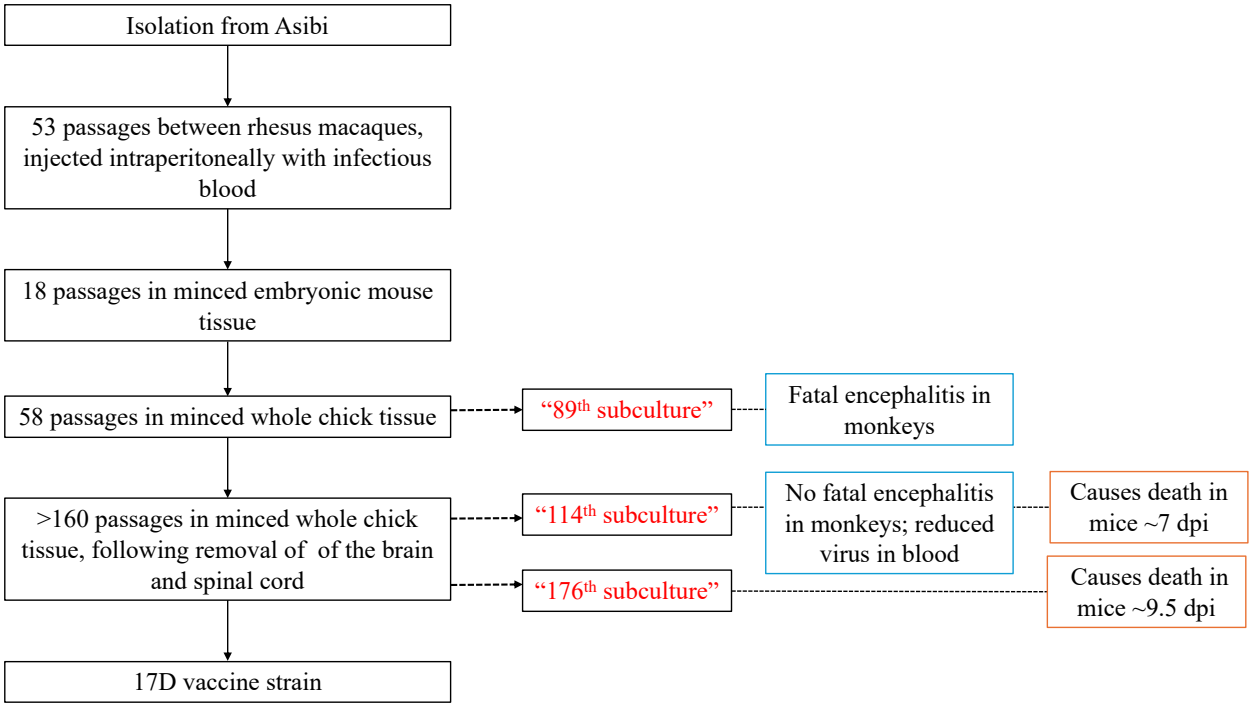

[Figure 1.8]

Figure 1.8 ***Passage history and attenuation of 17D***

Flow chart showing the passage history and key experiments demonstrating attenuation of the 17D vaccine strain following isolation of the parental Asibi strain, as described by Theiler and Smith, 1937.[84] Passage history is shown in black boxes on the left. Subculture strains are shown in red text, with dashed arrows indicating the stage of subculture from which that strain was taken. Subculture numbers are enclosed within quotation marks to indicate uncertainty around which passage was designated as the first passage by the authors. Experimental results that demonstrate key attenuation events performed in monkeys (blue boxes) and mice (orange boxes) are indicated with dashed lines joining the specified strain to the result. "dpi": days post-infection.

1.8.1d Vaccine production

Since early production in 1937, the 17D vaccine was, and continues to be, produced by inoculation of specific pathogen-free embryonated chicken eggs. [121, 122] A single dose of 17D vaccine must contain a minimum of 10^3 internation units (IU),[2] which is equivalent to 4.74 $\log_{10}$ plaque forming units,[123] however there no upper limit and great variation in IU per single dose is reported, with up to $10^{6.5}$ IU per dose.

1.8.2 Early trials of biosafety and immunogenicity

During the vaccine development process, less attenuated versions of the virus were used to vaccinate humans with the addition of an important safety measure: the attenuated virus was co-administered with human-immune serum that was known to inhibit viremia in monkeys.[124] The 17D vaccine was eventually administered to humans without the addition of human-immune sera in a series of incremental trials detailed by Smith et al, 1938.[68] Beginning in February 1937 in New York and continued in Brazil following manufacturing of the 17D vaccine in the Yellow Fever Service in Rio de Janeiro, trials began with vaccination with different doses of 17D performed in the laboratory. Small groups of 6-10 individuals were closely monitored to assess safety and immunogenicity. For two weeks following vaccination, temperature, blood, and urine samples were taken to assess fever, viremia, white blood cell count, and the presence of albumin in the urine, in addition to symptoms reported by the vaccinees. Aside from headaches and minor local inflammation at the site of vaccination, no serious side effects were noted. Blood was then taken at one-, two-, three-, four-, five-, seven-, and 10-weeks post-vaccination to perform antibody

titration. Following "satisfactory results" of few serious side effects and the detection of protective antibodies in 28/29 individuals, the vaccine was administered to larger groups of individuals.

In June of 1937, field trials began in the municipality of Varginha within the State of Minas Gerais, Brazil. Smith *et al.*,[68] noted the interest of the local people in prophylactic measures against YF; however, ultimately these trials involved vaccination of workers at three coffee fazendas (farms) following agreement with the local public health authorities and while cooperation of these individuals was noted, they were not given the opportunity to provide informed consent. Nonetheless, the trials continued and expanded to more fazendas and groups of vaccinees incrementally increased in size, and including children >2 years old and pregnant women. As larger cohorts received vaccination, rarer and more serious side-effects were alluded to with 1.4% of individuals having taken time off following vaccination, and less than 1% reportedly confined to bed rest for several days. Notably, the nature of these adverse events was measured by time missed from work and detailed clinical descriptions were not provided. Between June and August 1937, 2,746 individuals were vaccinated across 18 fazendas. Pre-vaccination antibody titers were detected in 5% (9/188) of individuals tested, and post-vaccination antibodies were detected in 94% (624/633) of individuals tested.

With few reports of serious adverse events, and apparent safety in children and pregnant women, these trials progressed to large-scale routine administration under the Cooperative Yellow Fever Service. Operations were streamlined as the number of vaccination sites increased, with doctors conducting post-vaccinal visits to fazendas to enquire about side effects, with no "serious or alarming" reactions noted from 26 different batches of vaccine. Beginning in late 1937, an outbreak of cases increased demand for doses and for the first time, the 17D vaccine was administered as an outbreak response measure. Between February 1937 and January 1938, more than 59,000 individuals were vaccinated, and the vaccine became widely accepted by the global community.

1.8.3 French neurotropic virus: an alternative vaccine

French neurotropic virus (FNV) is an obsolete attenuated vaccine strain derived from the parental French viscerotropic virus (FVV) strain that was originally isolated in Dakar, Senegal in December of 1927 from a Syrian individual named Francois Mayali.[125, 126] Attenuation of FVV was initiated by members of the Yellow Fever Commission including Theiler who serially passaged FVV through mouse brain tissue which resulted in enhanced neurotropism in NHPs.[126] The vaccine was ultimately developed at the Pasteur Institute, Dakar,[127] and was widely administered by scarification throughout French speaking countries in West Africa, with greater than 20 million doses administered by 1948.[128] Studies conducted in French soldiers showed that FNV was highly immunogenic, with the development of NAbs in 97% of soldiers (n=210) that protected mice against fatal challenge.[105] Unfortunately, there were reports of post-vaccinal encephalitis, including 73 cases and 29 deaths amongst children <10 years old following a vaccination campaign of 42,400 people in Enugu, Nigeria in 1952.[127] Ultimately, these serious complications contributed to discontinued use of FVV vaccine which was deemed to have a "greater danger of serious neurologic reactions" compared to the favored 17D vaccine.[105]

Section 1.9: Yellow fever immunity

1.9.1 Viremia

During natural human YFV infection, viral RNA can be detected by RT-PCR in serum between zero and 14 days following symptom onset,[19, 21] with peak viremia occurring 3-5 days post-symptom onset.[19, 95] Following vaccination, peak viremia occurs 5-7 days post-vaccination,[19, 129] which is short and self-limiting in comparison to natural infection.[19] The mechanism underlying the variation in viremia kinetics has been attributed to differences observed in the cell-entry pathway between strain wild-type Asibi and 17D vaccine strain. While the Asibi strain infects cells via clathrin-mediated endocytosis, the 17D vaccine strain utilizes the clathrin-independent pathway. Consequently, cell surface binding and entry is more efficient in the 17D vaccine strains compared to wild-type Asibi, and lower levels of viremia have been noted amongst vaccinees at 5-7 days post-vaccination, compared to naturally infected individuals who exhibit lower levels of prolonged viremia.[19] It has been suggested that the low level viral replication observed by wild-type strains may result in early immune evasion, in turn allowing the virus to disseminate, while

more efficient vaccine replication early on may play a key role in eliciting a robust anti-viral response resulting in rapid viral clearance.[130]

1.9.2 Soluble mediators

In 2004, ter Meulen *et al.*,[131] studied the cytokine response amongst individuals with YF infected during the large 2000 outbreak in the Republic of Guinea in West Africa which reported 688 suspected cases and 225 deaths. With the goal of understanding the role of inflammatory mediators in pathogenesis, the authors characterized cytokine responses amongst participants with IgM-confirmed YF with fatal- (n=7), non-fatal hemorrhagic- (n=11), and non-fatal non-hemorrhagic disease (n=18). Pro-inflammatory cytokines interleukin (IL)-8, MCP-1, tumor necrosis factor (TNF)-α, IL-6, and IL-1RA, and anti-inflammatory cytokine IL-10 were most elevated amongst fatal cases, followed by non-fatal hemorrhagic cases, and then non-fatal non-hemorrhagic cases. Unfortunately, the time interval between symptom onset and blood draw was not accurately recorded, and so the timing of soluble modulators cannot be determined.

A more comprehensive study conducted by Fradico *et al.*, 2023[19] in Brazil between 2017 and 2018 characterized soluble modulators amongst 92 acute phase hospitalized patients, 1-15 days post-symptom onset. The authors found significant increases in most soluble mediators: CCL11, CXCL8, CCL3, CCL4, CCL2, CXCL10, IL-1β, IL-6, TNFα, IL-12, IFN-γ, IL-17, IL-1Ra, IL-9, IL-10, FGF-basic, GM-CSF, and IL-2; representing a significant cytokine storm, with higher level of these mediators associated with higher morbidity scores. Amongst vaccinees, increased levels of soluble mediators were also noted compared to healthy controls but were reduced in magnitude compared to individuals with natural infection.

Regarding disease severity, the authors observed that CCL11, CXCL8, CCL3, CCL4, CCL2, CXCL10, IL-6, IL-17, FGF-basic, and GM-CSF were increased amongst fatal cases of YF and cases requiring intensive care, compared to patients who survived and patients who did not require intensive care, suggesting a signature of severe disease.

1.9.3 T cells

Akondy *et al.*, 2015[129] found that effector CD8+ T cell expansion begins seven days post-vaccination and reaches peak levels between day 11 and 14. They also found that the magnitude of the CD8+ T cell response is positively correlated with a peak viremia of <225 genomes per mL, and that vaccinees with peak viremia above this threshold exhibit an essentially saturated CD8+ T cell response. Regarding functionality, Co *et al.*, 2002 demonstrated IFNγ production by ELISPOT, high levels of T cell proliferation, and cytolytic activity against target cells infected with vaccina constructs expressing E, NS1, NS2a, and NS2b at 14-days post-vaccination (n=4), while Akondy *et al.*, 2009[132] identified NS4B-specific CD8+ IFNγ+ T cells as dominant in five vaccinees, accounting for 42% of CD8+ T cells at 2 months post-vaccination. James *et al.*, 2013[133] observed peak expansion of CD4+ T cells at 14 days post-vaccination (n=40), with specificity against C, prM, E, NS1, NS2a, NS3, and NS5 within a subset of participants (n=16), with the highest frequency specific to NS1.

While expansion of functional CD8+ and CD4+ T cells following vaccination has been demonstrated, the role of T cells in providing protective immunity is disputed in a review by Amanna & Slifka, 2016[134] who summarize the findings of two important clinical trials. The success of the 17D vaccine has inspired design of chimeric vaccines against related orthoflaviviruses, Japanese encephalitis virus (JEV) and DENV. The chimeric vaccines utilize the 17D vaccine backbone, consisting of structural protein C and non-structural proteins NS1 through NS5, with the important addition of structural proteins prM and E from JEV and DENV (Figure 1.9).

The power of these clinical trials in deducing the relevance of CD8+ T cell memory comes from the distinct chimeric make-up of each live attenuated vaccine and previous work that looked at the composition of the CD8+ T cells following 17D vaccination. Akondy *et al.*, 2009 found that less than 14% of functional CD8+ T cells are specific to peptides derived from M and E, while most memory CD8+ T cells recognize non-structural proteins.[132] As each chimeric vaccine elicits viremia in a varying proportion of vaccinees, secondary or boost vaccination conducted in 17D-immune vaccinees, offers a controlled attenuated challenge experiment. The results, summarized

in Figure 1.9, demonstrate viremia elicited from DENV or JEV vaccination is no different between vaccinees with and without prior 17D vaccination, suggesting that any existing T cell memory established from primary vaccination with 17D does not protect against viral replication with heterologous vaccines.

Figure[1.9]

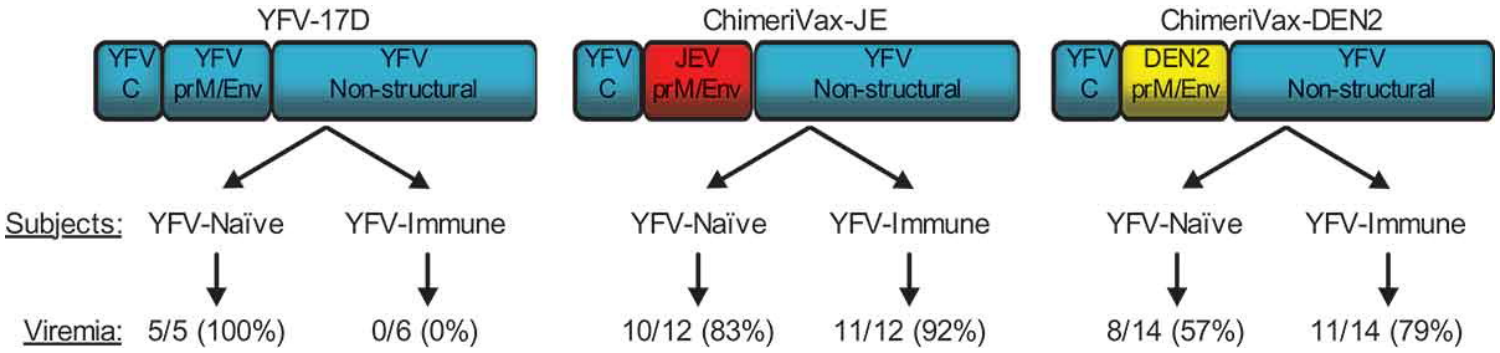

[Figure 1.9]

Figure 1.9 ***17D-specifc T cells fail to protect against vaccine-viremia from chimeric viruses***

Reprinted from Amanna & Slifka, 2016[134] with permission from Taylor & Francis obtained via Copyright Clearance Center RightsLink®.

1.9.4 B cells

1.9.4a General B cell immunology

The general immunology of B lymphocytes (B cells) from B cells activation to antibody secretion is reviewed at length.[135] A brief account is given below.

Briefly, B cells develop and mature in the bone marrow. Following maturation, mature but naïve B cells enter the circulation and secondary lymphoid tissues where they may encounter their cognate antigen and become activated. Antigens may be recognized by number immune receptors, including the B cell receptor (BCR). BCRs are membrane-bound immunoglobulins (Ig) antibodies bound to the surface of mature B cell via the crystallizable fragment (Fc). Following antigen recognition via the BCR, the BCR/antigen complex is internalized via clathrin-mediated

endocytosis. Proteolytic processing of the BCR/antigen complexes occurs in the lysosome and results in the generation of antigen-derived peptides which are then loaded onto major histocompatibility complexes (MHC) class II molecules for presentation to CD4+ T helper cells, which play an important role in B cell activation. Within lymph nodes, B cells present antigen via MHC-II, and subsequent recognition by CD4+ T helper cells result in co-stimulation of B cells via CD40-CD40L drives further B cells activation, resulting in proliferation and differentiation into centroblasts and centrocytes. Within the lymph node, these newly activated centroblasts and centrocytes are organized within the dark zone of germinal centers where they undergo somatic hypermutation. Somatic hypermutation is a process that increases BCR variability though activation-induced cytidine deaminase (AID)-mediated introduction of mutation within the variable region, and ultimately results in the production of high affinity antibodies. The process of somatic hypermutation produces a population of centrocytes that possess a range of related but non-clonal BCRs, derived from a parental BCR. The centrocytes are then presented to antigen via T follicular helper (T_{FH}) cells during a process called affinity maturation, where centrocytes with high affinity BCRs are positively selected, and centrocytes with reduced affinity BCRs are deleted. Following positive selection, B cells further differentiated to become either memory B cells (MBCs) or plasmablast cells, which secrete their BCR and become antibody-secreting cells.

1.9.4b YFV B cell immunology

Wec *et al.*, 2020[89] conducted a detailed study of B cells responses following 17D vaccination in two participants. They observed peak expansion of plasmablast cells at 10- and 14-days post-vaccination, with high levels of somatic hypermutation observed at day 14 post-vaccination, which continued for 6-9 months post-vaccination. By 14 days post-vaccination, 75-80% of total B cells expressed CD71 and had low expression of CD21, which are markers of B cell activation/proliferation, and activated memory B cells (MBCs), respectively. Between 14 days- and 1-year post-vaccination, populations of these cells steadily declined, reflecting the contraction of the expanding B cells following antigen clearance, and by 1-year post-vaccination, 100% of these cells had undergone somatic hypermutation. Finally, the authors found that monoclonal antibodies derived from these MBC bound to the YFV E glycoprotein II domain and were highly neutralizing.

1.9.5 Neutralizing antibodies as a correlate of protection

The concept of "protective antibodies" in the context of YF entered the literature as early as 1937, following challenge experiments in mice conducted by Theiler and Smith.[84] Serum taken from experimentally inoculated NHPs was serially diluted and combined with a lethal dose of YFV, before being inoculated into suckling mice. By counting the number mice per group that died and survived at each serum dilution, the theoretical serum dilution that is protective to 50% of the mice may be calculated, known as the "lethal dose 50," or LD50.[84]

In 1972, Mason *et al.* conducted an elegant experiment in rhesus macaques demonstrating the protective nature of 17D-elicited NAbs in a dose-dependent manner.[136] The authors vaccinated groups of NHPs with six different doses of the 17D vaccine—undiluted, 10^{-1}, 10^{-2}, 10^{-3}, 10^{-4}, and 10^{-5}—before determining NAb titers at 20 weeks post-infection, and subjecting animals to a lethal challenge with the parental Asibi strain. The key observations, which are summarized in Table 1.7, include a decrease in NAbs, measured as log neutralization index (LNI) with decreasing doses of 17D. An important functional readout from Mason *et al.*'s experiments is that this decrease in NAbs corresponded with a decrease in survival of animals following lethal challenge, from which they were able to calculate a protective threshold of 0.7 LNI, with 90-100% survival in NHPs receiving a dose of $\geq 10^{-3}$. By demonstrating the production of protective NAbs following vaccination with 17D in a NHP model, this paper was instrumental in establishing NAbs as a correlate of protection.

Table[1.7]

17D dose	***LNI at 20 wpv (log_{10})***	***Survival n/n (%) following challenge with Asibi at 20 wpv***
Undiluted	3.3	11/11 (100)
10^{-1}	2.4	11/12 (92)

10^{-2}	2.5	11/11 (100)
10^{-3}	3.3	10/11 (91)
10^{-4}	1.7	10/12 (83)
10^{-5}	0.62	3/11 (27)

[Tab1.7]

Table 1.7 17D elicits NAbs in a dose-response manner that protective against lethal YFV challenge/Summary of key findings from Mason *et al.*, 1973 that demonstrate protective nature of NAbs

Summary of key findings by Mason *et al.*, 1973 that show dose-response of 17D-elicited NAbs, and effects on survival in a NHP model challenged with the Asibi strain, 20 weeks post-vaccination (wvp).

1.9.6 Durability of NAbs

The durability of 17D-elicited NAbs has been extensively assessed[35, 137-173] and reviewed.[174-176] While the vaccine has been said to induce "life-long" immunity, research from our lab in a paper published by Kareko *et al.*, 2020[171] demonstrated waning potency of NAbs with time since vaccination. Plaque reduction neutralization tests (PRNT) were performed using sera from non-endemic vaccinees who received a single dose of 17D between zero and 61 ypv, and the serum dilution at which 90% of the input virus was neutralized ($PRNT_{90}$) was plotted against time since vaccination (Figure 1.10). When stratified by ypv, an increasing proportion of vaccines were found to be seronegative, i.e with $PRNT_{90}$ below the limit of detection of 1:10; 8% of vaccinees were found to be seronegative between zero and three ypv, 24% were seronegative 3-12 ypv, and 33% were seronegative by 12 ypv.

Figure[1.10]

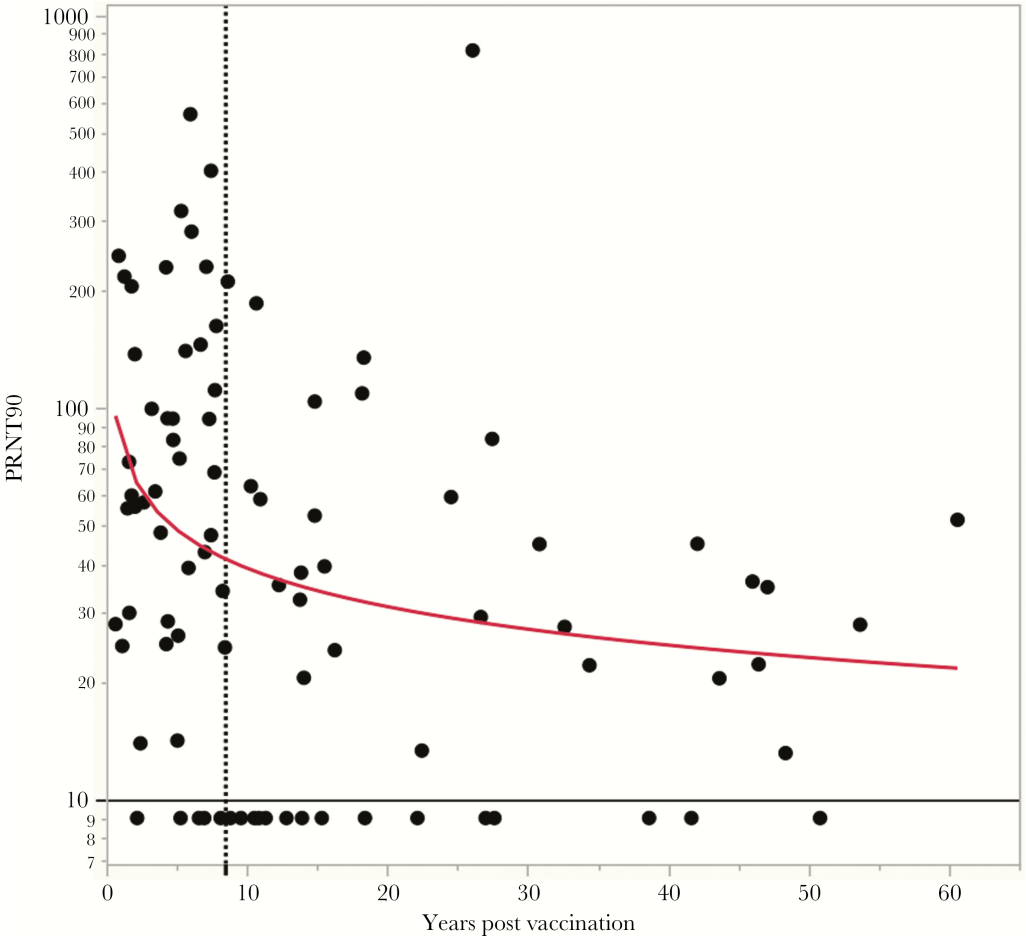

[Figure 1.10]

Figure 1.10 Potency of neutralizing antibodies wane with time since vaccination

Scatterplot showing plaque reduction neutralization test $(PRNT)_{90}$ against years post-vaccination. Each dot represents sera from non-endemic vaccinees following a single dose of 17D. Participants with a $PRNT_{90}$ above the limit of detection of 1:10 are considered seropositive, and participants with $PRNT_{90}$ below the limit of detection are considered seronegative. Reprinted from Kareko *et al.*, 2020[171] with permission from Oxford University Press obtained via Copyright Clearance Center RightsLink®.

Next, Kareko *et al.* next compared their seropositivity results to four other published studies of non-endemic cohorts,[137, 141, 150, 163] and found a summary proportion estimate of 21% of vaccinees who were seronegative ≥10 ypv (Figure 1.11), which is the historical interval for booster doses.

Figure[1.11]

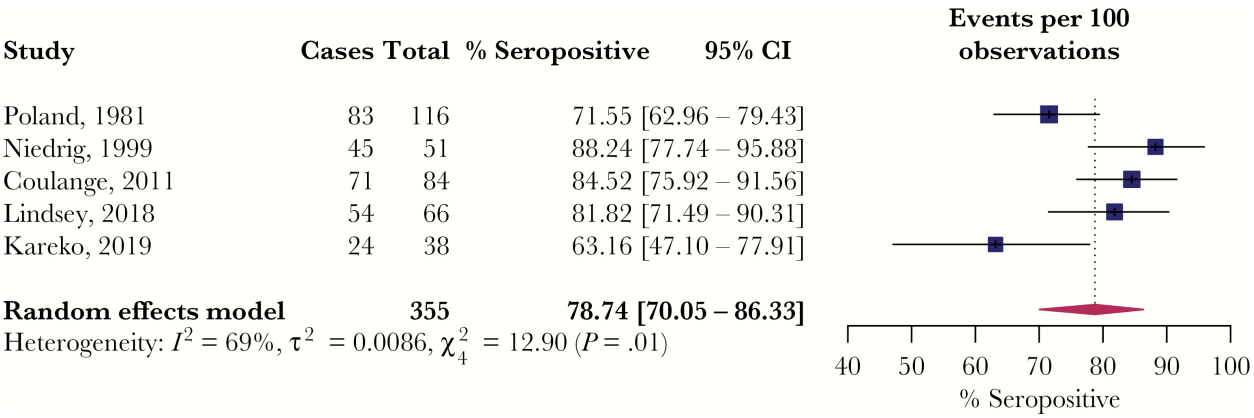

[Figure 1.11]

Figure 1.11 Twenty-one percent of non-endemic vaccinees are seronegative ≥10 years post-vaccination

Reprinted from Kareko *et al.*, 2020[171] with permission from Oxford University Press obtained via Copyright Clearance Center RightsLink®.

More recently, Kling *et al.*, 2022[176] reviewed the durability of NAbs from 36 studies including non-endemic and endemic cohorts, healthy adults, immunocompromised adults, and children, with time intervals post-vaccination ranging 1 month to 31years.[35, 138-140, 142-149, 151-162, 164-173] Following a single dose of 17D, Kling at el. found 29% of healthy adult vaccinees were seronegative >5 years up to 10 years from five studies (four endemic and one non-endemic). Notably, when studied as a standalone population, the duration of NAbs has been reported to be greatly reduced, with 50% of infant vaccinees seronegative by 5-10 ypv when vaccinated before the age of two years,[35] reflecting increased risk of secondary vaccine failure amongst infant populations who receive a single dose of 17D early in life.

The studies on the durability of NAbs following vaccination with 17D discussed here demonstrate that adhering to current recommendations of a single dose of 17D renders approximately one-in-five healthy adult vaccinees seronegative by 10 ypv. Yet, recommendations that a single dose of 17D confers lifelong immunity are maintained by global health entity the WHO, in addition to countries including the United States and the United Kingdom. The review by Kling *et al.*, 2022 led to Germany's STIKO (Standing Committee on Vaccination at the Robert-Koch Institute) to

reintroduce the recommendation for a booster dose of 17D every 10 years, which was met with criticism[177] and sparked debate.[178, 179] The controversy continues.

1.9.7 Potency and breadth of neutralizing antibodies

In addition to titers of NAbs, it is important to understand the characteristics of NAbs in terms of how well they neutralize, so that we can make comparison between individuals or experimental conditions and identify thresholds that define protective immunity.

1.9.7a Potency of NAbs

Potency refers to the capacity of NAbs antibodies to effectively neutralize a virus. Experimentally, potency may be measured using neutralization assays which determine the amount of antibody required to neutralize a proportion of a known amount of input virus within the assay, typically 50%, 80%, or 90%. Neutralization assay readouts may be an absolute concentration per volume, for example the inhibitory concentration that neutralizes 50% of input virus (IC_{50}). Alternatively, neutralization titers may be used, which describe the serum dilution at which 50% of input virus is neutralized (NT_{50}). While inhibitory concentrations based on human monoclonal antibody standards are commonly used in some fields, for example the study of human immunodeficiency virus,[180] NAbs titers (NTs) are the common standard within the YFV and orthoflavivirus field. These units of measurement allow us to compare the potency of NAbs between individuals based on a physiologic starting point – undiluted serum from each individual - and determine various neutralization thresholds, for example the threshold of seropositivity, or a "protective threshold" required for either preventing symptomatic disease or viral replication, known as clinical- and sterilizing- immunity, respectively.

1.9.7b Breadth

Another important and useful concept is the breadth of neutralization, defined as the range of antigenically diverse viruses against which the specified threshold is met. Experimentally, breadth

of a single serum is characterized by determining and comparing NTs against a panel of viruses. The composition and size of the virus panel used to characterize breadth depends upon the research question being asked. Breadth neutralization may be reported the number of viruses within a given panel that are successfully neutralized at a specific serum dilution, or above the limit of detection, for example at a serum dilution of 1:10. Sera that neutralize are large proportion of viruses within the given panel are considered to have increased breadth of neutralization compared to sera that neutralize only one or a few viruses within the same virus panel, which are considered to have a reduced breadth or neutralization in comparison. Breadth of neutralization may result from a single B cell clone with a BCR that recognizes a broad range of antigens. More likely, however, is the expansion of multiple B cells with varying BCRs that individually recognize a narrow range of antigen, but collectively contribute to an expansive polyclonal response that increases in potency and avidity over time. With increased exposure to antigen, the BCR undergoes multiple rounds of somatic hypermutation and affinity maturation, resulting in B cells with high affinity BCRs and plasmablast cell populations that secrete highly potent antibodies. By characterizing breath of NAbs, we can strategically design vaccines to combat a wide range of antigenic variation across different virus strains and make informed predictions about potential vaccine escape mutants as well as the risk of emerging and re-emerging pathogens.

1.9.7c Potency and breadth in the literature

The potency and breadth of neutralizing antibodies within the YFV field has been relatively unexplored. One reason for this is the requirement of a BSL-3 facility to study wild-type YF viruses, which represents a barrier to research. Haslwanter *et al.*, 2022[88] and Goncalves *et al.*, 2024[17] have both demonstrated reduced potency of 17D immune sera against wild-type SA-I strains. However, with seven genotypes of antigenically diverse YFVs distributed throughout Africa and South America, and ongoing conversations around the need for 17D booster doses, this represents a major knowledge gap.

Recently, Shinde *et al.*,2024[181] demonstrated that NHPs with heterologous orthoflavivirus immunity, as determined by the presence of NAbs against DENV and ZIKV following DENV or ZIKV infection, had decreased YFV viremia compared to orthoflavivirus naïve NHP infected with

the same dose of a wild-type SA-I strain. The authors also found that mosquitos that fed on NHPs with prior DENV or ZIKV immunity were refractory to infection compared to mosquitos fed on NHP without prior immunity. These data demonstrate cross-protection amongst NHP primates with heterologous orthoflavivirus infection histories that has not been previously demonstrated. Such cross-protection has not, to our knowledge, been explored in humans.

Chapter 2: Breakthroughs and insights: a comprehensive review of yellow fever vaccine breakthrough infection across 8 decades

Felicity J. Coulter[1] and William B. Messer[1,2,3]

[1]Department of Molecular Microbiology and Immunology, OHSU, Portland, Oregon, USA
[2] Department of Medicine, Division of Infectious Diseases, OHSU, Portland, Oregon, USA,
[3]Program in Epidemiology, OHSU–PSU School of Public Health, Portland, Oregon, USA

Publication info: *Accepted, 3rd October,2024, Vaccine.*
Doi: TBD

Section 2.1: Abstract

The yellow fever vaccine 17D is one of the most successful live-attenuated vaccines ever developed, controlling mosquito-borne yellow fever virus and yellow fever disease worldwide. Introduced in 1937, 17D never underwent rigorous phase III clinical trials to evaluate safety or efficacy, and while protection in the field was quickly established, no prospective evaluation of vaccine efficacy has ever been conducted. One important measure of vaccine efficacy is breakthrough infection resulting from vaccine failure. Yellow fever breakthrough infection was previously formally evaluated in a policy-changing report conducted by the Advisory Committee on Immunization Practices in 2015 but has not been reviewed since despite several recent outbreaks in South America and Africa. To address this knowledge gap, we conducted a literature search and reviewed 19 papers documenting breakthrough yellow fever infection between 1944 and 2023, including thirteen cohort studies, four case reports, and two case series, which we summarize, evaluate the approaches used, and identify strengths and weakness. We identified up to 7,793 and up to 773 breakthrough yellow fever infection amongst suspected- and confirmed

cases, respectively. This review provides an important and much needed update on the topic of yellow fever breakthrough infection, drawing from recent outbreaks, highlighting limitations, and suggesting future approaches to further advance the field.

Section 2.2: Introduction

In 1927, Adrian Stokes isolated and characterized yellow fever virus (YFV) as a "filterable agent" from an infected Ghanaian man named Asibi, establishing YFV as the etiological agent of yellow fever (YF).[107, 182] In 1928, Max Theiler began vaccine development by serial passage of the Asibi virus through embryonic chick and mouse tissues.[84] Following 176 passages, the live-attenuated virus, "17D", was subcutaneously injected into NHPs, where it elicited a neutralizing antibody (NAb) response without causing viscerotropic organ damage or neurotropic encephalitis and protected against a follow-up lethal YFV challenge.[84] Consequently, 17D was considered a good potential vaccine candidate, and in 1937, the first doses were administered to humans during an outbreak in Minas Gerais, Brazil.[68] Since then, approximately one billion doses of 17D have been distributed globally[183], and in 1951, Theiler was awarded the Nobel prize for this work.[119]

In 1959, the International Health Regulations (IHR) implemented a 9-year booster interval that was later amended to 10 years.[184] In 2013, the World Health Organization (WHO) commissioned an extensive literature review[174] on Nab durability which showed seropositivity rates of 75-100% amongst various vaccinee cohorts ≥10 years post vaccination. Based on these findings, WHO changed their policy recommendation from booster doses ever 10 years to a single life-time dose.[33] This prompted the US Advisory Committee on Immunization Practices (ACIP) to conduct Grading of Recommendations, Assessments, Development, and Evaluation (GRADE evaluation) of evidence pertaining to the need for 17D booster doses. In this policy- and practice-changing 2015 publication, ACIP identified critical outcomes, including "lack of vaccine failures" as a measure of vaccine effectiveness, representing the first and, to our knowledge, only consolidation and review of the literature on YF breakthrough infection.[175]

Breakthrough infection may occur because of primary vaccine failure, when an individual fails to seroconvert—produce virus-specific NAbs—following 17D vaccination, or because of secondary vaccine failure, defined as the loss of immunity following seroconversion,[185] or through vaccine-virus mismatch, as has been well documented with influenza A and COVID-19 vaccines, when the vaccine immune response lacks the potency and breadth required to protect against evolving virus variants. For simplicity in this review, we use the terms "breakthrough infection" when referring to infection in a vaccinee[186] ≥10 days following vaccination, and "vaccine failure" to refer the underlying mechanism.

Although ACIP's 2015 GRADE publication[175] transformed vaccination practices, the analyses of data were not peer-reviewed. Following an extensive review of articles retrieved from PubMed and Embase using "yellow fever vaccine" as a keyword, ACIP's GRADE evaluation identified 18 breakthrough cases amongst individuals ≥10 days post vaccination from eight observational studies between 1944 and 2014.[187-194] The GRADE authors note inferior evidence from observational studies due to a higher risk of bias resulting from incomplete capture of cases and lack of a comparison group[195] compared to randomized controlled trials, which were not conducted for 17D prior to widespread use.

ACIP's GRADE evaluation identified inconsistencies in the number of reported breakthrough cases in Brazil across 4 publications,[191-194] ranging from five to 459 cases, depending on the publication which cover varying and overlapping time-periods between 1973 and 2009. The GRADE authors resolved these inconsistencies using data requested from the Brazilian Ministry of Health (MoH), and provided new summary count of seven, but they did not specify how the inconsistencies were resolved or adjudicated against the peer-reviewed research and the raw data from the MoH was not provided.

An additional limitation of the GRADE publication is the use of "lack of evidence of vaccine failure" as a proxy for vaccine effectiveness. Specifically, GRADE documented a handful of breakthrough infections in the context of ">540 million [administered vaccine] doses", which could be misconstrued as a denominator of exposed individuals, and would be an excessive over-estimation of efficacy given that the number of vaccinated individuals truly exposed to YFV

through the bite of an infected mosquito is likely very small compared to the number of administered vaccine doses, and ultimately unknown. Nevertheless, absent prospective vaccine efficacy studies in high-risk settings, administered doses can serve as a surrogate for vaccine coverage in these high-risk settings. Despite limitations, the GRADE finding of "very few" documented breakthrough cases served as evidence for vaccine effectiveness, and ultimately contributed to ACIP's removal of the recommendation for booster doses for most travelers in 2015.[196]

Although IHR removed the booster requirement in 2016,[8] the need for booster doses remains controversial, and recommendations differ between countries. For non-endemic traveler populations, current US and UK guidelines suggest that individuals traveling to high-risk endemic areas consider a booster dose if the last dose was received ≥10 years prior[8] while Germany reinstated the 10-year booster requirement in 2023 based on a systematic review looking at NAbs duration in vaccinees.[176]

Investigators continue to document YF outbreaks in South America and Africa in reports ranging in scale from case- to nationwide-reports, offering additional knowledge and insight into 17D vaccine efficacy in YFV transmission settings such as active outbreaks. Here we comprehensively examine publications that report YF vaccine breakthrough cases, as well as re-examine the literature initially reported in the ACIP GRADE, offering an updated perspective on what is known and what remains to be understood about 17D efficacy in humans.

Section 2.3: Approach

We conducted a PubMed-based literature search using the search term "[yellow fever] AND [*country*]" (Supplementary Table 2.1)[25, 49], limiting to English full text reports. We identified 3,304 reports published by March 28, 2024. We initially rejected papers based on a title or abstract that did not describe human cases of YF. Otherwise, the full texts were searched for keywords "vaccin*"* and *"*immun", to determine if vaccination status was reported, and ultimately read in full.

Section 2.4: Findings

Our search identified potential breakthrough infection occurring between 1944 and 2019, with 7,724 to 7,793 cases amongst suspected/reported cases, and 341 to 773 amongst confirmed cases, where ranges reflect incomplete or ambiguous data. Amongst cohort and case series studies, breakthrough cases constituted 8-34% of suspected cases,[29, 30, 52, 197, 198] and 2-49% of confirmed cases.[30, 41, 52, 53, 74, 191, 193, 197, 199, 200] Studies with incalculable proportion of breakthrough cases were excluded from these ranges.[194, 201] Cases were reported by 18 papers published between 1953 and 2023, including six identified by the GRADE report.[188, 189, 191-194] We identified five additional papers published before 2015,[29, 53, 197, 201, 202] and seven published since.[30, 41, 52, 74, 198-200] One report identified by the GRADE report was not identified by our search.[187] Reports included ten source countries: three South American—Bolivia, Brazil, and French Guiana—and five African—Angola, Cameroon, the Central African Republic, Sudan, and Uganda. Two reports described infection in West Africa. Our findings are summarized in Table 2.1.

Table[2.1]

Reference	Study type	Source locale	Study population	Study period; date(s)	Sample size, (N)	Case definition	Vaccination to symptom onset	Vaccinated, % (n)	Unvaccinated, % (n)	Vaccination status unknown, % (n)	Vaccination verification	<10 days† or <14 days‡ post vaccination interval documented?	Age(s) at breakthrough	Fatality rate of breakthrough cases, % (n/n)
Elliott et al., 1944	Case series	West Africa	Patients at a hospital	*NA; 1944*	3	Suspected	8 months 2 years 1.5 years	*NA*	*NA*	*NA*	*NR*	No	32 years 35 years 25 years	66.7% (2/3)
Ross et al., 1953	Case report	Uganda	*NA*	*NA; 1952*	1	Suspected	4 years	*NA*	*NA*	*NA*	*NR*	No	39 years	100% (1/1)
De Cock et al., 1988	Cohort	Oju, Nigeria	Patients of treatment centers and a hospital	6 months; *Jul - Dec, 1986*	87	Suspected; *without jaundice*	*NR*	0 or 79.3% (0 or 69)*	20.7% (18)*	0 or 79% (0 or 69)*	*NR*	No	*NR*	*NR*
Nolla-Sallas et al., 1989	Case report	Niger, Mali, Burkina-Faso, or Mauritania	*NA*	*NA; 1988*	1	Confirmed; *IgM+ and CF+*	5 years	*NA*	*NA*	*NA*	Vaccine certificate	Yes†	37 years	0% (0/1)
Heraud et al., 1999	Case report	French Guiana	*NA*	*NA; 1998*	1	Confirmed; *RT-PCR from liver*	1 year and 13 years	*NA*	*NA*	*NA*	*NR*	Yes†	*NR*	100% (1/1)

Van der Stuyft et al., 1999	Cohort	Santa Cruz, Bolivia	Patients of hospitals and health centers	7 months; *Dec, 1997 - Jun, 1998*	6	Confirmed; *IgM+*	*NR 6m - 1y*	33.3% (2)	66.7% (4)	0	Combination of medical records and interviews with physician and family members	No Yes†	4 years 58 years	100% (2/2)
de Filippis et al., 2004	Case report	Minas Gerais, Brazil	*NA*	*NA; 2001*	1	Confirmed; *Viral isolation from liver and PCR sequencing*	*14 days*	*NA*	*NA*	*NA*	*NR*	Yes†	69 years	100% (1/1)
Tuboi et al., 2006	Cohort	Brazil	Nationally reported cases	5 years; *1988 - 2002*	251	Confirmed; *IgM+, viral isolation, liver pathology, YF Ag+ (IHC), or 4-fold increase in NAbs*	*8 months 5 years 1.5 years 1 year 5 months*	2.0% (5)	78.5% (197)	19.5% (49)	"Written evidence"	Yes†	21 years 20 years 17 years 62 years 30 years	40% (2/5)
Câmara et al, 2013	Cohort	Brazil	Nationally reported cases	35 years; 1973-2008	831	Confirmed; *IgM+, viral isolation, liver pathology, YF Ag+ (IHC), or 4-fold increase in NAbs*	*Unclear*	3.2% or 55.2% (27 or 459)	0% or 52.0% (0 or 432)	44.8% (372)	Data obtained from MoH	No	*NR*	*NR*
Saraiva et al., 2013	Cohort	Amazonas, Brazil	Nationally reported cases	13 years; *1996 - 2009*	42	Confirmed; *IgM+ or histopathology*	*NR*	14.3% (6)	64.3% (27)	21.4% (9)	Participant-reported, one participant provided vaccination certificate	No	*NR*	83.3% (5/6)
					12	*Survived*		*8.3 % (1)*	*83.3% (10)*	*8.3% (1)*				

				30	*Died*		*16.7% (5)*	*56.7% (17)*	*26.7% (8)*				
Rachas et al., 2014	Cohort	The Central African Republic	Nationally reported cases	5.6 years; *Jan 2007 - Jul 2012*	55	Confirmed; *IgM+ and PRNT+*	*>10 ypv*	49.1% (27)	50.9% (28)	0%	Participant reported	No	*NR*	*NR*
							≤ 10 ypv	*11.1% (3)*						
					3,220	Suspected; *fever and jaundice*	*>10 ypv*	*40.7% (11)*						
							≤ 10 ypv	28.5% (919)	71.5% (2,301)	0%				
								17.4% (160)						
								76.7% (705)						
Alhakimi et al., 2015	Cohort	Darfur, Sudan	Nationally reported cases	3.6 months; Sep 1 – Dec 20, 2012	844	Reported		7.9% (67)	77.0% (650)	15.0% (127)	*NR*	No	*NR*	*NR*
					48	Confirmed; *IgM+ or RT-PCR+*	*NR*							
					655	*Epi linked*								
					37	*YFV+HEV*								
					13	*HEV*								
Boyd et al., 2017	Cohort	Angola	Nationally reported cases	4.4 months; *Jan 1 – May 11, 2016*	2,907	Suspected; *fever and jaundice*	*NR*	15.7% (459)	*NR*	*NR*	"Documented"	Yes†‡	Median (SD) 20 (12)	*NR*
					NR	Confirmed; *RT-PCR+*	*See main text*	*NR* (32)	*NR*	*NR*				40.6% (13/32)
Song et al., 2018	Case series	Angola	Chinese workers returning from Angola	*NA; Mar - Apr, 2016*	11	Confirmed; *RT-PCR+*	10 months 5 years	18.2% (2)	81.8% (9)	0%	*NR*	Yes‡	*NR*	0% (0/2)

Ho et al., 2019	Cohort	São Paulo, Brazil	Hospitalized patients within a single ICU	2 months; *Jan 10 - Mar 11, 2018*	79	Confirmed; *RT-PCR+*	~20 years 3-5 months < 1month	3.8% (3)	96.2% (76)	0%	Vaccination records and participant-reported	Yes†	*NR*	*NR*
de Rezende et al., 2022	Cohort	Belo Horizonte, Brazil	Hospitalized patients within a single hospital	2 years; *2017 - 2018*	60	Confirmed; *RT-PCR+ or IgM+*	>20 days	3.3% (2)	96.7% (58)	0%	*NR*	Yes†	*NR*	*NR*
Ferreira et al., 2022	Cohort	Minas Gerais, Brazil	Nationally reported cases	3 years; *2016-2018*	3,304	Reported	*NR*	33.6% (1,109)	45.1% (1,491)	21.3% (704)	*NR*	No	*NR*	*NR*
					905	Confirmed; *"laboratory criteria or clinical epidemiological criteria"*		12.4% (112)	64.1% (580)	23.5% (213)			*NR*	1.7% (15/905)
Nemg et al., 2022	Cohort	Cameroon	Nationally reported cases	10 years; *2010 - 2020*	20,261	Suspected; *fever and jaundice*	*"Days to years"*	25.5% (5,167)	74.5% (15,094)	0%	*NR*	No	*NR*	*NR*
					360	Confirmed; *IgM+ or PRNT50+*		33.1% (119)	66.9% (241)	0%				
Giugni et al., 2023	Cohort	São Paulo, Brazil	Single morgue	2 years; *2017 – 2019*	68	Confirmed; *IgM+, RT-PCR+ or IHC*	*NR*	2.9% (2)	13.2% (9)	83.8% (57)	Medical records	Yes†	*NR*	*NA*

[Figure 2.1]

Table 2.1 Peer-reviewed published articles reporting yellow fever breakthrough infection between 1944 and 2023

NA: not applicable; NR: not reported by the authors; IHC: immunohistochemistry; *n calculated from percentages; **denominator missing, cannot calculate percentages.

2.4.1 Africa

Elliott 1944[187] reports a series of suspected YF in three European military personnel treated at a West African military hospital in 1942, with symptom onset between 8 months- and 2 years- post vaccination (ypv), and 66.7% (2/3) fatality. Ross *et al*., 1953[188] similarly reports a suspected fatal case of YF in a European worker in Uganda in 1952, with symptom onset four ypv. Elliott references "occasional failure to develop immunity" following vaccination, and Ross *et al.* suggest manufacturer-specific differences in vaccine efficacy. However, these earliest accounts of potential breakthrough infection are limited by the authors' lack of confirmation of YF disease. During these early years, uncontrolled passage of the 17D vaccine resulted simultaneous use of multiple substrains which had post-vaccination complications that ranged from life-threatening adverse events to reduced immunogenicity.[121] It is plausible, therefore, that the cases reported by Elliott 1944 occurred following vaccination with a batch with reduced immunogenicity which failed to elicit a protective response, as these cases predate introduction of the seed lot system in 1945 which aimed to reduced such undesirable outcome.

De Cock *et al.* 1988,[201] report an outbreak in eastern Nigeria in 1986, representing the first documentation of possible breakthrough infection amongst indigenous individuals. Among 87 acute phase samples collected from suspected cases at treatment centers or a hospital in Oju, ≤7 days following symptom onset, 21% were reported as unvaccinated, implying that the remaining 79% were either vaccinated or of unknown vaccination status. However, the authors did not make this specific claim and our interpretation is therefore limited to speculation. Moreover, the authors describe the 17D vaccine as "probably effective for life", a contextual reflection of the central dogma that simultaneously and atypically acknowledges that immunity may not be "lifelong".

In 1989 Nolla-Sallas *et al.*[189] provide a case report of a 37-year-old Spanish woman with a "valid international vaccination certificate" with symptom onset five ypv following travel through Niger, Mali, Burkina Faso, and Mauritania. YF was confirmed by IgM-ELISA and CF, and after hospitalization in Mauritania and transfer to an intensive care unit (ICU) in Barcelona, she fully recovered. Nolla-Sallas *et al*. note that vaccine failure due to an immunological defect is unlikely in this otherwise healthy patient, instead referencing several 17D vaccines that failed to meet WHO

quality control,[203] suggesting that vaccine failure may have resulted from vaccine instability. A strength of this paper is that the authors warn against discounting the possibility of breakthrough infection, stating that "YF should not be ruled out by history of YF vaccination".

Twenty-five years later in 2014 Rachas *et al.*[197] investigated nationally reported cases in the Central African Republic between January 2007 and July 2012, aiming to assess effectiveness of the national YF surveillance system. The authors identified 28.5% (919/3,220) breakthrough infections amongst suspected cases, and 49.1% (27/55) amongst cases confirmed by IgM-ELISA and plaque reduction neutralization test (PRNT), with known vaccination status for all cases. A strength of this paper is the documentation of interval post-vaccination. Amongst suspected cases, 76.7% (705/919) were ≤10 ypv, and 17.4% (160/919) were >10 ypv. For confirmed infections, 40.7% were ≤10 ypv (11/27), and 11.1% were >10 ypv (3/27). The larger proportion of breakthrough infections ≤10 ypv compared to >10 ypv is surprising, given the literature showing reduced proportion of seropositive vaccinees by 10 ypv.[141, 159, 171] However, these data are difficult to interpret given the large quantity of individuals with unknown vaccination dates, and the lack of additional demographic characteristics of the breakthrough cases.

The following year, 2015, Alhakimi *et al.*,[29] examined national surveillance data from Darfur, Sudan, reporting 7.9% (67/844) breakthrough infections amongst reported cases, between September 1 and December 20, 2012. The authors report a scarcity of laboratory reagents amidst political instability, resulting in only 15.9% (134/844) of reported cases being tested, with 35.8% (48/134) positive for IgM-ELISA and/or PCR. In lieu of diagnostic testing, 77.6% of cases (655/844) were confirmed by epidemiological link. These numbers likely include false reports of YF cases due to a concurrent outbreak of Hepatitis E, which also presents with jaundice; the authors note that 27.6% (37/134) of samples were Hepatitis E virus (HEV) positive, and 9.7% (13/134) of samples were positive for both YFV and HEV. A weakness of this paper is the lack of data regarding vaccination status amongst confirmed cases, and timing between vaccination and symptom onset. Furthermore, the case definition of a "reported" case was not provided. In the context of a resource-limited setting with reduced capacity to conduct thorough diagnostic testing, this represents a loss of valuable data.

In 2017, publication Boyd *et al.*[198] aim to identifying vaccine failure and serious adverse events following a mass vaccination campaign launched in Angola in 2016 that administered >11.6 million doses between January and June 2016. Using nationally reported cases between January 1 and May 11, 2016, 16% (459/2,907) of suspected cases occurred in vaccinated individuals. The authors report breakthrough infection in 18 individuals with a *positive RT-PCR* ≥14 days after vaccination, and in 15 individuals with *symptom onset* ≥10 days after vaccination, amongst RT-PCR-confirmed cases, however, the total number of RT-PCR confirmed cases is not given, and it is not possible to calculate breakthrough infections as a proportion of all confirmed infections. A strength of this study is the primary goal of identifying breakthrough infection and the documentation of days between vaccination and symptom onset that allows the important distinction between vaccine failure, and cases where insufficient time has passed for an immune response to develop following vaccination. Because of the overlap of the study period with the vaccination campaign, many of the study population are likely 0-4-months post vaccination, presenting a unique opportunity to identify potential breakthrough cases due to primary vaccine failure. However, time since vaccination is not given beyond 14 days following vaccination, rendering a more nuanced assessment of the likely timing of vaccine failure impossible.

Song *et al*., 2018,[41] report RT-PCR-confirmed YF amongst Chinese workers returning from Angola in March and April of 2016. Combined with a previously reported case from the same group of workers,[39] 18.2% (2/11) breakthrough infection constituted 18.2% (2/11) of total imported cases, occurring 10 months- and five years- post vaccination and both with non-fatal outcomes.[39-41] With a total fatality rate of 18.2% (2/11), the number of deaths is too small to assess true mortality benefit of 17D, but the survival of the two breakthrough cases weakly suggests mortality is lower in breakthrough infections. This paper uniquely provides data on breakthrough infection in travelers, highlighting the importance of this topic for endemic and non-endemic traveler populations alike.

Most recently, Nemg *et al*., 2022[30] aimed to identify high-risk districts in Cameroon by characterizing YF cases between 2010 and 2020, documenting 25.5% (5,167/20,261) breakthrough cases amongst suspected cases, and 33.1% (119/360) amongst confirmed cases. Like Alhakimi *et al.*, the authors note a scarcity of reagents, relying on IgM-ELISA to confirm most

cases (339/360), and PRNT for some (21/360). Two-thousand-and-twenty samples collected ≤10 days after symptom onset were RT-PCR-negative. As with other reports, time since vaccination in breakthrough cases was not documented but is simply reported as "days to years", making it impossible to assess the proportion breakthrough infections erroneously attributed to vaccinees infected <10 days after vaccination.

2.4.2 South America

The earliest reports of breakthrough infections in South America in our search were published in 1999. Heraud *et al*.[202] is a fatal case report of a female of unknown age with symptom onset in 1998, one- and 13- years following vaccination, confirmed by RT-PCR from a post-mortem liver sample. Uniquely, the authors had access to a blood sample taken in 1994 which tested negative for YFV NAbs, indicating vaccine failure following primary vaccination. This paper importantly documents the first reported in French Guiana in 97 years, which initiated an immunization campaign.

Van der Stuyft *et al*. 1999[53] conducted six months of active YF surveillance amongst hospitals and clinics during an outbreak in Santa Cruz, Bolivia between 1997 and 1998. Amongst suspected cases, 33.3% (2/6) are fatal breakthrough infections, with 83.3% (5/6) total fatalities. Time intervals between vaccination and symptom onset were 6-12 months and unknown. The researchers also conducted a household serosurvey finding 5.7% (16/281) IgM-ELISA-positive participants, indicating possible asymptomatic YF. The authors reported 75% (12/16) vaccinees: 10 were two-months post vaccination, one was one ypv, and another was four ypv. However, the finding that vaccine-elicited IgM is detectable up to 4 ypv,[204] confounds these results.

In 2004, de Filippis *et al.*[192] investigate fatalities temporally associated with 17D vaccination, reporting breakthrough infection in a 69-year-old Brazilian man with symptom onset 14 days following vaccination, confirmed by sequencing of post-mortem viral isolates from the liver. The authors note the possibility that this individual had been naturally infected before mounting a protective response, especially given his "regular use of corticoids for allergies". This report was

one of the four reports for which the ACIP GRADE authors sought clarification from the Brazilian MoH.[175]

In 2006, Tuboi *et al*.[191] use Brazilian national YF surveillance data between 1998 and 2002 to assess risk factors for death among hospitalized YF patients. The authors document 2% (5/251) breakthrough infections amongst cases confirmed by either IgM-ELISA, viral isolation, liver pathology, immunohistochemistry, or neutralization assay. The cases were three females and two males, aged 17-62 years vaccinated 0.5-5 years before symptom onset, with a 40% (2/5) fatality rate amongst total breakthrough cases. Of note, one of two case definitions used in this report for suspected YF was "a person with an acute febrile disease not previously vaccinated against YF who had been in an endemic or epidemic area" meaning that vaccinees and therefore possible breakthrough cases were systematically excluded. Clarification for this report was also sought from the Brazilian MoH by the GRADE authors.

In 2013, two additional reports utilizing Brazilian national surveillance YF data were published. Câmara et al.[194] report either 3.2% (27/831) or 55.2% (459/831) breakthrough infections; where 432 individuals are reported as either "non-vaccinated" in the report's Table 1, and vaccinated >10 years prior in the main text. The discussion section of the manuscript implies that the 432 had been vaccinated but were "overdue" for a booster and therefore not up to date on their vaccination and considered unvaccinated. This distinction is paramount, and the inconsistency was one clarified in the GRADE evaluation, yet remains unresolvable using publicly available data including data made available by the Pan American Health Organization.[49]

The second report, by Saraiva *et al*.[193] documents 14.3% (6/42) breakthrough cases from 1996-2009 in the state of Amazonas, Brazil, with 71% (30/42) overall fatalities, and 66.7% (22/33) fatalities amongst individuals with known vaccination status. Whilst the authors provide number of deaths among vaccinated (5/6, 83.3%) and unvaccinated (17/22, 77.3%), the large proportion of individuals with unknown vaccination status (9/42; 21.4%) make these numbers difficult to interpret. As in Nolla-Sallas *et al.*[189] the authors suggest improper vaccine storage as a potential cause of high mortality amongst vaccinees. Additionally, they emphasize the need to ensure vaccines are given every 10 years, although their data do not address interval between vaccination

and symptom onset. The ACIP GRADE authors also sought clarification for these data via the Brazilian MoH.

Four papers report cases during a significant outbreak in Brazil between 2016 and 2019.[52] Ho *et al*., 2019[199] characterized RT-PCR-confirmed cases of severe YF amongst patients admitted to an intensive care unit (ICU) in São Paulo, Brazil between January 10, and March 11, 2018. The authors report 3.8% (3/79) breakthrough infections with time since vaccination <1 month-, 3-5 months-, and ~20 years- post vaccination. The relatively high fatality rate of 67% (53/79) is comparable with rates reported for severe YF in the literature. Unfortunately, the authors do not report deaths amongst vaccinees and we are unable to determine the protective efficacy of vaccination against death. The low number of vaccinated cases in this cohort could be interpreted as supportive, overall, for vaccine effectiveness in preventing severe disease while simultaneously demonstrating that protection is not absolute.

de Rezende et al., 2022,[200] investigated detection of YFV RNA by RT-PCR in urine samples from YF cases admitted to a hospital in Belo Horizonte, between 2017 and 2018. Amongst cases confirmed by either RT-PCR or IgM-ELISA, 3.3% (2/60) were breakthrough infections, with symptom onset >20 days- and 16 years- post vaccination. Described as "mild to severe", this hospitalized cohort likely represent increased overall YF severity, compared to national data. Consistent with our speculation for Ho *et al*,[199] the low proportion of hospitalized vaccinated cases supports potential protective efficacy of vaccination against severe disease.

The third report from Brazil examined nationally reported cases from 2016 to 2018. Ferreira *et al*., 2022[52] report 33.6% (1,109/3,304) breakthrough infections amongst suspected cases with 21.3% (704/3,304) of unknown vaccination status, and 12.4% (112/905) breakthrough infections amongst confirmed cases with 23.5% (213/905) unknown vaccination status. A weakness of this paper is a lack of detailed case definitions, how vaccination status was verified, and timing between vaccination and symptom onset, specifically what proportion of vaccines may have been vaccinated <10 days prior.

Finally, Giugni *et al.,* 2023,[74] characterized YF-associated myocardial injury, reporting 2.9% (2/57) breakthrough infections amongst YF fatalities in morgue in São Paulo, Brazil confirmed by RT-PCR, IgM-ELISA, or immunohistochemistry between 2017 and 2019. This unique cohort has a low rate of breakthrough infection, which again, may suggest good vaccine efficacy against severe YF. Like other papers, the authors only report vaccination as having occurred >10 days before symptom onset, which allowed the identification of true breakthrough cases, but prevents further interpretation regarding the timing of vaccine failure.

Section 2.5: Discussion

We reviewed 19 papers consisting of 13 cohort studies,[29, 30, 52, 53, 74, 191, 193, 194, 197-201] four case reports,[188, 189, 202, 205] and two case series[41, 187] reporting possible YF breakthrough infection. All studies were observational. Of the cohort studies, eight study populations were formed using national surveillance data, with six reporting cases across an entire nation[29, 30, 191, 194, 197, 198] and two within single states.[52, 193] Three studies documented YF cases receiving medical treatment at a single hospital,[53, 187, 200] two collected data from multiple hospitals and treatment centers,[53, 201] another studied ICU patients within a single hospital,[199] and one investigated YF fatalities within a single morgue.[74] Breakthrough infection was documented in individuals living in endemic areas by all cohort studies[29, 30, 52, 53, 74, 191, 193, 194, 197-201] and by two case reports,[189, 192] and in non-endemic travelers, workers, and military personnel via a case report and two case series.[41, 187, 188] These studies represent a range of disease severity, including a broad range of symptoms captured by national surveillance data,[29, 30, 52, 191, 193, 194, 197, 198] and more severe YF warranting treatment center- and hospital-level care,[53, 187, 188, 200, 201] ICU-level care,[199] or resulting in death.[74]

As noted above, observational studies have multiple limitations and sources of bias.

2.5.1 Asymptomatic infections

Asymptomatic cases represent 55% of total YFV infections,[7] yet we identified only one study that potentially identified breakthrough infection amongst asymptomatic individuals via a

serosurvey.[53] Furthermore, no studies performed population-level analyses of vaccination status in the context of disease severity, which would help inform vaccine efficacy against asymptomatic, mild, and severe disease. Whilst asymptomatic individuals are indeed harder to study, it is possible, even likely, that asymptomatic infections account for a measurable proportion of breakthrough infections, with symptoms diminished or masked because of partial protective immunity still conferred by the vaccine.

2.5.2 Case definitions

Other potential sources of bias include the use of suspected versus confirmed cases, where suspected cases will likely capture most true cases of YF, this definition does not exclude other diseases that cause similar symptoms. In contrast, laboratory confirmed cases are more likely to include a higher proportion of true positive YF cases. However, because laboratory testing can rely on the accessibility of samples and test reagents during a narrow testing window, confirmed case definitions are likely to exclude some true positive cases of YF, resulting in an underestimation of total and breakthrough cases.

2.5.3 Clinical definitions

Reports defined suspected and reported cases using clinical symptoms, typically centered around symptoms of febrile illness, with jaundice as a qualifying symptom in three papers,[30, 197, 198] and not a qualifying symptom in two papers.[29, 201] Whilst characteristic of YF, not all YF patients experience jaundice, as demonstrated Ho *et al.*[199] who report jaundice in only 19% (15/79) ICU patients, and inclusion of jaundice in the case definition within this study would have resulted in an underestimation. Conversely, patients may present with jaundice due to an unrelated illness, such as Hepatitis E, as demonstrated by Alhakimi *et al.*,[29] and using jaundice as a qualifying symptom likely resulted in an overestimation of cases. Defining cases as suspected is a useful tool, especially in resource-limited settings, however, these examples emphasize the need to examine case definition limitations within the context of the specific study population, highlighting the value of confirming cases with laboratory testing.

2.5.4 Laboratory confirmation

The first two published reports, by Elliott[187] and Ross *et al.*[188] failed to confirm YF disease using laboratory methods. Given that other hemorrhagic diseases that mimic YF are incident in Africa, misdiagnosis is a moderately strong possibility for these cases. This potential bias extends to other studies that report suspected, rather than confirmed cases. Cases were otherwise confirmed by virus isolation, serology (IgM-ELISA or PRNT), molecular methods (RT-PCR or sequencing), and pathological techniques like immunohistochemistry. Serological techniques indirectly detect changes in the immune response that are specific to and indicate YFV infection. The use of IgM-ELISA to confirm YF is a standard diagnostic method that detects anti-YFV IgM produced early following infection before Ig-class switching events, and in the absence of a differential diagnosis, a positive IgM-ELISA is typically interpreted as recent YFV infection.[21] However, Gibney *et al*., 2012 detected IgM by ELISA in 75.2% (29/40) of vaccinees 3-4 ypv,[204] and a positive IgM-ELISA may reflect recent vaccination rather wild-type YFV infection. Similarly, the PRNT does not discriminate between NAbs induce by vaccination versus natural infection. Consequently, studies confirming cases by IgM-ELISA[29, 30, 53, 74, 191, 193, 194, 197, 200] and PRNT[30, 197] may represent an overestimation of breakthrough infection, particularly during outbreaks where vaccination is initiated for outbreak containment and control.

While confirmation by RT-PCR is not susceptible to the confounding issues of serology, there are other limitations. First, viremia is detectable up to 10 days following symptom onset[21] which may result in false negatives in samples collected after viremia subsides, potentially underestimating both total and breakthrough cases in the six studies that confirmed cases with RT-PCR.[29, 41, 74, 198-200] Additionally, positive results may be confounded by detection of vaccine-induced viremia in individuals vaccinated <10 days before testing, a time frame too short for the vaccine to have elicited a protective immune response. Data to resolve this important interval was provided by 12 papers,[41, 53, 74, 187-189, 191, 192, 198-200, 202] but was missing from seven.[29, 30, 52, 193, 194, 197, 201]
Finally, we note the need to perform virus isolation followed by sequencing to distinguish wild-type infection from vaccine viremia in cases where symptoms occur shortly following vaccination,[192] which is common when vaccination campaigns are launched in response to ongoing outbreaks. Notably, such cases occurring before a sufficient antibody response has mounted should

be discounted as breakthrough infection. Distinguishing between vaccine viremia and wild-type infection is especially important in the context of the serious adverse events, YF vaccine associated neurotropic and viscerotropic disease (YEL-AND and YEL-AVD), which have overlapping symptoms with natural infection,[206] and failure to distinguish such cases may result in over estimation of breakthrough cases.

2.5.5 Vaccination status

Methods used to capture vaccine status varied widely. Some studies used vaccination records, medical records, or "written evidence", in all[74, 189, 191] or 66.7% (2/3)[199] of study participants. Other studies used a combination of medical records, surveillance forms, and interviews;[53, 198] whilst others relied on self-reporting.[30, 197] Many studies did not state how vaccination status was determined.[29, 41, 52, 192, 194, 200-202] Requiring documentation, especially in settings where hard-copy records are not reliably kept or access to records is either limited or impossible will result in underestimations of cases but maintains rigor in assessing breakthrough. On the other hand, self-reporting is susceptible to recall bias, which could lead to either over- or under-estimation of cases. For example, Teichmann *et al*. report hemorrhagic disease in a German traveler from Côte d'Ivoire who "confirmed several times that he had received yellow-fever vaccination 6 years previously", which was not corroborated by his vaccination certificate and explained by the authors as a confusion by the patient between the German terms used for hepatitis, "gelbsucht", and YF, "gelbfieber".[207] Even robust vaccination databases do not guaranteed that all individuals will be captured, and the limitations of self-reporting and verification must be contextually considered.

2.5.6 Primary and secondary vaccine failure

Breakthrough infection may occur because of primary or secondary vaccine failure. Primary YF vaccine failure may be caused by failures in manufacturing, storage, cold chain, resuspension, and administration, resulting in the vaccine failing to elicit a sustained immune response. Whilst this may have been responsible for some cases of breakthrough infection and was considered by the authors of several studies discussed above,[188, 189, 191-193] validation of these failures is lacking. Additionally, fractional dosing of 17D of one-fifth of a standard dose elicits high initial

seroconversion rates of 97-100% by 30-45 days post vaccination in healthy adults,[155, 208, 209] comparable with seroconversion rates elicited by standard dosing,[176, 210] suggesting that the vaccine may withstand ≤5-fold reduction in viability with little impact on short-term vaccine efficacy. Whilst adults who do not seroconvert following vaccination certainly represent individuals at risk for breakthrough infection due to primary vaccine failure, such individuals likely represent a small portion of total breakthrough infections. Meanwhile, reduced initial vaccine efficacy has been observed in children and immunocompromised individuals at 30-45 days post vaccination, with initial seroconversion rates of 85%-95%[165, 210] and 78%-100%,[158, 172] respectively, and these groups may be at higher risk of breakthrough infection due to primary vaccine failure.

Cross-sectional studies have found that around 20% of adult vaccinees are "seronegative" by 10 ypv,[141, 159, 171] depending on the definition of serostatus, potentially contributing a substantial proportion of breakthrough infections due to secondary vaccine failure. Similarly, seronegativity rates are approximately 50% by 5-10 ypv in infants vaccinated before the age of two years.[35, 167, 170, 211] Given that many countries, particularly in Africa where 90% of cases occur, routinely vaccinate children against YF at 9-12 months of age under the Expanded Program of Immunization[33, 35] infant vaccinees may have an increased risk of vaccine breakthrough due to secondary vaccine failure.

The breakthrough infections reviewed here cannot be distinguished between primary and secondary vaccine failure, which would require pre-infection serology. Whilst such serology may not be a reasonable public health measure, prospective cohort studies in endemic and high-risk areas to determine YFV serology of vaccinated cohorts on a seasonal basis would identify breakthrough cases, allowing identification of breakthrough infection amongst both symptomatic and asymptomatic cases, as well as indication of both primary and secondary vaccine failures.

2.5.7 Review limitations

There are limitations to our review. First, our literature search was performed manually, was limited to PubMed and articles published in English. Additionally, while PAHO maintains

publicly available databases of YF cases, including vaccinated cases[212] we elected to limit our review to peer-reviewed reports. In this report, we make no effort to determine breakthrough rates in the systematic manner of a meta-analysis. In fact, we suspect the quality of data available on breakthrough cases overall to be too low to support a formal meta-analysis. Instead, our goal was to consolidate and summarize the current literature on YF breakthrough infection to bring a much-needed perspective on the quantity and quality of reports on 17D breakthrough cases. In so doing, we have highlighted important limitations in the field, including the inherent limitations of case reports, case series, and observational studies in establishing vaccine efficacy. We note substantial inconsistencies in case definitions and documentation of vaccination status, all of which represent large barriers to accurately identifying breakthrough cases and comparing rates of breakthrough infection across populations. Closing this knowledge gap will call for prospective studies, quality documentation of vaccination status, and setting aside incompletely substantiated claims regarding "lifelong" immunity. Indeed, much of what is assumed to be "known" about 17D efficacy, for example the durability of NAb following a single dose, is incompletely understood at best, and such assumptions become barriers to rigorous scientific evaluation of breakthrough infection. An archetypical example of this was the exclusion of vaccinated patients from the case definition of YF in a study that aimed to improve case detection timeliness during an outbreak in the Democratic Republic of Congo in 2018.[38] This assumption-based exclusion almost certainly leads to under-reporting of breakthrough infections, and at worst, inappropriate care for such individuals. Finally, data on breakthrough infection provides insight into the longevity of protective 17D-elicited immunity, which adds crucially to the controversial topic on the requirement to boost. 17D is an old and highly successful vaccine, but one not without limitations. Ultimately, risk assessment of infection, disease outcomes, and adverse events need to be continuously studied and balanced against available resources for individuals and populations across the age and risk spectrum for YF, to inform country- and population-specific decisions regarding the need for a booster requirement.

Section 2.6: Supplementary materials

Table[2.S1]

Continent	Country	Source
Africa	Angola	Garske et al., 2014
	Benin	Garske et al., 2014
	Burkina Faso	Garske et al., 2014
	Burundi	Garske et al., 2014
	Cameroon	Garske et al., 2014
	Central African Republic	Garske et al., 2014
	Chad	Garske et al., 2014
	Cote d'Ivoire	Garske et al., 2014
	Democratic Republic of the Congo	Garske et al., 2014
	Equatorial Guinea	Garske et al., 2014
	Ethiopia	Garske et al., 2014; Nwaiwu et al., 2021
	Eritrea	Garske et al., 2014
	Gabon	Garske et al., 2014
	Guinea	Garske et al., 2014
	Guinea-Bissau	Garske et al., 2014
	Kenya	Garske et al., 2014
	Liberia	Garske et al., 2014
	Mali	Garske et al., 2014
	Mauritania	Garske et al., 2014
	Niger	Garske et al., 2014
	Nigeria	Garske et al., 2014

	Republic of the Congo	Garske et al., 2014
	Rwanda	Garske et al., 2014
	Senegal	Garske et al., 2014
	Sierra Leone	Garske et al., 2014
	Somalia	Garske et al., 2014
	South Sudan	Garske et al., 2014
	Sudan	Garske et al., 2014
	Tanzania	Garske et al., 2014
	The Gambia	Garske et al., 2014
	Togo	Garske et al., 2014
	Uganda	Garske et al., 2014
South American	Argentina	PAHO, 2023
	Bolivia	PAHO, 2023
	Brazil	PAHO, 2023
	Colombia	PAHO, 2023
	Ecuador	PAHO, 2023
	French Guiana	PAHO, 2023
	Guyana	PAHO, 2023
	Panama	PAHO, 2023
	Paraguay	PAHO, 2023
	Peru	PAHO, 2023
	Suriname	PAHO, 2023
	Trinidad and Tobago	PAHO, 2023
	Venezuela	PAHO, 2023

[Figure 2.S1]

Figure 2.S1 Summary of continent and country of yellow fever cases and source.

Countries were used to search PubMed using the search term “[yellow fever] AND [country]”.

Chapter 3: Optimization of the micro-immunofocus assay for use with wild-type yellow fever viruses

Author list
Felicity J. Coulter, Courtney A. Micheletti, Benjamin J. Burwitz, and William B. Messer

Publication info: *In preparation*
Doi: TBD

Section 3.1: Abstract

Yellow fever virus (YFV), the etiological agent of yellow fever remains a pathogen of public health concern, with recent outbreaks in both Africa and South America. Almost all studies of YFV rely upon the plaque assay, which remains the gold standard assay for identification and quantification of infectious YFV. However, the plaque assay is both time- and resource intensive, posing barriers to surveillance and research. While the micro-immunofocus assay has been developed and used extensively by the dengue- and Zika virus fields, it has not yet been standardized and widely adopted for wild-type YFV strains. We have adapted and optimized a micro-immunofocus assay for successful characterization of wild-type YFV strains belonging to all known genotypes. Here we provide a detailed protocol for a 96-well format wild-type YFV immunofocus assay using the pan-orthoflavivirus monoclonal antibody 4G2. Compared to the plaque assay, our protocol delivers equivalent virus quantification for all wild-type viruses tested using fewer reagents and laboratory consumables. Additionally, our assay produces results within five days, compared to the plaque assay which can take up to seven days. Overall, the micro-immunofocus assay described here advances the field by offering increased throughput, reduced cost, and rapid results compared to the current gold-standard. These advantages offer increased accessibility of an assay with applications in research, diagnostics, and surveillance of emerging YFV strains.

Section 3.2: Introduction

In 1927, yellow fever virus (YFV) became the first human pathogenic virus to ever be isolated,[107] and it is the prototypic virus of the genus orthoflavivirus which was named using the Latin root word "flavus" meaning yellow, after the yellowing jaundice it causes in yellow fever (YF) disease.

After isolation of the Asibi strain in 1927, the virus was initially maintained by serial inoculation in NHPs. Between NHPs, the presence of the virus was confirmed with observation of YF symptoms in the inoculated animal, which were often fatal.[114] Before the establishment of viral propagation in cell culture system, crude viral quantification involved inoculating groups of mice to determine a "mortality ratio", the number of mice that died out of the total number of mice inoculated,[124] where high ratios were indicative of high viral loads.

As virological and immunological techniques progressed side-by-side, the "protection test", later known as the mouse neutralization test, was developed to assess presence and potency of serum neutralizing antibodies by determining the dilution of sera from immunized animals that was protective against fatal infection, again performed in groups of mice.[213] In 1932 a tissue culture method to cultivate YFV was established. Using minced chick embryos eight- to 10-days old, and media containing normal monkey serum, Haagen and Theiler, 1932[116] describe successfully passaging YFV without loss of infectivity. These techniques played a fundamental role in not only maintaining the virus outside of vertebrate animals but also in the attenuation process that was used to make the highly successful live attenuated virus (LAV) YFV vaccine 17D that is still used today. In 1959, Porterfield developed the "plaque assay" for YFV, describing areas of "cell destruction" (i.e. plaques), that developed following the infection of chicken embryo fibroblasts monolayers with YFV that were overlaid with agar.[214] More specifically, plaques are small circular spots of dead cells that form within a cell monolayer as a result of a virus infecting and lysing a cluster of neighboring cells. Later that year, Porterfield applied his new plaque assay method as a titration technique of both virus and immune sera.[215] Unfortunately, Porterfield's plaque assay suffered poor reproducibility and despite its high potential for viral and immunological applications, it was not widely used.

In 1968, Spector and Tauraso[216] developed a protocol for conducting the plaque neutralization test using MA-104 cell monolayers derived from embryonic rhesus monkey kidney. Compared to the previous mouse neutralization test which took 21 days to produce a result, Spector and Tauraso's plaque assay produced results in just five or six days, did not require the use of mice, used 400μL of test sera compared to the 2mL required in mice, and was significantly cheaper. These developments represented a significant advance within the field which dramatically increased accessibility that would permit the production of valuable data.

In the modern era, the plaque assay and related plaque reduction neutralization test (PRNT) are gold standard techniques used for quantification of YFV, serological diagnosis of YF,[21, 217] and clinical vaccine trials.[218] Yet the plaque assay has limitations. Most notable is its reliance upon plaque formation, which renders it unsuitable for non-plaque-forming viruses, which infect cells and replicate but do not cause sufficient cell lysis to form distinct plaques in *in vitro* assays. Non-plaque-forming viruses have been reported for YFV[219] and other orthoflaviviruses.[220-222] Additionally, heterogeneous plaque morphology, especially in low passage clinical isolates[223] can pose challenges for generating reducible and accurate titers. To overcome these challenges, study of dengue virus (DENV) and Zika virus (ZIKV) utilize the immunofocus assay, which involves the application of immunostaining. Briefly, cell monolayers are infected with virus and incubated with a viscous overlay media such that newly synthesized virions are restricted to infect neighboring cells, as opposed to being secreted freely into a cell supernatant and infecting the cell monolayer at random. Resulting foci of infected neighboring cells can be visualized directly by immunostaining the virus within these clusters of cells. In order to visualize the immunofoci, cells must first be fixed and permeabilized, followed by addition of a primary monoclonal antibody that recognizes the envelope glycoprotein on the surface of the virion, followed by secondary antibody that binds to the species-specific antibody class (IgG, etc) of the primary antibody. This secondary antibody is also conjugated to a horseradish peroxidase enzyme that can oxidize a colorimetric substrate. The final step involves the addition of substrate, resulting in a color change and allowing the visualization of viral foci.

Within the YFV field, the plaque assay has remained the gold-standard for virus quantification, but challenges with the plaque assay have prompted the exploration of alternative methods of viral quantification.[219, 224] The focus assay has been successfully used to characterize neutralization against the attenuated and highly passaged 17D vaccine strain[108]and recently validated against the plaque assay.[225] Other studies have successfully used the focus assay to detect wild-type strains DakH1279[108] and ES-504[88], belonging to the West Africa-II and South American-I genotypes, respectively. However, beyond these studies the focus assay has not yet been successfully used to detect a broader range of antigenically diverse wild-type YFV strains. Here we describe a micro-immunofocus assay using pan-orthoflavivirus monoclonal antibody 4G2[226] to successfully visualize 10 wild-type YFV strains, including a representative strain from each of the seven genotypes.

Section 3.3: Results

3.3.1 Viruses

Ten virus strains were titrated by for plaque and focus assays (Table 3.1) including the 17D vaccine strain (WA-II genotype), parental Asibi strain (WA-II), non-human primate-adapted DakAr 1279 strain (WA-II), Jose Cachatra (WA-II), Ogbomosho (WA-I), Uganda48a (EA), Couma (E/CA), 321_Br_MG_2018 (SA-I) which was isolated during the recent outbreak in Brazil, and HEB 4263 (SA-II). The Angola strain 14FA/Angola71 was also titrated by focus assay. The year of isolation of these strains ranges from 1927 to 2018, and total number of passages ranges from three (Uganda48a and HEB 4236) to 50 (Couma). We note that only a partial passage history is available for Ogbomosho. Additionally, while the 17D virus used is denoted as passage five, this virus has an extensive prior passage history of over 289 sub-inoculations and subcultures through non-human primates and *ex vivo* tissues.[114]

Table[3.1]

Strain	Date of isolation	Locale of isolation	Genotype	Host source	Isolate history	Passage history†	Contributor history‡	Total passages
17D	1937	N/A	West Africa II	N/A	N/A	Vaccine vial – Vero (1) – C6/36 (2) – VF (2)	Sanofi Pasteur commercial vaccine vial – OHSU	5
Asibi	1927	Kpeve Village, **Ghana**	West Africa II	Human	Male, 28 yo. Patient survived.	Human – Monkey (6) – C636 (3) – VF (2)	YARU, Yale University – WRCEVA – OHSU	11
DakAr 1279	1965	Djeurbel, **Senegal**	West Africa II	Mosquito	No further isolate history provided	Mosquito – SM (6) – VF (2)	J.P. Digoutte, Institut Pasteur de Dakar – Robert E. Shope, YARU, Yale University – ARC (lot:M18524A WSV) –	8

							OHSU	
Jose Cachatra	23-Aug-1965	**Guinea Bissau**	West Africa II	Human	No further isolate history provided	Human – SM (6) – Mosquito – VF (2)	YARU – WRCEVA – OHSU	9
Ogbomosho	1946	Ogbomosho, **Nigeria**	West Africa I	Human	No further isolate history provided	Human – P? – C636 (2) – VF (2)	YARU – WRCEVA – OHSU	>5
Uganda48a/ MR896	Jul-1948	**Uganda**	East Africa	*Aedes* spp. mosquito	No further isolate history provided	Mosquito – C636 – VF (2)	Institute Pasteur Bangai, Central African Republic – YARU – WRCEVA	3
Couma	Jun-1961	**Ethiopia**	East/Central Africa	*Human*	No further isolate history provided	Human – SM (46) – Mosquito (2) – VF (2)	Institute Pasteur Paris, France – YARU – WRCEVA – OHSU	50

						–		
321_BR_MG_2018	2018	Minas Gerais, **Brazil**	South America I	Human	Female, 71 yo. Patient survived.	Human – Vero (2) – C636 (4) – VF (2)	Instituto de Ciências Biológicas, Universidade Federal de Minas Gerais, Brazil – OHSU	8
HEB 4236	5-Mar-1995	**Peru**	South America II	Human	No further isolate history provided	Human – C636 – VF (2)	D. Watts, NAMRID, Peru – WRCEVA – OHSU	3
14FA	1971	**Angola**	Angola	Human	No further isolate history provided	Humam – SM (7) – Mosquito (2) – C6/36 (1) – Vero (1) – VF (2)	Robert E. Shope, YARU, Yale University – ARC (lot: TC00885 WSV) – OHSU	13

[Table 3.1]

Table 3.1 Isolation and passage history of viruses

Representative virus strains from each genotype.

**yo: years old;*

†VF: Vero-furin+ cells, SM: suckling mouse, P?: missing passage history;

‡OHSU: Oregon Health & Science University, YARU: Yale Arbovirus Research Unit, WRCEVA: World Reference Center for Emerging Viruses and Arboviruses, ARC: Arboviruses Reference Collection (Centers for Disease Control and Prevention).

3.3.2 Incubation time of focus assays using wild-type YFVs

Building upon established in-house and published protocols of focus assays using the 17D vaccine strain which is incubated for 48 hours following infection,[88] we found an extended incubation time ≥72 hours produces foci with optimal diameters for counting for most of our wild-type viruses. The exception to this was the Couma strain, which in our hands produced overlapping foci at ~72 hours and optimal foci after ~48 hours.

3.3.3 Biosafety modifications and challenges

Operating within the BSL-3 poses challenges, including reduced dexterity resulting from extra personal protective equipment (PPE), additional precautions taken when discarding liquids to avoid unnecessary aerosolization and spills, and thorough decontamination steps. To account for these time consuming and important precautions, we developed a modified protocol. One major modification involved carefully removing overlay media from 96-wells plates by pipetting. Typically, plates are washed three times at this stage to removed residual overlay, which we reduced to a single wash to save time before fixing. As a result of reduced washing, we found a high level of "background" which is the result of non-specific binding of monoclonal antibodies used for visualization of foci, presumably the result of residual overlay media. Additionally, we found that some virus foci were faint and had poorly defined foci borders, reducing the accuracy of foci recognition by the CTL Immunospot software.

3.3.4 Assay optimization

To account for these challenges, we adjusted our methods. To reduce background, we extended our blocking step to overnight at 4°C. To improve focus recognition, we increased our primary antibody incubation step to a minimum of overnight at 4°C. Finally, we allowed the TrueBlue substrate to incubate until clear foci were visible by eye – typically 60 minutes at room temperature and sometimes overnight at 4°C. Total assay time with these modifications from and including the day of infection to image acquisition was 5 days (4 days for Couma).

3.3.5 Immunostaining of wild-type YFV strains

We successfully visualized foci for every wild-type YFV strain assayed, including a strain from every known genotype (Figure 3.1). Furthermore, our modified immunostaining protocol allowed easy detection of individual foci using the CTL Immunospot.

Figure[3.1]

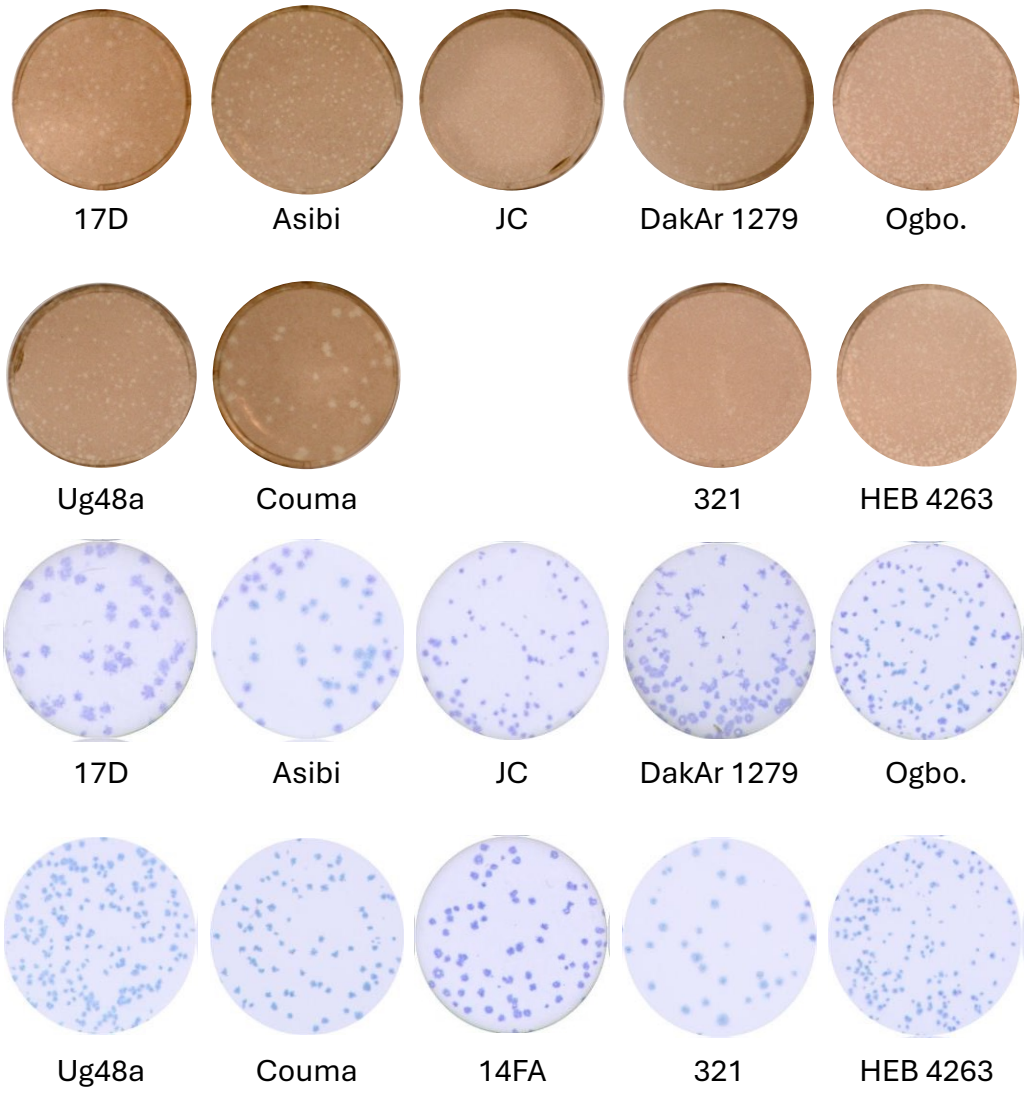

[Figure 3.1]

Figure 3.1 Representative plaques and foci

Representative wells from plaque assays (top two rows) and focus assays (bottom two rows) for 17D vaccine strains and wild type viruses from each genotype. Plaque assays were conducted in 6-well plates and focus assay were conducted in 96-well plates.

JC: Jose Cachatra, Ogbo.: Ogbomosho, Ug48a: Uganda48a. 321: 321_Br_MG_2018.

Courtney Micheletti conducted plaque assays and provided images of individual representative wells.

3.3.6 Comparison of plaque- and focus assays

3.3.6a Viral titers

We found a high level of agreement between plaque- and focus- assay-derived titers, with fold differences between PFU/mL and FFU/mL ranging 1.0-3.6 (Table 3.2).

3.3.6b Time

From infection to plaque/foci visualization, the plaque assay took 4-7 days, and the focus assay took 4-5 days. All steps of the plaque assay must be performed within the BSL-3 facility. Comparatively, focus assay plates may be removed from the BSL-3 on day 2-3 post infection following fixation with paraformaldehyde, and the remaining steps can be performed at BSL-2, without the need for a biosafety cabinet and with minimal personal protective equipment. Reduced time spent in the BSL-3 represent a significant reduction of risk of accidental exposure to lab personal through reduced time spent in a high stress environment, reduced interactions with infectious virus, and reduced operation while donning extra personal protective equipment which can limit dexterity.

3.3.6c Other resources

The plaque assay requires two 6-well plates to conduct a single titration in duplicate, compared to the focus assay, where eight titrations can be performed in duplicate within a single 96-well plate. This represents a significant reduction in cost of consumables and reduced incubator space required to conduct assays. The 96-well format also requires fewer cells and less cell culture media, representing reduced cost in reagents.

Table[3.2]

Virus strain	Focus/ plaque assay	Titer per individual dilution (FFU/mL or PFU/mL)					GMT	Fold difference
		1.0E-02	*1.0E-03*	*1.0E-04*	*1.0E-05*	*1.0E-06*		
17D	FA			1.1E+07	6.7E+06		8.7E+06	2.0
	PA			4.1E+06	5.4E+06	3.9E+06	4.4E+06	
Asibi	FA	6.5E+05	1.1E+06	1.0E+06			8.8E+05	1.0
	PA	1.1E+06	7.2E+05	9.5E+05			9.1E+05	
Jose Cachatra	FA		1.7E+06	2.5E+06			2.1E+06	1.6
	PA		3.1E+06	3.5E+06	3.3E+06		3.3E+06	
DakAR	FA		2.9E+06	6.0E+06			4.2E+06	1.3
	PA			4.8E+06	2.0E+06	3.3E+06	3.2E+06	
Ogbomosho	FA		2.6E+06	4.4E+06			3.4E+06	1.2
	PA			4.5E+06	3.5E+06		4.0E+06	
Uganda48	FA	6.0E+05	1.1E+06	3.3E+05			5.9E+05	1.7
	PA		8.3E+05	1.2E+06	1.0E+06		1.0E+06	
Couma	FA			2.5E+07	3.3E+07		2.9E+07	3.0
	PA			7.1E+06	1.3E+07		9.5E+06	
321_Br_MG_2018	FA		3.1E+06	5.3E+06	3.3E+06		3.8E+06	3.6
	PA			1.7E+06	6.7E+05		1.1E+06	
HEB4263	FA		6.4E+06	9.5E+06	1.0E+07		8.5E+06	2.6
	PA			3.1E+06	3.5E+06		3.3E+06	

[Figure 3.2]

Table 3.2 Comparison of titers determined by plaque and focus assay

Courtney Micheletti provided plaque counts and titers. FFU: focus forming units, PFU: plaque-forming units.

Section 3.4: Discussion

Here we have successfully optimized the micro-focus assay in 96-well format to visualize and titrate wild-type YFV strains representative of all seven genotypes. Notably, using pan-orthoflavivirus anti-E monoclonal antibody 4G2, we were able to visualize foci formed by DakAr 1279, a strain which has been previously described as non-plaque- and non-focus forming using the YFV-specific mAb, 3A8.B6,[219] offering a valuable quantification method for a strain that causes robust viscerotropic infection in rhesus macaques that mimics severe human disease.[72, 108]

In contrast to previous reports of low passage and clinical isolates of orthoflaviviruses as non-plaque forming,[220-222] we successfully visualized foci from low passage (p3) isolates Uganda48a and HEB4236, suggesting that our protocol is suitable for visualizing other low passage strains and clinical isolates, and has the potential to identify newly emerged strains that pose a risk to public health.

The focus assay has many advantages compared to the plaque assay. Notably, the focus assay requires less overall time, and fewer consumables and reagents which together represent reduced cost on material items and salary of lab personnel. Wild-type YFV must be handled at BSL-3. While the focus assay still requires a BSL-3 facility to handle live virus, we emphasize a small but important increase in biosafety through the reduced time of lab personnel spent in the BSL-3 handling infectious virus.

The focus assay has many important applications. Beyond titration, we have successfully used the methods described here to conduct FRNTs (data not shown). The FRNT is an invaluable tool for conducting serosurveys to determine immunity of a given population with the goal of assessing vaccination coverage and risk of an outbreak. The FRNT has been adopted by many.[88, 108, 227, 228] However, the PRNT remains the gold standard serological diagnostic, boasting greater specificity than the IgM ELISA which is especially valuable in areas of co-circulating orthoflaviviruses.[21] The FRNT is a higher throughput and rapid alternative that offers to crucially reduce time needed to provide diagnoses, the provision of care, and public health efforts such as ring vaccination to prevent spread of disease.

Our study has limitations. While we were able to visualize foci for all viruses tested, we recognize that successful staining is not guaranteed, especially for true clinical isolates which were not validated here below passage three. Our approach of inter-assay validation required titers within fourfold of each another which represents the accepted variation for titration assays and neutralization tests within the field. However, no statistical analyses were conducted to robustly validate a correlation between the two assays.

Our focus assay offers a time- and cost saving approach to characterize wild-type YFVs that have proven to be challenging to characterize using historical methods. The ability to reliably characterize wild-type YFV strains advances the field by increasing the accessibility of a powerful assay with applications in diagnostics, surveillance, and research, ultimately enhancing our potential to reduce disease transmission and improve public health outcomes.

Section 3.5: Materials & Methods

Viruses

Viruses were obtained from collections with the World Reference Centre for Emerging Viruses and Arboviruses and University of Texas Medical Branch, the Centre for Disease Control's Reference, and gifted by Betânia Paiva Drumond with the Universidade Federal de Minas Gerais. Source, isolate history, and passage history are summarized in Table 1.

Tissue culture

Vero cells (ATCC CCL-81) were used for virus titration. Vero cells over-expressing furin (Vero-furin+) were used for virus propagation (ref or note that they were made in house). Vero cells were maintained in Vero complete media (VCM): MEM/EBSS (Hyclone, SH30024.01) supplemented with L-glutamine (Gibco, 25030-081) non-essential amino acids (NEAA; Gibco, 11140-050), antibiotic-antimycotic (Gibco, 15240-062) and 10% v/v fetal bovine serum (FBS; Avantor, 89510-186). Vero-furin+ cells were maintained in Vero-furin+ (VF) media (VFM): VCM supplemented with 460µg/mL G418 (Thermo, 10131035), which required to elicit selective pressure for over expression of furin G418-reistant gene during the infection stage of virus propagation in Vero-Furin+ cells. All cells were incubated at 37°C, 5% CO_2. Cells were passaged by rinsing with phosphate buffered saline without calcium or magnesium (PBS; HyClone, SH30256.01), trypsinized with 0.25% Trypsin-EDTA (Gibco, 25200-056), quenched in VCM, and pelleted at 200 x g for 5 minutes. All cells used in assays were below passage 25.

Virus propagation

All unfixed viruses were handled within a biosafety level 3 (BSL-3) facility at OHSU. T75 tissue culture flasks (Fisherbrand, FB012937) were seeded with 5 x 10^6 Vero-Furin+ cells in VFM and

grown overnight at 37°C, 5% CO_2 and cell confluence was confirmed prior to infection. Flasks were washed twice with PBS, and infected with virus suspended in virus dilution media (VDM): MEM/EBSS supplemented with L-glutamine, NEAA, Gibco, antibiotic-antimycotic, and 2% v/v FBS and incubated for 1 hour at 37°C, 5% CO_2, rocking the flasks every 15 minutes. Next, the viral inoculum was removed and discarded, and 12mL of VCM was added to each flask before incubating at 37°C, 5% CO_2. Flasks were observed for cytopathic effect (CPE), compared to uninfected cells over the subsequent days, and harvested when ≥40% CPE was first observed (4-8 days post infection for all viruses). Tissue culture supernatants were collected and clarified at 1000 x g for 10 minutes at room temperature (RT). Clarified supernatants were supplemented with 10% v/v sucrose phosphate glutamate (SPG; 2.18M sucrose, 38mM KH_2PO_4, 72mM K_2HPO4, 60mM L-Glutamic acid), aliquoted, and stored immediately at -80°C. All virus aliquots were stored at -80°C for ≥48 hours before use.

Upon receipt of virus stocks from external sources, an initial passage (p1) stock was generated by infecting with an unknown multiplicity of infection (MOI). "p1" stocks were used solely to seed subsequent working stocks at an MOI of ~0.01. All neutralization assays were conducted using second passage "p2" stocks.

Plaque assay

Plaque assays were performed in biological duplicate. Virus quantification by plaque assay was conducted using standard virological methods as previously described.[229-233] VeroE6 cells (ATCC CRL-1586) were seeded into 6-well flat-bottom plates, with $5.0x10^5$ cells/well, 24 hours prior to infection. Virus was diluted 10-fold with a range of 10^{-2} - 10^{-7} in OptiMEM (Gibco 31985-070) supplemented with 2% heat-inactivated fetal bovine serum (Avantor 89510-186, Lot#015B20), and 1% Antibiotic-Antimycotic 100X (Gibco 15240062). Infection was performed by adding 0.3 mL of diluted virus to each well containing 80-90% confluent monolayers for 1 hour at 37°C and gently rocked every 15 minutes. After 1 hour, the inoculum was removed from the wells and replaced with 3.0 mL of a molten primary overlay, equilibrated to 42°C. The overlay consisted of a 1:1 ratio of agarose and nutrient media, composed of 1% SeaPlaque agarose (Lonza 50100), 2x EMEM (Quality Biological, 115-073-101), 2.5% heat-inactivated fetal bovine serum (Avantor 89510-186 Lot#015B20), and 0.5% Antibiotic-Antimycotic 100X (Gibco 15240062). The primary

overlay was left to solidify completely for >20 minutes before incubation at 37°C with 5% CO2 for 3-5 days, varying based on the viral strain. After initial plaque formation, 2.0 mL of molten secondary overlay containing 3.3 mg/mL Neutral Red (Sigma-Aldrich 861251) was added to each well and allowed to solidify before incubating at 37°C for 24 hours. Plaques were then visually inspected and counted using an LED transilluminator. Images of the inverted plates were captured using a digital camera attached to an adjustable vertical mount to minimize vignetting of individual wells.

Focus assay

Serum dilution and infection

Focus assays were performed in biological duplicate. Vero cells were seeded in 96-wells plates at 2 x 10^4 cells per well in 200µL of VCM, and incubated at 37°C, 5% CO_2, overnight. Virus stocks were thawed at room temperature, and serially diluted 10-fold starting at 10^{-1} through 10^{-5} in VDM. Serial dilutions were prepared by adding 30µL of neat virus to 270µL of VDM, mixing by pipetting up and down 30X before transferring 30µL to the next well. Virus dilutions were performed in duplicate, and no-virus (VDM only) well was prepared per dilution. Ninety percent confluency of Vero cell monolayers was confirmed, and VCM media discarded. Cells were infected by pipetting 30mL of diluted virus carefully down the side of wells, so as not to disturb the cell monolayer. Plates were manually rocked immediately to ensure even distribution of the virus inoculum over the cell monolayer, and then every 15 minutes for a total of 45-60 minutes incubation at 37°C, 5% CO_2. Cells were then overlaid with 180µL of overlay media: OptiMEM (Gibco, 31985-070) with 1% methylcellulose (Sigma, M0512) supplemented with NEAA, anti-anti, and 10% v/v fetal bovine serum (FBS). Infected plates were incubated at 37°C, 5% CO_2, for 68 hours (±4), except for Couma 1961 which was incubated for 48 hours (±6).

Fixation and staining

Forty-eight to 72 hours post infection, overlay media was aspirated and discarded by careful pipetting so as not to disturb the cell monolayer. Wells were washed once by adding 200µL of PBS gently down the side of the wells, then PBS was aspirated and discarded as before. Entire plates were fixed in 4% paraformaldehyde (PFA) in PBS by adding 100µL carefully down the side of wells before completely submerging plates and lids and transferring to a resealable bag. Plates

were incubated at RT for 20 minutes to allow for complete viral inactivation before removal from the BSL-3 suite. Following inactivation, PFA was discarded, and plates washed twice by submerging in PBS. PBS was discarded and plates blotted on absorbent paper towels to remove residual PBS. Cells were permeabilized by incubating for 10 minutes at RT, rocking, with 30mL of permeabilization buffer: PBS with 0.074g sodium azide (Sigma S8032), 0.875% bovine serum albumin (Sigma, A-7409), 0.01% saponin (Sigma, S8032). Plates were washed twice with PBS, blotted as before, and blocked by adding 150µL of blocking buffer (BB; PBS with 2% heat inactivated normal goat serum (Rockland Immunochemicals, Inc., 0204-00-0100), and 0.4% Titron-X) and incubated overnight (or up to 4 days) at 4°C. BB was discarded, 30µL of primary antibody—pan-flavivirus anti-E antibody 4G2[226] (1mg/mL, generated from hybridoma, ATCC cat # HB-112)—diluted 1:750 in BB added, and incubated overnight at 4°C. Primary antibody was discarded, and plates were washed 3 times with PBS, and blotted. Thirty µL of secondary antibody—Horse Radish Peroxidase goat-anti-mouse-IgG antibody (BioLegend, Cat# 405306)—diluted 1:1000 in BB was added to each well and incubated for 45 minutes (<90 minutes) at RT. Due to the light sensitivity of peroxidase, plates were protected with foil in all subsequent steps. Plates were washed 3 times with PBS, and blotted, before adding 30µL of TrueBlue™ Peroxidase Substrate (Kirkegaard & Perry Laboratories Inc., 5510-0030) per well. Plates were allowed to develop for a minimum of 20 minutes, or until foci were visible (occasionally overnight). TrueBlue™ was discarded, and plates washed once by submerging in de-ionized water. Water was discarded, plates blotted, and allowed to air dry for ≥20 minutes. Images of individual wells were acquired, foci counted, and quality controlled using a CTL ImmunoSpot 7.0.26.0 (Cellular Technology LTD, Cleveland, OH, USA).

Comparison of viral titers by plaque and focus assay

To establish the reproducibility of results using either assay, plaque and focus counting was performed on blinded samples with one lab member counting plaques and another counting foci. Next, we calculated plaque forming units (PFU/mL) or focus forming units (FFU/mL) for each dilution that had countable plaques or foci, and geometric mean titers (GMTs) were calculated. Intra-assay validation required biological duplicates with titer values within fourfold of each other. Fold differences were then calculated between GMTs from plaque- and focus assays determined

using the same virus. For inter-assay validation we required virus-paired GMTs within fourfold of each other.

Table3.2

Strain	Date of isolation	Country of Isolation	Genotype	Host source	Isolate history	Passage history†
17D	1937*	N/A	West Africa II	N/A	N/A	Vaccine vial ↓ ???
Asibi	1927	Kpeve Village, **Ghana**	West Africa II	Human	Male, 28 yo. Patient survived.	Human ↓ Monkey (6) ↓ C636 (3) ↓ VFc2 ↓ VFc2
DakAr 1279	1965	Djeurbel, **Senegal**	West Africa ???	Mosquito	No further isolate history provided	SM (6) ↓ VFc2 ↓ VFc2
Couma	Jun-61	**Ethiopia**	East/Central Africa	Human	No further isolate history provided	Human ↓ SM (46) ↓ Mosquito (2) ↓ VFc2 ↓ VFc2

HEB 4236	05-Mar-95	**Peru**	South America II	Human	No further isolate history provided	Human ↓ C636 ↓ VFc2 ↓ <u>VFc2</u>
Ogbomosho	1946	Ogbomosho, **Nigeria**	West Africa I	Human	No further isolate history provided	Human ↓ P? ↓ C636 (2) ↓ VFc2 ↓ <u>VFc2</u>
Uganda48a/ MR896	Jul-48	**Uganda**	East Africa	*Aedes* spp.	No further isolate history provided	Mosquito ↓ C636 ↓ VFc2 ↓ <u>VFc2</u>
Jose Cachatra	23-Aug-65	**Guinea Bissau**	West Africa II	Human	No further isolate history provided	Human ↓ SM (6) ↓ Mosquito ↓ VFc2

						↓ VFc2
321_BR_MG_2018	2018	Minas Gerais, **Brazil**	South America I	Human	Female, 71 yo. Patient, survived, no further isolate history provided	Human ↓ Vero (2) ↓ C636 (4) ↓ VFc2 ↓ VFc2

[Table 2.1]

Table 2.1 Isolation and passage history of viruses

*Date of development.

†Number of passages within specified tissue/animal in parentheses; "P?" indicates unknown passage history; viral passage used for experiments is underlined.

Section 3.6: Acknowledgements

Thank you to Courtney Micheletti for conducting all plaque assays and writing the associated methods section. Thank you to Betânia Drumond from Universidade Federal de Minas Gerais for kindly gifting us the viral isolate 321_Br_MG_2018 used in these experiments. Thank you to Alec Hirsch and Hirsch lab for kindly supplying us with 4G2 antibody which was generated in-house using their hybridoma.

Chapter 4: New insights into an old vaccine: potency and breadth of the yellow fever vaccine 17D-elicted neutralizing antibodies is enhanced by heterologous orthoflavivirus infection

Author list
Felicity J Coulter, Courtney A Micheletti, Abram E Estrada, Samantha R Osman, Shuhua Luo, and William B. Messer.

Publication info: *In preparation, Journal of Infectious Diseases*
Doi: TBD

Section 4.1: Abstract

The yellow fever 17D vaccine has been distributed worldwide for almost 90 years and is considered highly successful, eliciting neutralizing antibodies in almost all vaccinees. However, with recent outbreaks in South America, and Africa, yellow fever continues to represent a significant public and global health concern. Despite the longevity of the 17D vaccine, few studies have characterized the capacity of 17D-immune sera to neutralize wild-type yellow fever viruses. To our knowledge, we provide the first extensive characterization of the potency and breadth of 17D-immune sera, using an expanded panel of wild-type yellow fever viruses that represent all known genotypes together with a unique cohort of non-endemic vaccinees with diverse orthoflavivirus infection histories. Importantly, we identified significantly reduced neutralization titers and rates of seropositivity of 17D-immune sera against South American SA-I virus strains. However, this effect was observed exclusively amongst 17D-only vaccinees, suggesting a boosting effect following heterologous orthoflavivirus infection. We believe this boosting effect is the result of cross-reactivity of neutralizing antibodies to N67 epitopes within the envelope glycoprotein that

are exclusive to SA-I strains and conserved across dengue serotypes. These data fill an important knowledge gap and have implications for future vaccine strategies.

Section 4.2: Introduction

Mosquito-borne yellow fever virus (YFV), the prototypic orthoflavivirus and etiological agent of yellow fever (YF), is estimated to cause up to 173,000 severe infections and up to 82,000 deaths annually across Africa and South America.[234] With no current antiviral therapies, the YFV vaccine 17D continues to play an essential role in controlling disease since its creation in the early 1930s. The millions of doses distributed globally are estimated to prevent up to 119,000 of YF cases annually.[234]

The 17D vaccine is a live-attenuated vaccine derived from the wild-type Asibi strain of YFV originally isolated from and named after a Ghanaian man in 1927.[182] Over the next decade, Max Theiler and colleagues serially passaged the Asibi strain first through non-human primates, and then over 180 times *in vitro* in embryonic mouse, embryonic chick, and finally embryonic chick tissues lacking brain and central nervous tissue.[84] The resulting virus was named 17D, and had reduced neuro- and viscerotropism, and importantly, elicited neutralizing antibodies in non-human primates that were protective against a lethal challenge with the parental Asibi strain.[84] Shortly thereafter, newly invented techniques permitted large scale production of the vaccine in embryonated chicken eggs,[235] and the first doses of the 17D vaccine were administered to humans during an YF outbreak in Minas Gerais, Brazil in December of 1937,[68] and the 17D vaccine rapidly became widely accepted throughout the global community.

Despite a strong safety record and huge success controlling yellow fever disease, 17D predated the modern-day FDA-approval process, bypassing rigorous validation of safety and efficacy. Nonetheless, 17D is highly immunogenic, eliciting NAbs in 95 to >99% of vaccinees by 30 days post-vaccination.[176, 210] NAbs against the 17D vaccine strain are widely accepted as a correlate of protection.[83, 136] The gold standard for characterizing 17D-elicited neutralizing antibodies is the plaque reduction neutralization test (PRNT), which determines the serum-dilution at which a given percentage of input virus within the assay is neutralized, for example 50, 80, or 90%.

Notably, most characterization of 17D-immune sera, including studies determining the durability of 17D-elicited NAbs have used either the attenuated vaccines strains 17D[137, 141, 236-238] or, to a lesser degree, the French neurotropic strain[239-241] as the test virus, both of which belong to the West African WA-II genotype,[242] and neglect the antigenic diversity of wild-type viruses. Crucially, these studies,[137, 141, 236-238] played a key role in shaping recommendations made by the USA Advisory Committee of Immunization Practices that rescinded the need for administration of booster doses to most travelers.[196] This decision was made despite the significant knowledge gap regarding the capacity of 17D-elicited NAb to neutralize circulating and clinically relevant wild-type strains that remain today.

YFV strains are genetically grouped into seven genotypes originally distinguished by nucleotide sequence variation of >9% within a 670bp fragment bridging the pre-membrane (prM) and envelope (E) genes.[78] Phylogenetic analyses estimate that currently circulating strains in Africa emerged in West Africa (WA) ~1,500 years ago, that South American (SA) strains diverged from WA strains almost 500 years, and that currently circulating SA strains were introduced into the Americas during the slave trade[75] and diverged into SA-I and SA-II genotypes ~300 years ago. The seven genotypes currently recognized are WA-I, WA-II, East Africa (EA), and East/Central Africa (E/CA), Angola (A), and SA-I and SA-II. Strains belonging to the SA-I genotype were responsible for causing the largest outbreak in the 21st century, which occurred in Brazil between 2016 and 2019.[48] A total of 2,205 confirmed cases and 734 deaths were reported to the Pan American Health Organization,[49] although the number of actual cases was likely much higher. This outbreak prompted a new wave of scientific investigation of YFV, including epidemiological-, immunological-, and clinical studies.

To our knowledge, 17D-immune sera has been characterized using authentic YFV strains only twice before. Haslwanter *et al.*, 2022[88] and Goncalves *et al.*, 2024[17] showed reduced potency of 17D-immune sera against SA-I strains amongst vaccinee cohorts in Brazil; an important finding that suggests that the neutralization capacity of 17D-elicited NAbs is significantly reduced against clinically relevant strains, contrary to previous estimates. Haslwanter *et al.* also showed reduced potency using a cohort of vaccinees from the United States; however, these data were produced using reporter viral particles. Additionally, they identified five amino acid residue

substitutions within the E glycoprotein, that were found exclusively in SA-I strains, that increased resistance to neutralization by 17D-immune sera. Interestingly, one of these residues is a glycosylation site highly conserved across related orthoflavivirus dengue virus (DENV) strains, where it plays a crucial role in cell attachment and entry of dendritic cell and macrophages via cell surface receptor DC-SIGN.[243] Importantly, co-circulation of YFV and DENV in Brazil and other YFV-endemic regions generates diverse orthoflavivirus immunity amongst these populations. However, the potential for heterologous orthoflavivirus infection to modify the capacity of 17D-elicited NAbs against wild-type YFV strains has not yet been explored, possibly because of research barriers imposed by the requirement of a biosafety level (BSL)-3 facility to handle wild-type strains.

To address this important knowledge gap, we generated a panel of 12 wild-type YFVs including archival and contemporary strains representing all seven YFV genotypes. Using our unique cohort of non-endemic 17D-vaccinees with diverse orthoflavivirus infection histories, we performed focus reduction neutralization tests (FRNTs) against our unique virus panel. Additionally, we employed antigenic cartography to provide the most extensive characterization of YFV potency and breadth to date and establishing the previously unexplored YFV antigenic landscape. By assessing geometric mean titers (GMTs) and rates of seropositivity amongst our vaccinees, we demonstrated a novel role for heterologous orthoflavivirus infection in boosting 17D-immunity. Taken together, our findings have implications for future public health efforts, including surveillance and vaccination strategies.

Section 4.3: Results

4.3.1 Viruses

A total of 13 YFV virus strains were used for characterizing potency and breadth of NAbs induced by 17D vaccination (Supplementary Table 4.1). The E gene (ectodomain) of working stocks of the 13 viruses evaluated in this study were sequenced using Sanger sequencing and phylogenetic relatedness was confirmed (Figure 4.1A). We identified 33 amino acid differences across all viruses, with 10 differences restricted to 17D and 23 differences between wild-type viruses (Figure

4.1B, C). Seven differences were within E domain (ED) I, 16 were within EDII, and 10 were within EDIII. We confirmed the presence of a novel H67N glycosylation site, as well as additional sites previously implicated by Haslwanter *et al.*, 2022 to influence neutralization by 17D-immine sera—A83E, D270E, N271S, and N272K—which are all unique to the SA strains, with all five changes unique to SA-I strains, except for N271S which is also found in SA-II. WA-I strains showed least variation with 10-11 amino acid changes (2.5-2.8%), followed by WA-II strains with 11 amino acid changes (2.8%). EA strains differed by 18-19 amino acids (4.5-4.8%), the E/CA, A, and SA-I strains each differed by 19 amino acids (4.8%), while SA-II strains showed the most variation with 22-23 amino acid changes (5.5-5.8%).

Figure[4.1]

A

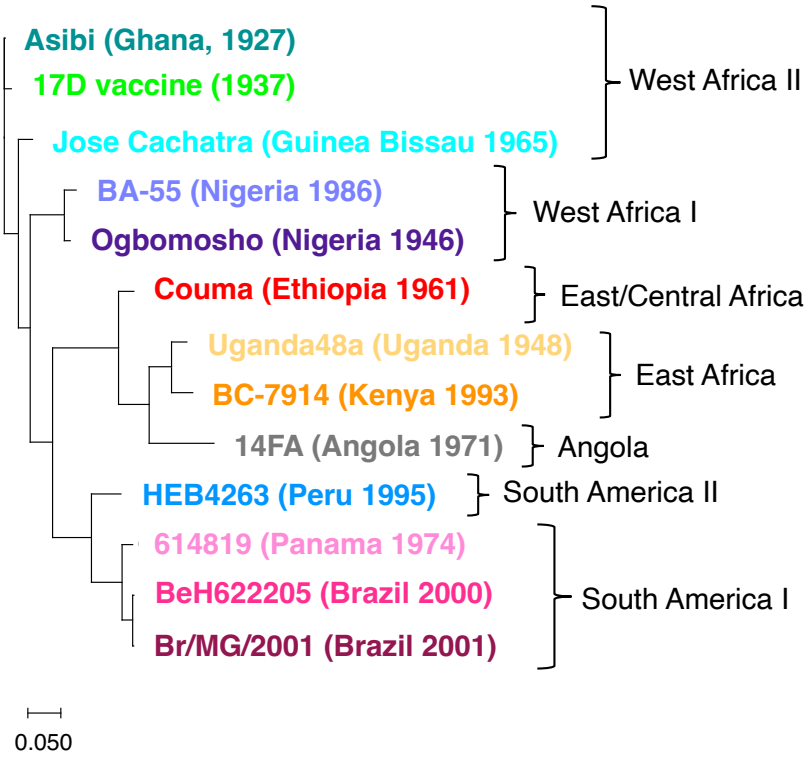

B

Domain	EDI	EDII								EDI					EDII									EDI	EDIII								
Position	46	52	56	62	67	70	83	87	90	153	154	170	173	191	200	201	207	224	268	270	271	272	282	299	305	318	325	331	335	344	345	360	380
17D	E	R	V	N	H	I	A	E	N	T	T	V	I	G	T	E	R	V	T	D	N	N	S	I	F	V	S	R	I	I	N	D	R
Asibi	E	G	A	N	H	I	A	E	N	N	T	A	T	G	K	E	R	V	T	D	N	N	S	M	S	V	P	K	I	I	N	D	T
Ogbomosho	E	G	A	N	H	I	A	E	N	N	T	A	T	G	K	E	R	V	T	D	N	N	S	M	S	V	P	R	I	I	N	D	T
BA-55	E	G	A	N	H	I	A	E	N	N	T	A	T	G	K	E	R	V	T	D	N	N	S	M	S	V	P	K	I	I	N	D	T
Jose	E	G	A	N	H	I	A	E	N	N	T	A	T	G	K	E	R	V	T	D	N	N	S	M	S	V	P	K	I	I	N	D	T
Uganda48a	Q	G	A	S	H	I	A	D	N	N	T	A	T	G	K	D	R	I	E	D	N	N	S	M	S	V	P	K	I	V	N	D	T
Couma	Q	G	A	S	H	I	A	D	N	N	T	A	T	G	K	D	R	I	E	D	N	N	S	M	S	V	P	K	I	V	K	D	T
BC-7914	Q	G	A	S	H	I	A	D	N	N	T	A	T	G	K	D	R	I	E	D	N	N	S	M	S	V	P	K	I	V	N	D	T
14FA	Q	G	A	S	H	I	A	D	N	N	T	A	T	G	K	D	R	I	E	D	N	N	S	M	S	V	P	K	I	V	N	D	T
HEB4263	E	G	A	S	H	I	A	E	H	N	A	A	T	S	K	E	R	V	T	G	S	N	S	M	S	A	P	R	M	V	N	E	T
Br/MG/2001	E	G	A	S	N	I	E	E	N	N	T	A	T	S	K	E	D	V	T	N	S	K	A	M	S	A	P	R	M	V	N	D	T
BEH622205	E	G	A	S	N	I	E	E	N	N	T	A	T	S	K	E	D	V	T	N	S	K	A	M	S	A	P	R	M	V	N	D	T
614819	E	G	A	S	N	V	E	E	N	N	A	A	T	S	K	E	D	V	T	N	S	K	S	M	S	A	P	R	M	V	N	D	T

C

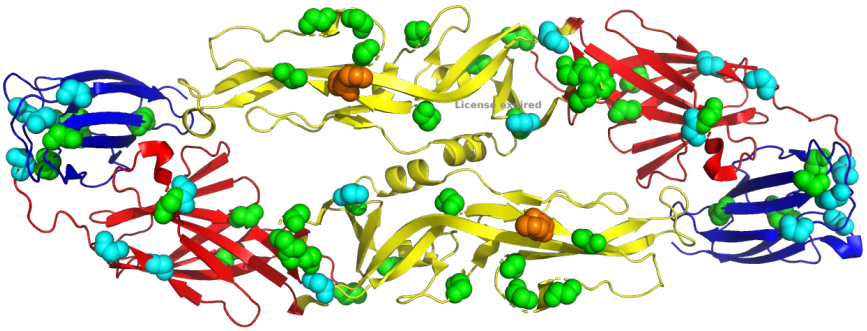

[Figure 4.1]

4.1 Amino acid changes within the ectodomain of the envelope glycoprotein amongst wild-type YFV strains

*Table **(A)** and ribbon diagram **(B)** showing amino acid variation within the E glycoprotein ectodomain between 17D and wild-type strains, with 33 total amino acid changes, 10 restricted to 17D (cyan) and 23 between wild-type viruses (green and orange). Residues implicated in modifying neutralization, including glycosylation site H67N (Haslwanter et al., 2022) restricted to SA-I strains are shown in orange. **(C)** Phylogenetic tree constructed using the amino acid sequence of the ectodomain of E. Virus strain names are colored and year of isolation is given in parentheses. Genotype names are in black.*

Abram Estrada designed primers and analyzed sequences including sequence alignments.

*William Messer performed phylogenetic analysis and generated the summary table (A), ribbon diagram (B), and phylogenetic tree **(C).***

4.3.2 Immune sera

All study participants (n=36) had previously received a single dose of 17D vaccine (Table 4.1). The interval post-vaccination ranged 1-11 years (median 6 years). Age at vaccination ranged 19-69 years (median 29.5 years). Vaccinees were either flavivirus naïve (n=18; "17D only vaccinees") or showed serological evidence of heterologous flavivirus infection (n=18; "heterologous vaccinees"). Heterologous vaccinee immune profiles were identified by self-reported histories which were confirmed by serology and included: primary DENV infection to DENV-1 (n=3), DENV-2 (n=6), DENV-3 (n=1), and DENV-4 (n=2), secondary DENV (n=3), ZIKV infection (n=2), and DENV and ZIKV infection (n=1). Most participants were female (78%, n=28). Eighty-three percent of participants identified as white (n=30), 5% reported another race/ethnicity or "other" (n=5, grouped for anonymity) and 2% (n=1) were of unknown race/ethnicity.

Table[4.1]

Sex, n (%)	
Female	28 (77.8)
Male	8 (22.2)
Race/Ethnicity, n (%)	
White	30 (83.3)
Other	5 (13.9)
Unknown	1 (2.3)
Age (years) at vaccination, median (min-max)	29.5 (19-69)
Years post vaccination, median (min-max)	6 (1-11)
Orthoflavivirus infection history, n (%)	
17D only vaccinees	18 (50.0)
Heterologous vaccinees	18 (50.0)
DENV-1	3 (16.7)
DENV-2	6 (33.3)
DENV-3	1 (5.6)
DENV-4	2 (11.1)
DENV secondary	3 (16.7)
ZIKV	2 (11.1)
DENV and ZIKV	1 (5.6)

[Table 4.1]

[4.1] **Study participants**

Summary demographics of study participants, including sex, race/ethnicity, age at vaccination, years' post-vaccination, and Orthoflavivirus infection history.

4.3.3 Potency and breadth of vaccinee immune sera

To characterize the potency and breadth of 17D-immune sera, we conducted FRNTs using our panel of 13 viruses. Pooled GMTs (Supplementary Table 4.2) of wild-type viruses were reduced 1.0-12.5-fold compared to 17D (Figure 4.2A and D). Friedman test with Dunn's multiple comparison comparing pooled GMTs to every other pooled GMT shows that Uganda48a (1:52, adj.p<0.0001), Couma (1:58, adj.p=0.0003), Br/MG/2001 (1:18, adj.p<0.0001), BeH622205 (1:13, adj.p<0.0001), 614819 (1:13, adj.p<0.0001), HEB4263 (1:40, adj.p<0.0001), and 14FA

(1:56, adj.p=0.0014) are significantly reduced compared to 17D, while GMTs against Asibi (1:83), Jose Cachatra (1:96), Ogbomosho (1:69), and BC-7914 (1:66) are not (Figure 4.2D). No significant differences were observed between pooled GMTs of viruses within the same genotype. Notably, pooled GMTs of SA-I strains—Br/MG/2001, BeH622205, and 614819—were significantly lower compared to most other viruses, except HEB4263, with significant differences ranging from 3.1-12.5-fold-changes (Figure 4.2D). Additionally, the pooled GMT of Br/MG/2001 trended towards reduced potency compared to Uganda48a, although this was not statistically significant.

We next determined proportion of vaccinees seropositive for each virus, using a cut-off of an NT_{50} <1:10 (Figure 4.2B). We found >90% of vaccinees were seropositive for all virus strains except SA-I and SA-II strains, with 86% percent of vaccinees seropositive against HEB4263 and a significantly lower proportion of vaccinees seropositive against SA-I strains with 64% against Br/MG/2001 ($p<0.001$), 50% against BeH622205 ($p<0.0001$), and 47% against 614819 ($p<0.0001$).

Neutralization titers (NT) against 17D are widely accepted as a correlate of protection, yet an evaluation of how well 17D NT titers correlate with wild-type YFV NT titers has never been performed. To address this knowledge gap, we analyzed the correlation between 17D and wild-type GMTs, finding that 17D titers were correlated significantly with all wild-type YFVs, ranging 0.40-0.68 ($p<0.0001–0.0168$) except for SA-I strains (Figure 4.2C), for which we found no correlation. This result suggests that while potency of vaccinee sera against 17D may predict potency against most other wild-type strains, it does not predict potency against SA-I strains.

We next examined the relationship between virus E glycoprotein primary amino-acid sequences and potency of serum neutralizing antibodies using Dayhoff distances. Dayhoff distances[244] are a weighted measure of amino acid similarity between primary amino acid sequences. We found a highly significant negative correlation (Pearson $R^2 = -0.84$, $p=0.0002$) between wild-type virus amino-acid distance from 17D and wild-type virus neutralization titers (Supplementary Figure 4.1), suggesting that as antigenic similarity to 17D decreases, serum antibody potency decreases as well.

Figur[4.2]

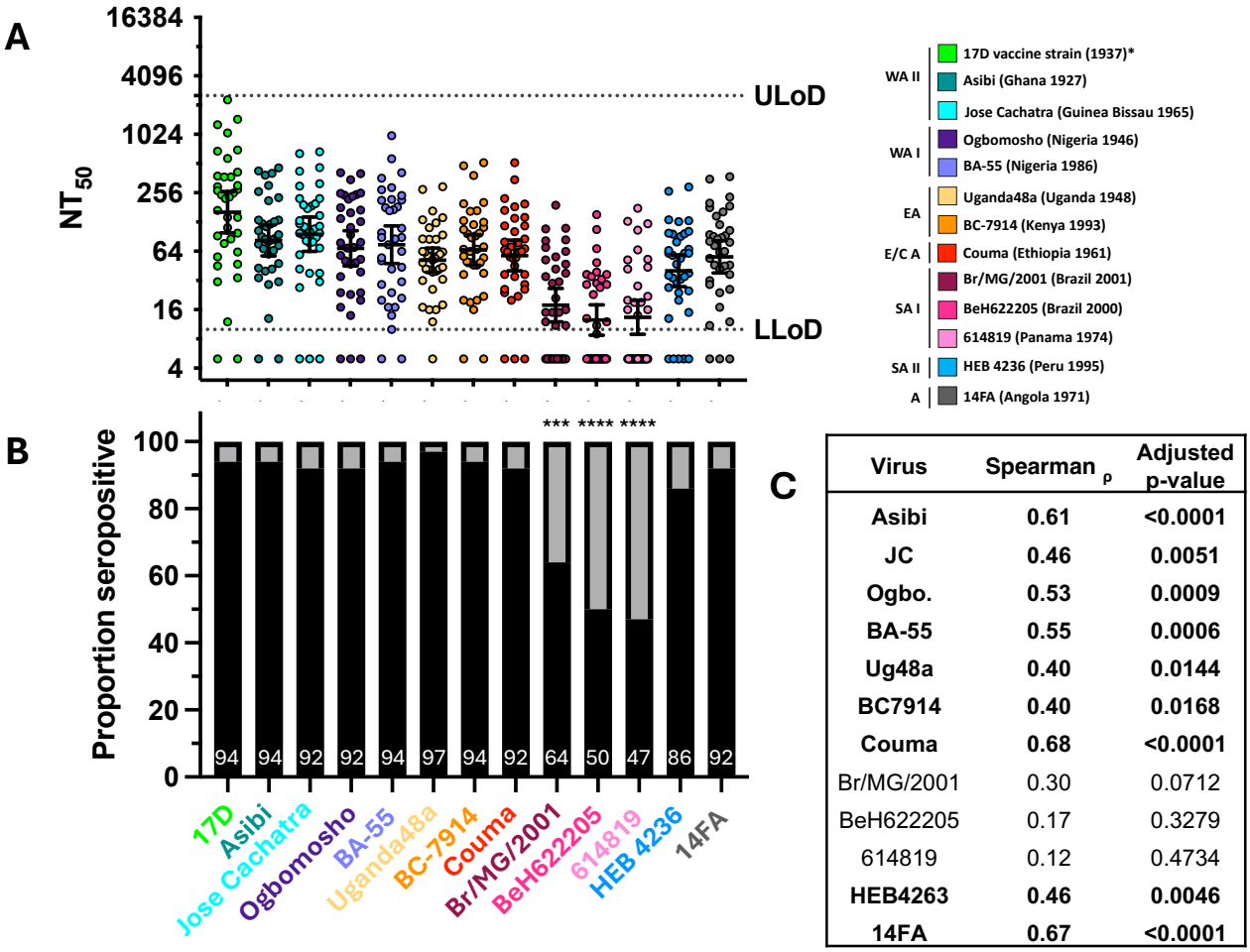

C

Virus	Spearman ρ	Adjusted p-value
Asibi	**0.61**	**<0.0001**
JC	**0.46**	**0.0051**
Ogbo.	**0.53**	**0.0009**
BA-55	**0.55**	**0.0006**
Ug48a	**0.40**	**0.0144**
BC7914	**0.40**	**0.0168**
Couma	**0.68**	**<0.0001**
Br/MG/2001	0.30	0.0712
BeH622205	0.17	0.3279
614819	0.12	0.4734
HEB4263	**0.46**	**0.0046**
14FA	**0.67**	**<0.0001**

D

	17D	Asibi	JC	Ogbomosho	BA-55	Ug48a	BC-7914	Couma	Br/MG/2001	BeH622205	614819	HEB4263	14FA
17D		2.0	1.7	2.3	2.2	3.1	2.5	2.8	9.0	12.5	12.5	4.1	2.9
Asibi			1.2	1.2	1.1	1.6	1.3	1.4	4.6	6.4	6.4	2.1	1.5
JC				1.4	1.3	1.8	1.5	1.7	5.3	7.4	7.4	2.4	1.7
Ogbomosho					1.1	1.3	1.0	1.2	3.8	5.3	5.3	1.7	1.2
BA-55						1.4	1.1	1.3	4.2	5.8	5.8	1.9	1.3
Uganda48a							1.3	1.1	2.9	4.0	4.0	1.3	1.1
BC-7914								1.1	3.7	5.1	5.1	1.7	1.2
Couma									3.2	4.5	4.5	1.5	1.0
Br/MG/2001										1.4	1.4	2.2	3.1
BeH622205											1.0	3.1	4.3
614819												3.1	4.3
HEB4263													1.4
14FA													

Adjusted p-value

ns
<0.05
<0.01
<0.001
<0.0001

[Figure 4.2]

4.2 Potency of vaccinee sera against wild-type viruses are reduced compared to 17D

(A) *NT_{50} for all participants against each virus. Each dot represents the geometric mean titer (GMT) of a single participant serum, calculated from biological duplicates. Horizontal bars and whiskers are geometric means with 95% confidence intervals. ULoD and LLoD indicate upper (1:2560) and lower (1:10) limits of detection. GMTs <1:10 were given an arbitrary value of 5. Virus strains are color-coded according to the key and arranged by genotype.* ***(B)*** *Bar graph showing proportion of seropositive (NT_{50} <1:10, black) and seronegative (NT_{50} ≥1:10, grey) participants, with percentage of total (n=36) shown with white numbers. Chi-squared analysis shows statistically greater proportion of seronegative participants for SA-I strains Br/MG/2001, BeH622205, and 614819 compared to the model prediction. *** indicates a p-value <0.001, **** p-value < 0.0001.* ***(C)*** *Table showing Spearman's rank correlation coefficients and adjusted p-values between Log-GMTs of 17D and wild-type viruses. Statistically significant values are in bold.* ***(D)*** *Matrix showing GMT fold differences between viruses. Boxes are colored by Friedman test with Dunn's multiple comparisons test adjusted p-values.*

Samantha Osman, Chad Nix, and Shuhua Luo generated data for 17D neutralization assays.

4.3.4 Heterologous vaccinees have increased potency of NAbs against SA-I strains and increased breadth of neutralization

Historically, antibodies elicited by heterologous infection with other orthoflaviviruses have not been thought to significantly impact the neutralizing capacity of 17D-elicited neutralizing antibodies. However, this thinking has arisen from 17D-based neutralization tests, and the impact of heterotypic Orthoflavivirus immunity on wild-type YFV neutralizing antibodies has not, to our knowledge, been previously examined. To explore potential effects of heterologous flavivirus infection history on GMTs, we stratified NT_{50} results by 17D only- and heterologous vaccinees (Figure 4.3). We found that pooled GMTs of heterologous vaccinees were significantly higher compared to 17D only vaccinees against the SA-I strains Br/MG/2001 (p=0.0236), BeH622205 (p=0.0328), and 614819 (p=0.0061) that showed reduced potency in the combined dataset (Figure 4.3), with fold differences between the SA-I strains and the other strains ranging 1.1-24.9 (Figure 4.4A and 4.5A). With no other significant differences observed, this demonstrates that heterologous vaccinees have increased potency of NAbs against SA-I strains and increased breadth of NAbs overall compared to 17D vaccinees alone.

To further investigate the increased potency and breadth of NAbs observed amongst heterologous vaccinees, we stratified GMTs by orthoflavivirus infection history (Figure 4.4A and C) and

compared pooled GMTs. Overall, fewer significant differences were observed between pooled GMTs amongst heterologous vaccinees (15/78 pairs) compared to 17D only vaccinees (28/78 pairs) (Figure 4.5). Again, pooled GMTs were significantly reduced for SA-I strains—Br/MG/2001, BeH622205, and 614819—against most other viruses for 17D only vaccinees (23/30 pairs), excluding HEB4263 (Figure 4.5A). Contrastingly, fewer significant differences were observed for SA-I strains amongst heterologous vaccinees (12/30 pairs) (Figure 4.5B), supporting our previous observation that heterologous infection increases potency and breadth of 17D-immune sera.

Figure[4.3]

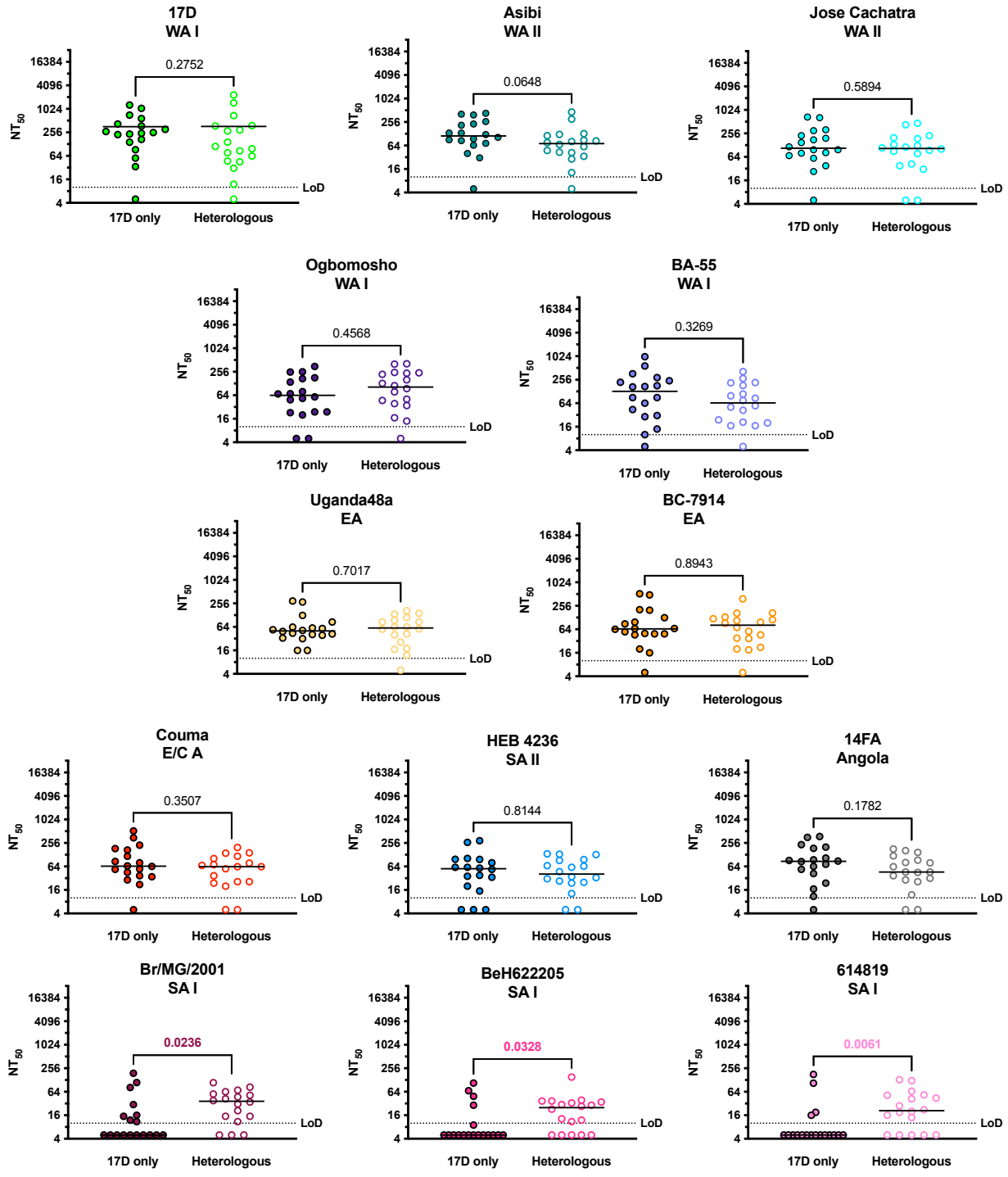

[Figure 4.3]

4.3 Heterologous vaccinees have increased potency against SA-I strains compared to 17D-only vaccinees
Individual plots show GMTs of 17D only- (open circles, right) and heterologous vaccinees (filled circles, left) against a single virus, with virus strain and genotype indicated at the top. Horizontal lines indicate medians, and p-values (Mann-Whitney U) are indicated for each plot. Statistically significant p-values are in bold and color.
Samantha Osman, Chad Nix, and Shuhua Luo generated data for 17D neutralization assays.

4.3.5 Vaccinees with heterologous flavivirus infection have increased seropositivity to SA-I strains

We next examined the impact of heterologous immunity on the proportion of vaccinees that were seropositive against each virus. By stratifying by orthoflavivirus infection history, we observed significantly reduced proportions of seropositive vaccinees against SA-I strains amongst 17D-only vaccinees, with 44% seropositive against Br/MG/2001 ($p<0.05$), 28% against BeH622205 ($p<0.001$), and 22% against 614819 ($p<0.001$) (Figure 4.4B). Interestingly, HEB4263 had the next lowest proportion of seropositive vaccinees amongst 17D only vaccines, with 83% compared to ≥89% for all other viruses. Contrastingly, amongst heterologous vaccinees the proportion of seropositive vaccinees against SA-I was not significantly reduced compared to other viruses, with 83% seropositive against Br/MG/2001, 72% against BeH622205, and 82% against 614819 (Figure 4.4D), with ≥89% seropositive vaccinees for all other viruses. We re-examined NT_{50} values and Dayhoff distances by orthoflavivirus infection history and found again strong negative correlations between wild-type virus amino-acid distance from 17D and neutralization titers for both 17D-only vaccinees (Pierson R=-0.800, p=0.0005) and heterologous vaccinees (Pierson R=-0.810, p=0.0004) (Supplementary Figure 4.2).

We also asked if order of vaccination and infection impacted our observations of increased potency and breadth. Amongst our heterologous vaccinees, seven were orthoflavivirus infected before vaccination, 10 were infected after vaccination, and one was unknown. We found no significant differences between these two groups regarding GMT ($p>0.80$) and seropositivity ($p>0.30$).

Figure[4.4]

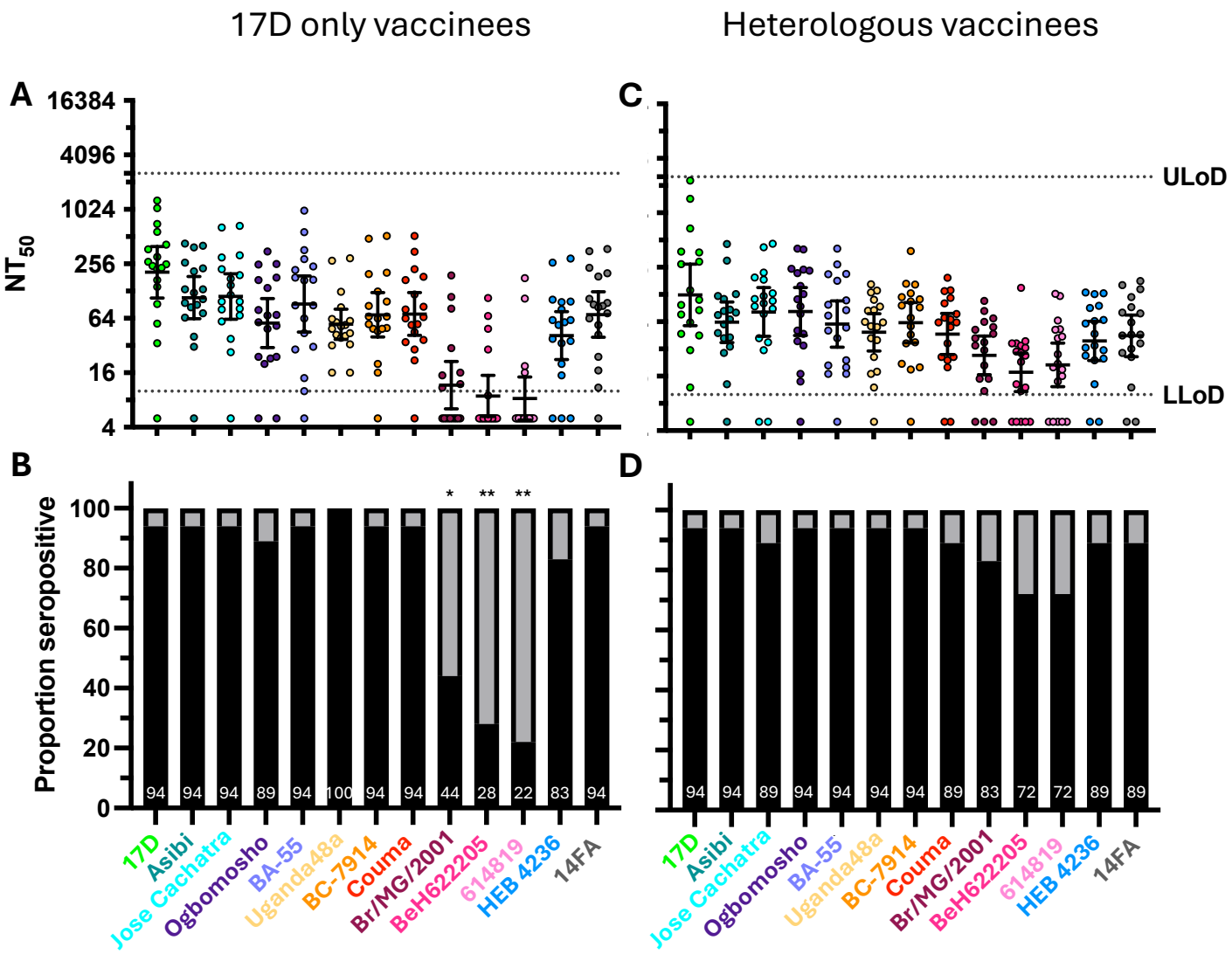

[Figure 4.4]

[4.4] **Heterologous vaccinees have increased seropositivity to SA-I strains**

(A) NT_{50} against each virus for 17D only vaccinees (left panel) and heterologous vaccinees (right panel). Each dot represents the geometric mean titer (GMT) of a single participant serum, calculated from biological duplicates.

Horizontal bars and whiskers are geometric means with 95% confidence intervals. ULoD and LLoD indicate upper (1:2560) and lower (1:10) limits of detection. GMTs <1:10 were given an arbitrary value of 5. Virus strains are color-coded according to the key in Figure 4.2 and arranged by genotype. **(B)** Bar graphs showing proportion of seropositive (NT_{50} <1:10, black) and seronegative (NT_{50} ≥1:10, grey) amongst 17D only- (left panel) and heterologous vaccinees (right panel). White numbers indicate percentage of total (n=18). Analysis of means of proportions (ANOMP) shows statistically greater proportion of seronegative vaccinees for SA-I stains Br/MG/2001 ($p<0.05$), BeH622205 ($p<0.001$), and 614819 ($p<0.001$) compared to other viruses, for 17D only vaccinees. No differences were observed heterologous vaccinees.

Samantha Osman, Chad Nix, and Shuhua Luo generated data for 17D neutralization assays.

Figure[4.5]

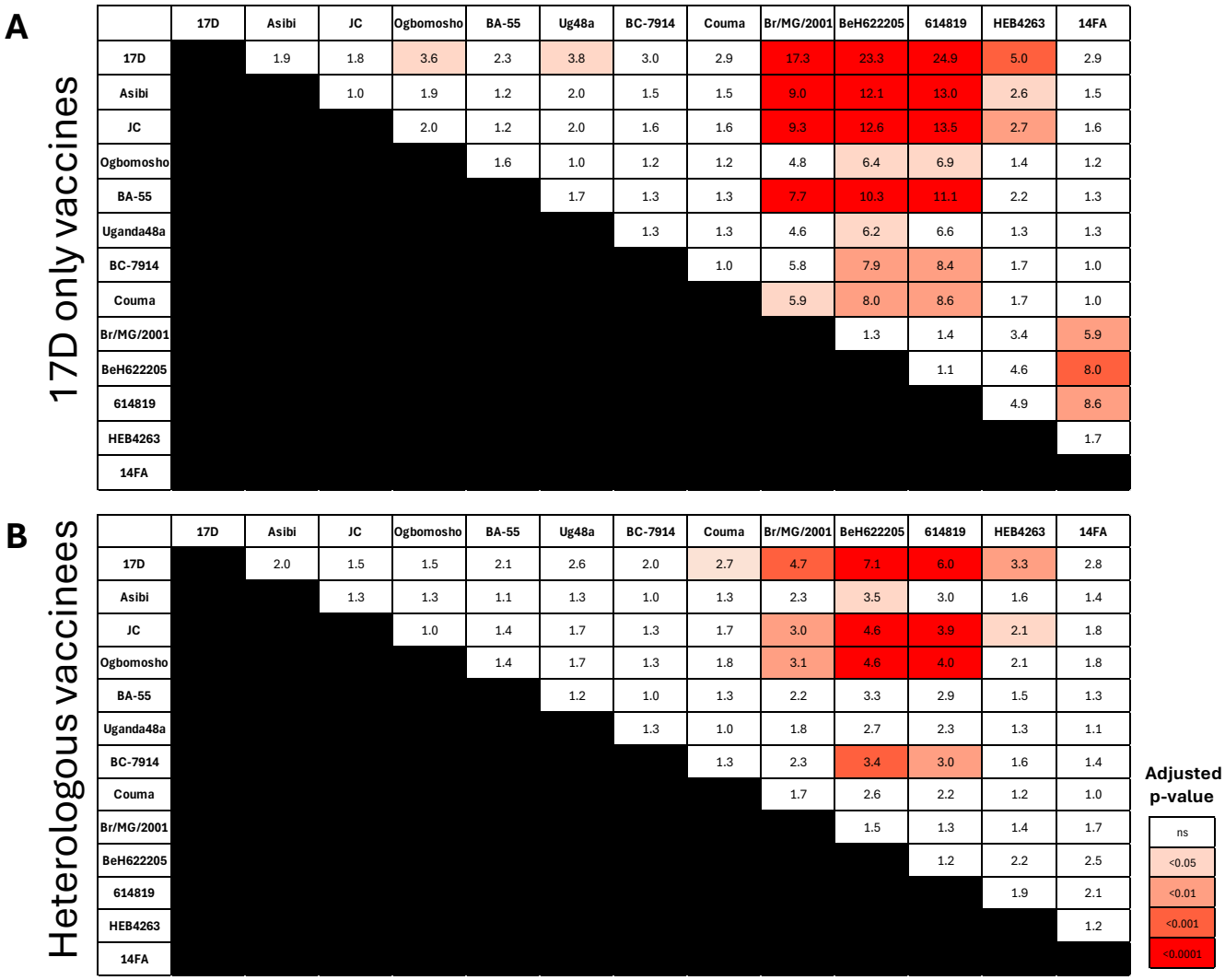

A	17D	Asibi	JC	Ogbomosho	BA-55	Ug48a	BC-7914	Couma	Br/MG/2001	BeH622205	614819	HEB4263	14FA
17D		1.9	1.8	3.6	2.3	3.8	3.0	2.9	17.3	23.3	24.9	5.0	2.9
Asibi			1.0	1.9	1.2	2.0	1.5	1.5	9.0	12.1	13.0	2.6	1.5
JC				2.0	1.2	2.0	1.6	1.6	9.3	12.6	13.5	2.7	1.6
Ogbomosho					1.6	1.0	1.2	1.2	4.8	6.4	6.9	1.4	1.2
BA-55						1.7	1.3	1.3	7.7	10.3	11.1	2.2	1.3
Uganda48a							1.3	1.3	4.6	6.2	6.6	1.3	1.3
BC-7914								1.0	5.8	7.9	8.4	1.7	1.0
Couma									5.9	8.0	8.6	1.7	1.0
Br/MG/2001										1.3	1.4	3.4	5.9
BeH622205											1.1	4.6	8.0
614819												4.9	8.6
HEB4263													1.7
14FA													

B	17D	Asibi	JC	Ogbomosho	BA-55	Ug48a	BC-7914	Couma	Br/MG/2001	BeH622205	614819	HEB4263	14FA
17D		2.0	1.5	1.5	2.1	2.6	2.0	2.7	4.7	7.1	6.0	3.3	2.8
Asibi			1.3	1.3	1.1	1.3	1.0	1.3	2.3	3.5	3.0	1.6	1.4
JC				1.0	1.4	1.7	1.3	1.7	3.0	4.6	3.9	2.1	1.8
Ogbomosho					1.4	1.7	1.3	1.8	3.1	4.6	4.0	2.1	1.8
BA-55						1.2	1.0	1.3	2.2	3.3	2.9	1.5	1.3
Uganda48a							1.3	1.0	1.8	2.7	2.3	1.3	1.1
BC-7914								1.3	2.3	3.4	3.0	1.6	1.4
Couma									1.7	2.6	2.2	1.2	1.0
Br/MG/2001										1.5	1.3	1.4	1.7
BeH622205											1.2	2.2	2.5
614819												1.9	2.1
HEB4263													1.2
14FA													

[Figure 4.5]

[4.5] Heterologous vaccinees have reduced GMT fold-differences between wild-viruses and 17D

Boxes are colored by adjusted p-values derived from Friedman test with Dunn's multiple comparisons test.

Samantha Osman, Chad Nix, and Shuhua Luo generated data for 17D neutralization assays.

4.3.6 SA-I strains form a distinct antigenic cluster

Antigenic cartography (AC) is a method used to visualize the antigenic relationship between virus strains. AC was developed first within the influenza field[245] and has subsequently been used to characterize DENV,[246, 247] ZIKV[248], and SARS CoV-2,[249] among others. Antigenic maps are constructed by plotting virus strains and immune sera on a single map. The coordinates of any given virus and serum on the map are the result of optimization that attempts to minimize the sum of squares between the tables distances (derived from a matrix of neutralization titers), and map distances (straight-line distances) between any given virus-serum pair.[250] The resulting map is a relational visualization of all viruses and all sera within the model where the proximity of objects suggests antigenic similarity and a single box represents a twofold serum dilution.[246] Antigenic cartography offers a nuanced understanding of the antigenic relationship between viruses based on the functional readout of neutralization, which allows us to make predictions about the immune response that may not be obvious from linear sequence data alone. The antigenic relationship of wild-type yellow fever viruses using antigenic cartography has not, to our knowledge, been previously explored. We constructed an antigenic map using GMTs against all 13 viruses for all sera (Figure 4.6A). As expected, SA-I strain viruses were most antigenically distant from 17D and formed a distinct cluster. Additionally, the antigenic distances between virus strains and sera were greatest for SA-I strains at 3.7-4.3 antigenic units compared to 1.4-2.4 for all other wild-type strains (Supplementary Table 4.3). To follow up on our observation of differences in NT_{50} between 17D-only and heterologous vaccinees, we constructed antigenic maps using GMTs stratified by orthoflavivirus infection history. The antigenic distances between sera and SA-I strains increased when constructed using 17D-only vaccinee GMTs (4.69-5.17) (Figure 4.6B, Supplementary Table 3) and decreased with heterologous vaccinee GMTs (2.79-3.15) (Figure 4.6C, Supplementary Table 3). Strikingly, heterologous immune sera were also more centered within the wild-type viruses compared to 17D only vaccinees. Overall, these data suggest that heterologous immune sera recognize a wider breadth of antigenically diverse wild-type YFVs compared to 17D-only immune sera.

Figure[4.6]

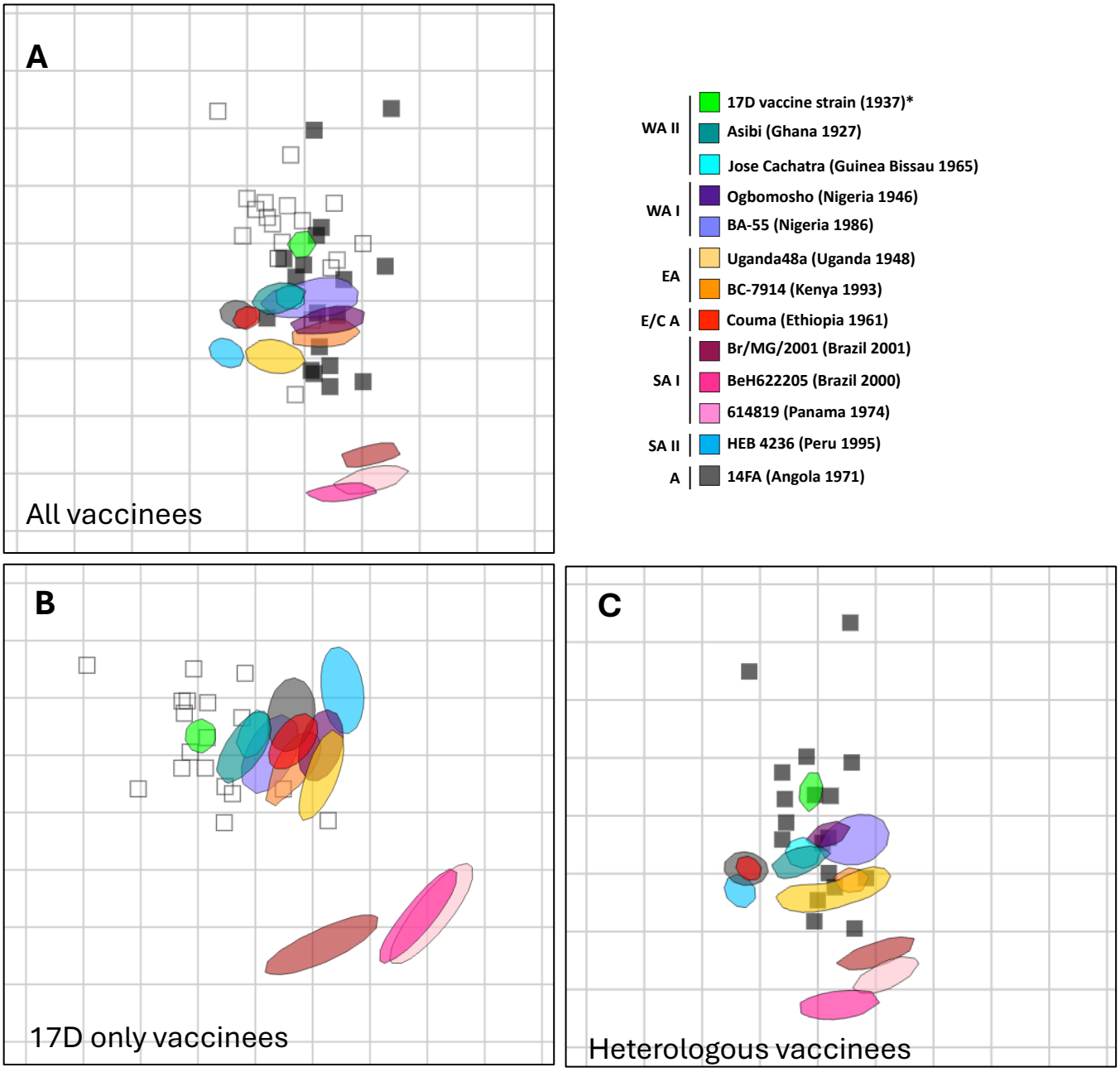

[Figure 4.6]

[4.6] Antigenic cartography of 17D and wild-type YFV strains, using 17D-immune sera

Antigenic cartography maps generated using **(A)** all 17D-vaccinees sera (n=36), including 17D only- (open squares) and heterologous vaccinees (filled squares), **(B)** 17D only vaccinees, and **(C)** heterologous vaccinees. Maps were generated using the Racmacs package in R (version 4.3.1) and RStudio (version 2023.06.1+524). A single gridline-define box represents a two-fold serum dilution of a neutralization titer.

Samantha Osman, Chad Nix, and Shuhua Luo generated data for 17D neutralization assays.

4.3.7 Reduced potency against SA-I strains is observed at 28 days post-vaccination

To begin to investigate whether the reduced potency 17D immune sera observed against the SA-I strains is the result of primary vaccine failure (failure to seroconvert following vaccination) or secondary vaccine failure (waning immunity following successful seroconversion) we performed FRNTs on seven vaccinee sera at 28 days post-vaccination against a subset of our wild-type virus panel, including 17D, BA-55 (WA-I), HEB 4236 (SA-II), and Br/MG/2001 (SA-I) (Figure 4.7). Study participants were aged 23-49 years (median 30) at vaccination and 43% female. Race/ethnicity data is omitted to maintain anonymity. As with our earlier data, we observed significantly reduced pooled GMTs against SA-I strain Br/MG/2001 (1:23, adjusted p=0.0017) compared to 17D (1:786), with no other significant differences observed between BA-55 (1:368) or HEB4263 (1:242) (Figure 4.7A). We also evaluated at the proportion of vaccinees who were seropositive against individual viruses and found only 29% of vaccinees were seropositive against Br/MG/2001, compared to 100% of vaccinees who were seropositive against every other strain (Figure 4.7B). Although limited by a small samples size, these data suggest an increased rate of primary 17D vaccine failure against SA-I strains, which may have the potential to increase risk of breakthrough infection.

Figure[4.7]

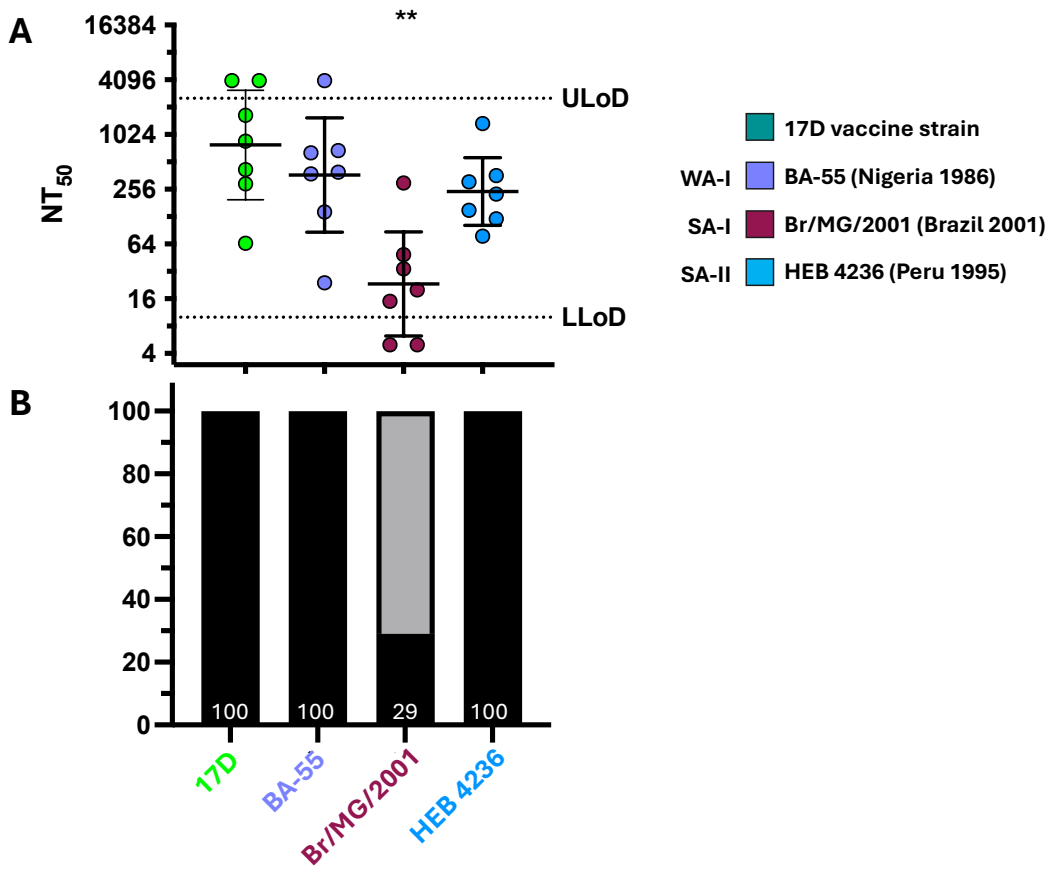

[Figure 4.7]

[4.7] **Reduced potency against the SA-I genotype is observed 28 days post-vaccination**

(A) NT_{50} GMTs of vaccinee sera 28 days post-vaccination against representative wild-type viruses. Each dot represents the geometric mean titer (GMT) of a single participant serum, calculated from biological duplicates. ULoD and LLoD indicate upper (1:2560) and lower (1:10) limits of detection. GMTs <1:10 were given an arbitrary value of 5. ** indicates an adjusted p-value of 0.0017 compared to 17D, following Friedman test with Dunn's multiple comparisons test of all GMTs. **(B)** Bar graphs showing proportion of seropositive (NT_{50} <1:10, black) and seronegative (NT_{50} ≥1:10, grey) amongst vaccinees at 28 days post-vaccination.

4.3.8 DENV immune sera from unvaccinated individuals

Because we found increased potency and breadth of heterologous vaccinee sera against wild-type YFV, we wanted to assess baseline cross-reactivity of DENV-immune sera, without 17D vaccination, against wild-type YFV, a comparison that has not, to our knowledge, been previously

made. We tested 18 primary and 16 secondary DENV-immune sera from individuals who denied prior 17D vaccination (Supplementary Figure 4.7). Six of 34 (23%) were seropositive against 17D, a significantly lower proportion than both 17D-only and 17D heterologous vaccinees, with positive NT_{50} titers ranging from 1:12 to 1:50. Cross-reactivity was greatest against the WA-I strain BA-55, with 59% (20/34) seropositive and a titer range from 1:10 to 1:993, but still significantly lower than either vaccinee group. Finally, cross-reactivity was reduced against the SA-I strain BEH622205, with 26% (9/34) seropositive with an NT_{50} range among the positives of 1:12 to 1:586. The proportion of seropositive sera among DENV-only immunes was significantly lower than both 17D-only and heterologous immune vaccinees, and the GMTs for DENV-only sera against BEH622205 were significantly lower than both vaccinee groups. Taken together, these data demonstrate background cross-neutralization by some DENV-only immune sera against wild-type YFV, but not to the degree that such cross-reactivity alone could explain the greater potency and breadth of heterotypic vaccinee sera against SA-I YFV strains.

Section 4.4: Discussion

To our knowledge, this is the most extensive characterization of the potency and breadth of 17D-vaccinee sera with diverse vaccination and host immune backgrounds. Using a panel of 12 antigenically diverse and genotypically representative wild-type yellow fever strains, we discovered reduced potency of vaccinee sera against these wild-type YFVs compared to the 17D vaccine strain, with the most significant differences observed amongst vaccinees who were, otherwise, orthoflavivirus naïve. Potency was particularly reduced against SA-I genotype viruses, consistent with previous findings by Haslwanter *et al.*, 2022.[88] Importantly, we observed this phenomenon as early as 28 days post-vaccination, raising the possibility of primary vaccine failure amongst most naïve vaccinees against SA-I strains and reduced effectiveness of ring vaccination strategies during SA-I outbreaks. By using a panel of wild-type viruses that represent all known YFV genotypes, we have demonstrated that the potency of 17D-vaccinee sera decreased against wild-type viruses with decreasing amino acid similarity to 17D (Dayhoff distances), with a surprisingly low proportion vaccinees who were seropositive against the SA-I strains.

We identified a key host factor—heterologous orthoflavivirus infection—that significantly increased the potency and breath of 17D-immune sera against SA-I strains, and the proportion of vaccinees who were seropositive against SA-I. Taken together, these data suggest that heterologous orthoflavivirus infection effectively "boosts" the immunity elicited by the 17D vaccine which has implications for 17D vaccination strategies between DENV endemic and non-endemic populations. Interestingly, Haslwanter *et al.* found 88% (21/24) of vaccinees to be seropositive against their SA-I strain, which is similar to the rates of seropositivity against SA-I strain observed amongst our heterologous vaccinees (72-83%). While Haslwanter *et al.* did not characterize orthoflavivirus infection history of their participants, DENV is endemic to Brazil, and we suspect that this cohort may include heterologous vaccinees.

Antigenic cartography is a powerful tool used for surveillance of circulating viruses and vaccine design. Each year, the influenza vaccine is updated to include strains such that the antigenic distance between the vaccine strains and anticipated circulating strains is less than two antigenic units.[245] Here we constructed, to our knowledge, the first antigenic map of wild-type YFVs, finding that SA-I strains form a distinct antigenic cluster and that heterologous vaccinee sera has reduced antigenic distance to SA-I strains compared to 17D only vaccinees, suggesting the potential for increased 17D vaccine efficacy amongst heterologous vaccinees. Beyond defining the antigenic landscape of YFV, continued application of antigenic cartography could enhance surveillance of circulating YFV strains and facilitate the prediction regarding risk of an outbreak within a specific population and potentially inform future vaccine design strategies.

Historically, most studies establishing 17D-elicited neutralization titers have used the 17D vaccine strain and occasionally the parental Asibi strain.[83, 216, 251] Recent studies have found decreased potency of 17D-vaccinee sera, using authentic SA-I strain viruses, isolated during the recent outbreak in Brazil.[17, 88] Haslwanter *et al.*, 2022[88] observed a ~7-8fold reduction between $FRNT_{50}$ between 17DD and SA-I strain ES-504 (n=24) and Goncalves *et al.*, 2024[17] observed ~2-3-fold reduction between 17DD and SA-I strain Hu-BR2018 (n=23) which are similar to the fold-reduction observed amongst our heterologous vaccinees (4.7-7.1). Meanwhile, other data generated using reporter viral particles (RVPs),[88] which may or may not recapitulate the tertiary

and quaternary epitopes formed across adjacent E glycoprotein dimers on the surface of authentic viruses, should be interpreted with care.

Haslwanter *et al.*, 2022[88] additionally demonstrated decreased potency of 17D vaccinee sera amongst 16 non-endemic US vaccinees, but only using RVPs. Using purified monoclonal antibodies and an elegant set of chimeric RVPs they mapped two sites within domain II (EDII) and the DII-DI hinge domain, containing five amino acid substitutions between SA-I and African strains 17D and Asibi; H67N, A83E, D270E, N271S, and N272K, located within the discontinuous sequence encoding EDII that is responsible for the reduced neutralization observed against their SA-I strain. Using our expanded library of authentic viruses consisting of all known genotypes, including three SA-I strains, we confirmed the presence of all five amino acid substitutions in our SA-I strains: Br/MG/2001, BeH622205, and 614819 which was isolated from Panama in 1974. Therefore, these mutations arose at least 42 years before the recent outbreak in Brazil. We also identified the N271S mutation in our representative SA-I strain HEB4263 which trended towards decreased GMTs and fewer seropositive vaccinees compared to 17D and other African wild-type viruses, supporting the previous finding that N271S alone sufficiently impedes neutralization by 17D-immune sera.[88]

Our work does not determine the basis for increased potency of heterologous immune sera against SA-I strains. However, we note that N67 glycosylation is otherwise unique to and highly conserved across the DENV serotypes. For DENV, N67 has been shown to interact with host cell receptor dendritic cell-specific ICAM3 grabbing nonintegrin (DC-SIGN),[252] is required for DENV infectivity and has been implicated in pathogenesis.[243] The cell-mediated process of glycosylation can result in the carbohydrate protrusions that may either contribute to immune evasion by masking key neutralizing epitopes,[253] or by simply altering the topology and therefore epitopes of the virion surface in a glycosylation specific manner. It is striking that 26% of our DENV-only participant sera include antibodies that neutralize Br/MG/2001, and we believe this novel cross-neutralizing effect hints at an underlying antibody selection and affinity maturation in infection with both DENV and 17D vaccine results in the generation of memory B cells that are programmed to secrete antibodies that recognize N67 epitopes.

Specifically, we hypothesize that DENV infection results in the generation of memory B cells (MBCs) capable of recognizing N67 epitopes that have low level cross-reactivity to YFV SA-I strains, even in the absence of 17D vaccination. Similarly, we suspect that vaccination with 17D elicits MBCs with low level cross-reactivity against DENV strains. We propose that following a secondary exposure (heterologous infection or vaccination), affinity maturation of these low-level cross-reactivity MBCs results in the differentiation and proliferation of multiple progeny plasmablast cells that secrete a broad range of NAbs that all contribute to a polyclonal response with enhanced breadth of neutralization, that confers increased cross-reactivity to N67 epitopes and therefore SA-I strains.

Strengths of this study include the use of a diverse, authentic wild-type YFV panel that represents all YFV genotypes, enabling us to establish potency and breadth of the previously unexplored wild-type YFV antigenic landscape. Within our cohort, we found a balanced distribution of years post-vaccination, and a distribution of ages at vaccination that is particularly representative of traveler populations worldwide. Additionally, the balanced distribution of heterologous- and 17D-only vaccinees which was confirmed by serology provides confidence in our finding that heterologous infection plays a role in boosting 17D immunity.

Our study also has limitations. This cohort is relatively small, lacking children, or individuals vaccinated over the age of 69 years, and it is overrepresented by white and female participants so some statistical analyses, particularly of our smaller heterologous- and 17D only vaccinee subsets, should be interpreted with these limitations in mind. We found significantly decreased seropositivity against SA-I strains suggesting an increased rate of primary vaccine failure against SA-I strains, however it is not known if this translates to increased risk of infection. Additionally, our antigenic maps were constructed exclusively using 17D vaccinee immune sera which deviates from typical antigenic cartography utilizing immune sera and homologous viruses, for example, to properly define SA-I strains, sera from an individual naturally infected with a SA-I virus should be included. Importantly, we did not include vaccinees who were >11 years post-vaccination in our study, and so our findings cannot be generalized beyond this interval. Future studies to validate our findings should include larger and more diverse cohorts to ensure generalizability to a broader population.

Our data suggest the potential for increased risk of breakthrough infection with SA-I strains and calls for further evaluation of this risk. 17D breakthrough infections are not systematically reported and the extent to which breakthrough infections have or have not contributed to the large number of cases in South America in the past decade is not known, despite the serious public health implications of such breakthroughs. It is also possible that baseline DENV immunity in highly endemic countries like Brazil confers heterologous immunity which increases resistance to SA-I outbreaks, however this has not been explored. With recent outbreaks and ongoing sylvatic transmission that maintains viral reservoirs within which viral evolution continues, YFV continues to pose a threat to public and global health. Within this context, our study amongst many others' raises the question: is it time to update this historical and important vaccine?

Section 4.5: Materials & Methods

Human research ethics

This study was reviewed by and approved by the Oregon Health & Science University Institutional Review Board (IRB#10212 and #20910). All study participants provided consent upon enrollment.

Study participants

All participants had previously received a single dose of 17D vaccine, which was confirmed by vaccination record or serology, were ≥18 years of age, and living in the Portland metropolitan area, Oregon, USA at the time of enrollment. Participants were recruited through two observational studies. The first cohort recruited based on prior suspected or confirmed orthoflavivirus infection or history of vaccination with 17D. The second study, conducted in collaboration with Kaiser Permanente Health Research Center, recruited previously unvaccinated individuals based on upcoming scheduled 17D vaccination. Upon enrollment, travel histories, prior infections, and information from vaccination records were documented. orthoflavivirus infection against DENV and Zika virus (ZIKV) was characterized by FRNT.

Serum

Serum was collected in serum separator tubes, allowed to clot at room temperature for ≥30 minutes before centrifugation at 1000 x g for 10 minutes. Serum was heat inactivated at 56°C for 30 minutes and stored at -20°C or -80°C until use.

Viruses

Viruses were obtained from the Centers for Disease Control and Prevention (CDC) and the World Reference Center for Emerging Viruses and Arboviruses (WRCEVA) at the University Texas Medical Branch (UTMB). The following viruses were used: Ogbomosho (WA-I), BA-55 (WA-I), Asibi (WA-II), Jose Cachatra (WA-II), Uganda48a (EA), BC-7914 (EA), Couma (ECA), 14FA (A), Br/MG2001 (SA-I), BeH622205 (SA-I), 614819 (SA-I), HEB 4263 (SA-II) and IQT 5591 (SA-II). All unfixed viruses were handled within the Biosafety Level 3 (BSL-3) facility at OHSU.

Virus sequencing

Viral RNA was extracted using the *Quick*-RNA Viral Kit (Zymo Research Corporation, catalog #R1034). Complementary DNA (cDNA) was synthesized using the primer YFVAmp2A and the SuperScript III First-Strand Synthesis System (Thermo Fisher,catalog #18080051). To synthesize cDNA, 1µL 10µM YFVAmp2A, 1µL 10mM dNTP Mix, 10µL RNA, and 13µL DEP-C treated water were combined, mixed, and incubated at 65°C for 5 minutes, then placed on ice for 2 minutes. A separate mix of 2µL 10x RT Buffer, 4µL 25mM $MgCl_2$, 2µL 0.1M DTT, and 1µL 40 U/µL RNase OUT was prepared, added to the previous mix, and incubated at 25°C for 2 minutes. 1µL 200 U/µL SuperScript III RT was then added to each tube and incubated in the thermocycler under the following conditions: 50°C for 1 hour, then 85°C for 5 minutes. PCR amplification of the prM, E and NS1 genes was performed using Phusion High-Fidelity DNA Polymerase (New England Biolabs) and primers YFVAmp1A and YFVAmp2A. Fifty µL reactions were prepared,

composed of 5µL cDNA, 2.5µL 2000 U/mL Phusion polymerase, 2.5µL 10µM forward primer (YFVAmp1A), 2.5µL 10µM reverse primer (YFVAmp2A), 1µL 10mM dNTPs, 1.5uL 100% DMSO, 10µL 5x Phusion HF Reaction Buffer, and 25µL molecular biology-grade water. Thermocycler conditions were as follows: 98°C for two minutes, 35 cycles of 98°C for 10 seconds, 60°C for 20 seconds, and 72°C for two minutes and 18 seconds, followed by 72°C for 5 minutes. PCR products were visualized on 1% agarose gel with SYBR Safe DNA gel stain (Thermo Fisher, catalog #S33102). The band of interest (approximately 3.5kb) was excised and purified using the QIAquick Gel Extraction kit (Qiagen, catalog #28704) per the manufacturer's instructions. Purified products were sequenced commercially (Genewiz), via Sanger sequencing. Primers 857R_YFV, 996F_YFV, 1300F_YFV, 1520R_YFV, 2144F_YFV, 2340R_YFV, 2843F_YFV, 3010R_YFV, YFVAmp1A, and YFVSeq2A (Table xx) were used to sequence the region of interest. Additional primers, 1805F_Couma, 3011R_Couma, and 2466R_Couma, were designed specifically for the Couma YFV strain due to poor performance in some areas of the sequence. Contigs were assembled from .ab1 files and aligned using Geneious Prime (version 2024.0.7). Geneious Prime (version 2024.0.7) was used to assemble contigs from .ab1 files and align them to a consensus sequence derived from an untrimmed alignment of 14 YFV sequences from GenBank.

Phylogenetic analysis

Phylogenetic analysis was conducted in MEGA11.[254, 255] The evolutionary history was inferred by using the Maximum Likelihood method and Dayhoff matrix-based model.[256] Initial tree(s) for the heuristic search were obtained automatically by applying Neighbor-Join and BioNJ algorithms to a matrix of pairwise distances estimated using the Dayhoff model, and then selecting the topology with superior log likelihood value. A discrete Gamma distribution was used to model evolutionary rate differences among sites (5 categories (+G, parameter = 0.7260)). The tree is drawn to scale, with branch lengths measured in the number of substitutions per site. This analysis involved 16 amino acid sequences. There was a total of 493 positions in the final dataset. Evolutionary analyses were conducted in MEGA11.[254, 256]

Virus propagation

All unfixed viruses were handled within a biosafety level 3 (BSL-3) facility at OHSU, except for 17D which was handled at BSL-2. Viruses were propagated in Vero-furin (VF) cells (VFc2). T75 flasks (Fisherbrand, FB012937) were seeded with 5E06 cells (< p25) in 12mL of VF media: MEM/EBSS (Hyclone, SH30024.01) supplemented with L-glutamine (Gibco, 25030-081) non-essential amino acids (NEAA; Gibco, 11140-050), antibiotic-antimycotic (Gibco, 15240-062), 10% v/v fetal bovine serum (FBS; Avantor, 89510-186), and 460µg/mL G148 (Thermo, 10131035) and incubated at 37°C, 5% CO_2 overnight. Near confluent flasks were washed with 25mL of Dulbecco's phosphate buffered saline (dPBS; HyClone, SH30256.01). Virus was either thawed at room temperature (RT) or reconstituted with dilution media (DM; MEM/EBSS with antibiotic-antimycotic and glutamine) and added to flasks in 4mL of DM, rocked every 15 minutes at 37°C, 5% CO_2 for 1 hour before the inoculum was discarded and 12mL of Vero complete media (VCM; MEM/EBSS with 10% FBS, antibiotic-antimycotic, L-glutamine) added. Flasks were observed for cytopathic effect (CPE) and tissue culture supernatants harvested when CPE was ≥40%. Tissue culture supernatants were clarified at 1000 x g for 10 minutes at RT, resuspended in 10% v/v sucrose phosphate glutamate (SPG; 2.18M sucrose, 38mM KH_2PO_4, 72mM K_2HPO4, 60mM L-Glutamic acid), and stored at -80°C for ≥48 hours before use. Seed stocks (p1) were propagated with an unknown multiplicity of infection (MOI) using 100µL of virus suspension and used to propagate working stocks (p2) using an MOI of 0.01, and viruses were harvested 4-6 days post infection. All assay described here were performed using single batch p2 virus stocks.

Focus reduction neutralization assay (FRNT)

Methods were adapted from established in-house protocols used for 17D, DENV and ZIKV.[248] Vero cells were seeded in 96-wells plates at 2 x 10^4 cells per well in 200µL of VCM, and incubated at 37°C, 5% CO_2, overnight. Using U-bottom plates, participant serum (6µL) was diluted 4-fold in VDM starting at 1:5 through 1:1280 (working dilution), for a final volume of 45µL per well. Biological duplicates of serum dilutions were prepared for each virus, with a virus only control well per each serum-dilution. Virus was thawed at RT and diluted to 2X in DM to obtain 40-150 foci per well. Virus-serum inoculums were made by adding 45µL of virus the diluted serum (1:1)

to give final serum dilutions of 1:10 through 1:2560 which were incubated for 45-60 minutes at 37°C, 5% CO_2 to allow binding of neutralizing antibodies to the surface of virions. For infection of cell monolayers, plates were retrieved from the incubator and VCM media discarded. Thirty microliters of virus-serum inoculum were added carefully by pipetting down the side of wells, so as not to disturb the cell monolayer, and rocked immediately to ensure even distribution of the inoculum over the cell monolayer. Infected plates were incubated for 45-60 minutes at 37°C, 5% CO_2 and rocked manually every 15 minutes. Cells were overlaid with overlay media OptiMEM (Gibco, 31985-070) supplemented with NEAA, antibiotic-antimycotic and 10% v/v FBS. Infected plates were incubated for 48±6 hours (Couma) or 68±4 hours for all other viruses. On the second- or third-day post infection, overlay media was removed and plates were washed once with dPBS and fixed with 4% paraformaldehyde (Sigma, P6148) before removing from the BSL-3. Plates were incubated overnight at 4°C with 150µL of blocking buffer (BB; PBS with 2% heat inactivated normal goat serum, (Rockland Immunochemicals Inc., 0204-00-0100), and 0.4% Titron-X) per well and then incubated overnight again at 4°C with 30µL of primary antibody 1mg/mL 4G2 (hybridoma-derived ATCC cat #HB-112) diluted 1:750 in BB. The following day, plates were washed three times with dPBS and incubated for 46-60 minutes with 30 µL secondary Horse Radish Peroxidase goat-anti-mouse-IgG antibody (BioLegend, Cat# 405306) diluted 1:1000 in BB and subsequently protected from light. Plates were washed three times with dPBS and 30µL of TrueBlue™ Peroxidase Substrate (Kirkegaard & Perry Laboratories Inc., 5510-0050) added per well. Plates were allowed to develop for a ≥20 minutes until foci were clearly visible by eye (occasionally overnight), quenched with water and allowed to air-dry for 20 minutes. Wells were imaged, and foci counted, and quality controlled using controlled using a CTL ImmunoSpot 7.0.26.0 (Cellular Technology LTD, Cleveland, OH, USA). $FRNT_{50}$ were calculated in GraphPad Prism® (version 10.3.0) using a sigmoidal dose-response curve fitting percent neutralization against serum-dilution.

Antigenic cartography

Antigenic maps were constructed as previously described[245, 246, 248] using $FRNT_{50}$ data produce for our core 36 participants against 17D and 12 wildtype viruses, using the Racmacs package in R (version 4.3.1) and RStudio (version 2023.06.1+524).

Statistical methods

Statistical analyses were conducted GraphPad Prism® (version 10.3.0) and JMP® (version 17.2.0). After establishing our log-transformed GMT data was not normally distributed, specifically for SA-I strains which skew-right, we employed non-parametric statistical analyses. Friedman test with Dunn's multiple pairwise comparisons was used to compare pooled GMTs, chi-squared was used to compare the proportion of seropositive and seronegative vaccines for each virus, and Mann-Whitney U was used to compare GMTs between 17D only and heterologous vaccinees for each virus. For analysis of Dayhoff values against GMTs we first established significance using a Spearman rank correlation and then applied Pearson correlation to use an indicator of fit.

Section 4.6: Acknowledgements

We would like to acknowledge the World Reference Center for Emerging Viruses and Arboviruses for the provision of virus strains Couma, Uganda48a, Ogbomosho, Jose Cachatra, HEB4236, and Asibi. Additionally, we acknowledge the Center for Disease Control Arbovirus Reference Collection for the provision of virus strains Br/MG/2001, BeH622205, BC-7914, BA-55, 614819, and 14FA. We would like to thank Alec Hirsch, PhD, OHSU, Vaccine and Gene Therapy Institute for generously providing the 4G2 antibody. Thank you to Bill Messer for conducting phylogenetic analysis, generating Figure 4.1, for writing the associated methods section, and the results section for DENV-immune sera. Thank you to Abram Estrada for sequencing the viruses and for writing the associated methods sections. Thank you to Courtney Micheletti for help propagating viruses, and for conducting assays using DENV-immune sera. Thank you to Shuhua Luo, Sam Osman, and

Chad Nix for conducting 17D neutralization assays. Thank you to Sophia Hu, who helped with quality control.

Section 4.7: Supplementary materials

Figure[4.S1]

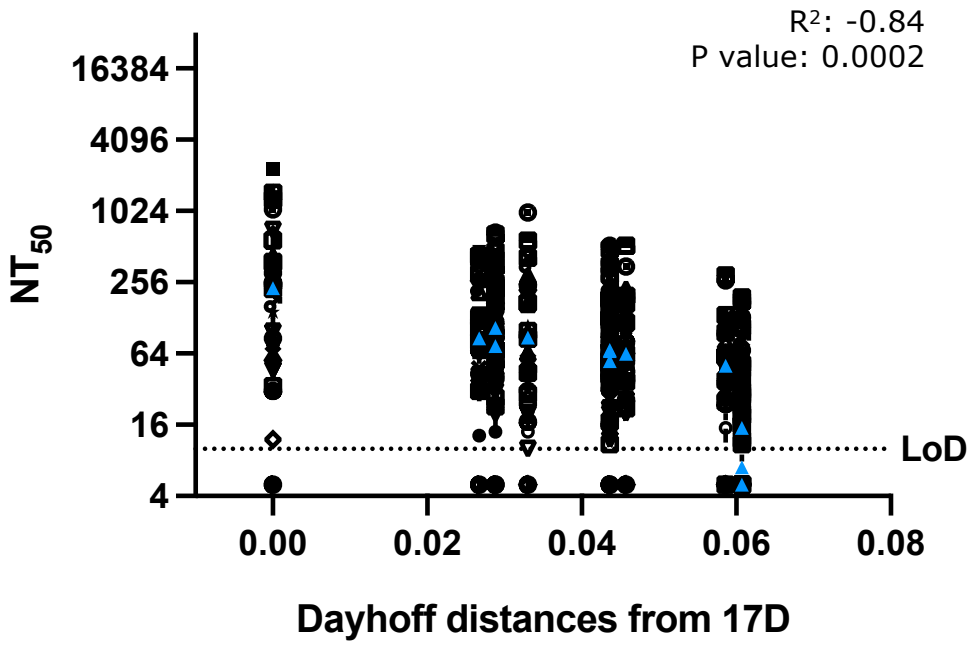

[Figure 4.S1]

Figure 4.S1 NTs versus Dayhoff distances from 17D

Dayhoff distance for each virus are shown in Table 4.S1. Each dot represents the geometric mean titer (GMT) of a single participant serum, calculated from biological duplicates. Blue triangles indicate median GMT for individual viruses. Pearson R^2 calculated excluding the median value for 17D.

Table 4.S1

857R_YFV	AGCCATCTCTCAATCTTYTGS
996F_YFV	YGACAGRGAYTTCATTGAGGG
1300F_YFV	GGGAAAGGRAGCATTGTGG
1520R_YFV	CAYTCCAGTGTRGCTTTYCC
2144F_YFV	ACAAAGARGGAAGYTCAATAGG
2340R_YFV	GACCTTTGTTATCCAGYTCAAGC
2843F_YFV	ATGGAAGCTTCATCATAGAYGG
3010R_YFV	CACCCARGATRGATCCATCR
YFVAmp1A	ACCTTCAAGAGGTGTTCAAGG
YFVAmp2A	CTCCTCCATTGTTCATCTCATG
YFVSeq2A_R	CTATCATCATGCTCACCAAMCC
1805F_Couma	GGTGGTCATGTCTCTT
2129F_Couma	TCAGTCTTGAGTCTCC
3011R_Couma	TGCACCTAGTATAGCC
2466R_Couma	GCACATCCTTGGTCTGCC

[Table 4.S1]

Takkle 4.S1 Table of primers

Table 4.S2

Virus strain	Dayhoff distance from 17D	Pooled GMTs – all vaccinees	Pooled GMTs – 17D only	Pooled GMTs – Heterologous
17D vaccine	0.0	162	207	127
Asibi	0.0267	83	108	63
Jose Cachatra	0.0288	96	112	82
Ogbomosho	0.0288	69	57	83
BA-55	0.0330	75	92	60
Uganda48a	0.0436	52	55	49
BC-7914	0.0436	66	70	62
14FA	0.0436	56	71	45
Couma	0.0457	58	71	47
HEB4263	0.0586	40	41	39
Br/MG/2001	0.0607	18	12	27
BEH622205	0.0607	13	8.9	18
614819	0.0607	13	8.3	21

[Table 4.S2]

Table 4.S1 Dayhoff distances and pooled GTMs for all-, 17D only-, and heterologous vaccinees.

Figure[4.S2]

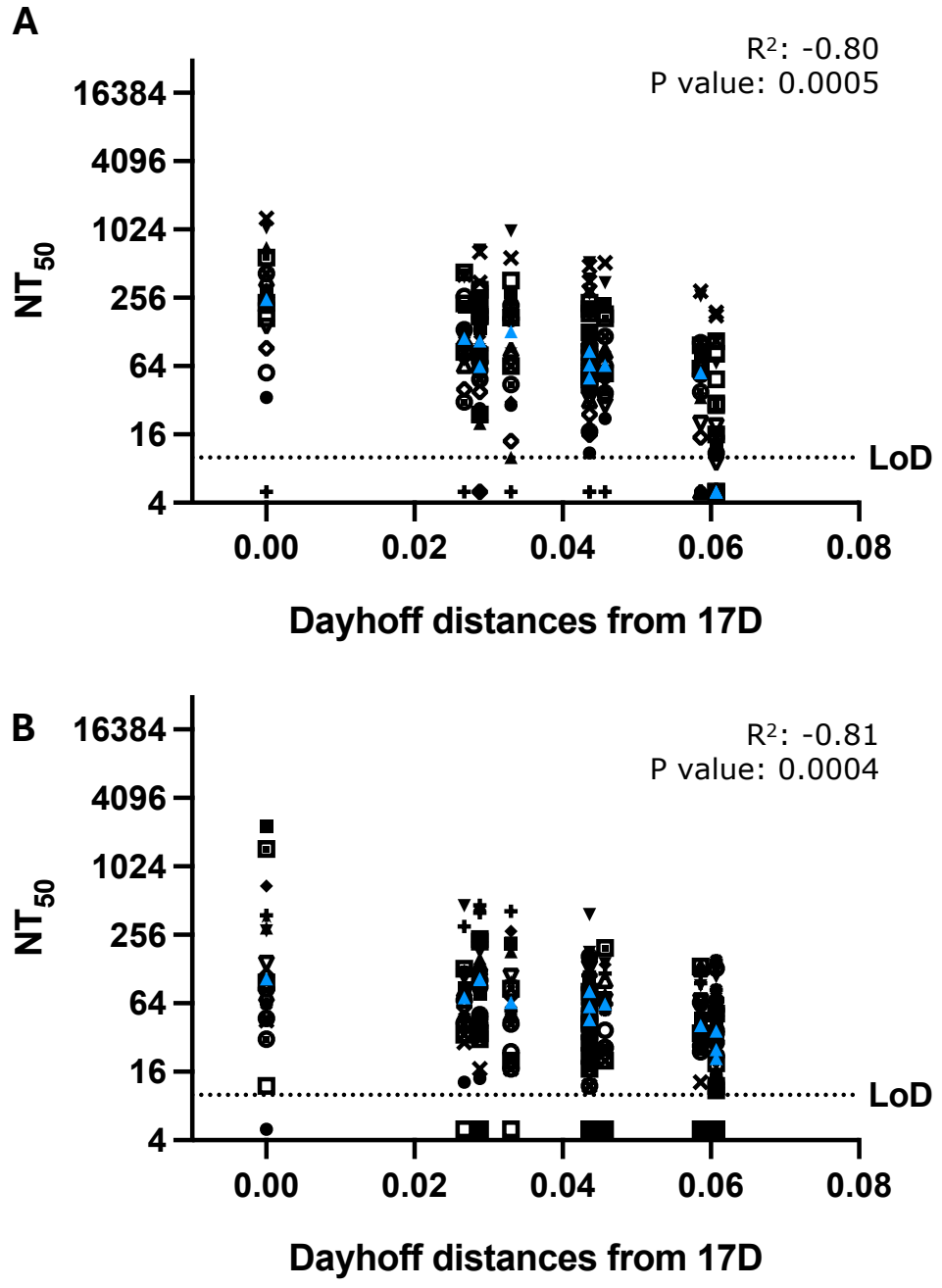

[Figure 4.S2]

[4.S2] NTs versus Dayhoff distances from 17D

(A) 17D only vaccinees, and **(B)** heterologous vaccinees. Dayhoff distance for each virus are shown in Table 4.S1. Each dot represents the geometric mean titer (GMT) of a single participant serum, calculated from biological duplicates. Blue triangles indicate median GMT for individual viruses. Pearson R^2 calculated excluding the median value for 17D.

Table[4.S3]

Virus strain	All vaccinees	17D only	Heterologous	Fold-antigenic difference (17D only – heterologous)
17D vaccine	1.06	0.98	0.96	0.02
Asibi	1.40	1.37	1.19	0.18
Jose Cachatra	1.37	1.35	1.12	0.24
Ogbomosho	1.49	2.33	1.00	1.32
BA-55	1.46	1.62	1.45	0.16
Uganda48a	2.07	2.38	1.73	0.65
BC-7914	1.66	1.87	1.48	0.39
14FA	1.89	2.00	1.74	0.26
Couma	1.84	1.92	1.70	0.22
HEB4263	2.44	2.76	2.01	0.75
Br/MG/2001	3.72	4.69	2.79	1.90
BEH622205	4.25	5.08	3.15	1.93
614819	4.14	5.17	3.07	2.10

[Table 4.S3]

Table 4.S3 Antigenic distances between virus strains and sera

Table of median antigenic distances between sera and viruses, extracted from antigenic cartography models constructed using total-, 17D-only-, and heterologous vaccinee sera (Figure 4.6A, B, and C). Values represent antigenic units corresponding to a single box within the antigenic map, where each box represents a two-fold serum dilution of a neutralization titer.

Figure[4.S3]

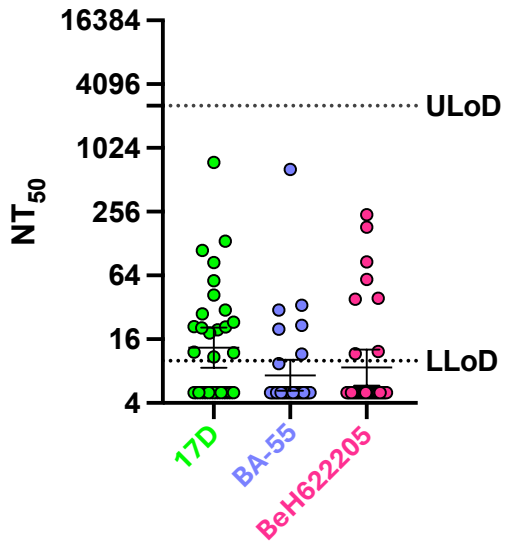

[Figure 4.S3]

Figure 4.S3 Cross-neutralization of DENV-immune unvaccinated participants

Chapter 5: Thesis Summary

Section 5.1: Highlights

5.1.1 Chapter 2 highlights: Breakthroughs and insights: a comprehensive review of yellow fever vaccine breakthrough infection across 8 decades

1. Our review provides an important update on breakthrough YF infection since the ACIP GRADE evaluation in 2015, including contemporary outbreaks.
2. Breakthrough infection results in a range of disease severity.
3. The low proportion of breakthrough cases amongst severe cases suggests the potential for protective efficacy of the 17D vaccine against severe disease.
4. Inconsistent case definitions, inadequate records of vaccination status, and the absence of prospective studies, impede the overall quality of data on breakthrough infection.
5. Unsubstantiated claims of "lifelong" immunity contribute to underreporting of breakthrough infection.

5.1.2 Chapter 3 highlights: Optimization of the micro-immunofocus assay for use with wild-type yellow fever viruses

1. Almost all studies of wild-type YFVs have previously relied on the time- and resource intensive plaque assay.
2. The micro-focus assay is compatible with YFV strains that represent of all seven genotypes.
3. With increased throughput, reduced cost, and more rapid results, the focus assay significantly more accessible, with important application in surveillance of emerging strains and diagnostics.

5.1.2 Chapter 4 highlights: New insights into an old vaccine: potency and breadth of the yellow fever vaccine 17D-elicted neutralizing antibodies is enhanced by heterologous Orthoflavivirus *infection*

1. Current knowledge of the 17D-elciited NAbs and vaccination policy relies on neutralization data generated almost exclusively using the 17D vaccine strain.
2. Until now, the capacity of the 17D-elicited neutralizing antibodies to neutralize wild-type YFVs represented a huge knowledge gap with significant implications for public and global health.
3. 17D-vaccinee sera has reduced potency against SA-I strains, which has been previously attributed to five amino acid substitutions within the E glycoprotein.
4. The E N67 residue found exclusively in SA-I amongst YFV strains is a highly conserved glycosylation site found exclusively in DENV amongst orthoflaviviruses.
5. Our work establishes potency and breadth of 17D immune sera against all seven YFV genotypes within a previously unexplored antigenic landscape.
6. Potency and breadth of 17D-elicited NAbs are boosted by heterologous orthoflavivirus infection.
7. Reduced potency of NAbs at 28 days post-vaccination suggests an increased risk of primary vaccine failure against SA-I strains.

Section 5.2: Future Directions

Our much-needed review of breakthrough YF infection has highlighted limitations within the field that warrant attention. Within the context of endemic countries and outbreaks, we call for improved documentation of vaccination status, by both governmental and public health agencies and researchers alike. Additionally, we emphasize the need for collectors of YF and 17D vaccination

data to document the time interval between most recent 17D vaccination dose and infection, which was largely missing from the studies we reviewed, and could provide valuable insight into the controversial topic regarding the need for booster doses. Moving forward, we propose the design and execution of robust prospective studies in endemic regions, as has been done with dengue,[257] with the goal of capturing breakthrough infection events in real-time. With a longitudinal study design, one could identify NAbs thresholds below which breakthrough infection occurs, detect boosting of NAbs as the result of asymptomatic infection, and monitor NAbs kinetics over time. Studies such as these would provide valuable insight regarding the incidence of primary versus secondary 17D vaccine failure.

Our data showing 29% seronegativity against SA-I strain Br/MG/2001 at 28 days post-vaccination suggests an increased risk of primary vaccine failure against SA-I amongst orthoflavivirus naïve vaccinees that has not been previously described. However, these data are preliminary and warrant validation user a larger cohort of individuals. In June 2022, we established our Yellow fever Long-Term Immunity Study (Yellow LoTIS), recruiting prospective 17D vaccinees with no prior orthoflavivirus immunity. Through this study, we have established a biobank of pre- and post-vaccination serum samples, with 28 days samples for over 70 participants. Using these samples, we will perform neutralization assays against SA-I strains and others to validate our preliminary findings that have significant implications regarding 17D vaccine efficacy and risk of breakthrough infection.

To test our hypothesis that increased potency of NAbs and seropositivity against SA-I strains amongst our heterologous vaccinees is mediated through the production of cross-reactive antibodies that recognize epitopes containing the N67 glycosylation site, we propose to generate chimeric YFV viruses with single nucleotide mutations. Per our hypothesis, we expect that introduction of an SA-I strain H67N substitution into the 17D vaccine strain will result in reduced neutralization by our 17D-only vaccinee sera, with unchanged potency of neutralization by our heterologous vaccinee sera. By generating the reciprocal chimeric virus—introducing an N67H

substitution into SA-I strain viruses—we expect increased neutralization by 17D-only vaccine sera, with no changes in neutralization observed amongst out heterologous vaccinees.

Finally, to validate our findings that heterologous orthoflavivirus infection boosts 17D-elicited immunity against SA-I strains, we propose a clinical trial involving 17D vaccination of individuals with prior DENV immunity. To conduct our study, we will recruit DENV-immune individuals from our existing cohort of >200 individuals with serological evidence of orthoflavivirus infection. First, we will use pre-vaccination serum samples to establish baseline neutralization titers against SA-I strains and compare them to paired samples taken 28-days post-vaccination, which we expect to increase. Additionally, we will compare 28-day post-vaccination neutralization titers between these DENV-immune vaccinees to our orthoflavivirus naïve cohort discussed above, where we expect to see an increased proportion of vaccinees against SA-I strains amongst vaccinee participants with prior DENV immunity. Based on a power calculation using the observed differences in seropositivity against SA-I strain Br/MG/2001 which was the least significant SA-I strain in our analyses (Figure 4.4B), between 17D-only and heterologous vaccinees, we determined that enrolling a minimum of 46 participants would be necessary to achieve 80% power (with an alpha level of 0.05). Beyond NAbs, we propose to identify and characterize pre-vaccination DENV-specific plasmablast, MBC lineages, and T follicular helper cells that preferentially expand following 17D vaccination. We believe these results will be instrumental in shaping future and improved vaccination strategies.

Section 5.3: References

1. McNeill JR. Yellow jack and geopolitics: environment, epidemics, and the struggles for empire in the American tropics. The Environment and World History. 2004;27(4):22.
2. Barrett AD. Yellow Fever in Angola and Beyond--The Problem of Vaccine Supply and Demand. N Engl J Med. 2016;375(4):301-3. Epub 20160608. doi: 10.1056/NEJMp1606997. PubMed PMID: 27276108.
3. Hall CM. The saffron scourge in New Orleans. Country Roads. 2018 23 March 2018.
4. Runge JS. Yellow Fever and the Emotional Consequences of Untreatable Epidemic Disease. Einstein Journal of Biology and Medicine. 2015;30(30):7.
5. Prinzi A. History of Yellow Fever in the U.S.: American Society for Microbiology; 2021 [updated 17 May 2021; cited 2024 11 July 2024]. Available from: https://asm.org/articles/2021/may/history-of-yellow-fever-in-the-u-s.
6. Kopperman PE. "Venerate the Lancet": Benjamin Rush's yellow fever therapy in context. Bull Hist Med. 2004;78(3):539-74. doi: 10.1353/bhm.2004.0126. PubMed PMID: 15356370.
7. Johansson MA, Vasconcelos PF, Staples JE. The whole iceberg: estimating the incidence of yellow fever virus infection from the number of severe cases. Trans R Soc Trop Med Hyg. 2014;108(8):482-7. Epub 20140630. doi: 10.1093/trstmh/tru092. PubMed PMID: 24980556; PMCID: PMC4632853.
8. Gershman M, Staples JE. Yellow Fever, CDC Yellow Book 2024: Centers for Disease Control and Prevention; 2024 [cited 2024 4/19/2024]. Available from: https://wwwnc.cdc.gov/travel/yellowbook/2024/infections-diseases/yellow-fever#risk.
9. Simon LV, Hashmi MF, Torp KD. Yellow Fever: StatPearls Publishing; 2024. Available from: https://www.ncbi.nlm.nih.gov/books/NBK470425/.
10. Jones EM, Wilson DC. Clinical features of yellow fever cases at Vom Christian Hospital during the 1969 epidemic on the Jos Plateau, Nigeria. Bull World Health Organ. 1972;46(5):653-7. PubMed PMID: 4538038; PMCID: PMC2480786.
11. Staples JE, Martin S. Control of Communicable Disease Manual. 21st ed. Heymann DL, editor: APHA; 2024.
12. Weir E, Haider S. Yellow fever: readily prevented but difficult to treat. CMAJ. 2004;170(13):1909-10. doi: 10.1503/cmaj.1040826. PubMed PMID: 15210636; PMCID: PMC421715.

13. CDC. Yellow Fever: Symptoms, Diagnosis, and Treatment 2024 [cited 2024 August 14, 2024]. Available from: https://www.cdc.gov/yellow-fever/symptoms-diagnosis-treatment/index.html#:~:text=Initial%20symptoms%20can%20include%20sudden,tired)%20might%20last%20several%20months.

14. Denis B, Chirio D, Ponscarme D, Brichler S, Colin de Verdiere N, Simon F, Molina JM. Hepatitis Rebound after Infection with Yellow Fever Virus. Emerg Infect Dis. 2019;25(6):1248-9. Epub 20190617. doi: 10.3201/eid2506.190069. PubMed PMID: 30870138; PMCID: PMC6537733.

15. Rezende IM, Pereira LS, Fradico JRB, Pascoal Xavier MA, Alves PA, Campi-Azevedo AC, Speziali E, Dos Santos LZM, Albuquerque NS, Penido I, Santos TA, Bom A, da Silva AMV, Fernandes CB, Calzavara CE, Kroon EG, Martins-Filho OA, Teixeira-Carvalho A, Drumond BP. Late-Relapsing Hepatitis after Yellow Fever. Viruses. 2020;12(2). Epub 20200217. doi: 10.3390/v12020222. PubMed PMID: 32079143; PMCID: PMC7077229.

16. Osorio FMF, Cancado GGL, Nardelli MJ, Vidigal PVT, Xavier MAP, Clemente WT. Hepatitis Relapse after Yellow Fever Infection: Is There Another Wave? Rev Soc Bras Med Trop. 2020;53:e20200152. Epub 20200622. doi: 10.1590/0037-8682-0152-2020. PubMed PMID: 32578715; PMCID: PMC7310355.

17. Goncalves AP, Almeida LT, Rezende I, Fradico JRB, Pereira LS, Ramalho DB, Pascoal Xavier MA, Calzavara Silva CE, Monath TP, LaBeaud AD, Drumond BP, Campi-Azevedo AC, Martins-Filho OA, Teixeira-Carvalho A, Alves PA, Grupo de Estudos de Pesquisa e Resposta em Febre Amarela do Estado de Minas G. Evaluation of humoral immune response after yellow fever infection: an observational study on patients from the 2017-2018 sylvatic outbreak in Brazil. Microbiol Spectr. 2024;12(5):e0370323. Epub 20240321. doi: 10.1128/spectrum.03703-23. PubMed PMID: 38511952; PMCID: PMC11064539.

18. Rezende IM, McClure MA, Pereira LS, Fradico JRB, Cenachi ARC, Moura AS, Paladino LLA, Dutra MRT, Alves PA, Xavier MAP, Said R, Ramalho DB, Gama TDP, Martins-Filho OA, Monath TP, Teixeira-Carvalho A, Drumond BP, LaBeaud AD, Yellow Fever Collaborative G. Characterization and Investigation of Risk Factors for Late-Relapsing Hepatitis After Yellow Fever. Clin Infect Dis. 2023;77(4):565-73. doi: 10.1093/cid/ciad249. PubMed PMID: 37099356; PMCID: PMC10444002.

19. Fradico JRB, Campi-Azevedo AC, Speziali E, do Valle Antonelli LR, Peruhype-Magalhaes V, de Rezende IM, Alves PA, Pascoal-Xavier MA, Pereira LS, Dutra MRT, Ramalho DB, Cenachi A, de Paula L, Santos TA, do Carmo Said RF, Calzavara-Silva CE, Coelho-Dos-Reis JGA, de Magalhaes CR, Rabelo LLC, Valim V, Brito-de-Sousa JP, da Costa-Rocha IA, de Souza Gomes M, Amaral LR, de Lima SMB, Trindade GF, Santos RT, da Silva JFA, Monath T, LaBeaud AD, Drumond BP, Martins-Filho OA, Teixeira-Carvalho A, Yellow Fever Collaborative G. Serum soluble mediators as prognostic biomarkers for morbidity, disease outcome, and late-relapsing hepatitis in yellow fever patients. Clin Immunol. 2023;251:109321. Epub 20230403. doi: 10.1016/j.clim.2023.109321. PubMed PMID: 37019421.

20. CDC. Yellow Fever 2019 Case Definition: U.S. Department of Health & Human Services; 2019 [updated April 16, 2021; cited 2024]. Available from: https://ndc.services.cdc.gov/case-definitions/yellow-fever-2019/.

21. PAHO, WHO. Laboratory Diagnosis of Yellow Fever Virus infection 2018 [updated 9 September 2018; cited 2024 18 February 2024]. Available from: https://www.paho.org/en/documents/laboratory-diagnosis-yellow-fever-virus-infection.

22. data I-. 2024 ICD-10-CM Diagnosis Code A95.9 2023 [cited 2024]. Available from: https://www.icd10data.com/ICD10CM/Codes/A00-B99/A90-A99/A95-/A95.9#:~:text=Yellow%20fever%2C%20unspecified,-2016%202017%202018&text=Billable%2FSpecific%20Code-,A95.,a%20diagnosis%20for%20reimbursement%20purposes.

23. CDC. Treatment and Prevention of Yellow Fever 2024 [updated May 14, 2024; cited 2024 August 15, 2024]. Available from: https://www.cdc.gov/yellow-fever/hcp/treatment-prevention/index.html#:~:text=Treatment-,There%20is%20no%20specific%20treatment%20for%20yellow%20fever%3B%20clinical%20management,use%20of%20analgesics%20and%20antipyretics.

24. WHO. Yellow fever 2023 [updated May 31, 2023; cited 2024 August 16, 2024]. Available from: https://www.who.int/news-room/fact-sheets/detail/yellow-fever.

25. Garske T, Van Kerkhove MD, Yactayo S, Ronveaux O, Lewis RF, Staples JE, Perea W, Ferguson NM, Yellow Fever Expert C. Yellow Fever in Africa: estimating the burden of disease and impact of mass vaccination from outbreak and serological data. PLoS Med.

2014;11(5):e1001638. Epub 20140506. doi: 10.1371/journal.pmed.1001638. PubMed PMID: 24800812; PMCID: PMC4011853.

26. Mutebi JP, Barrett AD. The epidemiology of yellow fever in Africa. Microbes Infect. 2002;4(14):1459-68. doi: 10.1016/s1286-4579(02)00028-x. PubMed PMID: 12475636.

27. Nasidi A, Monath TP, DeCock K, Tomori O, Cordellier R, Olaleye OD, Harry TO, Adeniyi JA, Sorungbe AO, Ajose-Coker AO, et al. Urban yellow fever epidemic in western Nigeria, 1987. Trans R Soc Trop Med Hyg. 1989;83(3):401-6. doi: 10.1016/0035-9203(89)90518-x. PubMed PMID: 2617590.

28. Nwaiwu AU, Musekiwa A, Tamuzi JL, Sambala EZ, Nyasulu PS. The incidence and mortality of yellow fever in Africa: a systematic review and meta-analysis. BMC Infect Dis. 2021;21(1):1089. Epub 20211023. doi: 10.1186/s12879-021-06728-x. PubMed PMID: 34688249; PMCID: PMC8536483.

29. Alhakimi HA, Mohamed OG, Khogaly HSE, Arafa KAO, Ahmed WA. Epidemiological, Clinical and Entomological Characteristics of Yellow Fever Outbreak in Darfur 2012. AIMS Public Health. 2015;2(1):132-41. Epub 20150325. doi: 10.3934/publichealth.2015.1.132. PubMed PMID: 29546100; PMCID: PMC5690374.

30. Nemg FBS, Abanda NN, Yonga MG, Ouapi D, Samme IE, Djoumetio MD, Endegue-Zanga MC, Demanou M, Njouom R. Sustained circulation of yellow fever virus in Cameroon: an analysis of laboratory surveillance data, 2010-2020. BMC Infect Dis. 2022;22(1):418. Epub 20220429. doi: 10.1186/s12879-022-07407-1. PubMed PMID: 35488234; PMCID: PMC9055699.

31. WHO. Yellow fever – African Region (AFRO) 2024 [cited 2024 August 5, 2024]. Available from: https://www.who.int/emergencies/disease-outbreak-news/item/2024-DON510.

32. Monath TP, Craven RB, Adjukiewicz A, Germain M, Francy DB, Ferrara L, Samba EM, N'Jie H, Cham K, Fitzgerald SA, Crippen PH, Simpson DI, Bowen ET, Fabiyi A, Salaun JJ. Yellow fever in the Gambia, 1978--1979: epidemiologic aspects with observations on the occurrence of orungo virus infections. Am J Trop Med Hyg. 1980;29(5):912-28. doi: 10.4269/ajtmh.1980.29.912. PubMed PMID: 7435793.

33. WHO. Vaccines and vaccination against yellow fever. WHO position paper -- June 2013. Wkly Epidemiol Rec. 2013;88(27):269-83. PubMed PMID: 23909008.

34. Chopra H, Patel N, Sethi Y, Emran TB. Resurgence of yellow fever in Africa in 2022: a glance on protective measures. Int J Surg. 2023;109(2):112-4. Epub 20230201. doi: 10.1097/JS9.0000000000000117. PubMed PMID: 36799819; PMCID: PMC10389304.

35. Domingo C, Fraissinet J, Ansah PO, Kelly C, Bhat N, Sow SO, Mejia JE. Long-term immunity against yellow fever in children vaccinated during infancy: a longitudinal cohort study. Lancet Infect Dis. 2019;19(12):1363-70. Epub 20190919. doi: 10.1016/S1473-3099(19)30323-8. PubMed PMID: 31543249; PMCID: PMC6892259.

36. WHO. Situation report: yellow fever 2016 [updated October 28, 2016; cited 2024 August 13, 2024]. Available from: https://iris.who.int/bitstream/handle/10665/250661/yellowfeversitrep28Oct16-eng.pdf;jsessionid=F46BF6410A79A8F01D053CBF34FD3FD8?sequence=1.

37. Manuel E, Armando A, Francisco M, Paixao J, Aramburu J, de Oliveira MDS, Freitas H, Pedro AM, Jandondo D, Carderon PB, Lamezon SL, Fortes F, Mariscal J, Cardoso Y, Moreira R, Morais J, Francisco NM. Assessment of the yellow fever outbreak in Angola from December 2015 through December 2016: A retrospective study. Health Sci Rep. 2024;7(2):e1924. Epub 20240215. doi: 10.1002/hsr2.1924. PubMed PMID: 38444843; PMCID: PMC10913757.

38. Ingelbeen B, Weregemere NA, Noel H, Tshapenda GP, Mossoko M, Nsio J, Ronsse A, Ahuka-Mundeke S, Cohuet S, Kebela BI. Urban yellow fever outbreak-Democratic Republic of the Congo, 2016: Towards more rapid case detection. PLoS Negl Trop Dis. 2018;12(12):e0007029. Epub 20181207. doi: 10.1371/journal.pntd.0007029. PubMed PMID: 30532188; PMCID: PMC6300298.

39. Wang L, Zhou P, Fu X, Zheng Y, Huang S, Fang B, Zhang G, Jia K, Li S. Yellow fever virus: Increasing imported cases in China. J Infect. 2016;73(4):377-80. Epub 20160713. doi: 10.1016/j.jinf.2016.07.003. PubMed PMID: 27422700.

40. Chen Z, Liu L, Lv Y, Zhang W, Li J, Zhang Y, Di T, Zhang S, Liu J, Li J, Qu J, Hua W, Li C, Wang P, Zhang Q, Xu Y, Jiang R, Wang Q, Chen L, Wang S, Pang X, Liang M, Ma X, Li X, Wang Q, Zhang F, Li D. A fatal yellow fever virus infection in China: description and lessons. Emerging microbes & infections. 2016;5(7):e69. doi: https://dx.doi.org/10.1038/emi.2016.89.

41. Song R, Guan S, Lee SS, Chen Z, Chen C, Han L, Xu Y, Li A, Zeng H, Ye H, Zhang F. Late or Lack of Vaccination Linked to Importation of Yellow Fever from Angola to China.

Emerg Infect Dis. 2018;24(7):1383-6. Epub 20180717. doi: 10.3201/eid2407.171868. PubMed PMID: 29723485; PMCID: PMC6038747.

42. Wilder-Smith A, Massad E. Estimating the number of unvaccinated Chinese workers against yellow fever in Angola. BMC Infect Dis. 2018;18(1):185. Epub 20180417. doi: 10.1186/s12879-018-3084-y. PubMed PMID: 29665797; PMCID: PMC5905133.

43. Kuno G. The Absence of Yellow Fever in Asia: History, Hypotheses, Vector Dispersal, Possibility of YF in Asia, and Other Enigmas. Viruses. 2020;12(12). Epub 20201125. doi: 10.3390/v12121349. PubMed PMID: 33255615; PMCID: PMC7759908.

44. Brink S. Yellow Fever Timeline: The History Of A Long Misunderstood Disease 2016 [cited 2024 August 16, 2024]. Available from: https://www.npr.org/sections/goatsandsoda/2016/08/28/491471697/yellow-fever-timeline-the-history-of-a-long-misunderstood-disease.

45. Chippaux JP, Chippaux A. Yellow fever in Africa and the Americas: a historical and epidemiological perspective. J Venom Anim Toxins Incl Trop Dis. 2018;24:20. Epub 20180825. doi: 10.1186/s40409-018-0162-y. PubMed PMID: 30158957; PMCID: PMC6109282.

46. de Oliveira Figueiredo P, Stoffella-Dutra AG, Barbosa Costa G, Silva de Oliveira J, Dourado Amaral C, Duarte Santos J, Soares Rocha KL, Araujo Junior JP, Lacerda Nogueira M, Zaza Borges MA, Pereira Paglia A, Desiree LaBeaud A, Santos Abrahao J, Geessien Kroon E, Bretas de Oliveira D, Paiva Drumond B, de Souza Trindade G. Re-Emergence of Yellow Fever in Brazil during 2016-2019: Challenges, Lessons Learned, and Perspectives. Viruses. 2020;12(11). Epub 20201030. doi: 10.3390/v12111233. PubMed PMID: 33143114; PMCID: PMC7692154.

47. Lowy I. Leaking Containers: Success and Failure in Controlling the Mosquito Aedes aegypti in Brazil. Am J Public Health. 2017;107(4):517-24. Epub 20170216. doi: 10.2105/AJPH.2017.303652. PubMed PMID: 28207332; PMCID: PMC5343710.

48. Cunha MDP, Duarte-Neto AN, Pour SZ, Ortiz-Baez AS, Cerny J, Pereira BBS, Braconi CT, Ho YL, Perondi B, Sztajnbok J, Alves VAF, Dolhnikoff M, Holmes EC, Saldiva PHN, Zanotto PMA. Origin of the Sao Paulo Yellow Fever epidemic of 2017-2018 revealed through molecular epidemiological analysis of fatal cases. Sci Rep. 2019;9(1):20418. Epub 20191231. doi: 10.1038/s41598-019-56650-1. PubMed PMID: 31892699; PMCID: PMC6938505.

49. PAHO. Yellow fever: number of confirmed human cases and deaths in endemic countries of the Americas, since 1960: Pan American Heath Organization Health Emergencies Department World Health Organization; 2023 [1 April 2024]. Available from: https://ais.paho.org/phip/viz/ed_yellowfever.asp.

50. Silva NIO, Sacchetto L, de Rezende IM, Trindade GS, LaBeaud AD, de Thoisy B, Drumond BP. Recent sylvatic yellow fever virus transmission in Brazil: the news from an old disease. Virol J. 2020;17(1):9. Epub 20200123. doi: 10.1186/s12985-019-1277-7. PubMed PMID: 31973727; PMCID: PMC6979359.

51. Garcia-Oliveira GF, Guimaraes A, Moreira GD, Costa TA, Arruda MS, de Mello EM, Silva MC, de Almeida MG, Hanley KA, Vasilakis N, Drumond BP. YELLOW ALERT: Persistent Yellow Fever Virus Circulation among Non-Human Primates in Urban Areas of Minas Gerais State, Brazil (2021-2023). Viruses. 2023;16(1). Epub 20231223. doi: 10.3390/v16010031. PubMed PMID: 38257732; PMCID: PMC10818614.

52. Ferreira F, Bastos Camacho LA, Villela DAM. Occurrence of yellow fever outbreaks in a partially vaccinated population: An analysis of the effective reproduction number. PLoS Negl Trop Dis. 2022;16(9):e0010741. Epub 20220915. doi: 10.1371/journal.pntd.0010741. PubMed PMID: 36108073; PMCID: PMC9514630.

53. Van der Stuyft P, Gianella A, Pirard M, Cespedes J, Lora J, Peredo C, Pelegrino JL, Vorndam V, Boelaert M. Urbanisation of yellow fever in Santa Cruz, Bolivia. Lancet. 1999;353(9164):1558-62.

54. PAHO, WHO. Epidemiological Update Yellow fever in the Region of the Americas 2024 [cited 2024 August 13, 2024]. Available from: https://www.paho.org/en/documents/epidemiological-update-yellow-fever-region-americas-21-march-2024.

55. Postler TS, Beer M, Blitvich BJ, Bukh J, de Lamballerie X, Drexler JF, Imrie A, Kapoor A, Karganova GG, Lemey P, Lohmann V, Simmonds P, Smith DB, Stapleton JT, Kuhn JH. Renaming of the genus Flavivirus to Orthoflavivirus and extension of binomial species names within the family Flaviviridae. Arch Virol. 2023;168(9):224. Epub 20230810. doi: 10.1007/s00705-023-05835-1. PubMed PMID: 37561168.

56. Postler TS, Kuhn JH. Rename one genus and all species in the family to comply with the ICTV-mandated binomial format (Amarillovirales: Flaviviridae)2022.

57. Neufeldt CJ, Cortese M, Acosta EG, Bartenschlager R. Rewiring cellular networks by members of the Flaviviridae family. Nat Rev Microbiol. 2018;16(3):125-42. doi: 10.1038/nrmicro.2017.170. PubMed PMID: 29430005; PMCID: PMC7097628.
58. Simmonds P, Becher P, Bukh J, Gould EA, Meyers G, Monath T, Muerhoff S, Pletnev A, Rico-Hesse R, Smith DB, Stapleton JT, Ictv Report C. ICTV Virus Taxonomy Profile: Flaviviridae. J Gen Virol. 2017;98(1):2-3. doi: 10.1099/jgv.0.000672. PubMed PMID: 28218572; PMCID: PMC5370391.
59. Mukhopadhyay S, Kuhn RJ, Rossmann MG. A structural perspective of the flavivirus life cycle. Nat Rev Microbiol. 2005;3(1):13-22. doi: 10.1038/nrmicro1067. PubMed PMID: 15608696.
60. Hahn CS, Dalrymple JM, Strauss JH, Rice CM. Comparison of the virulent Asibi strain of yellow fever virus with the 17D vaccine strain derived from it. Proc Natl Acad Sci U S A. 1987;84(7):2019-23. doi: 10.1073/pnas.84.7.2019. PubMed PMID: 3470774; PMCID: PMC304575.
61. Pierson TC, Diamond MS. Degrees of maturity: the complex structure and biology of flaviviruses. Curr Opin Virol. 2012;2(2):168-75. Epub 20120323. doi: 10.1016/j.coviro.2012.02.011. PubMed PMID: 22445964; PMCID: PMC3715965.
62. Kuhn RJ, Zhang W, Rossmann MG, Pletnev SV, Corver J, Lenches E, Jones CT, Mukhopadhyay S, Chipman PR, Strauss EG, Baker TS, Strauss JH. Structure of dengue virus: implications for flavivirus organization, maturation, and fusion. Cell. 2002;108(5):717-25. doi: 10.1016/s0092-8674(02)00660-8. PubMed PMID: 11893341; PMCID: PMC4152842.
63. Stiasny K, Kossl C, Lepault J, Rey FA, Heinz FX. Characterization of a structural intermediate of flavivirus membrane fusion. PLoS Pathog. 2007;3(2):e20. doi: 10.1371/journal.ppat.0030020. PubMed PMID: 17305426; PMCID: PMC1797619.
64. Scaturro P, Cortese M, Chatel-Chaix L, Fischl W, Bartenschlager R. Dengue Virus Non-structural Protein 1 Modulates Infectious Particle Production via Interaction with the Structural Proteins. PLoS Pathog. 2015;11(11):e1005277. Epub 20151112. doi: 10.1371/journal.ppat.1005277. PubMed PMID: 26562291; PMCID: PMC4643051.
65. Puerta-Guardo H, Glasner DR, Espinosa DA, Biering SB, Patana M, Ratnasiri K, Wang C, Beatty PR, Harris E. Flavivirus NS1 Triggers Tissue-Specific Vascular Endothelial

Dysfunction Reflecting Disease Tropism. Cell Rep. 2019;26(6):1598-613 e8. doi: 10.1016/j.celrep.2019.01.036. PubMed PMID: 30726741; PMCID: PMC6934102.

66. de Sousa FTG, Warnes CM, Manuli ER, Ng A, D'Elia Zanella L, Ho YL, Bhat S, Romano CM, Beatty PR, Biering SB, Kallas EG, Sabino EC, Harris E. Yellow fever disease severity and endothelial dysfunction are associated with elevated serum levels of viral NS1 protein and syndecan-1. medRxiv. 2023. Epub 20230630. doi: 10.1101/2023.06.29.23292053. PubMed PMID: 37425955; PMCID: PMC10327263.

67. Yu IM, Zhang W, Holdaway HA, Li L, Kostyuchenko VA, Chipman PR, Kuhn RJ, Rossmann MG, Chen J. Structure of the immature dengue virus at low pH primes proteolytic maturation. Science. 2008;319(5871):1834-7. doi: 10.1126/science.1153264. PubMed PMID: 18369148.

68. Smith HH, Penna HA, Paoliello A. Yellow fever vaccination with cultured virus (17D) without immune serum. American Journal of Tropical Medicine. 1938;19(5):437-68.

69. Douam F, Ploss A. Yellow Fever Virus: Knowledge Gaps Impeding the Fight Against an Old Foe. Trends Microbiol. 2018;26(11):913-28. Epub 20180619. doi: 10.1016/j.tim.2018.05.012. PubMed PMID: 29933925; PMCID: PMC6340642.

70. Barba-Spaeth G, Longman RS, Albert ML, Rice CM. Live attenuated yellow fever 17D infects human DCs and allows for presentation of endogenous and recombinant T cell epitopes. J Exp Med. 2005;202(9):1179-84. Epub 20051031. doi: 10.1084/jem.20051352. PubMed PMID: 16260489; PMCID: PMC2213233.

71. Woodson SE, Holbrook MR. Infection of hepatocytes with 17-D vaccine-strain yellow fever virus induces a strong pro-inflammatory host response. J Gen Virol. 2011;92(Pt 10):2262-71. Epub 20110622. doi: 10.1099/vir.0.031617-0. PubMed PMID: 21697351.

72. Engelmann F, Josset L, Girke T, Park B, Barron A, Dewane J, Hammarlund E, Lewis A, Axthelm MK, Slifka MK, Messaoudi I. Pathophysiologic and transcriptomic analyses of viscerotropic yellow fever in a rhesus macaque model. PLoS neglected tropical diseases. 2014;8(11):e3295. doi: https://dx.doi.org/10.1371/journal.pntd.0003295.

73. Vieira WT, Gayotto LC, de Lima CP, de Brito T. Histopathology of the human liver in yellow fever with special emphasis on the diagnostic role of the Councilman body. Histopathology. 1983;7(2):195-208. doi: 10.1111/j.1365-2559.1983.tb02235.x. PubMed PMID: 6303935.

74. Giugni FR, Aiello VD, Faria CS, Pour SZ, Cunha MDP, Giugni MV, Pinesi HT, Ledesma FL, Morais CE, Ho YL, Sztajnbok J, de Morais Fernezlian S, Ferraz da Silva LF, Mauad T, Ferreira Alves VA, Hilario do Nascimento Saldiva P, Antonangelo L, Dolhnikoff M, Duarte-Neto AN. Understanding yellow fever-associated myocardial injury: an autopsy study. EBioMedicine. 2023;96:104810. Epub 20230925. doi: 10.1016/j.ebiom.2023.104810. PubMed PMID: 37757571; PMCID: PMC10550587.

75. Bryant JE, Holmes EC, Barrett AD. Out of Africa: a molecular perspective on the introduction of yellow fever virus into the Americas. PLoS Pathog. 2007;3(5):e75. doi: 10.1371/journal.ppat.0030075. PubMed PMID: 17511518; PMCID: PMC1868956.

76. Domingo C, Charrel RN, Schmidt-Chanasit J, Zeller H, Reusken C. Yellow fever in the diagnostics laboratory. Emerging microbes & infections. 2018;7(1):129. doi: https://dx.doi.org/10.1038/s41426-018-0128-8.

77. Moreira Salles AP, de Seixas Santos Nastri AC, Ho YL, Vilas Boas Casadio L, Emanuel Amgarten D, Justo Arevalo S, Soares Gomes-Gouvea M, Jose Carrilho F, de Mello Malta F, Rebello Pinho JR. Updating the Phylodynamics of Yellow Fever Virus 2016-2019 Brazilian Outbreak With New 2018 and 2019 Sao Paulo Genomes. Front Microbiol. 2022;13:811318. Epub 20220414. doi: 10.3389/fmicb.2022.811318. PubMed PMID: 35633726; PMCID: PMC9132216.

78. Mutebi JP, Wang H, Li L, Bryant JE, Barrett AD. Phylogenetic and evolutionary relationships among yellow fever virus isolates in Africa. J Virol. 2001;75(15):6999-7008. doi: 10.1128/JVI.75.15.6999-7008.2001. PubMed PMID: 11435580; PMCID: PMC114428.

79. de Souza RP, Foster PG, Sallum MA, Coimbra TL, Maeda AY, Silveira VR, Moreno ES, da Silva FG, Rocco IM, Ferreira IB, Suzuki A, Oshiro FM, Petrella SM, Pereira LE, Katz G, Tengan CH, Siciliano MM, Dos Santos CL. Detection of a new yellow fever virus lineage within the South American genotype I in Brazil. J Med Virol. 2010;82(1):175-85. doi: 10.1002/jmv.21606. PubMed PMID: 19950229.

80. Mir D, Delatorre E, Bonaldo M, Lourenco-de-Oliveira R, Vicente AC, Bello G. Phylodynamics of Yellow Fever Virus in the Americas: new insights into the origin of the 2017 Brazilian outbreak. Sci Rep. 2017;7(1):7385. Epub 20170807. doi: 10.1038/s41598-017-07873-7. PubMed PMID: 28785067; PMCID: PMC5547128.

81. Vasconcelos PF, Bryant JE, da Rosa TP, Tesh RB, Rodrigues SG, Barrett AD. Genetic divergence and dispersal of yellow fever virus, Brazil. Emerg Infect Dis. 2004;10(9):1578-84. doi: 10.3201/eid1009.040197. PubMed PMID: 15498159; PMCID: PMC3320275.
82. CDC. Biosafety in Microbiological and Biomedical Laboratories 2020; 6th:[Available from: https://www.cdc.gov/labs/pdf/SF__19_308133-A_BMBL6_00-BOOK-WEB-final-3.pdf.
83. Hepburn MJ, Kortepeter MG, Pittman PR, Boudreau EF, Mangiafico JA, Buck PA, Norris SL, Anderson EL. Neutralizing antibody response to booster vaccination with the 17d yellow fever vaccine. Vaccine. 2006;24(15):2843-9. Epub 20060118. doi: 10.1016/j.vaccine.2005.12.055. PubMed PMID: 16494976.
84. Theiler M, Smith HH. The Effect of Prolonged Cultivation in Vitro Upon the Pathogenicity of Yellow Fever Virus. J Exp Med. 1937;65(6):767-86. doi: 10.1084/jem.65.6.767. PubMed PMID: 19870633; PMCID: PMC2133530.
85. Bredenbeek PJ, Kooi EA, Lindenbach B, Huijkman N, Rice CM, Spaan WJM. A stable full-length yellow fever virus cDNA clone and the role of conserved RNA elements in flavivirus replication. J Gen Virol. 2003;84(Pt 5):1261-8. doi: 10.1099/vir.0.18860-0. PubMed PMID: 12692292.
86. McElroy KL, Tsetsarkin KA, Vanlandingham DL, Higgs S. Characterization of an infectious clone of the wild-type yellow fever virus Asibi strain that is able to infect and disseminate in mosquitoes. J Gen Virol. 2005;86(Pt 6):1747-51. doi: 10.1099/vir.0.80746-0. PubMed PMID: 15914853.
87. Jiang X, Dalebout TJ, Lukashevich IS, Bredenbeek PJ, Franco D. Molecular and immunological characterization of a DNA-launched yellow fever virus 17D infectious clone. J Gen Virol. 2015;96(Pt 4):804-14. Epub 20141216. doi: 10.1099/jgv.0.000026. PubMed PMID: 25516543; PMCID: PMC4811652.
88. Haslwanter D, Lasso G, Wec AZ, Furtado ND, Raphael LMS, Tse AL, Sun Y, Stransky S, Pedreno-Lopez N, Correia CA, Bornholdt ZA, Sakharkar M, Avelino-Silva VI, Moyer CL, Watkins DI, Kallas EG, Sidoli S, Walker LM, Bonaldo MC, Chandran K. Genotype-specific features reduce the susceptibility of South American yellow fever virus strains to vaccine-induced antibodies. Cell Host Microbe. 2022;30(2):248-59 e6. Epub 20220107. doi: 10.1016/j.chom.2021.12.009. PubMed PMID: 34998466; PMCID: PMC10067022.

89. Wec AZ, Haslwanter D, Abdiche YN, Shehata L, Pedreno-Lopez N, Moyer CL, Bornholdt ZA, Lilov A, Nett JH, Jangra RK, Brown M, Watkins DI, Ahlm C, Forsell MN, Rey FA, Barba-Spaeth G, Chandran K, Walker LM. Longitudinal dynamics of the human B cell response to the yellow fever 17D vaccine. Proc Natl Acad Sci U S A. 2020;117(12):6675-85. Epub 20200309. doi: 10.1073/pnas.1921388117. PubMed PMID: 32152119; PMCID: PMC7104296.

90. Shustov AV, Mason PW, Frolov I. Production of pseudoinfectious yellow fever virus with a two-component genome. J Virol. 2007;81(21):11737-48. Epub 20070822. doi: 10.1128/JVI.01112-07. PubMed PMID: 17715227; PMCID: PMC2168813.

91. Kain MP, Bolker BM. Predicting West Nile virus transmission in North American bird communities using phylogenetic mixed effects models and eBird citizen science data. Parasit Vectors. 2019;12(1):395. Epub 20190808. doi: 10.1186/s13071-019-3656-8. PubMed PMID: 31395085; PMCID: PMC6686473.

92. Shinde DP, Plante JA, Plante KS, Weaver SC. Yellow Fever: Roles of Animal Models and Arthropod Vector Studies in Understanding Epidemic Emergence. Microorganisms. 2022;10(8). Epub 20220805. doi: 10.3390/microorganisms10081578. PubMed PMID: 36013996; PMCID: PMC9412558.

93. CDC. Transmission of yellow fever 2024 [cited 2024 July 20, 2024]. Available from: https://www.cdc.gov/yellow-fever/php/transmission/index.html.

94. Kallas EG, D'Elia Zanella L, Moreira CHV, Buccheri R, Diniz GBF, Castineiras ACP, Costa PR, Dias JZC, Marmorato MP, Song ATW, Maestri A, Borges IC, Joelsons D, Cerqueira NB, Santiago ESNC, Morales Claro I, Sabino EC, Levi JE, Avelino-Silva VI, Ho YL. Predictors of mortality in patients with yellow fever: an observational cohort study. Lancet Infect Dis. 2019;19(7):750-8. Epub 20190516. doi: 10.1016/S1473-3099(19)30125-2. PubMed PMID: 31104909.

95. Avelino-Silva VI, Thomazella MV, Marmorato MP, Correia CA, Dias JZC, Maestri A, Cerqueira NB, Moreira CHV, Buccheri R, Felix AC, Zanella L, Costa PR, Kallas EG. Viral Kinetics in Sylvatic Yellow Fever Cases. J Infect Dis. 2023;227(9):1097-103. doi: 10.1093/infdis/jiac435. PubMed PMID: 36316804.

96. Cunha MS, da Costa AC, de Azevedo Fernandes NCC, Guerra JM, Dos Santos FCP, Nogueira JS, D'Agostino LG, Komninakis SV, Witkin SS, Ressio RA, Maeda AY, Vasami FGS,

Kaigawa UMA, de Azevedo LS, de Souza Facioli PA, Macedo FLL, Sabino EC, Leal E, de Souza RP. Epizootics due to Yellow Fever Virus in Sao Paulo State, Brazil: viral dissemination to new areas (2016-2017). Sci Rep. 2019;9(1):5474. Epub 20190402. doi: 10.1038/s41598-019-41950-3. PubMed PMID: 30940867; PMCID: PMC6445104.

97. Julander JG. Animal models of yellow fever and their application in clinical research. Curr Opin Virol. 2016;18:64-9. Epub 20160416. doi: 10.1016/j.coviro.2016.03.010. PubMed PMID: 27093699.

98. Almeida MA, Cardoso Jda C, Dos Santos E, da Fonseca DF, Cruz LL, Faraco FJ, Bercini MA, Vettorello KC, Porto MA, Mohrdieck R, Ranieri TM, Schermann MT, Sperb AF, Paz FZ, Nunes ZM, Romano AP, Costa ZG, Gomes SL, Flannery B. Surveillance for yellow Fever virus in non-human primates in southern Brazil, 2001-2011: a tool for prioritizing human populations for vaccination. PLoS Negl Trop Dis. 2014;8(3):e2741. Epub 20140313. doi: 10.1371/journal.pntd.0002741. PubMed PMID: 24625681; PMCID: PMC3953010.

99. de Azevedo Fernandes NCC, Guerra JM, Diaz-Delgado J, Cunha MS, Saad LD, Iglezias SD, Ressio RA, Dos Santos Cirqueira C, Kanamura CT, Jesus IP, Maeda AY, Vasami FGS, de Carvalho J, de Araujo LJT, de Souza RP, Nogueira JS, Spinola RMF, Catao-Dias JL. Differential Yellow Fever Susceptibility in New World Nonhuman Primates, Comparison with Humans, and Implications for Surveillance. Emerg Infect Dis. 2021;27(1):47-56. doi: 10.3201/eid2701.191220. PubMed PMID: 33350931; PMCID: PMC7774563.

100. Kuno G. Mechanisms of Yellow Fever Transmission: Gleaning the Overlooked Records of Importance and Identifying Problems, Puzzles, Serious Issues, Surprises and Research Questions. Viruses. 2024;16(1). Epub 20240104. doi: 10.3390/v16010084. PubMed PMID: 38257784; PMCID: PMC10820296.

101. Bryan CS, Moss SW, Kahn RJ. Yellow fever in the Americas. Infect Dis Clin North Am. 2004;18(2):275-92, table of contents. doi: 10.1016/j.idc.2004.01.007. PubMed PMID: 15145381.

102. Finlay C. The Mosquito Hypothetically Considered as an Agent in the Transmission of Yellow Fever Poison. Yale J Biol Med. 1937;9(6):589-604. PubMed PMID: 21433746; PMCID: PMC2601727.

103. Reed W, Carroll J, Agramonte A, Lazear JW. The Etiology of Yellow Fever-A Preliminary Note. Public Health Pap Rep. 1900;26:37-53. PubMed PMID: 19600960; PMCID: PMC2329228.

104. Mehra A. Politics of Participation: Walter Reed's Yellow-Fever Experiments: AMA Journal of Ethics; 2009 [cited 2024]. Available from: https://journalofethics.ama-assn.org/article/politics-participation-walter-reeds-yellow-fever-experiments/2009-04.
105. Strode GK. Yellow fever. 1st ed. New York: McGraw-Hill; 1951 1951.
106. Staples JE, Monath TP. Yellow fever: 100 years of discovery. JAMA. 2008;300(8):960-2. doi: 10.1001/jama.300.8.960. PubMed PMID: 18728272.
107. Stokes A, Bauer JH, Hudson NP. Experimental transmission of yellow fever to laboratory animals. American Journal of Tropical Medicine. 1928;8:103-64.
108. Ricciardi MJ, Rust LN, Pedreno-Lopez N, Yusova S, Biswas S, Webb GM, Gonzalez-Nieto L, Voigt TB, Louw JJ, Laurino FD, DiBello JR, Raue HP, Barber-Axthelm AM, Chun K, Uttke S, Raphael LMS, Yrizarry-Medina A, Rosen BC, Agnor R, Gao L, Labriola C, Axthelm M, Smedley J, Julander JG, Bonaldo MC, Walker LM, Messaoudi I, Slifka MK, Burton DR, Kallas EG, Sacha JB, Watkins DI, Burwitz BJ. Therapeutic neutralizing monoclonal antibody administration protects against lethal yellow fever virus infection. Sci Transl Med. 2023;15(689):eade5795. Epub 20230329. doi: 10.1126/scitranslmed.ade5795. PubMed PMID: 36989376; PMCID: PMC10617428.
109. Tesh RB, Guzman H, da Rosa AP, Vasconcelos PF, Dias LB, Bunnell JE, Zhang H, Xiao SY. Experimental yellow fever virus infection in the Golden Hamster (Mesocricetus auratus). I. Virologic, biochemical, and immunologic studies. J Infect Dis. 2001;183(10):1431-6. Epub 20010417. doi: 10.1086/320199. PubMed PMID: 11319679.
110. Xiao SY, Zhang H, Guzman H, Tesh RB. Experimental yellow fever virus infection in the Golden hamster (Mesocricetus auratus). II. Pathology. J Infect Dis. 2001;183(10):1437-44. Epub 20010417. doi: 10.1086/320200. PubMed PMID: 11319680.
111. Baldon LVR, de Mendonca SF, Ferreira FV, Rezende FO, Amadou SCG, Leite T, Rocha MN, Marques JT, Moreira LA, Ferreira AGA. AG129 Mice as a Comprehensive Model for the Experimental Assessment of Mosquito Vector Competence for Arboviruses. Pathogens. 2022;11(8). Epub 20220803. doi: 10.3390/pathogens11080879. PubMed PMID: 36015000; PMCID: PMC9412449.
112. Foundation TR. The Rockefeller Foundation Annual Report1926.
113. Noguchi H. Leptospira Icteroides and Yellow Fever. Proc Natl Acad Sci U S A. 1920;6(3):110-1. doi: 10.1073/pnas.6.3.110. PubMed PMID: 16576471; PMCID: PMC1084441.

114. Lloyd W, Theiler M, Ricci NI. Modification of the virulence of yellow fever virus by cultivation in tissues in vitro. Transactions of the Royal Society of Tropical Medicine and Hygiene. 1936;29(5):481-529.
115. Bauer JH, Mahaffy AF. Studies on the filterability of yellow fever virus. American Journal of Epidemiology. 1930;12(1):175-95.
116. Haagen E, Theiler M. Studies of Yellow Fever Virus in Tissue Culture. Experimental biology and medicine. 1932;29(4):2.
117. Tang S, Hu S, Xiao J, Zhang Z, Su Z, Wu Q, Yang J, Liu X, Zhu Q, Shi J, Moming A, Deng Y, Fan Z, Guo R, Sun S, Zhang Y, Shen S, Deng F. Monitoring the Process and Characterizing Symptoms of Suckling Mouse Inoculation Promote Isolating Viruses from Ticks. Zoonoses. 2023;3(1).
118. NPO. The Nobel Prize: Max Theiler – Facts: Nobel Prize Outreach AB; 2024 [cited 2024 August 8, 2024]. Available from: https://www.nobelprize.org/prizes/medicine/1951/theiler/facts/.
119. Norrby E. Yellow fever and Max Theiler: the only Nobel Prize for a virus vaccine. J Exp Med. 2007;204(12):2779-84. doi: 10.1084/jem.20072290. PubMed PMID: 18039952; PMCID: PMC2118520.
120. NPO. NOBEL PRIZES 2023 Nobel Prize Outreach AB2024 [August 8, 2024]. Available from: https://www.nobelprize.org/all-nobel-prizes-2023/.
121. Post PR, de Carvalho R, da Silva Freire M, Galler R. The early use of yellow fever virus strain 17D for vaccine production in Brazil--a review. Memorias do Instituto Oswaldo Cruz. 2001;96(6):849-57.
122. Pato TP, Souza MCO, Mattos DA, Caride E, Ferreira DF, Gaspar LP, Freire MS, Castilho LR. Purification of yellow fever virus produced in Vero cells for inactivated vaccine manufacture. Vaccine. 2019;37(24):3214-20. Epub 20190430. doi: 10.1016/j.vaccine.2019.04.077. PubMed PMID: 31047674.
123. FDA. Package insert - YF-Vax 2019 [updated Dec17, 2019; cited 2024 Sep 18, 2024]. Available from: https://www.fda.gov/media/76015/download?attachment.
124. Sawyer WA, Kitchen SF, Lloyd W. Vaccination against Yellow Fever with Immune Serum and Virus Fixed for Mice. J Exp Med. 1932;55(6):945-69. doi: 10.1084/jem.55.6.945. PubMed PMID: 19870044; PMCID: PMC2132143.

125. Sellards AW, Hindle E. The Preservation of Yellow Fever Virus. Br Med J. 1928;1(3512):713-4. doi: 10.1136/bmj.1.3512.713. PubMed PMID: 20773851; PMCID: PMC2455522.
126. Beck AS, Barrett AD. Current status and future prospects of yellow fever vaccines. Expert Rev Vaccines. 2015;14(11):1479-92. Epub 20150914. doi: 10.1586/14760584.2015.1083430. PubMed PMID: 26366673; PMCID: PMC5563254.
127. Stones PB, Macnamara FN. Encephalitis following neurotropic yellow fever vaccine administered by scarification in Nigeria: epidemiological and laboratory studies. Trans R Soc Trop Med Hyg. 1955;49(2):176-86. doi: 10.1016/0035-9203(55)90044-4. PubMed PMID: 14373854.
128. Beck A, Guzman H, Li L, Ellis B, Tesh RB, Barrett ADT. Phylogeographic reconstruction of African yellow fever virus isolates indicates recent simultaneous dispersal into east and west Africa. PLoS neglected tropical diseases. 2013;7(3):e1910. doi: https://dx.doi.org/10.1371/journal.pntd.0001910.
129. Akondy RS, Johnson PL, Nakaya HI, Edupuganti S, Mulligan MJ, Lawson B, Miller JD, Pulendran B, Antia R, Ahmed R. Initial viral load determines the magnitude of the human CD8 T cell response to yellow fever vaccination. Proc Natl Acad Sci U S A. 2015;112(10):3050-5. Epub 20150223. doi: 10.1073/pnas.1500475112. PubMed PMID: 25713354; PMCID: PMC4364194.
130. Fernandez-Garcia MD, Meertens L, Chazal M, Hafirassou ML, Dejarnac O, Zamborlini A, Despres P, Sauvonnet N, Arenzana-Seisdedos F, Jouvenet N, Amara A. Vaccine and Wild-Type Strains of Yellow Fever Virus Engage Distinct Entry Mechanisms and Differentially Stimulate Antiviral Immune Responses. mBio. 2016;7(1):e01956-15. Epub 20160209. doi: 10.1128/mBio.01956-15. PubMed PMID: 26861019; PMCID: PMC4752603.
131. ter Meulen J, Sakho M, Koulemou K, Magassouba N, Bah A, Preiser W, Daffis S, Klewitz C, Bae HG, Niedrig M, Zeller H, Heinzel-Gutenbrunner M, Koivogui L, Kaufmann A. Activation of the cytokine network and unfavorable outcome in patients with yellow fever. J Infect Dis. 2004;190(10):1821-7. Epub 20041012. doi: 10.1086/425016. PubMed PMID: 15499539.
132. Akondy RS, Monson ND, Miller JD, Edupuganti S, Teuwen D, Wu H, Quyyumi F, Garg S, Altman JD, Del Rio C, Keyserling HL, Ploss A, Rice CM, Orenstein WA, Mulligan MJ, Ahmed R. The yellow fever virus vaccine induces a broad and polyfunctional human memory

CD8+ T cell response. J Immunol. 2009;183(12):7919-30. doi: 10.4049/jimmunol.0803903. PubMed PMID: 19933869; PMCID: PMC3374958.
133. James EA, LaFond RE, Gates TJ, Mai DT, Malhotra U, Kwok WW. Yellow fever vaccination elicits broad functional CD4+ T cell responses that recognize structural and nonstructural proteins. J Virol. 2013;87(23):12794-804. Epub 20130918. doi: 10.1128/JVI.01160-13. PubMed PMID: 24049183; PMCID: PMC3838168.
134. Amanna IJ, Slifka MK. Questions regarding the safety and duration of immunity following live yellow fever vaccination. Expert Rev Vaccines. 2016;15(12):1519-33. Epub 20160620. doi: 10.1080/14760584.2016.1198259. PubMed PMID: 27267203; PMCID: PMC5171234.
135. Adler LN, Jiang W, Bhamidipati K, Millican M, Macaubas C, Hung SC, Mellins ED. The Other Function: Class II-Restricted Antigen Presentation by B Cells. Front Immunol. 2017;8:319. Epub 20170323. doi: 10.3389/fimmu.2017.00319. PubMed PMID: 28386257; PMCID: PMC5362600.
136. Mason RA, Tauraso NM, Spertzel RO, Ginn RK. Yellow fever vaccine: direct challenge of monkeys given graded doses of 17D vaccine. Appl Microbiol. 1973;25(4):539-44. doi: 10.1128/am.25.4.539-544.1973. PubMed PMID: 4633476; PMCID: PMC380857.
137. Poland JD, Calisher CH, Monath TP, Downs WG, Murphy K. Persistence of neutralizing antibody 30-35 years after immunization with 17D yellow fever vaccine. Bull World Health Organ. 1981;59(6):895-900. PubMed PMID: 6978196; PMCID: PMC2396120.
138. Coursaget P, Fritzell B, Blondeau C, Saliou P, Diop-Mar I. Simultaneous injection of plasma-derived or recombinant hepatitis B vaccines with yellow fever and killed polio vaccines. Vaccine. 1995;13(1):109-11. doi: 10.1016/0264-410x(95)80020-e. PubMed PMID: 7598769.
139. Sibailly TS, Wiktor SZ, Tsai TF, Cropp BC, Ekpini ER, Adjorlolo-Johnson G, Gnaore E, DeCock KM, Greenberg AE. Poor antibody response to yellow fever vaccination in children infected with human immunodeficiency virus type 1. Pediatr Infect Dis J. 1997;16(12):1177-9. doi: 10.1097/00006454-199712000-00015. PubMed PMID: 9427466.
140. Lang J, Zuckerman J, Clarke P, Barrett P, Kirkpatrick C, Blondeau C. Comparison of the immunogenicity and safety of two 17D yellow fever vaccines. Am J Trop Med Hyg. 1999;60(6):1045-50. doi: 10.4269/ajtmh.1999.60.1045. PubMed PMID: 10403341.

141. Niedrig M, Lademann M, Emmerich P, Lafrenz M. Assessment of IgG antibodies against yellow fever virus after vaccination with 17D by different assays: neutralization test, haemagglutination inhibition test, immunofluorescence assay and ELISA. Trop Med Int Health. 1999;4(12):867-71. doi: 10.1046/j.1365-3156.1999.00496.x. PubMed PMID: 10632996.
142. Stefano I, Sato HK, Pannuti CS, Omoto TM, Mann G, Freire MS, Yamamura AM, Vasconcelos PF, Oselka GW, Weckx LW, Salgado MF, Noale LF, Souza VA. Recent immunization against measles does not interfere with the sero-response to yellow fever vaccine. Vaccine. 1999;17(9-10):1042-6. doi: 10.1016/s0264-410x(98)00320-x. PubMed PMID: 10195613.
143. Osei-Kwasi M, Dunyo SK, Koram KA, Afari EA, Odoom JK, Nkrumah FK. Antibody response to 17D yellow fever vaccine in Ghanaian infants. Bull World Health Organ. 2001;79(11):1056-9. PubMed PMID: 11731813; PMCID: PMC2566698.
144. Monath TP, Nichols R, Archambault WT, Moore L, Marchesani R, Tian J, Shope RE, Thomas N, Schrader R, Furby D, Bedford P. Comparative safety and immunogenicity of two yellow fever 17D vaccines (ARILVAX and YF-VAX) in a phase III multicenter, double-blind clinical trial. The American journal of tropical medicine and hygiene. 2002;66(5):533-41.
145. Camacho LA, Freire Mda S, Leal Mda L, Aguiar SG, Nascimento JP, Iguchi T, Lozana Jde A, Farias RH, Collaborative Group for the Study of Yellow Fever V. Immunogenicity of WHO-17D and Brazilian 17DD yellow fever vaccines: a randomized trial. Rev Saude Publica. 2004;38(5):671-8. Epub 20041018. doi: 10.1590/s0034-89102004000500009. PubMed PMID: 15499438.
146. Belmusto-Worn VE, Sanchez JL, McCarthy K, Nichols R, Bautista CT, Magill AJ, Pastor-Cauna G, Echevarria C, Laguna-Torres VA, Samame BK, Baldeon ME, Burans JP, Olson JG, Bedford P, Kitchener S, Monath TP. Randomized, double-blind, phase III, pivotal field trial of the comparative immunogenicity, safety, and tolerability of two yellow fever 17D vaccines (Arilvax and YF-VAX) in healthy infants and children in Peru. Am J Trop Med Hyg. 2005;72(2):189-97. PubMed PMID: 15741556.
147. Guirakhoo F, Kitchener S, Morrison D, Forrat R, McCarthy K, Nichols R, Yoksan S, Duan X, Ermak TH, Kanesa-Thasan N, Bedford P, Lang J, Quentin-Millet MJ, Monath TP. Live attenuated chimeric yellow fever dengue type 2 (ChimeriVax-DEN2) vaccine: Phase I clinical trial for safety and immunogenicity: effect of yellow fever pre-immunity in induction of cross

neutralizing antibody responses to all 4 dengue serotypes. Hum Vaccin. 2006;2(2):60-7. Epub 20060315. doi: 10.4161/hv.2.2.2555. PubMed PMID: 17012873.

148. Roukens AH, Vossen AC, Bredenbeek PJ, van Dissel JT, Visser LG. Intradermally administered yellow fever vaccine at reduced dose induces a protective immune response: a randomized controlled non-inferiority trial. PloS one. 2008;3(4):e1993. doi: https://dx.doi.org/10.1371/journal.pone.0001993.

149. Nasveld PE, Marjason J, Bennett S, Aaskov J, Elliott S, McCarthy K, Kanesa-Thasan N, Feroldi E, Reid M. Concomitant or sequential administration of live attenuated Japanese encephalitis chimeric virus vaccine and yellow fever 17D vaccine: randomized double-blind phase II evaluation of safety and immunogenicity. Hum Vaccin. 2010;6(11):906-14. Epub 20101101. doi: 10.4161/hv.6.11.12854. PubMed PMID: 20864814; PMCID: PMC3060385.

150. Coulange Bodilis H, Benabdelmoumen G, Gergely A, Goujon C, Pelicot M, Poujol P, Consigny PH. [Long term persistence of yellow fever neutralising antibodies in elderly persons]. Persistance a long terme des anticorps neutralisants de la fievre jaune chez les personnes agees de 60 ans et plus. 2011;104(4):260-5. doi: https://dx.doi.org/10.1007/s13149-011-0135-7.

151. Roukens AH, Soonawala D, Joosten SA, de Visser AW, Jiang X, Dirksen K, de Gruijter M, van Dissel JT, Bredenbeek PJ, Visser LG. Elderly subjects have a delayed antibody response and prolonged viraemia following yellow fever vaccination: a prospective controlled cohort study. PloS one. 2011;6(12).

152. S.r.l. NVaD. Study to evaluate the safety and immunogenicity of travel vaccines when administered concomitantly with meningococcal ACWY conjugate vaccine in healthy adults. ICTRP. 2011;11:1056-9.

153. Edupuganti S, Eidex RB, Keyserling H, Akondy RS, Lanciotti R, Orenstein W, del Rio C, Pan Y, Querec T, Lipman H, Barrett A, Ahmed R, Teuwen D, Cetron M, Mulligan MJ, Team YF-IS. A randomized, double-blind, controlled trial of the 17D yellow fever virus vaccine given in combination with immune globulin or placebo: comparative viremia and immunogenicity. Am J Trop Med Hyg. 2013;88(1):172-7. Epub 20121203. doi: 10.4269/ajtmh.2012.12-0179. PubMed PMID: 23208880; PMCID: PMC3541731.

154. Kerneis S, Launay O, Ancelle T, Iordache L, Naneix-Laroche V, Mechai F, Fehr T, Leroy J-P, Issartel B, Dunand J, van der Vliet D, Wyplosz B, Consigny P-H, Hanslik T. Safety and immunogenicity of yellow fever 17D vaccine in adults receiving systemic corticosteroid therapy:

an observational cohort study. Arthritis care & research. 2013;65(9):1522-8. doi: https://dx.doi.org/10.1002/acr.22021.

155. Campi-Azevedo AC, de Almeida Estevam P, Coelho-Dos-Reis JG, Peruhype-Magalhaes V, Villela-Rezende G, Quaresma PF, Maia Mde L, Farias RH, Camacho LA, Freire Mda S, Galler R, Yamamura AM, Almeida LF, Lima SM, Nogueira RM, Silva Sa GR, Hokama DA, de Carvalho R, Freire RA, Filho EP, Leal Mda L, Homma A, Teixeira-Carvalho A, Martins RM, Martins-Filho OA. Subdoses of 17DD yellow fever vaccine elicit equivalent virological/immunological kinetics timeline. BMC Infect Dis. 2014;14:391. Epub 20140715. doi: 10.1186/1471-2334-14-391. PubMed PMID: 25022840; PMCID: PMC4223624.

156. Collaborative Group for Studies of Yellow Fever V. A randomised double-blind clinical trial of two yellow fever vaccines prepared with substrains 17DD and 17D-213/77 in children nine-23 months old. Mem Inst Oswaldo Cruz. 2015;110(6):771-80. doi: 10.1590/0074-02760150176. PubMed PMID: 26517656; PMCID: PMC4667580.

157. Michel R, Berger F, Ravelonarivo J, Dussart P, Dia M, Nacher M, Rogier S, Moua D, Sarr FD, Diop OM, Sall AA, Baril L. Observational study on immune response to yellow fever and measles vaccines in 9 to 15-month old children. Is it necessary to wait 4 weeks between two live attenuated vaccines? Vaccine. 2015;33(20):2301-6. doi: https://dx.doi.org/10.1016/j.vaccine.2015.03.069.

158. Avelino-Silva VI, Miyaji KT, Hunt PW, Huang Y, Simoes M, Lima SB, Freire MS, Caiaffa-Filho HH, Hong MA, Costa DA, Dias JZ, Cerqueira NB, Nishiya AS, Sabino EC, Sartori AM, Kallas EG. CD4/CD8 Ratio and KT Ratio Predict Yellow Fever Vaccine Immunogenicity in HIV-Infected Patients. PLoS Negl Trop Dis. 2016;10(12):e0005219. Epub 20161212. doi: 10.1371/journal.pntd.0005219. PubMed PMID: 27941965; PMCID: PMC5179051.

159. Campi-Azevedo AC, Costa-Pereira C, Antonelli LR, Fonseca CT, Teixeira-Carvalho A, Villela-Rezende G, Santos RA, Batista MA, Campos FM, Pacheco-Porto L, Melo Junior OA, Hossell DM, Coelho-dos-Reis JG, Peruhype-Magalhaes V, Costa-Silva MF, de Oliveira JG, Farias RH, Noronha TG, Lemos JA, von Doellinger Vdos R, Simoes M, de Souza MM, Malaquias LC, Persi HR, Pereira JM, Martins JA, Dornelas-Ribeiro M, Vinhas Ade A, Alves TR, Maia Mde L, Freire Mda S, Martins Rde M, Homma A, Romano AP, Domingues CM, Tauil PL, Vasconcelos PF, Rios M, Caldas IR, Camacho LA, Martins-Filho OA. Booster dose after 10 years is recommended following 17DD-YF primary vaccination. Human vaccines &

immunotherapeutics. 2016;12(2):491-502. doi: 10.1080/21645515.2015.1082693. PubMed PMID: 26360663; PMCID: PMC5049740.

160. Chan KR, Wang X, Saron WAA, Gan ES, Tan HC, Mok DZL, Zhang SL, Lee YH, Liang C, Wijaya L, Ghosh S, Cheung YB, Tannenbaum SR, Abraham SN, St John AL, Low JGH, Ooi EE. Cross-reactive antibodies enhance live attenuated virus infection for increased immunogenicity. Nat Microbiol. 2016;1(12):16164. Epub 20160919. doi: 10.1038/nmicrobiol.2016.164. PubMed PMID: 27642668; PMCID: PMC7097525.

161. Lopez P, Lanata CF, Zambrano B, Cortes M, Andrade T, Amemiya I, Terrones C, Gil AI, Verastegui H, Marquez V, Crevat D, Jezorwski J, Noriega F. Immunogenicity and Safety of Yellow Fever Vaccine (Stamaril) When Administered Concomitantly With a Tetravalent Dengue Vaccine Candidate in Healthy Toddlers at 12-13 Months of Age in Colombia and Peru: A Randomized Trial. Pediatr Infect Dis J. 2016;35(10):1140-7. doi: 10.1097/INF.0000000000001250. PubMed PMID: 27254034.

162. Colin de Verdiere N, Durier C, Samri A, Meiffredy V, Launay O, Matheron S, Mercier-Delarue S, Even S, Aboulker J-P, Molina J-M, Autran B, Simon F. Immunogenicity and safety of yellow fever vaccine in HIV-1-infected patients. AIDS (London, England). 2018;32(16):2291-9. doi: https://dx.doi.org/10.1097/QAD.0000000000001963.

163. Lindsey NP, Horiuchi KA, Fulton C, Panella AJ, Kosoy OI, Velez JO, Krow-Lucal ER, Fischer M, Staples JE. Persistence of yellow fever virus-specific neutralizing antibodies after vaccination among US travellers. Journal of travel medicine. 2018;25(1). doi: https://dx.doi.org/10.1093/jtm/tay108.

164. Veit O, Domingo C, Niedrig M, Staehelin C, Sonderegger B, Hequet D, Stoeckle M, Calmy A, Schiffer V, Bernasconi E, Flury D, Hatz C, Zwahlen M, Furrer H, Swiss HIVCS. Long-term Immune Response to Yellow Fever Vaccination in Human Immunodeficiency Virus (HIV)-Infected Individuals Depends on HIV RNA Suppression Status: Implications for Vaccination Schedule. Clin Infect Dis. 2018;66(7):1099-108. doi: 10.1093/cid/cix960. PubMed PMID: 29140432.

165. Campi-Azevedo AC, Reis LR, Peruhype-Magalhaes V, Coelho-Dos-Reis JG, Antonelli LR, Fonseca CT, Costa-Pereira C, Souza-Fagundes EM, da Costa-Rocha IA, Mambrini JVM, Lemos JAC, Ribeiro JGL, Caldas IR, Camacho LAB, Maia MLS, de Noronha TG, de Lima SMB, Simoes M, Freire MDS, Martins RM, Homma A, Tauil PL, Vasconcelos PFC, Romano

APM, Domingues CM, Teixeira-Carvalho A, Martins-Filho OA. Short-Lived Immunity After 17DD Yellow Fever Single Dose Indicates That Booster Vaccination May Be Required to Guarantee Protective Immunity in Children. Front Immunol. 2019;10:2192. Epub 20190926. doi: 10.3389/fimmu.2019.02192. PubMed PMID: 31616412; PMCID: PMC6775283.

166. Collaborative group for studies on yellow fever v. Duration of immunity in recipients of two doses of 17DD yellow fever vaccine. Vaccine. 2019;37(35):5129-35. Epub 20190603. doi: 10.1016/j.vaccine.2019.05.048. PubMed PMID: 31171393.

167. Jia Q, Jia C, Liu Y, Yang Y, Qi J, Tong L, Chen H, Zhang M, Che J, Li B, Li Z. Clinical evidence for the immunogenicity and immune persistence of vaccination with yellow fever virus strain 17D in Chinese peacekeepers deployed to Africa. Antiviral research. 2019;162:1-4. doi: https://dx.doi.org/10.1016/j.antiviral.2018.12.001.

168. Asante KP, Ansong D, Kaali S, Adjei S, Lievens M, Nana Badu L, Agyapong Darko P, Boakye Yiadom Buabeng P, Boahen O, Maria Rettig T, Agutu C, Benard Ekow Harrison S, Ntiamoah Y, Adomako Anim J, Adeniji E, Agordo Dornudo A, Gvozdenovic E, Dosoo D, Sambian D, Owusu-Boateng H, Ato Wilson E, Prempeh F, Vandoolaeghe P, Schuerman L, Owusu-Agyei S, Agbenyega T, Ofori-Anyinam O. Immunogenicity and safety of the RTS,S/AS01 malaria vaccine co-administered with measles, rubella and yellow fever vaccines in Ghanaian children: A phase IIIb, multi-center, non-inferiority, randomized, open, controlled trial. Vaccine. 2020;38(18):3411-21. Epub 20200317. doi: 10.1016/j.vaccine.2020.03.014. PubMed PMID: 32192811; PMCID: PMC7611265.

169. Burkhard J, Ciurea A, Gabay C, Hasler P, Muller R, Niedrig M, Fehr J, Villiger P, Visser LG, de Visser AW, Walker UA, Hatz C, Buhler S. Long-term immunogenicity after yellow fever vaccination in immunosuppressed and healthy individuals. Vaccine. 2020;38(19):3610-7. doi: https://dx.doi.org/10.1016/j.vaccine.2019.12.042.

170. Idoko OT, Domingo C, Tapia MD, Sow SO, Geldmacher C, Saathoff E, Kampmann B. Serological Protection 5-6 Years Post Vaccination Against Yellow Fever in African Infants Vaccinated in Routine Programmes. Front Immunol. 2020;11:577751. Epub 20201008. doi: 10.3389/fimmu.2020.577751. PubMed PMID: 33133096; PMCID: PMC7578390.

171. Kareko BW, Booty BL, Nix CD, Lyski ZL, Slifka MK, Amanna IJ, Messer WB. Persistence of Neutralizing Antibody Responses Among Yellow Fever Virus 17D Vaccinees

Living in a Nonendemic Setting. J Infect Dis. 2020;221(12):2018-25. doi: 10.1093/infdis/jiz374. PubMed PMID: 31545367; PMCID: PMC7289542.

172. Valim V, Machado K, Miyamoto ST, Pinto AD, Rocha PCM, Serrano EV, Dinis VG, Gouvea SA, Dias JGF, Campi-Azevedo AC, Teixeira-Carvalho A, Peruhype-Magalhaes V, da Costa-Rocha IA, de Lima SMB, Miranda EH, Trindade GF, Maia MLS, Gavi M, da Silva LB, Duque RH, Gianordoli APE, Casagrande TZ, Oliveira KG, Moura B, Nicole-Batista F, Rodrigues LC, Clemente TB, Magalhaes ES, Bissoli MF, Gouvea M, Pinto-Neto L, Costa CZ, Giovelli RA, Brandao LR, Polito ETL, Koehlert IO, Borjaille BP, Pereira DB, Dias LH, Merlo DL, Genelhu LFF, Pretti FZ, Giacomin MDS, Burian APN, Fantinato F, Pileggi GS, da Mota LMH, Martins-Filho OA. Planned Yellow Fever Primary Vaccination Is Safe and Immunogenic in Patients With Autoimmune Diseases: A Prospective Non-interventional Study. Front Immunol. 2020;11:1382. Epub 20200717. doi: 10.3389/fimmu.2020.01382. PubMed PMID: 32765496; PMCID: PMC7379374.

173. Juan-Giner A, Kimathi D, Grantz KH, Hamaluba M, Kazooba P, Njuguna P, Fall G, Dia M, Bob NS, Monath TP, Barrett AD, Hombach J, Mulogo EM, Ampeire I, Karanja HK, Nyehangane D, Mwanga-Amumpaire J, Cummings DAT, Bejon P, Warimwe GM, Grais RF. Immunogenicity and safety of fractional doses of yellow fever vaccines: a randomised, double-blind, non-inferiority trial. Lancet (London, England). 2021;397(10269):119-27. doi: https://dx.doi.org/10.1016/S0140-6736(20)32520-4.

174. Gotuzzo E, Yactayo S, Cordova E. Efficacy and duration of immunity after yellow fever vaccination: systematic review on the need for a booster every 10 years. Am J Trop Med Hyg. 2013;89(3):434-44. doi: 10.4269/ajtmh.13-0264. PubMed PMID: 24006295; PMCID: PMC3771278.

175. ACIP. Grading of Recommendations, Assessment, Development, and Evaluation (GRADE) for Use of Yellow Fever Vaccine Booster Doses 2015 [updated 06/17/201504/22/2024]. Available from: https://www.cdc.gov/vaccines/acip/recs/grade/yf-vac-boost.html.

176. Kling K, Domingo C, Bogdan C, Duffy S, Harder T, Howick J, Kleijnen J, McDermott K, Wichmann O, Wilder-Smith A, Wolff R. Duration of Protection After Vaccination Against Yellow Fever: A Systematic Review and Meta-Analysis. Clin Infect Dis. 2022;75(12):2266-74. doi: 10.1093/cid/ciac580. PubMed PMID: 35856638; PMCID: PMC9761887.

177. Schaumburg F, Schuler F, Grobusch MP. New recommendation on yellow fever booster vaccination in Germany. Travel Med Infect Dis. 2022;50:102487. Epub 20221029. doi: 10.1016/j.tmaid.2022.102487. PubMed PMID: 36342037.
178. Kling K, Domingo C, Bogdan C, Mertens T, Wolff R, Wiedermann U. Comment on: "New recommendation on yellow fever booster vaccination in Germany". Travel Med Infect Dis. 2023;52:102561. Epub 20230324. doi: 10.1016/j.tmaid.2023.102561. PubMed PMID: 36967051.
179. Schaumburg F, Grobusch MP. Reply to comments by Kling et al. On 'new recommendation on yellow fever booster vaccination in Germany' by Schaumburg et al. Travel Med Infect Dis. 2023;52:102562. Epub 20230324. doi: 10.1016/j.tmaid.2023.102562. PubMed PMID: 36967050.
180. Mascola JR, Louder MK, Winter C, Prabhakara R, De Rosa SC, Douek DC, Hill BJ, Gabuzda D, Roederer M. Human immunodeficiency virus type 1 neutralization measured by flow cytometric quantitation of single-round infection of primary human T cells. J Virol. 2002;76(10):4810-21. doi: 10.1128/jvi.76.10.4810-4821.2002. PubMed PMID: 11967298; PMCID: PMC136170.
181. Shinde DP, Plante JA, Scharton D, Mitchell B, Walker J, Azar SR, Campos RK, Sacchetto L, Drumond BP, Vasilakis N, Plante KS, Weaver SC. Yellow Fever Emergence: Role of Heterologous Flavivirus Immunity in Preventing Urban Transmission. bioRxiv. 2024. Epub 20240303. doi: 10.1101/2024.03.03.583168. PubMed PMID: 38463973; PMCID: PMC10925309.
182. Stokes A, Bauer JH, Hudson NP. The transmission of yellow fever to macacus rhesus: a preliminary note. Journal of the American Medical Association. 1928;90(4):253-4.
183. Hansen CA, Barrett ADT. The Present and Future of Yellow Fever Vaccines. Pharmaceuticals (Basel). 2021;14(9). Epub 20210901. doi: 10.3390/ph14090891. PubMed PMID: 34577591; PMCID: PMC8468696.
184. Staples JE, Barrett ADT, Wilder-Smith A, Hombach J. Review of data and knowledge gaps regarding yellow fever vaccine-induced immunity and duration of protection. NPJ vaccines. 2020;5(1):54. doi: https://dx.doi.org/10.1038/s41541-020-0205-6.
185. Wiedermann U, Garner-Spitzer E, Wagner A. Primary vaccine failure to routine vaccines: Why and what to do? Hum Vaccin Immunother. 2016;12(1):239-43. doi: 10.1080/21645515.2015.1093263. PubMed PMID: 26836329; PMCID: PMC4962729.

186. CDC. Vaccine & Immunizations Glossary 2022 [cited 2024 27 May 2024]. Available from: https://www.cdc.gov/vaccines/terms/glossary.html.
187. Elliott M. Yellow fever in the recently inoculated. Trans R Soc Trop Med Hyg. 1944;38(3):4.
188. Ross RW, Haddow AJ, Raper AB, Trowell HC. A fatal case of yellow fever in a European in Uganda. East Afr Med J. 1953;30(1):1-11. PubMed PMID: 13033776.
189. Nolla-Sallas J, Saballs-Radresa J. Imported yellow fever in vaccinated tourist. The Lancet. 1989;334(8674):1275.
190. Akoua-Koffi C, Ekra KD, Kone AB, Dagnan NS, Akran V, Kouadio KL, Loukou YG, Odehouri K, Tagliante-Saracino J, Ehouman A. [Detection and management of the yellow fever epidemic in the Ivory Coast, 2001]. Med Trop (Mars). 2002;62(3):305-9. PubMed PMID: 12244930.
191. Tuboi SH, Costa ZG, da Costa Vasconcelos PF, Hatch D. Clinical and epidemiological characteristics of yellow fever in Brazil: analysis of reported cases 1998-2002. Trans R Soc Trop Med Hyg. 2007;101(2):169-75. Epub 20060630. doi: 10.1016/j.trstmh.2006.04.001. PubMed PMID: 16814821.
192. de Filippis AM, Nogueira RM, Jabor AV, Schatzmayr HG, Oliveira JC, Dinis SC, Galler R. Isolation and characterization of wild type yellow fever virus in cases temporally associated with 17DD vaccination during an outbreak of yellow fever in Brazil. Vaccine. 2004;22(9-10):1073-8. doi: 10.1016/j.vaccine.2003.11.002. PubMed PMID: 15003633.
193. Saraiva M, Amorim RD, Moura MA, Santos EC, Sampaio LS, Barbosa M, Buhrer-Sekula S. Historical analysis of the records of sylvan yellow fever in the State of Amazonas, Brazil, from 1996 to 2009. Rev Soc Bras Med Trop. 2013;46(2):223-6. doi: 10.1590/0037-8682-1573-2013. PubMed PMID: 23740065.
194. Camara FP, de Carvalho LM, Gomes AL. Demographic profile of sylvatic yellow fever in Brazil from 1973 to 2008. Trans R Soc Trop Med Hyg. 2013;107(5):324-7. Epub 20130226. doi: 10.1093/trstmh/trt014. PubMed PMID: 23442573.
195. Ahmed F, Temte JL, Campos-Outcalt D, Schunemann HJ, Group AEBRW. Methods for developing evidence-based recommendations by the Advisory Committee on Immunization Practices (ACIP) of the U.S. Centers for Disease Control and Prevention (CDC). Vaccine.

2011;29(49):9171-6. Epub 20110811. doi: 10.1016/j.vaccine.2011.08.005. PubMed PMID: 21839794.

196. Staples JE, Bocchini JA, Jr., Rubin L, Fischer M, Centers for Disease C, Prevention. Yellow Fever Vaccine Booster Doses: Recommendations of the Advisory Committee on Immunization Practices, 2015. MMWR Morb Mortal Wkly Rep. 2015;64(23):647-50. PubMed PMID: 26086636; PMCID: PMC4584737.

197. Rachas A, Nakoune E, Bouscaillou J, Paireau J, Selekon B, Senekian D, Fontanet A, Kazanji M. Timeliness of yellow fever surveillance, Central African Republic. Emerg Infect Dis. 2014;20(6):1004-8. doi: 10.3201/eid2006.130671. PubMed PMID: 24857597; PMCID: PMC4036780.

198. Boyd AT, Dombaxe D, Moreira R, Oliveira MS, Manuel E, Colorado CN, Lanzieri TM. Notes from the Field: Investigation of Patients Testing Positive for Yellow Fever Viral RNA After Vaccination During a Mass Yellow Fever Vaccination Campaign - Angola, 2016. MMWR Morb Mortal Wkly Rep. 2017;66(10):282-3. Epub 20170317. doi: 10.15585/mmwr.mm6610a5. PubMed PMID: 28301446; PMCID: PMC5657865.

199. Ho YL, Joelsons D, Leite GFC, Malbouisson LMS, Song ATW, Perondi B, Andrade LC, Pinto LF, D'Albuquerque LAC, Segurado AAC, Hospital das Clinicas Yellow Fever Assistance G. Severe yellow fever in Brazil: clinical characteristics and management. J Travel Med. 2019;26(5). doi: 10.1093/jtm/taz040. PubMed PMID: 31150098.

200. de Rezende IM, Oliveira GFG, Costa TA, Khan A, Pereira LS, Santos TA, Alves PA, Calzavara-Silva CE, Martins-Filho OA, Teixeira-Carvalho A, LaBeaud AD, Drumond BP. Yellow Fever Molecular Diagnosis Using Urine Specimens during Acute and Convalescent Phases of the Disease. J Clin Microbiol. 2022;60(8):e0025422. Epub 20220802. doi: 10.1128/jcm.00254-22. PubMed PMID: 35916519; PMCID: PMC9383191.

201. De Cock KM, Monath TP, Nasidi A, Tukei PM, Enriquez J, Lichfield P, Craven RB, Fabiyi A, Okafor BC, Ravaonjanahary C, et al. Epidemic yellow fever in eastern Nigeria, 1986. Lancet. 1988;1(8586):630-3. doi: 10.1016/s0140-6736(88)91425-0. PubMed PMID: 2894558.

202. Heraud JM, Hommel D, Hulin A, Deubel V, Poveda JD, Sarthou JL, Talarmin A. First case of yellow fever in French Guiana since 1902. Emerging infectious diseases. 1999;5(3):429-32.

203. WHO. Yellow fever vaccines : thermostability of freeze-dried vaccines. Weekly empidemiological record. 1987(62):3.
204. Gibney KB, Edupuganti S, Panella AJ, Kosoy OI, Delorey MJ, Lanciotti RS, Mulligan MJ, Fischer M, Staples JE. Detection of anti-yellow fever virus immunoglobulin m antibodies at 3-4 years following yellow fever vaccination. Am J Trop Med Hyg. 2012;87(6):1112-5. Epub 20121029. doi: 10.4269/ajtmh.2012.12-0182. PubMed PMID: 23109371; PMCID: PMC3516084.
205. Motta E, Camacho LAB, Filippis AMB, Costa M, Pedro L, Cardoso SW, Souza MCO, Mendes YDS, Grinsztejn B, Coelho LE. Safety of the yellow fever vaccine in people living with HIV: a longitudinal study exploring post-vaccination viremia and hematological and liver kinetics. Braz J Infect Dis. 2024;28(1):103719. Epub 20240207. doi: 10.1016/j.bjid.2024.103719. PubMed PMID: 38341187; PMCID: PMC10904163.
206. Martin M, Tsai TF, Cropp B, Chang GJ, Holmes DA, Tseng J, Shieh W, Zaki SR, Al-Sanouri I, Cutrona AF, Ray G, Weld LH, Cetron MS. Fever and multisystem organ failure associated with 17D-204 yellow fever vaccination: a report of four cases. Lancet (London, England). 2001;358(9276):98-104.
207. Teichmann D, Grobusch MP, Wesselmann H, Temmesfeld-Wollbruck B, Breuer T, Dietel M, Emmerich P, Schmitz H, Suttorp N. A haemorrhagic fever from the Cote d'Ivoire. Lancet. 1999;354(9190):1608. doi: 10.1016/s0140-6736(99)09233-8. PubMed PMID: 10560677.
208. Abdala-Torres T, Campi-Azevedo AC, da Silva-Pereira RA, Dos Santos LI, Henriques PM, Costa-Rocha IA, Otta DA, Peruhype-Magalhaes V, Teixeira-Carvalho A, Araujo MSS, Fernandes EG, Sato HK, Fantinato F, Domingues C, Kallas EG, Tomiyama HTI, Lemos JAC, Coelho-Dos-Reis JG, de Lima SMB, Schwarcz WD, de Souza Azevedo A, Trindade GF, Ano Bom APD, da Silva AMV, Fernandes CB, Camacho LAB, de Sousa Maia ML, Collaborative Group for Studies of Yellow Fever V, Martins-Filho OA, do Antonelli L. Immune response induced by standard and fractional doses of 17DD yellow fever vaccine. NPJ Vaccines. 2024;9(1):54. Epub 20240308. doi: 10.1038/s41541-024-00836-w. PubMed PMID: 38459059; PMCID: PMC10923915.
209. Casey RM, Harris JB, Ahuka-Mundeke S, Dixon MG, Kizito GM, Nsele PM, Umutesi G, Laven J, Kosoy O, Paluku G, Gueye AS, Hyde TB, Ewetola R, Sheria GKM, Muyembe-Tamfum JJ, Staples JE. Immunogenicity of Fractional-Dose Vaccine during a Yellow Fever Outbreak -

Final Report. N Engl J Med. 2019;381(5):444-54. Epub 20180214. doi: 10.1056/NEJMoa1710430. PubMed PMID: 29443626; PMCID: PMC7064153.

210. Reis LR, Costa-Rocha IAD, Campi-Azevedo AC, Peruhype-Magalhaes V, Coelho-Dos-Reis JG, Costa-Pereira C, Otta DA, Freire LC, Lima SMB, Azevedo AS, Schwarcz WD, Ano Bom APD, Silva A, Souza AF, Castro TDM, Ferroco CLV, Filippis AMB, Nogueira FB, Homma A, Domingues CM, Sousa ESS, Camacho LAB, Maia MLS, Teixeira-Carvalho A, Martins-Filho OA. Exploratory study of humoral and cellular immunity to 17DD Yellow Fever vaccination in children and adults residents of areas without circulation of Yellow Fever Virus. Vaccine. 2022;40(5):798-810. Epub 20211227. doi: 10.1016/j.vaccine.2021.12.029. PubMed PMID: 34969545.

211. Campi-Azevedo AC, Peruhype-Magalhaes V, Coelho-Dos-Reis JG, Antonelli LR, Costa-Pereira C, Speziali E, Reis LR, Lemos JA, Ribeiro JGL, Bastos Camacho LA, de Sousa Maia ML, Barbosa de Lima SM, Simoes M, de Menezes Martins R, Homma A, Cota Malaquias LC, Tauil PL, Costa Vasconcelos PF, Martins Romano AP, Domingues CM, Teixeira-Carvalho A, Martins-Filho OA, Collaborative Group for Studies of Yellow Fever V. 17DD Yellow Fever Revaccination and Heightened Long-Term Immunity in Populations of Disease-Endemic Areas, Brazil. Emerg Infect Dis. 2019;25(8):1511-21. Epub 20190817. doi: 10.3201/eid2508.181432. PubMed PMID: 31298654; PMCID: PMC6649311.

212. PAHO. Yellow fever: vaccination status among confirmed nominal cases in the Americas, 2000-2014: Pan American Heath Organization Health Emergencies Department World Health Organization; 2023 [1 April 2024]. Available from: https://ais.paho.org/phip/viz/ed_yellowfever.asp.

213. Sawyer WA, Lloyd W. The Use of Mice in Tests of Immunity against Yellow Fever. J Exp Med. 1931;54(4):533-55. doi: 10.1084/jem.54.4.533. PubMed PMID: 19869938; PMCID: PMC2132022.

214. Porterfield JS. Plaque production with yellow fever and related arthropodborne viruses. Nature. 1959;183(4667):1069-70. doi: 10.1038/1831069b0. PubMed PMID: 13644293.

215. Porterfield JS. A plaque technique for the titration of yellow fever virus and antisera. Trans R Soc Trop Med Hyg. 1959;53:458-66. doi: 10.1016/0035-9203(59)90021-5. PubMed PMID: 14434289.

216. Spector S, Tauraso NM. Yellow fever virus. I. Development and evaluation of a plaque neutralization test. Appl Microbiol. 1968;16(11):1770-5. doi: 10.1128/am.16.11.1770-1775.1968. PubMed PMID: 4973067; PMCID: PMC547757.
217. Jonker EF, Visser LG, Roukens AH. Advances and controversies in yellow fever vaccination. Ther Adv Vaccines. 2013;1(4):144-52. doi: 10.1177/2051013613498954. PubMed PMID: 24757521; PMCID: PMC3991151.
218. Dia M, Bob NS, Talla C, Dupressoir A, Escadafal C, Thiam MS, Diallo A, Ndiaye O, Heraud JM, Faye O, Sall AA, Faye O, Fall G. Performance assessment and validation of a plaque reduction neutralization test (PRNT) in support to yellow fever diagnostic and vaccine clinical trials. J Med Virol. 2023;95(4):e28700. doi: 10.1002/jmv.28700. PubMed PMID: 36951314.
219. Hammarlund E, Amanna IJ, Dubois ME, Barron A, Engelmann F, Messaoudi I, Slifka MK. A flow cytometry-based assay for quantifying non-plaque forming strains of yellow fever virus. PLoS One. 2012;7(9):e41707. Epub 20120919. doi: 10.1371/journal.pone.0041707. PubMed PMID: 23028428; PMCID: PMC3446955.
220. Lambeth CR, White LJ, Johnston RE, de Silva AM. Flow cytometry-based assay for titrating dengue virus. J Clin Microbiol. 2005;43(7):3267-72. doi: 10.1128/JCM.43.7.3267-3272.2005. PubMed PMID: 16000446; PMCID: PMC1169137.
221. Blitvich BJ, Firth AE. Insect-specific flaviviruses: a systematic review of their discovery, host range, mode of transmission, superinfection exclusion potential and genomic organization. Viruses. 2015;7(4):1927-59. Epub 20150410. doi: 10.3390/v7041927. PubMed PMID: 25866904; PMCID: PMC4411683.
222. Nath H, Ghosh A, Basu K, Abhishek D, Biswas S. Dengue virus clinical isolates sustain viability of infected hepatic cells by counteracting apoptosis-mediated DNA breakage. bioRxiv. 2020.
223. Furtado ND, Raphael LM, Ribeiro IP, de Mello IS, Fernandes DR, Gomez MM, Dos Santos AAC, Nogueira MDS, de Castro MG, de Abreu FVS, Martins LC, Vasconcelos P, Lourenco-de-Oliveira R, Bonaldo MC. Biological Characterization of Yellow Fever Viruses Isolated From Non-human Primates in Brazil With Distinct Genomic Landscapes. Front Microbiol. 2022;13:757084. Epub 20220214. doi: 10.3389/fmicb.2022.757084. PubMed PMID: 35237244; PMCID: PMC8882863.

224. Scheck MK, Lehmann L, Zaucha M, Schwarzlmueller P, Huber K, Pritsch M, Barba-Spaeth G, Thorn-Seshold O, Krug AB, Endres S, Rothenfusser S, Thorn-Seshold J. FluoRNT: A robust, efficient assay for the detection of neutralising antibodies against yellow fever virus 17D. PLoS One. 2022;17(2):e0262149. Epub 20220209. doi: 10.1371/journal.pone.0262149. PubMed PMID: 35139078; PMCID: PMC8827462.
225. Simoes M, Camacho LA, Yamamura AM, Miranda EH, Cajaraville AC, da Silva Freire M. Evaluation of accuracy and reliability of the plaque reduction neutralization test (micro-PRNT) in detection of yellow fever virus antibodies. Biologicals. 2012;40(6):399-404. Epub 20120930. doi: 10.1016/j.biologicals.2012.09.005. PubMed PMID: 23034357.
226. Henchal EA, Gentry MK, McCown JM, Brandt WE. Dengue virus-specific and flavivirus group determinants identified with monoclonal antibodies by indirect immunofluorescence. Am J Trop Med Hyg. 1982;31(4):830-6. doi: 10.4269/ajtmh.1982.31.830. PubMed PMID: 6285749.
227. Medina-Magues LG, Muhe J, Jasny E, Medina-Magues ES, Roth N, Lopera-Madrid J, Salas-Quinchucua C, Knuese C, Petsch B, Osorio JE. Immunogenicity and protective activity of mRNA vaccine candidates against yellow fever virus in animal models. NPJ Vaccines. 2023;8(1):31. Epub 20230304. doi: 10.1038/s41541-023-00629-7. PubMed PMID: 36871059; PMCID: PMC9984760.
228. Vianna CM, Noronha TG, Camacho LAB, Andrade RC, de Souza Brum RC, Dos Santos EM, Aguiar DF, Dos Santos MLB, de Souza Cruz RL, de Lima SMB, de Souza Azevedo Soares A, Schwarcz WD, da Matta de Castro T, Xavier JR, da Conceicao DA, Homma A, de Lourdes de Sousa Maia M. Duration of post-vaccination immunity to yellow fever in volunteers ten years after a dose-response study - A complementary study. Vaccine. 2024;42(24):126083. Epub 20240625. doi: 10.1016/j.vaccine.2024.06.050. PubMed PMID: 38926068; PMCID: PMC11413730.
229. Dulbecco R. Production of Plaques in Monolayer Tissue Cultures by Single Particles of an Animal Virus. Proc Natl Acad Sci U S A. 1952;38(8):747-52. doi: 10.1073/pnas.38.8.747. PubMed PMID: 16589172; PMCID: PMC1063645.
230. Mendoza EJ, Manguiat K, Wood H, Drebot M. Two Detailed Plaque Assay Protocols for the Quantification of Infectious SARS-CoV-2. Curr Protoc Microbiol. 2020;57(1):ecpmc105. doi: 10.1002/cpmc.105. PubMed PMID: 32475066; PMCID: PMC7300432.

231. Gonzalez-Hernandez MB, Bragazzi Cunha J, Wobus CE. Plaque assay for murine norovirus. J Vis Exp. 2012(66):e4297. Epub 20120822. doi: 10.3791/4297. PubMed PMID: 22951568; PMCID: PMC3487293.
232. Kuno G. Serodiagnosis of flaviviral infections and vaccinations in humans. Adv Virus Res. 2003;61:3-65. doi: 10.1016/s0065-3527(03)61001-8. PubMed PMID: 14714429.
233. Shurtleff AC, Bloomfield HA, Mort S, Orr SA, Audet B, Whitaker T, Richards MJ, Bavari S. Validation of the Filovirus Plaque Assay for Use in Preclinical Studies. Viruses. 2016;8(4):113. Epub 20160421. doi: 10.3390/v8040113. PubMed PMID: 27110807; PMCID: PMC4848606.
234. Gaythorpe KA, Hamlet A, Jean K, Garkauskas Ramos D, Cibrelus L, Garske T, Ferguson N. The global burden of yellow fever. Elife. 2021;10. Epub 20210316. doi: 10.7554/eLife.64670. PubMed PMID: 33722340; PMCID: PMC7963473.
235. Frierson JG. The yellow fever vaccine: a history. The Yale journal of biology and medicine. 2010;83(2):77-85.
236. de Melo AB, da Silva Mda P, Magalhaes MC, Gonzales Gil LH, Freese de Carvalho EM, Braga-Neto UM, Bertani GR, Marques ET, Jr., Cordeiro MT. Description of a prospective 17DD yellow fever vaccine cohort in Recife, Brazil. Am J Trop Med Hyg. 2011;85(4):739-47. doi: 10.4269/ajtmh.2011.10-0496. PubMed PMID: 21976581; PMCID: PMC3183786.
237. Reinhardt B, Jaspert R, Niedrig M, Kostner C, L'Age-Stehr J. Development of viremia and humoral and cellular parameters of immune activation after vaccination with yellow fever virus strain 17D: a model of human flavivirus infection. J Med Virol. 1998;56(2):159-67. doi: 10.1002/(sici)1096-9071(199810)56:2<159::aid-jmv10>3.0.co;2-b. PubMed PMID: 9746073.
238. Machado VW, Vasconcelos PF, Silva EV, Santos JB. Serologic assessment of yellow fever immunity in the rural population of a yellow fever-endemic area in Central Brazil. Rev Soc Bras Med Trop. 2013;46(2):166-71. doi: 10.1590/0037-8682-0007-2012. PubMed PMID: 23740066.
239. Dick GW, Gee FL. Immunity to yellow fever nine years after vaccination with 17D vaccine. Trans R Soc Trop Med Hyg. 1952;46(4):449-58. doi: 10.1016/0035-9203(52)90062-x. PubMed PMID: 14958824.
240. Rosenzweig EC, Babione RW, Wisseman CL, Jr. Immunological studies with group B arthropod-borne viruses. IV. Persistence of yellow fever antibodies following vaccination with

17D strain yellow fever vaccine. Am J Trop Med Hyg. 1963;12:230-5. PubMed PMID: 13975014.

241. Groot H, Riberiro RB. Neutralizing and haemagglutination-inhibiting antibodies to yellow fever 17 years after vaccination with 17D vaccine. Bull World Health Organ. 1962;27(6):699-707. PubMed PMID: 13950710; PMCID: PMC2555840.

242. Beck AS, Wood TG, Widen SG, Thompson JK, Barrett ADT. Analysis By Deep Sequencing of Discontinued Neurotropic Yellow Fever Vaccine Strains. Sci Rep. 2018;8(1):13408. Epub 20180907. doi: 10.1038/s41598-018-31085-2. PubMed PMID: 30194325; PMCID: PMC6128858.

243. Carbaugh DL, Lazear HM. Flavivirus Envelope Protein Glycosylation: Impacts on Viral Infection and Pathogenesis. J Virol. 2020;94(11). Epub 20200518. doi: 10.1128/JVI.00104-20. PubMed PMID: 32161171; PMCID: PMC7269438.

244. Mount DW. Using PAM Matrices in Sequence Alignments. CSH Protoc. 2008;2008:pdb top38. Epub 20080601. doi: 10.1101/pdb.top38. PubMed PMID: 21356854.

245. Smith DJ, Lapedes AS, de Jong JC, Bestebroer TM, Rimmelzwaan GF, Osterhaus AD, Fouchier RA. Mapping the antigenic and genetic evolution of influenza virus. Science. 2004;305(5682):371-6. Epub 20040624. doi: 10.1126/science.1097211. PubMed PMID: 15218094.

246. Katzelnick LC, Fonville JM, Gromowski GD, Bustos Arriaga J, Green A, James SL, Lau L, Montoya M, Wang C, VanBlargan LA, Russell CA, Thu HM, Pierson TC, Buchy P, Aaskov JG, Munoz-Jordan JL, Vasilakis N, Gibbons RV, Tesh RB, Osterhaus AD, Fouchier RA, Durbin A, Simmons CP, Holmes EC, Harris E, Whitehead SS, Smith DJ. Dengue viruses cluster antigenically but not as discrete serotypes. Science. 2015;349(6254):1338-43. doi: 10.1126/science.aac5017. PubMed PMID: 26383952; PMCID: PMC4876809.

247. Wang L, Huang AT, Katzelnick LC, Lefrancq N, Escoto AC, Duret L, Chowdhury N, Jarman R, Conte MA, Berry IM, Fernandez S, Klungthong C, Thaisomboonsuk B, Suntarattiwong P, Vandepitte W, Whitehead SS, Cauchemez S, Cummings DAT, Salje H. Antigenic distance between primary and secondary dengue infections correlates with disease risk. Sci Transl Med. 2024;16(744):eadk3259. Epub 20240424. doi: 10.1126/scitranslmed.adk3259. PubMed PMID: 38657027.

248. Nix CD, Salberg J, Coulter FJ, Kareko BW, Lyski ZL, Booty BL, Messer WB. Potency and breadth of human primary ZIKV immune sera shows that Zika viruses cluster antigenically as a single serotype. PLoS Negl Trop Dis. 2020;14(4):e0008006. Epub 20200413. doi: 10.1371/journal.pntd.0008006. PubMed PMID: 32282800; PMCID: PMC7213746.
249. Wang W, Lusvarghi S, Subramanian R, Epsi NJ, Wang R, Goguet E, Fries AC, Echegaray F, Vassell R, Coggins SA, Richard SA, Lindholm DA, Mende K, Ewers EC, Larson DT, Colombo RE, Colombo CJ, Joseph JO, Rozman JS, Smith A, Lalani T, Berjohn CM, Maves RC, Jones MU, Mody R, Huprikar N, Livezey J, Saunders D, Hollis-Perry M, Wang G, Ganesan A, Simons MP, Broder CC, Tribble DR, Laing ED, Agan BK, Burgess TH, Mitre E, Pollett SD, Katzelnick LC, Weiss CD. Antigenic cartography of well-characterized human sera shows SARS-CoV-2 neutralization differences based on infection and vaccination history. Cell Host Microbe. 2022;30(12):1745-58 e7. Epub 20221021. doi: 10.1016/j.chom.2022.10.012. PubMed PMID: 36356586; PMCID: PMC9584854.
250. Wilks S. An introduction to antigenic cartography [cited 2024 Aug 5, 2024]. Available from: https://acorg.github.io/Racmacs/articles/intro-to-antigenic-cartography.html.
251. Mason RA, Tauraso NM, Ginn RK, O'Brien TC, Trimmer RW. Yellow fever vaccine. V. Antibody response in maonkeys inoculated with graded doses of the 17D vaccine. Appl Microbiol. 1972;23(5):908-13. doi: 10.1128/am.23.5.908-913.1972. PubMed PMID: 4624211; PMCID: PMC380469.
252. Pokidysheva E, Zhang Y, Battisti AJ, Bator-Kelly CM, Chipman PR, Xiao C, Gregorio GG, Hendrickson WA, Kuhn RJ, Rossmann MG. Cryo-EM reconstruction of dengue virus in complex with the carbohydrate recognition domain of DC-SIGN. Cell. 2006;124(3):485-93. doi: 10.1016/j.cell.2005.11.042. PubMed PMID: 16469696.
253. Yap SSL, Nguyen-Khuong T, Rudd PM, Alonso S. Dengue Virus Glycosylation: What Do We Know? Front Microbiol. 2017;8:1415. Epub 20170725. doi: 10.3389/fmicb.2017.01415. PubMed PMID: 28791003; PMCID: PMC5524768.
254. Stecher G, Tamura K, Kumar S. Molecular Evolutionary Genetics Analysis (MEGA) for macOS. Mol Biol Evol. 2020;37(4):1237-9. doi: 10.1093/molbev/msz312. PubMed PMID: 31904846; PMCID: PMC7086165.

255. Tamura K, Stecher G, Kumar S. MEGA11: Molecular Evolutionary Genetics Analysis Version 11. Mol Biol Evol. 2021;38(7):3022-7. doi: 10.1093/molbev/msab120. PubMed PMID: 33892491; PMCID: PMC8233496.
256. Schwarz R, Dayhoff M. Matrices for detecting distant relationships. Atlas of protein sequences: National Biomedical Research Foundation; 1979. p. 353-58.
257. Gordon A, Kuan G, Mercado JC, Gresh L, Aviles W, Balmaseda A, Harris E. The Nicaraguan pediatric dengue cohort study: incidence of inapparent and symptomatic dengue virus infections, 2004-2010. PLoS Negl Trop Dis. 2013;7(9):e2462. Epub 20130926. doi: 10.1371/journal.pntd.0002462. PubMed PMID: 24086788; PMCID: PMC3784501.

Appendix 1: Potency and breadth of human primary ZIKV immune sera shows that Zika viruses cluster antigenically as a single serotype

Chad D. Nix[1,2], Jonathan Salberg[3], Felicity J. Coulter[2], Bettie W. Kareko[2], Zoe L. Lyski[2], Brian L. Booty[4], William B. Messer[2,3,5*]

[1]Dept. of Infection Prevention and Control, Oregon Health and Science University, Portland, Oregon, United States of America.
[2]Dept. of Molecular Microbiology and Immunology, Oregon Health and Science University, Portland, Oregon, United States of America.
[3]Dept. of Medicine, Division of Infectious Diseases, Oregon Health and Science University, Portland, Oregon, United States of America.
[4]Oregon Clinical and Translational Research Institute, Oregon Health and Science University, Portland, Oregon, United States of America.
[5]Program in Epidemiology, Oregon Health & Science University–Portland State University School of Public Health, Portland, Oregon, United States of America.

Published: April 13, 2020, in PLOS Neglected Tropical Diseases
Doi: 10.1371/journal.pntd.0008006

Section A1.1: Abstract

Zika virus (ZIKV) emerged as a global public health threat throughout the Americas since 2014. Phylogenetically, the virus is composed of three main lineages, an African, Asian, and American lineage. The recent emergence and spread of ZIKV has raised questions regarding the breadth and potency of human primary ZIKV immune sera against antigenically diverse ZIKV. Although

ZIKV is thought to compose a single antigenic serotype, in-depth evaluation of the antigenic relatedness of ZIKV across genetic variants has been limited to a relatively small series of early convalescent human immune sera (4–12 weeks) against a limited number (3) of genetic variants. Using virus neutralization assays, we characterize the potency and breadth of twelve primary ZIKV immune sera from adults infected 5 to 38 months previously against a panel of 11 ZIKV isolates from the African, Asian and American lineages. We assess the variability of neutralization potency of immune sera from these subjects and the variability of susceptibility to neutralization for each virus isolate. Overall, we found all sera neutralized all viruses at $FRNT_{50}$ ranging from 1:271 to 1:4271, a 15.8-fold range, with only small differences between subject geometric mean titers (GMT) against all viruses and small differences between each ZIKV isolate and sensitivity to neutralization by all sera: when pooled, African strains were 1.3-fold more sensitive to neutralization by subject immune sera compared to pooled American strains. Finally, we subjected our data to analysis using antigenic cartography, finding that ZIKV are highly antigenically similar, with only a ~4-fold range across all antigenic distances between viruses, consistent with a single serotype.

Section A1.2: Author summary

The recent emergence of Zika virus as an important human pathogen has raised questions about the durability and breadth of Zika virus immunity following natural infection in humans. While global epidemic patterns suggest that Zika infection elicits a protective immune response that is likely to offer long-term protection against repeat infection by other Zika viruses, only one study to date has formally examined the ability of human Zika immune sera to neutralize different Zika viruses. That study was limited because it evaluated human immune sera no more than 13 weeks after Zika virus infection and tested a relatively small number of Zika viruses. In this study, we examine twelve human Zika immune sera as far as 3 years after infection and test the sera against a total of eleven Zika virus isolates. Our results confirm the earlier study and epidemic patterns that suggest Zika virus exists in nature as a single serotype, and infection with one Zika virus can be expected to elicit protective immunity against repeat infection by any Zika virus for years to decades after the first infection.

Section A1.3: Introduction

Although Zika virus (ZIKV) was first isolated in 1947 from a rhesus monkey in the Zika Forest of Uganda[1, 2], only in the last decade has ZIKV emerged as a global public health threat. The first large outbreak among humans was characterized by an epidemic of fever and rash on the Island of Yap in 2007.[3, 4] ZIKV then went largely quiescent until introduction to French Polynesia in 2013, where an epidemiologic association with Guillain-Barré syndrome (GBS) was identified.[5] A rapid expansion ensued as ZIKV spread throughout Oceania, progressing to the Americas in 2015.[6] Concern for the consequences of ZIKV infection heightened as an increased number of infants born with microcephaly were recorded in areas of confirmed ZIKV transmission in Brazil. The association between congenital abnormalities and GBS with ZIKV infection prompted the World Health Organization (WHO) to declare a Public Health Emergency of International Concern on February 1, 2016 (PHEIC).[7] Although ZIKV remains a significant long-term public health challenge, on November 18, 2016, the WHO announced that the ZIKV epidemic no longer met criteria for representing a PHEIC as the number of reported cases decreased.

ZIKV is a single-stranded positive-sense RNA of the *Flavivirus* genus transmitted by *Aedes spp*. mosquitoes. It has historically been assigned two major lineages, an African lineage and an Asian lineage.[8] However, recent analyses suggest a third, American lineage, has emerged from the Asian lineage.[9] The ZIKV virion contains three structural proteins: capsid (C), pre-membrane/membrane(prM/M), and the envelope (E) glycoprotein. The E glycoprotein is the primary target of virus-neutralizing antibodies following natural infection, and these antibodies are thought to be primarily responsible for long-term protection against repeat infection.[9] ZIKV E glycoproteins are highly conserved, with amino acid divergence at ~6% between ZIKV lineages and ~2% within lineages. Phylogenetic analyses suggest that ZIKV exists as a single serotype, however, significant differences in neutralization titers in dengue virus (DENV) have been explained by as few as two amino acid substitutions,[10] and the amount of amino acid variability needed to produce a distinct DENV serotype is difficult to predict.[11]

Historically, immune sera raised in humans, mice, or non-human primates (NHP) have been used to formally characterize flavivirus serotypes, with the first two DENV serotypes being defined

using five viruses isolates and four human convalescent immune sera[12]. What we now know of as the four DENV serotypes were first defined using fourteen clinical virus isolates, four NHP sera and an unreported number of mouse sera.[13] The original characterization of ZIKV as a distinct virus used a single ZIKV isolate and ZIKV immune sera from a single NHP and sera from fourteen NHPs infected with other known sylvatic viruses [2]. However, the correlation between serotype-specific antibodies raised in experimentally infected animals and human serotype-specific immunity following natural infection has never been established. To more fully characterize the potency and breadth of human ZIKV immune sera many months to years after primary (single flavivirus) natural infection and empirically evaluate the antigenic relationship between ZIKV, we tested a panel of twelve human sera collected 5 to 38 months following ZIKV infection against eleven genetically distinct ZIKV isolates. Immune sera potency and breadth were assessed using 50% focus reduction neutralization tests ($FRNT_{50}$) and we evaluated antigenic relatedness using antigenic cartography. These study results confirm and advance the early work by others and have important implications for ZIKV vaccine design and evaluation. Additionally they provide a solid basis for estimating and understanding the very limited potential for antigenically variant ZIKV viruses to penetrate otherwise ZIKV immune populations.

Section A1.4: Methods

A1.4.1 Human research ethics

The study has been reviewed and approved by the Oregon Health & Science University Institutional Review Board (IRB#10212). Informed consent was obtained from subjects on initiation of their participation in the study.

A1.4.2 Sample collection and storage

On enrollment, subjects provided approximately 80 mL of blood, with 30 mL collected in BD "red top" serum separator vacutainers (Becton-Dickson) for serologic studies and stored at -80°C until used for assays.

A1.4.3 Viruses and tissue culture

All ZIKVs and yellow fever virus strain 17D (YFVax®) were propagated in C6/36 mosquito cells (ATCC CRL 1660) in minimal essential media (MEM) supplemented with L-glutamine (Gibco), non-essential amino acids (NEAA) (Gibco), antibiotic-antimycotic (anti-anti) (Gibco) and 5% by volume fetal bovine serum (FBS) incubated at 32°C, 5% CO_2. Zika viruses included PRVABC59 (Puerto_Rico_2015) and FSS13025 (Cambodia_2010), both generously provided by the World Reference Center for Emerging Viruses and Arboviruses (WRCEVA), and ZIKV/Homo sapiens/COL/FLR/2015 (Colombia_2015), BeH819015 (Brazil_2015), MEX 2–81 (Mexico_2016), 41525 (Senegal_1984), IbH_30656 (Nigeria_1968), and H/PF/2013 (French_Polynesia_2013), generously provided by Alec Hirsch, PhD, OHSU Vaccine and Gene Therapy Institute. Strains MR766 (Uganda_1947), P 6–740 (Malaysia_1966), and PLCal_ZV (Thailand_2013) were obtained from BEI resources. 17D was obtained from the manufacturer (Sanofi USA). All DENV were propagated in Vero cells that over-express furn. [14, 15] VF cells were grown in MEM with 10% FBS, NEAA, anti-anti, and selection antibiotic G418 (InvivoGen) at 37°C and 5% CO_2 DENV used in neutralization assays included infectious clones of DENV3 UNC3001,[16] and DENV4 DV4SL1992a[17] as well as DENV1 WestPac'74 (generously provided by Stephen Whitehead, National Institutes of Health) and DENV2 16803 (WRCEVA). All neutralization assays were performed using Vero cells (ATCC CCL-81) similarly grown with MEM, NEAA, anti-anti and 10% by volume FBS incubated at 37°C and 5% CO_2.

A1.4.4 Neutralization assays

Fifty percent focus reduction neutralization test ($FRNT_{50}$) titers were used to characterize subject sera. Subject sera were first heat-inactivated at 56°C for 30 minutes. Sera were then diluted four-fold in MEM supplemented with 2% FBS from a starting dilution of 1:10 and mixed with an equal

volume of ~100 focus forming units (FFU) of ZIKV strains giving a final starting dilution of 1:20. Virus-dilution mixes without sera were prepared simultaneously as controls for input virus FFUs. After 1 hour of incubation, virus mixes were inoculated into individual wells of 96 well plates seeded with Vero cells, incubated for 1 hour, and overlaid with 1% methylcellulose in Opti-MEM (Gibco) supplemented with NEAA, anti-anti, amphotericin B, and 2% FBS. Plates were incubated for 24 hours at 37°C, 5% CO_2. The overlay was then removed, monolayers were fixed with 4% formaldehyde, incubated with the anti-flavivirus mouse monoclonal antibody (4G2) (ATCC HB 112) followed by a horse-radish peroxidase (HRP) conjugated secondary goat-anti-mouse antibody (ThermoFisher Scientific Cat # 62–6520). Plates were washed 3 times with PBS and HRP True Blue Peroxidase Substrate (KPL) was then applied for 15–60 minutes to visualize infected foci. Using a CTL ImmunoSpot instrument (CTL, Cleveland, OH, USA), foci in individual wells were scanned, counted, and counts underwent quality control. Proportion of virus neutralized per well was calculated and the serum dilution that neutralizes 50% of control input virus ($FRNT_{50}$) was determined by sigmoidal dose-response curve fitting of percent neutralization vs. fold serum dilution using GraphPad Prism® (Version 7.0). All assays were performed in biologic duplicates. Individual sera that showed a greater than 4-fold difference between biologic replicates were subjected to repeat neutralization assays. Initial neutralization assays against DENV1-4 and YFV 17D were conducted in a similar manner in a 24-well plate format with 30–40 PFU/well. DENV plates were incubated for 5 days and counter stained for infectious foci in the same manner as ZIKVs, 17D plates were incubated for 7 days and counter stained with crystal violet to visualize infectious plaques. Fifty-percent neutralization titers for all assays are reported as the fold-dilutions.

A1.4.5 Antigenic cartography

The ZIKV antigenic map was constructed as previously described[11, 18] and implemented using the Acmacs Web Cherry platform (https://acmacs-web.antigenic-cartography.org/). Briefly, antigenic maps are constructed by first generating a table of antigenic distances (D_{ij}) between each individual virus (i) and serum (j) using serum titers for each serum-titer pair (N_{ij}). To calculate table distance, the titer against the best neutralized virus for that serum is defined as b_i and the distances for that serum are calculated as $D_{ij} = log_2(b_i)-log(N_{ij})$. For the best neutralized virus for

that serum, $N_{ij} = b_i$, and this distance will be equal to 0. For the remaining serum-virus pairs, table distance D_{ij} is equivalent to the fold-difference in titer between b_{ij} and N_{ij}. Euclidean map distance (d_{ij}) for each serum-virus pair is found by minimizing the error between the table distance D_{ij} and map distance, d_{ij}, using the error function $E = \sum_{ij} e(D_{ij},d_{ij})$, where $e(D_{ij},d_{ij}) = (D_{ij}-d_{ij})^2$ when the neutralization titer is above 1:20. For viruses with neutralization titers <1:20, the error was defined as $e(D_{ij},d_{ij}) = (D_{ij}-1-d_{ij})^2(1/1+e^{-10(Dij-1-dij)})$. To make a map and derive d_{ij} for each serum-virus pair, viruses and sera are assigned random starting coordinates and the error function is minimized using the conjugate gradient optimization method. One thousand independent optimizations were conducted to generate the aintgenic map.

A1.4.6 Statistical analyses

The evolutionary history for the genetic relatedness of ZIKV was inferred by using the Maximum Likelihood method and General Time Reversible model. The tree with the highest log likelihood was retained. Initial tree(s) for the heuristic search were obtained automatically by applying Neighbor-Join and BioNJ algorithms to a matrix of pairwise distances estimated using the Maximum Composite Likelihood (MCL) approach, and then selecting the topology with superior log likelihood value. Codon positions included were 1st+2nd+3rd. There were a total of 2382 positions in the final dataset. Evolutionary analyses were conducted in MEGA X.[19]

Geometric mean titers between sera were plotted and compared in GraphPad Prism (Version 8.00 for Mac, GraphPad Software, La Jolla California USA, www.graphpad.com) using ANOVA followed by Bonferroni's correction for multiple comparisons. Potency and breadth survival curves were assembled in GraphPad Prism and compared using a Mantel-Cox non-parametric comparison followed by Bonferroni's correction for multiple comparisons (adjusted P = 0.05). Correlation between geometric mean titer (GMT) or area under the curve (AUC) for survival curves and months post-infection was assessed using standard least-squares fitting of $\log_{10}$transformed $FRNT_{50}$ or AUC and months post-infection (power model) using JMP® (Version 14.0.0. SAS Institute Inc., Cary, NC, 1989–2019.)

A1.4.7 Sequencing

Viral RNA was isolated from tissue culture supernatants using QIAamp Viral RNA Mini Kit (Qiagen). cDNA was generated using random hexamers and SuperScript II Reverse Transcriptase (Thermo Fisher), according to the manufacturer's instructions. Capsid genes were amplified from cDNA using primers ZV_seqA_s and ZV_seqA_a using Phusion Polymerase according to the manufacturer's instructions. Fifty µL reactions (1X HF buffer (Thermo Fisher), 200mM each dNTP, 0.5mM forward primer, 0.5mM reverse primer, 1U Phusion Polymerase and 4 mL cDNA) were subjected to thermocycling conditions of 98°C for 30 seconds, followed by 40 cycles of 98°C for 10 seconds, 58°C for 15 seconds and 72°C for 15 seconds, prior to final extension at 72°C for 10 minutes. prM, and E genes were amplified from cDNA using primers ZV_seqB_s and ZVseqF_a and Phusion Polymerase as 50 µL reactions as before (S1 Table). Thermocycling conditions consisted of 98°C for 30 seconds, followed by 40 cycles of 98°C for 10 seconds, 55°C for 15 seconds and 72°C for 80 seconds, prior to final extension at 72°C for 10 minutes. PCR products were visualized on 1.5% agarose gel with ethidium bromide, purified (QIAquick PCR Purification Kit, Qiagen) and mixed with sequencing primers (S1 Table) for submission to a commercial sequencing company (Genewiz) for Sanger sequencing. Contigs were assembled from chromatographs and aligned using Geneious Prime (version 2019.2.1).

Section A1.5: Results

A1.5.1 Study subjects

A total of 12 subjects with history of ZIKV infection (Table 1) and without serologic evidence of DENV infection (Table 2) were identified. Clinical infections were documented between February 2014 and December 2016 and individual subject sera were obtained anywhere from 5 to 38 months post-infection. Infections were primarily acquired in Latin America or the Caribbean with two infections documented in the Cook Islands, five subjects had documented yellow fever vaccinations, all of whom had detectable YFV neutralizing antibodies (Table 2).

Table[A1.1]

ID	Sex	Age	Country of infection	Months post-infection	Year received yellow fever vaccine
11884	Male	28	Nicaragua	5	NV
14269	Female	45	Cuba	10	NV
14278	Female	51	Mexico	10	NV
14276	Female	52	Virgin Islands	12	NV
14252	Female	24	Mexico	13	2013
14664	Female	39	Jamaica	14	2002
11981	Female	44	Dominican Republic	15	2008
14236	Male	55	Nicaragua	15	1997
14137	Female	41	Guatemala	18	2003
12451	Female	61	Cook Islands	24	NV
12462	Male	69	Cook Islands	27	NV
11942	Female	25	Haiti	38	NV

NV = Not Vaccinated

https://doi.org/10.1371/journal.pntd.0008006.t001

[Table A1.1]

[A1.1] Study subjects.

Table[A1.2]

ID	Sex	Age	Country of infection	Months post-infection	Year received yellow fever vaccine
11884	Male	28	Nicaragua	5	NV
14269	Female	45	Cuba	10	NV
14278	Female	51	Mexico	10	NV
14276	Female	52	Virgin Islands	12	NV
14252	Female	24	Mexico	13	2013
14664	Female	39	Jamaica	14	2002
11981	Female	44	Dominican Republic	15	2008
14236	Male	55	Nicaragua	15	1997
14137	Female	41	Guatemala	18	2003
12451	Female	61	Cook Islands	24	NV
12462	Male	69	Cook Islands	27	NV
11942	Female	25	Haiti	38	NV

NV = Not Vaccinated

https://doi.org/10.1371/journal.pntd.0008006.t001

[Table A1.2]

[A1.2] Subject neutralization profiles by fold serum dilution yielding 50% neutralization (FRNT50).

A1.5.2 Zika viruses

ZIKV immune sera from the 12 subjects were tested against eleven ZIKV strains (Table 3): five of American lineage, three of Asian lineage, and three of African lineage. Overall amino acid homology in the ZIKV structural proteins C/prM/E between these strains range from 95.7–99.7% (mean: 98.2%). The viruses grouped by area of geographic isolation with the French Polynesian isolate most closely related to the four Latin American isolates (Fig 1).

Figure[A1.1]

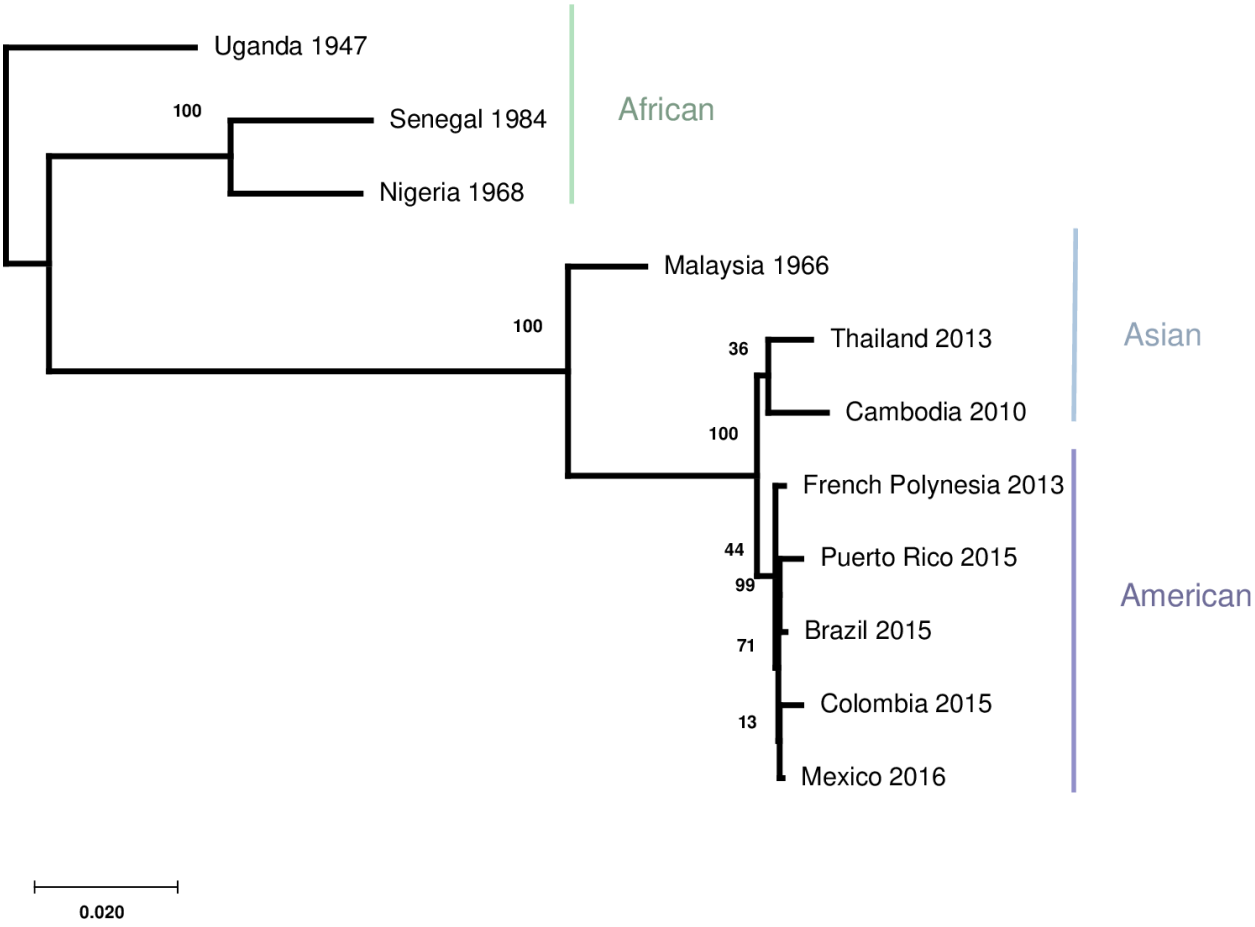

[Figure A1.1]

[A1.1] **Molecular phylogenetic analysis by maximum likelihood method.**

The percentage of trees in which the associated taxa clustered together is shown next to the branches. The tree is drawn to scale, with branch lengths measured in the number of substitutions per site. Colored bars correspond to virus strain region of isolation.

Table[A1.3]

Virus strain name	Isolate	Accession #	Year isolated	Location
Uganda_1947	MR766	MN755624	1947	Uganda
Senegal_1984	41525	MN755616	1984	Senegal
Nigeria_1968	IbH_30656	MN755617	1968	Nigeria
Malaysia_1966	P 6–740	MN755625	1966	Malaysia
Cambodia_2010	FSS13025	MN755621	2010	Cambodia
Thailand_2013	PLCal_ZV	MN755626	2013	Thailand
French_Polynesia_2013	H/PF/2013	MN755619	2013	French Polynesia
Puerto_Rico_2015	PRVABC59	MN755623	2015	Puerto Rico
Brazil_2015	BeH819015	MN755622	2015	Brazil
Colombia_2015	ZIKV/Homo sapiens/COL/FLR/2015	MN755620	2015	Colombia
Mexico_2016	MEX 2–81	MN755618	2016	Mexico

https://doi.org/10.1371/journal.pntd.0008006.t003

[Table A1.3]

Table A1.3 ZIKV strain.

A1.5.3 Virus specific neutralization by subject.

We first evaluated individual serum neutralizing potency against each of the eleven viruses (Fig 2). Individual $FRNT_{50}$ values between sera ranged from a serum dilution of 1:271 (serum 12462 vs Senegal_1968) to a serum dilution of 1:4271 (serum 14269 vs Malaysia_1966), a 15.8-fold range between all subjects and all viruses. However, within subject variability was substantially less, ranging from 2.28-fold (subject 14278) to 4.44-fold (subject 14236) (Fig 2). None of the titers showed significant differences within subjects (ANOVA).

Figure[A1.2]

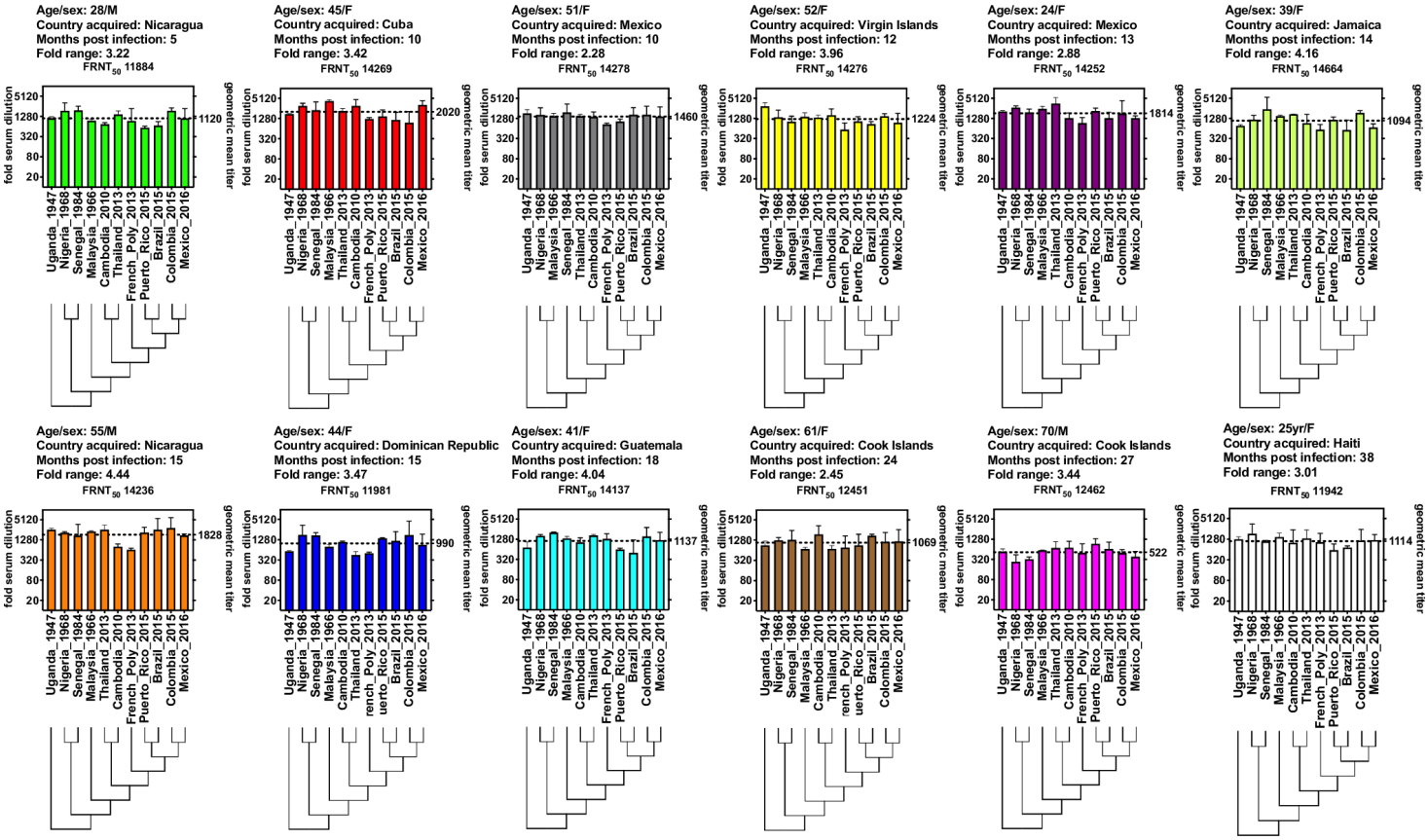

[Figure A1.2]

Figure A1.2 $FRNT_{50}$ titers for subject sera against each virus.

Fold serum dilution is shown on the left Y-axis, geometric mean titer (GMT) for each subject against all 11 viruses is plotted on the right Y-axis. Viruses and their relative phylogenetic relationships are shown on the X-axis. Subject age, gender, country infection acquired, months post-infection and fold-FRNT50 range are reported above each serum plot. The sera are ordered left to right from most recent to most remote infection.

A1.5.4 Between subject serum potency and breadth.

We next compared geometric mean titers between each subject (Fig 3A) by ANOVA and overall potency and breadth by survival curve analysis (Fig 3B). Overall, individual subject GMT against all eleven viruses had a relatively narrow range, from a low of 1:521(subject 12462) to a high of 1:2020 (subject 14269), or a 3.9-fold difference. Subject 12462 serum GMT was significantly lower than all other subject sera, subject 11981 had a significantly lower GMT (1:990) against 4

subject sera, and subject 14269 had a significantly higher GMT against 5 other subject sera (ANOVA followed by Tukey HSD, Fig 3A). As an alternate approach to visualizing and comparing individual subject neutralization profiles, we constructed potency and breadth curves for each subject (Fig 3B). Potency and breadth neutralization curves were first developed in the HIV field to characterize broadly neutralizing antibodies and immune sera against panels of HIV pseudoviruses (de Camp et al, 2014). These curves maintain resolution at the level of neutralization titer against each virus, rather than calculating a mean estimate based on all titers. Curves show the number of viruses neutralized at a given serum dilution over the range of all dilutions tested, analogous to survival over time in a Kaplan-Meier curve. Curves are compared using the non-parametric Mantel-Cox test followed by a Bonferroni correction for multiple comparisons. This approach does not assume a normal distribution of individual titers, but is also less sensitive to differences between curves. Upon inspection, 12462 again stands out as different from all other subjects' neutralization pattern, although the difference was only statistically significant for sera 14278, 14252, 14236, 11981, 12451 and 11942. None of the other eleven sera tested differed from one-another in potency or breadth. Finally, we tested whether there was a correlation between GMT (Fig 3A) or area under the curve (Fig 3B) and months post-infection, finding no correlation between time since infection and subsequent ZIKV neutralizing antibody titers (adjusted R^2 = -0.1, P = 0.80 for both GMT and AUC).

Figure A1.3

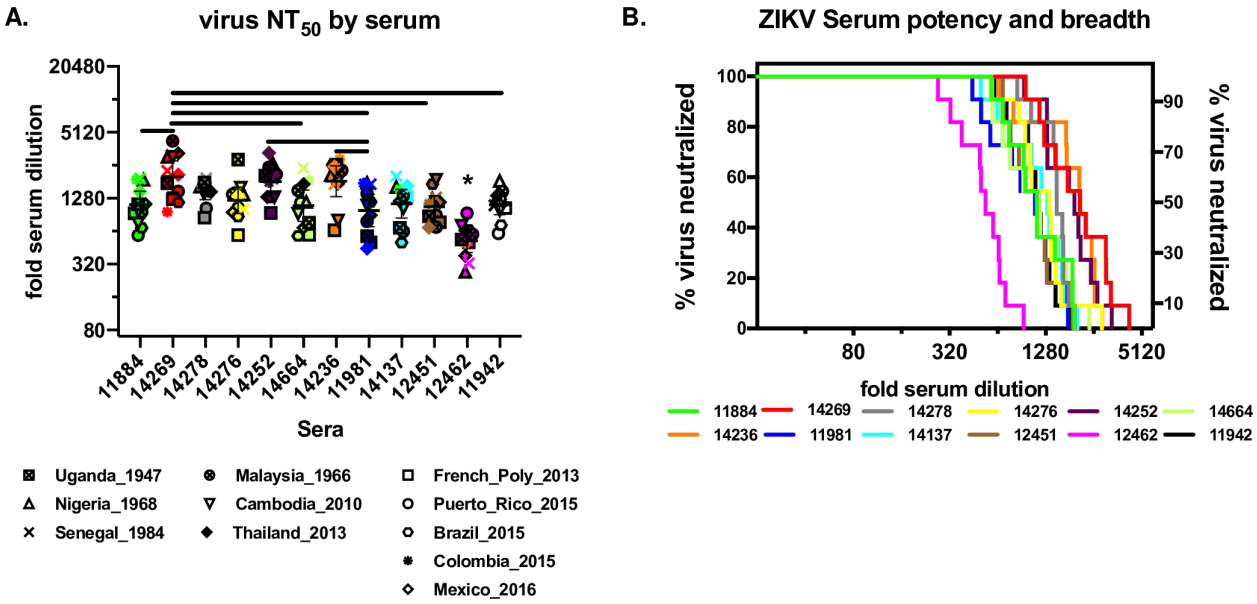

[Figure A1.3]

[A1.3] Potency and breadth of subject immune sera.

(A) GMT for each serum against eleven ZIKV isolates. Y-axis shows fold-serum dilution, each virus $FNRT_{50}$ value is plotted by the correlating symbol show in the legend below the plot. The symbols are color coded to match the sera indicated in Fig 2. Line and whiskers show serum GMT and 95% confidence. The GMT for subject 12462 (*) was significantly lower than all other sera (ANOVA followed by Tukey's correction for multiple comparisons, $P<0.05$). Remaining sera pairs that had GMTs that differed significantly are show by horizontal bars (ANOVA followed by Tukey's correction for multiple comparisons, $P<0.05$) **(B)** Potency and breadth curve for each subject serum. The Y-axes shows proportion of viruses neutralized (N = 11), X axis shows fold serum dilution. The plots are color coded to match the sera in Fig 2. The plot for each serum shows the proportion of viruses neutralized by $FRNT_{50}$ at a given serum dilution. Each step in each plot represents an $FRNT_{50}$ value for one virus; as fold serum dilution increases for each serum, the proportion of viruses neutralized decreases by 1/11 (9.1%) as each $FRNT_{50}$ dilution for each virus is crossed. *differs from 12462, Mantel-Cox followed by Bonferroni's correction for multiple comparisons, $P<0.05$.

A1.5.5 Neutralization by virus and antigenic cartography.

To specifically address the relative differences in virus sensitivity to neutralization by human immune sera, we first compared GMTs for each virus against all sera (Fig 4A). GMTs for each virus ranged from 1:836 for French_Poly_2013 to 1:1594 for Nigeria_1968, a 1.91-fold difference. None of the differences between any of the GMTs by virus were statistically significant (ANOVA followed by Tukey HSD post-hoc test). When comparted by strain, the GMTs for African, Asian, and American were 1:1400, 1:1306, and 1:1067, respectively, with the African and the American strains differing significantly from one another, a 1.31-fold difference (ANOVA followed by Bonferroni, P = 0.016).

Figure[A1.4]

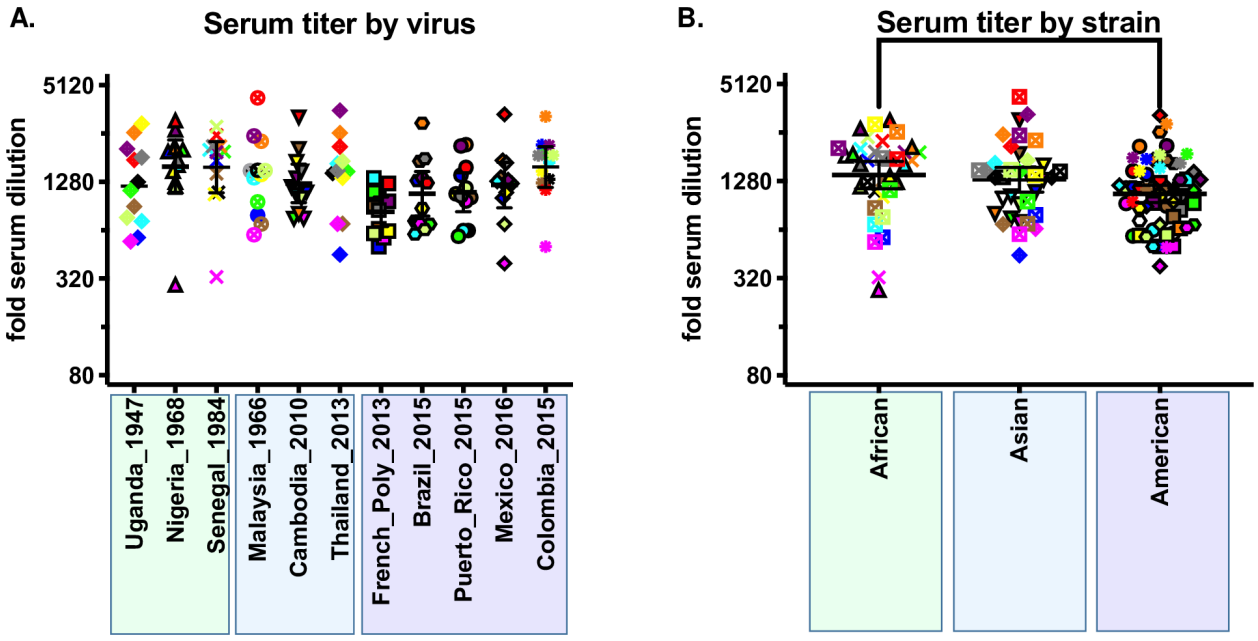

[Figure A1.4]

[A1.4] Neutralization by virus and strain.

(A) $FRNT_{50}$ titers for each serum against each virus. The Y-axis shows fold-serum dilution, the X-axis shows each virus, the phylogenetic tree below the X-axis shows the relative genetic relatedness of the viruses. Individual virus symbols are indicated below the figure and the symbols are color-coded to match the sera in Fig 2. **(B)** $FRNT_{50}$titers for ZIKV grouped by strain. Strain pairs found to be different by ANOVA followed by Tukey HSD correction for multiple comparisons are show by brackets (P = 0.038).

To further characterize the antigenic relationship between genetically distinct ZIKV, we turned to antigenic cartography.[11, 18] Antigenic cartography has been implemented previously to describe the antigenic relatedness of dengue viruses[11, 20] and influenza.[18, 21–23] Antigenic maps offer an alternate way to evaluate neutralization titers in that they are based on neutralization data that reflect the antigenic rather than genetic relatedness of pathogens. Viral antigenic maps fit neutralization titers for all sera against all viruses simultaneously: each virus is measured in relation to many immune sera, allowing for a more accurate estimate of antigenic relatedness than that which is provided by individual neutralization titers. Antigenically, ZIKV formed a discrete and compact map, with the greatest antigenic unit (AU) distances no greater than ~four-fold range across the two-dimensional map space (Fig 5), equivalent to a single dilution in the FRNT assay used to estimate $FRNT_{50}$ values for this map. The two African strains mapped to nearly identical

loci, while the American strains were located at relatively larger, but still quite small, antigenic distances from one another, while the lone Asian strain in our panel was centrally located among the American and African strains. Compared to the dengue viruses, ZIKV were more tightly clustered and more closely related antigenically than DENV viruses are when mapped using human primary DENV immune sera.[11]

Figure[A1.5]

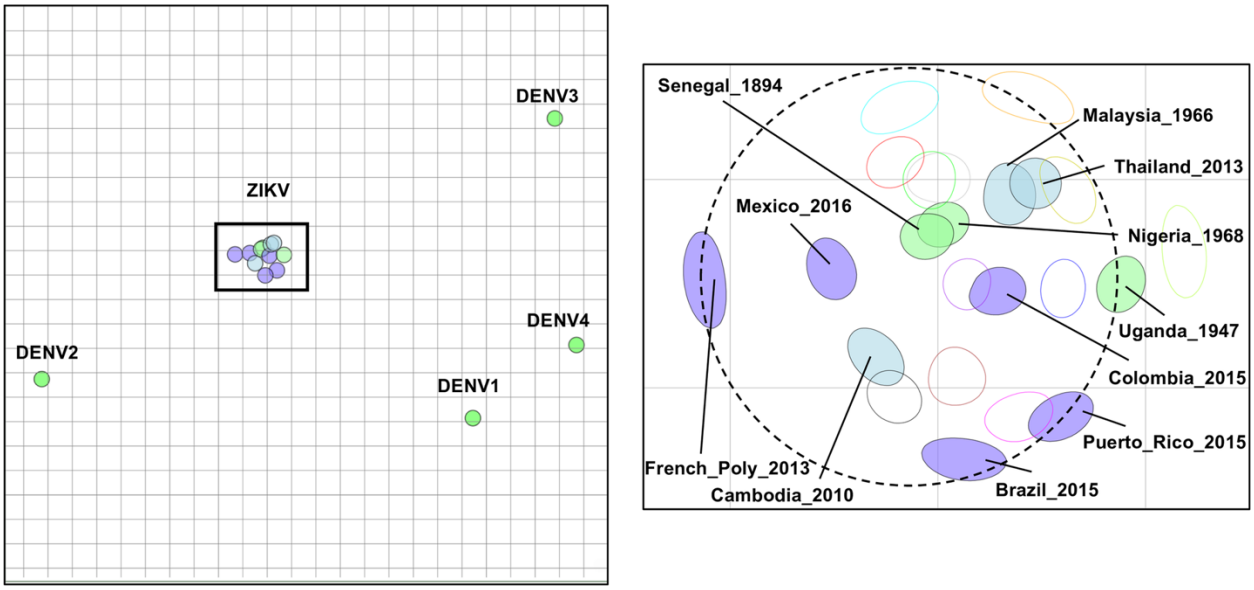

[Figure A1.5]

[A1.5] **Antigenic map of eleven ZIKVs against twelve human ZIKV immune sera from 5 to 38 months post-infection.**

Locator map shows the relative antigenic relatedness between ZIKV and the dengue viruses. Each unit of antigenic distance (AU), the length of one side of a grid square, is equivalent to a two-fold dilution in the neutralization assay. Inset map shows each serum and ZIKV. Sera are shown as open blobs colored to match each serum as in Fig 2. Each virus is shown as a filled blob and is colored according to virus strain (American = slate blue, African = turquoise, Asian = steel blue). The size and shape of each blob is the confidence area of its position. Dashed line circle has a diameter equal to 2 AU or four-fold, the difference of a single dilution in the FRNT assay used to estimate $FRNT_{50}$ titer.

Section A1.6: Discussion

Phylogenetic comparisons between historic and contemporary ZIKV isolates find minimal genetic variability, supporting the generally held hypothesis that ZIKVs antigenically form a single serotype.[9] However, within flaviviruses it has been shown that relatively few genetic—amino acid encoding—differences can be associated with significant differences in virus susceptibility to neutralization by human immune sera raised against otherwise genetically very similar viruses.[10, 16, 24] Consequently, the antigenic differences between closely related flaviviruses cannot be inferred by genetic analysis alone, and empiric characterization of closely related viruses using serologic assays is still necessary to validate assumptions about antigen relationships within genetically similar flaviviruses. Ideally, this characterization should be undertaken with a set of viruses that capture within virus genetic diversity and a set of sera from individuals with diverse exposure histories to the same group of genetically similar viruses. To date, only one study, Dowd *et al.*,[25] has examined the serotype specificity of contemporary human ZIKV convalescent immune sera from the most recent 2014–2016 epidemic against the three genetically distinct ZIKV strains. While Dowd *et al.* was a critically important first approximation of the potency and breadth of human ZIKV-specific immune sera following natural infection, the study had several limitations: only three ZIKV strains were fully evaluated against eight ZIKV-confirmed human convalescent sera; the convalescent sera were collected in an early convalescent time period 3 to 12.6 weeks post infection, when short-lived flavivirus cross-reactive IgM and IgG titers are expected to be high,[26, 27] and, finally, subject co-existent flavivirus immunity to DENV or other flaviviruses in the human subjects was not assessed. Here we conducted an in-depth analysis of a panel of genetically similar but distinct ZIKV against a panel of primary ZIKV-immune sera from individuals infected 5–38 months prior these immunologic studies. Our work builds upon and expands earlier results reported by Dowd *et al.*[25] which was limited to eight early convalescent ZIKV immune sera (<3 months) and only three ZIKV isolates. All subject sera in our study potently neutralized all ZIKV isolates at $FRNT_{50}$ >1:320 (Fig 2), and although the GMT against all viruses for one subject, 12462, was significantly lower compared to the GMTs for the other eleven subjects (Fig 3A), this may reflect a host factor such as subject age at infection–70 years old–rather than an underlying immunogenic difference between the infecting viruses. The identity of the infecting virus is not known, but can be reasonably assumed to be an American strain (infected in the Cook Islands in 2014), and another subject, 18451, was infected at the same time and location as subject 12462, presumably with the same virus strain, but did not develop

lower immune titers. We did not observe any trends towards a relationship between time post-infection, geographic location of infection, and specificity, breadth, or potency of immune sera titers.

When $FRNT_{50}$ titers were compared by virus (Fig 4A), none of the viruses differed in their GMT against the twelve subject sera. However, it is interesting to note that, when pooled by strain, we did find a statistically significant, but small, 1.4-fold difference between GMT for both African strains compared to the five American strains. These two strains have 8 conserved amino acid differences across the E glycoprotein (Supplemental Table), four of which are predicted to be surface-exposed: T120A, located on the E domain II (EDII) d-e loop; V169I, located on the EDI F_0 strand; V317I, located on the EDIII A strand; and D393E, located on the EDIII f-g loop, part of the EDIII lateral ridge epitope region. While it is beyond the scope of this research to evaluate whether these residues contribute to the small but robust differences in neutralization between the African and American ZIKV strains, all four regions have been implicated as targets for human ZIKV [28] and DENV neutralizing mAbs.[29–31] Even so, the overall magnitude of neutralization potency across all strains and sera suggests these differences are unlikely to play a meaningful role in antigenic escape in the context of existing primary ZIKV immunity.

Analysis of our data by antigenic cartography provided similar results, with some notable differences. While comparison of GMTs across titers and sera suggested some differences between sera and titers in pairwise comparisons, when plotted using all serum-virus pairs simultaneously, the resulting antigenic map is remarkably tight and homogeneous, with neither African or American strains grouping apart from the other strains, and while two African strains were the closest to one another by antigenic distance, the antigenic map distances between the African strains and the American strains are no greater than the antigenic map distances with the American strains. Overall, the antigenic distance spanned by all viruses was just over 2 AU, or four-fold, the difference of a single dilution in our FRNT assay, strongly supporting the hypothesis that ZIKV constitutes a single serotype.

Although our results add significantly to our understanding of the potency and breadth of antibodies elicited by primary ZIKV infection and the antigenic relationship between genetically distinct ZIKV, our study had several weaknesses: the virus strain(s) that infected our study subjects has been inferred to be American strains by epidemic association rather than virus isolation, and

subjects with history of primary ZIKV infection by African or Asia strains were not identified; our panel of viruses was biased towards recent American strain isolates, with only three Asian and three African strains represented; and, the study is cross-sectional and still only examines potency and breadth of immune sera through 3 years post-infection, true "long-term" immunity, and longitudinal ZIKV immunity in study subjects was not examined. Future studies that address these weaknesses would substantially add to our understanding of the natural history of ZIKV immunity in human populations, the limited role antibody neutralization escape may play in ZIKV evolution, and the potential for ZIKV vaccines currently under development to protect against likely future genetic ZIKV variants.

Section A1.6: Supporting information

Figure[A1.6]

Supplemental Table 1. primers used for ZIKV sequencing.

Name	5' - Sequence - 3'
ZV_seqA_s	ACAGTTCGAGTTTGAAGCG
ZV_seqA_a	TGTRGTCAGCAGGAGGC
ZV_seqB_s	TAGGAAGGAGARGAAGAGACG
ZV_seqB_a	TGTCAAGGTAGGCTTCAC
ZV_seqC_s	GAGGTRAGATCCTACTGC
ZV_seqC_a	ACCATCCATCTCAGCCTC
ZV_seqD_s	AACTCCACACTGGAACAAC
ZV_seqE_s	GAATGTCCTGGTTCTCAC
ZV_seqE_a	TAGCCTAGATCACTGTG
ZV_seqF_s	CTCAAACATAGAGCATGG
ZV_seqF_a	GTCACCATDGACCTYACTAAG

[Figure A1.6]

[A1.6] **Primers used for ZIKV sequencing.**

Figure[A1.7]

Supplemental Table 2. Raw P-values for pair wise comparisons of potency/breadth curves (Figure 3b). Cells highlighted in red show serum pairs that differ by P<0.05 by Bonferroni correction.

Serum	11942	11981	14278	12451	14137	11884	12462	14236	14252	14269	14276	14664
11942		0.845200	0.046900	0.968500	0.348100	0.474500	0.000014	0.0.000902	0.001700	0.001700	0.438200	0.521900
11981	0.845200		0.161300	0.930800	0.753600	0.287600	0.002200	0.001100	0.001400	0.002200	0.762500	0.449000
14278	0.046900	0.161300		0.114500	0.502200	0.415900	0.000002	0.002300	0.028400	0.021600	0.211500	0.720800
12451	0.968500	0.930800	0.114500		0.514600	0.000091	0.000091	0.000500	0.035700	0.001700	0.437900	0.638300
14137	0.348100	0.753600	0.502200	0.514600		0.826900	0.000200	0.000700	0.010700	0.005900	0.968100	0.861200
11884	0.474500	0.287600	0.415900	0.000091	0.826900		0.000055	0.002600	0.004600	0.003400	0.841000	0.988400
12462	0.000014	0.002200	0.000002	0.000091	0.000200	0.000055		0.000010	0.000001	0.255700	0.040800	0.000600
14236	0.0.000902	0.001100	0.002300	0.000500	0.000700	0.002600	0.000010		0.917100	0.255700	0.040800	0.007000
14252	0.001700	0.001400	0.028400	0.035700	0.010700	0.004600	0.000001	0.917100		0.450200	0.093500	0.014200
14269	0.001700	0.002200	0.021600	0.001700	0.005900	0.003400	0.255700	0.255700	0.450200		0.009900	0.009500
14276	0.438200	0.762500	0.211500	0.437900	0.968100	0.841000	0.040800	0.040800	0.093500	0.009900		0.854600
14664	0.521900	0.449000	0.720800	0.638300	0.861200	0.988400	0.000600	0.007000	0.014200	0.009500	0.854600	

[Figure A1.7]

[A1.7] Raw P-values for pair wise comparisons of potency/breadth curves (Fig 3B).

Cells highlighted in red show serum pairs that differ by P<0.05 by Bonferroni correction.

Figure[A1.8]

Supplemental Table 3. Summary of variable residues across ZIKV capsid (C), prM, and envelope (E) proteins.

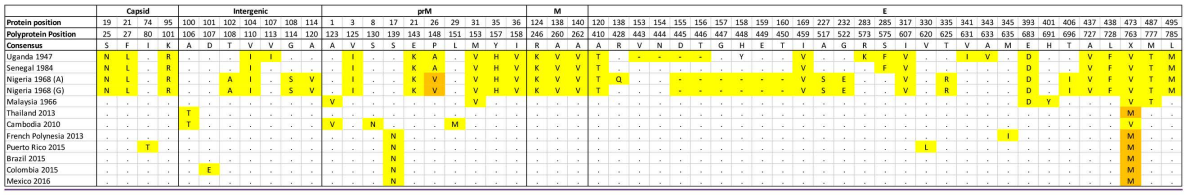

[Figure A1.8]

[A1.8] Summary of variable residues across ZIKV capsid (C), prM, and envelope (E) proteins.

Section A1.9: Acknowledgements

The authors would like to acknowledge Paul Cieslak, MD, Melissa Powell, MPH, and Lisa Takeuchi, MPH, with OHA for their assistance in recruiting individuals who tested positive for ZIKV.

Section A1.10: References

1. Dick GW. Zika virus. II. Pathogenicity and physical properties. Trans R Soc Trop Med Hyg. 1952;46(5):521–34. Epub 1952/09/01. pmid:12995441.

2. Dick GW, Kitchen SF, Haddow AJ. Zika virus. I. Isolations and serological specificity. Trans R Soc Trop Med Hyg. 1952;46(5):509–20. Epub 1952/09/01. pmid:12995440.

3. Lanciotti RS, Kosoy OL, Laven JJ, Velez JO, Lambert AJ, Johnson AJ, *et al.* Genetic and serologic properties of Zika virus associated with an epidemic, Yap State, Micronesia, 2007. Emerging infectious diseases. 2008;14(8):1232–9. pmid:18680646

4. Duffy MR, Chen TH, Hancock WT, Powers AM, Kool JL, Lanciotti RS, *et al.* Zika virus outbreak on Yap Island, Federated States of Micronesia. The New England journal of medicine. 2009;360(24):2536–43. pmid:19516034

5. Cao-Lormeau VM, Blake A, Mons S, Lastere S, Roche C, Vanhomwegen J, *et al.* Guillain-Barre Syndrome outbreak associated with Zika virus infection in French Polynesia: a case-control study. Lancet. 2016;387(10027):1531–9. Epub 2016/03/08. pmid:26948433; PubMed Central PMCID: PMC5444521.

6. Weaver SC, Costa F, Garcia-Blanco MA, Ko AI, Ribeiro GS, Saade G, *et al.* Zika virus: History, emergence, biology, and prospects for control. Antiviral Res. 2016;130:69–80. Epub 2016/03/22. pmid:26996139; PubMed Central PMCID: PMC4851879.

7. WHO statement on the first meeting of the International Health Regulations (2005) (IHR 2005) Emergency Committee on Zika virus and observed increase in neurological disorders and neonatal malformations: WHO; 2016 [updated Febraruy 1, 2016]. Available from: https://www.who.int/en/news-room/detail/01-02-2016-who-statement-on-the-first-meeting-of-the-international-health-regulations-(2005)-(ihr-2005)-emergency-committee-on-zika-virus-and-observed-increase-in-neurological-disorders-and-neonatal-malformations.

8. Gubler DJ, Vasilakis N, Musso D. History and Emergence of Zika Virus. J Infect Dis. 2017;216(suppl_10):S860–S7. Epub 2017/12/22. pmid:29267917; PubMed Central PMCID: PMC5853376.

9. Heinz FX, Stiasny K. The Antigenic Structure of Zika Virus and Its Relation to Other Flaviviruses: Implications for Infection and Immunoprophylaxis. Microbiol Mol Biol Rev. 2017;81(1). Epub 2017/02/10. pmid:28179396; PubMed Central PMCID: PMC5312239.

10. VanBlargan LA, Mukherjee S, Dowd KA, Durbin AP, Whitehead SS, Pierson TC. The type-specific neutralizing antibody response elicited by a dengue vaccine candidate is focused on two amino acids of the envelope protein. PLoS Pathog. 2013;9(12):e1003761. Epub 2013/12/19. pmid:24348242; PubMed Central PMCID: PMC3857832.

11. Katzelnick LC, Fonville JM, Gromowski GD, Bustos Arriaga J, Green A, James SL, *et al.* Dengue viruses cluster antigenically but not as discrete serotypes. Science (New York, NY). 2015;349(6254):1338–43. pmid:26383952

12. Smadel JE. Introduction, symposium on viral and rickettsial diseases. Bacteriol Rev. 1950;14(3):193–7. Epub 1950/09/01. pmid:14772192; PubMed Central PMCID: PMC440969.

13. Hammon WM, Rudnick A, Sather GE. Viruses associated with epidemic hemorrhagic fevers of the Philippines and Thailand. Science. 1960;131(3407):1102–3. Epub 1960/04/15. pmid:14399343.

14. Mukherjee S, Sirohi D, Dowd KA, Chen Z, Diamond MS, Kuhn RJ, *et al.* Enhancing dengue virus maturation using a stable furin over-expressing cell line. Virology. 2016;497:33–40. pmid:27420797; PubMed Central PMCID: PMC5502530.

15. Raut R, Corbett KS, Tennekoon RN, Premawansa S, Wijewickrama A, Premawansa G, *et al.* Dengue type 1 viruses circulating in humans are highly infectious and poorly neutralized by human antibodies. Proc Natl Acad Sci U S A. 2019;116(1):227–32. Epub 2018/12/07. pmid:30518559; PubMed Central PMCID: PMC6320508.

16. Messer WB, Yount B, Hacker KE, Donaldson EF, Huynh JP, de Silva AM, *et al.* Development and characterization of a reverse genetic system for studying dengue virus serotype 3 strain variation and neutralization. PLoS neglected tropical diseases. 2012;6(2):e1486. pmid:22389731

17. Widman DG, Young E, Nivarthi U, Swanstrom JA, Royal SR, Yount BL, *et al.* Transplantation of a quaternary structure neutralizing antibody epitope from dengue virus serotype 3 into serotype 4. Sci Rep. 2017;7(1):17169. pmid:29215033; PubMed Central PMCID: PMC5719398.

18. Smith DJ, Lapedes AS, de Jong JC, Bestebroer TM, Rimmelzwaan GF, Osterhaus AD, *et al.* Mapping the antigenic and genetic evolution of influenza virus. Science. 2004;305(5682):371–6. Epub 2004/06/26. pmid:15218094.

19. Kumar S, Stecher G, Li M, Knyaz C, Tamura K. MEGA X: Molecular Evolutionary Genetics Analysis across Computing Platforms. Mol Biol Evol. 2018;35(6):1547–9. Epub 2018/05/04. pmid:29722887; PubMed Central PMCID: PMC5967553.

20. Mansfield KL, Horton DL, Johnson N, Li L, Barrett AD, Smith DJ, *et al.* Flavivirus-induced antibody cross-reactivity. J Gen Virol. 2011;92(Pt 12):2821–9. Epub 2011/09/09. pmid:21900425; PubMed Central PMCID: PMC3352572.

21. Lewis NS, Daly JM, Russell CA, Horton DL, Skepner E, Bryant NA, *et al.* Antigenic and genetic evolution of equine influenza A (H3N8) virus from 1968 to 2007. J Virol. 2011;85(23):12742–9. Epub 2011/09/23. pmid:21937642; PubMed Central PMCID: PMC3209411.

22. Fouchier RA, Smith DJ. Use of antigenic cartography in vaccine seed strain selection. Avian Dis. 2010;54(1 Suppl):220–3. Epub 2010/06/05. pmid:20521635.

23. de Jong JC, Smith DJ, Lapedes AS, Donatelli I, Campitelli L, Barigazzi G, *et al.* Antigenic and genetic evolution of swine influenza A (H3N2) viruses in Europe. J Virol. 2007;81(8):4315–22. Epub 2007/02/09. pmid:17287258; PubMed Central PMCID: PMC1866135.

24. Gallichotte EN, Baric TJ, Nivarthi U, Delacruz MJ, Graham R, Widman DG, *et al.* Genetic Variation between Dengue Virus Type 4 Strains Impacts Human Antibody Binding and Neutralization. Cell Rep. 2018;25(5):1214–24. Epub 2018/11/01. pmid:30380413; PubMed Central PMCID: PMC6226424.

25. Dowd KA, DeMaso CR, Pelc RS, Speer SD, Smith ARY, Goo L, *et al.* Broadly Neutralizing Activity of Zika Virus-Immune Sera Identifies a Single Viral Serotype. Cell Rep. 2016;16(6):1485–91. Epub 2016/08/03. pmid:27481466; PubMed Central PMCID: PMC5004740.

26. Gallichotte EN, Baric RS, de Silva AM. The Molecular Specificity of the Human Antibody Response to Dengue Virus Infections. Adv Exp Med Biol. 2018;1062:63–76. Epub 2018/05/31. pmid:29845525.

27. Pasquier C, Joguet G, Mengelle C, Chapuy-Regaud S, Pavili L, Prisant N, *et al.* Kinetics of anti-ZIKV antibodies after Zika infection using two commercial enzyme-linked immunoassays. Diagn Microbiol Infect Dis. 2018;90(1):26–30. Epub 2017/11/07. pmid:29107414.

28. Stettler K, Beltramello M, Espinosa DA, Graham V, Cassotta A, Bianchi S, *et al.* Specificity, cross-reactivity, and function of antibodies elicited by Zika virus infection. Science. 2016;353(6301):823–6. Epub 2016/07/16. pmid:27417494.

29. Fibriansah G, Tan JL, Smith SA, de Alwis AR, Ng TS, Kostyuchenko VA, *et al.* A potent anti-dengue human antibody preferentially recognizes the conformation of E protein monomers assembled on the virus surface. EMBO molecular medicine. 2014;6(3):358–71. pmid:24421336

30. Fibriansah G, Tan JL, Smith SA, de Alwis R, Ng TS, Kostyuchenko VA, *et al.* A highly potent human antibody neutralizes dengue virus serotype 3 by binding across three surface proteins. Nature communications. 2015;6:6341. pmid:25698059

31. Wahala WM, Donaldson EF, de Alwis R, Accavitti-Loper MA, Baric RS, de Silva AM. Natural strain variation and antibody neutralization of dengue serotype 3 viruses. PLoS pathogens. 2010;6(3):e1000821. pmid:20333252

Appendix 2: A lyophilized colorimetric RT-LAMP test kit for rapid, low-cost, at-home molecular testing of SARS-CoV-2 and other pathogens

Xin Song[1,2,3], Felicity J Coulter[#,4], Ming Yang[#,5], Jessica L Smith[6], Fikadu G Tafesse [4], William B Messer[7,8,9], John H Reif[10,11]

[1]Department of Electrical and Computer Engineering, Duke University, Durham, NC, 27708, USA. xin.song@duke.edu.

[2]Department of Biomedical Engineering, Duke University, Durham, NC, 27708, USA. xin.song@duke.edu.

[3]Department of Computer Science, Duke University, Durham, NC, 27708, USA. xin.song@duke.edu.

[4]Department of Molecular Microbiology and Immunology, Oregon Health and Science University, Portland, OR, 97239, USA.

[5]Department of Computer Science, Duke University, Durham, NC, 27708, USA.

[6]Vaccine and Gene Therapy Institute, Oregon Health and Science University, Beaverton, OR, 97006, USA.

[7]Department of Molecular Microbiology and Immunology, Oregon Health and Science University, Portland, OR, 97239, USA. messer@ohsu.edu.

[8]Department of Medicine, Division of Infectious Diseases, Oregon Health and Science University, Portland, OR, 97239, USA. messer@ohsu.edu.

[9]Program in Epidemiology, OHSU-PSU School of Public Health, Oregon Health and Science University, Portland, OR, 97239, USA. messer@ohsu.edu.

[10]Department of Electrical and Computer Engineering, Duke University, Durham, NC, 27708, USA. reif@cs.duke.edu.

[11]Department of Computer Science, Duke University, Durham, NC, 27708, USA. reif@cs.duke.edu.

[#]Contributed equally.

Published: April 29, 2022, in Scientific Reports
Doi: 10.1038/s41598-022-11144-5

Section A2.1: Abstract

Access to fast and reliable nucleic acid testing continues to play a key role in controlling the COVID-19 pandemic, especially in the context of increased vaccine break-through risks due to new variants. We report a rapid, low-cost (~ 2 USD), simple-to-use nucleic acid test kit for self-administered at-home testing without lab instrumentation. The entire sample-to-answer workflow takes < 60 min, including noninvasive sample collection, one-step RNA preparation, reverse-transcription loop-mediated isothermal amplification (RT-LAMP) in a thermos, and direct visual inspection of a colorimetric test result. To facilitate long-term storage without cold-chain, a fast one-pot lyophilization protocol was developed to preserve all required biochemical reagents of the colorimetric RT-LAMP test in a single microtube. Notably, the lyophilized RT-LAMP assay demonstrated reduced false positives as well as enhanced tolerance to a wider range of incubation temperatures compared to solution-based RT-LAMP reactions. We validated our RT-LAMP assay using simulated infected samples, and detected a panel of SARS-CoV-2 variants with successful detection of all variants that were available to us at the time. With a simple change of the primer set, our lyophilized RT-LAMP home test can be easily adapted as a low-cost surveillance platform for other pathogens and infectious diseases of global public health importance.

Section A2.2: Introduction

The COVID-19 pandemic has cost millions of lives and presented unprecedented economic, social, and structural challenges across the world. While vaccination rollouts and improved access to testing have helped to control the pandemic[1], transmissions and infections (including post-vaccine breakthrough cases) due to the new variants of SARS-CoV-2[2,3] continue to pose a burden on global public health and economics. Effective SARS-CoV-2 surveillance requires frequent testing

with rapid results to quickly identify infected individuals to break transmission chains[4]. However, centralized testing models such as drive-through tests may increase the risk of exposure to health care workers and also rely on costly facilities, trained personnel, and sophisticated lab equipment (typically RT-qPCR) that in many cases still fail to deliver a timely test result. These delays can be detrimental to effective surveillance and disease control efforts due to the risk of presymptomatic/asymptomatic transmission of SARS-CoV-2[5]. While testing labs are widely available in many high-income countries, most low- and middle-income countries lack sufficient facilities and trained personnel for wide-spread application of sophisticated SARS-CoV-2 detection technologies. Rapid antigen tests are easy to use and less expensive, however, while they are effective at screening symptomatic patients with high viral loads[6], the overall higher rates of false positives and false negatives (compared to nucleic acid tests) make rapid antigen tests less suitable as a front-line diagnostic[7,8]. To quickly identify emerging SARS-CoV-2 transmission hotspots and curb the spread of virus from all potential transmission routes (presymptomatic, symptomatic, asymptomatic), a robust decentralized testing model would require the development of affordable nucleic acid home tests that are reliable, simple to use, and inexpensive to manufacture and distribute to large populations.

Since the beginning of the pandemic, researchers have sought to develop rapid molecular assays to overcome the practical limitations of standard RT-qPCR testing[9]. Among several candidate nucleic acids amplification protocols[10], RT-LAMP is a simple method that achieves rapid exponential amplification of RNA using a set of six primers to recognize eight distinct regions on the target RNA sequence, enabling highly specific and sensitive detection of target RNA without stringent requirement on sample purity[11]. This eliminates the need for the sophisticated RNA isolation and purification processes that have been a major bottleneck of current SARS-CoV-2 testing workflows. Further, the compatibility with simple pH-based colorimetric readout[12] allows easy interpretation of the test result by visual inspection, making RT-LAMP suitable for inexpensive point-of-care applications. To date, many RT-LAMP assays have been proposed for SARS-CoV-2 detection[13,14,15,16,17,18,19,20,21,22] including several that have obtained FDA Emergency Use Authorization (EUA)[23,24,25]. However, most of these tests still cannot meet the need for frequent at-home testing due to either un-optimized performance or the prohibitive cost per test.

Section A2.3: Results

A2.3.1 Assay development

Conventional molecular assays do not support convenient use at home by untrained individuals because of the complexity of the testing workflow, dependence on specialized instrumentation, stringent requirement of cold storage for reagents, and the high cost of the test platform manufacturing and distribution. To enable truly inexpensive, rapid, reliable at-home testing of COVID-19, we developed a simple all-in-one molecular home test kit based on lyophilized colorimetric RT-LAMP, requiring only a regular thermos and a thermometer to conduct the self-administered test. A rapid, one-pot lyophilization protocol was developed to quickly preserve all reagents needed for the colorimetric RT-LAMP test in a single microtube, facilitating long-term stability, inexpensive distribution, and convenient use of the home test kit. Notably, the lyophilized RT-LAMP assay demonstrated reduced false positives and higher tolerance to a wider range of incubation temperatures compared to conventional solution-based RT-LAMP reactions. To enable detection of viruses from clinical sample matrices, we adapted a one-step RNA preparation protocol19 based on low-cost shelf-stable reagents. The entire sample-to-answer workflow (Fig. 1) takes < 60 min, including noninvasive sample collection (anterior nasal swab or alternatively gingival swab), quick extraction-free RNA preparation, optimized RT-LAMP reaction in a thermos, and finally a colorimetric interpretation of the test result.

Figure[A2.1]

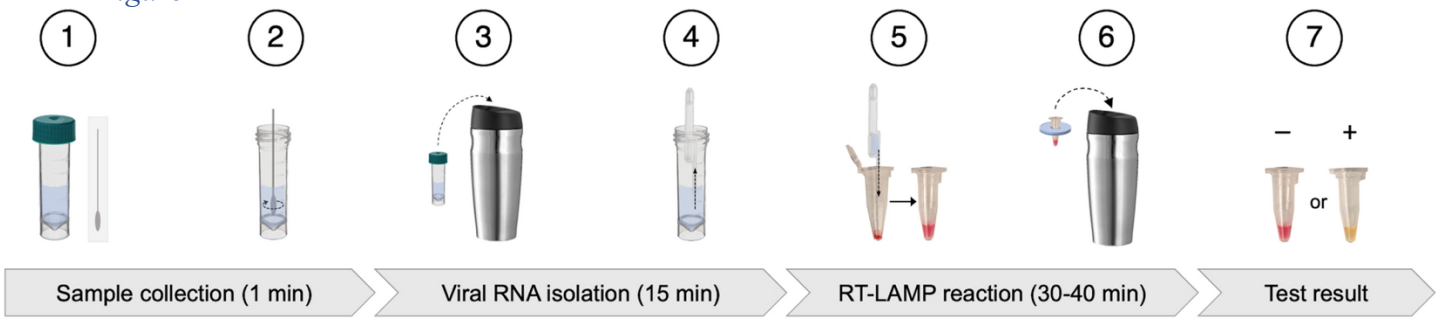

[Figure A2.1]

A2.1 Schematic illustration of the COVID-19 home test from sample collection to test result readout.
Step 1: Self-collect a sample using an anterior nasal swab (alternatively a gingival swab). Step 2: Plunge the swab into the media inside the collection tube. Gently rub and roll the swab against the tube wall for 10 times. Squeeze out the remaining liquid by pressing the swab against the side of the tube, discard the swab and recap the tube. Step 3: Add 95 °C hot water into a thermos. Ensuring the sample collection tube lid is tightly secured, place inside the thermos and close the lid, to incubate for 10 min. Step 4: Take out the collection tube and cool it on ice for 5 min, allowing any debris to settle to the bottom. Use a disposable transfer pipette to draw 20 µL of sample from the collection tube. Step 5: Quickly dispense the sample into the lyophilized RT-LAMP reaction tube. Recap and gently flick the side of the reaction tube to resuspend the mix (avoid introducing bubbles). Step 6: Use a thermometer or a temperature sticker (included in the kit) to adjust the water temperature to 65 °C in the thermos. Assemble the RT-LAMP reaction tube onto the foam floater and place it in the thermos. Close the lid and incubate for 40 min. Step 7: Take out the reaction tube and cool it on ice. Visually inspect the test result (pink = negative; yellow = positive).

RT-LAMP reactions rely on active enzymatic components (i.e., DNA polymerase and reverse transcriptase) that must be stored at a low temperature (typically − 20 °C). To preserve the RT-LAMP reagents for home test use, we employed lyophilization, also known as freeze-drying, to extend the shelf-life of the test kit and facilitate simple test kit distribution, handling, and storage under convenient temperatures (e.g., at typical home-refrigeration temperature or at room temperature). A lyophilized test kit also reduces the number of pipetting steps to improve usability and minimize contamination[26]. However, lyophilization is typically an expensive and time-consuming process involving three stages including freezing, primary drying, and secondary drying which can be difficult to design and optimize[27]. In this work, we developed a fast, one-pot lyophilization process that minimizes the drying time by completing both the primary and secondary drying under a single condition[28]. Unlike prior lyophilization protocols developed for molecular biology assays, our protocol eliminates the need to separately lyophilize the reaction buffer and the enzymes[17,26,29]. Instead, our simplified protocol enables one-pot lyophilization of all reagents needed for the colorimetric RT-LAMP in a single microtube (Table 1), and the entire lyophilization process can be completed in under 2 h (see Methods). We tested trehalose[30,31,32] and dextran[33,34] as candidate excipients to provide cryo- and lyoprotection during lyophilization, as well as enhanced stability for long-term storage. In addition, guanidine hydrochloride (GuHCl)[35] was included in the optimized formulation to improve the reaction

speed and the sensitivity of colorimetric RT-LAMP. We carefully screened multiple sets of recently published RT-LAMP primers[14,15,36,37,38] and optimized our RT-LAMP assay with a well-performing primer set[38] (Table 2), which targets the ORF1a gene of the viral genome and is minimally impacted by the mutations from recent SARS-CoV-2 variants.

Table[A2.1]

Component	Amount used per kit
WarmStart® colorimetric LAMP 2X master mix	10 µL
10X primer mix	2 µL
3 M Trehalose	3 µL
1 M GuHCl	0.8 µL

[Figure A2.1]

[A2.1] **Optimized formulation of the lyophilized colorimetric RT-LAMP test.**

Table[A2.2]

Primer	Sequence 5′ → 3′
F3	CGGTGGACAAATTGTCAC
B3	CTTCTCTGGATTTAACACACTT
FIP	TCAGCACACAAAGCCAAAAATTTATTTTTCTGTGCAAAGGAAATTAAGGAG
BIP	TATTGGTGGAGCTAAACTTAAAGCCTTTTCTGTACAATCCCTTTGAGTG
LoopF	TTACAAGCTTAAAGAATGTCTGAACACT
LoopB	TTGAATTTAGGTGAAACATTTGTCACG

[Figure A2.2]

[A2.2] Optimized formulation of the lyophilized colorimetric RT-LAMP test.

Compared to typical solution-based RT-LAMP reactions, we observed that the addition of trehalose at the optimized concentration significantly reduced the occurrence of RT-LAMP false positives. The slight decrease in reaction speed was mitigated by the addition of GuHCl. Notably, our lyophilized RT-LAMP reactions also enabled a wider compatible range of incubation temperatures compared to the solution-based RT-LAMP reactions, thus improving the assay's robustness to tolerate the use of regular thermoses for reaction incubation without precise temperature control. Specifically, as shown in Fig. S7, our lyophilized assay ("3 M trehalose + 1 M GuHCl) lyo") performed robustly across the entire temperature gradient tested (60.7–70.0 °C) with

clear readout of true positives as early as 20 min and no false positives by 50 min of incubation at most temperatures within the temperature gradient. In contrast, the solution-based RT-LAMP assay ("Fresh sol") based on the same primers and master mix formulation showed a narrower range of compatible temperatures, slower turnaround, and earlier occurrence of false positives. The beneficial effect of the one-pot lyophilization was also observed in Fig. S15, where we conducted a similar temperature gradient experiment for the assay based on a different published RT-LAMP primer set23. We hypothesize that the enhanced performance of the one-pot lyophilized assay is partly due to the inclusion of trehalose in the RT-LAMP formulation. In addition to its role as a lyo- and thermal-protectant, trehalose was found to have a DNA duplex destabilizing effect in prior literature39. Such an effect helps to improve the specificity and yield of isothermal amplification reactions, which agrees with the observations from our experiments.

A2.3.1 Assay validation

According to in-house validation using synthesized SARS-CoV-2 RNA (Twist Bioscience), our test kit remains stable for at least 30 days at typical home-refrigeration temperature (4 °C) (Fig. S11) and 10 days at room temperature (~ 20 to 22 °C) (Fig. S14), achieving ≥ 95% analytical sensitivity and > 99% specificity with a reproducible limit of detection (LoD) down to 100 RNA copies per reaction (i.e., 5 copies/μL) under both storage conditions. In addition, we conducted validation tests using simulated SARS-CoV-2 infected samples—heat-inactivated SARS-CoV-2 WA-1 virus serially diluted and spiked into pooled anterior nasal swab media (0.0025X TBE buffer in nuclease-free water)—from healthy donors (Fig. 2a). Sensitivity for authentic SARS-CoV-2 WA-1/2020 was significantly reduced in comparison to the sensitivity under laboratory conditions with commercially purified RNA, 15,514 viral copies per reaction, but at higher viral loads the assay demonstrated reliable sensitivity, specificity, and reproducibility for detection of SARS-CoV-2 virus (Fig. 2b). Specificity remained at ≥ 99% for the simulated samples (Fig. 2b). Aliquots of simulated SARS-CoV-2 infected samples were also subjected to qRT-PCR in the OHSU clinical lab using the Fisher Multiplex TaqPath platform with 15,514 viral copies returning a calculated CT value of 26.4. We next examined the distribution of CT values for 5897 samples tested across

symptomatic and asymptomatic patients tested in the OHSU clinical lab (data provided generously by Dr. Xuan Qin, OHSU Department of Pathology), finding that the RT-LAMP assay would be expected to have detected SARS-CoV-2 in approximately 4254 patients, the number of patients with a CT of < 26, yielding a real-world sensitivity of 72%.

Figure[A2.2]

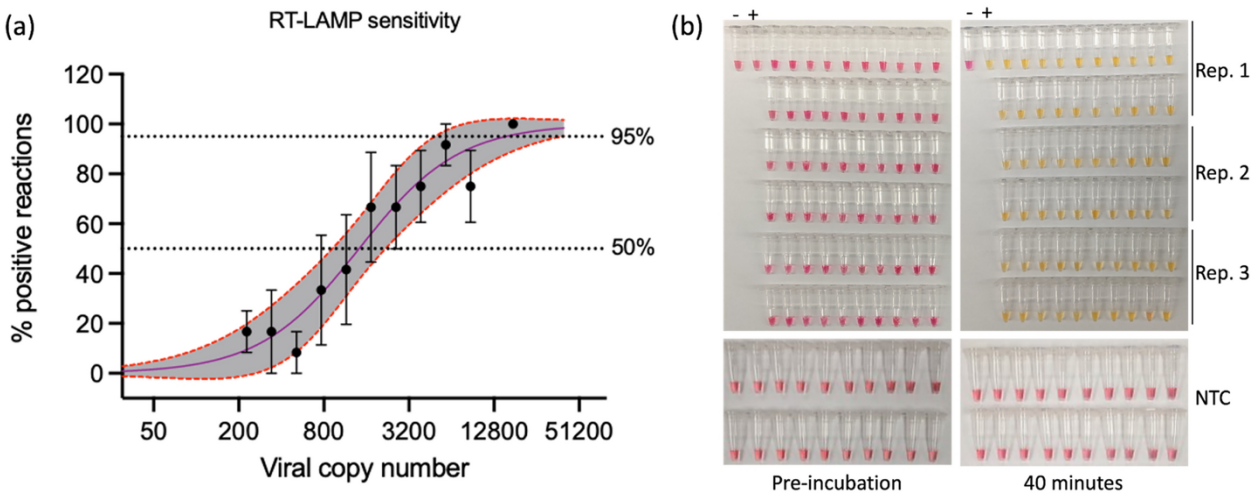

[Figure A2.2]

[A2.2] **Limit of detection and validation of analytical sensitivity and specificity on virus-spiked anterior nasal swab collection media.**

(A) Serial dilutions of heat-inactivated SARS-CoV-2 strain WA-1/2020 by percent positive samples. Three independent replicates of four-reactions per dilution were performed using samples from 227 copies per reaction to 17,473 copies per reaction. X-axis is log-scale showing copies per reaction, Y-axis shows % positive reactions. Each data point shows the average and standard error of the mean (SEM) for each set of replicates per dilution. A Sigmoidal dose–response curve was fit using the Find ECAnything least squares fit in Graphpad Prism 7.0 with lower and upper limits of 0 and 100 respectively. Red-dotted lines and grey area indicates 95% confidence interval around the dose–response curve. Straight dotted lines show 50 and 95% analytic sensitivity intercepts as predicted by the fitted curve. 95% limit of detection was 15,514 viral copies, 50% limit of detection was 1421 viral copies per reaction. **(B)** 20 replicates of non-template control (NTC, anterior nasal swab media only; bottom panels) versus 15,518 viral copies of heat-inactivated SARS-CoV-2 (top panels) in uninfected pooled anterior nasal swab media, demonstrating ≥ 99% analytical specificity and ≥ 95% analytical sensitivity at 15,518 copies/reaction. Nuclease-free water non-template control (−) and BEI RNA positive control (+), indicated. Pre-incubation and incubation times and colorimetric changes as above.

Like most RNA viruses, SARS-CoV-2 has and will continue to evolve genetically, and there are now several genetic variants of SARS-CoV-2, which the U.S. Centers for Disease Control and Prevention classifies as Variants Being Monitored (VBM), Variants of Interest (VOI), Variants of Concern (VOC) or Variants of High Consequence (VOHC). Classification depends on the presence of substitutions that may confer increased transmissibility, disease severity, immune and therapeutic escape, and interference with diagnostic test targets. It is thus important to assess the accuracy of our assay in detecting newly emerged SARS-CoV-2 variants. After carefully screening multiple sets of recently published RT-LAMP primers14,15,36,37,38, we optimized our RT-LAMP test with a well-performing primer set (Table 2)38 targeting the ORF1a gene of the SARS-CoV-2 viral genome. As shown in Figs. 3 and 4, our test successfully detected multiple SARS-CoV-2 variants and their isolates from different geographical locations, including WA1/2020 (USA), B.1.1.7 (“Alpha", UK), B.1.1.7 (“Alpha”, US-CA), B.1.351 (“Beta”, South Africa), P.2 (“Zeta”, Brazil), B.1.2 (US-LA/NM), B.1.427 (“Epsilon”, US-CA), B.1.429 (“Epsilon”, US-CA), B.1.526 (“Iota”, US-NY), B.1.617.1 (“Kappa”, India), and B.1.617.2 (“Delta”, India). The simplicity of our assay allows quick change of the primer sets to detect emerging variants of SARS-CoV-2 and other pathogens and diseases of public health importance.

Figure[A2.3]

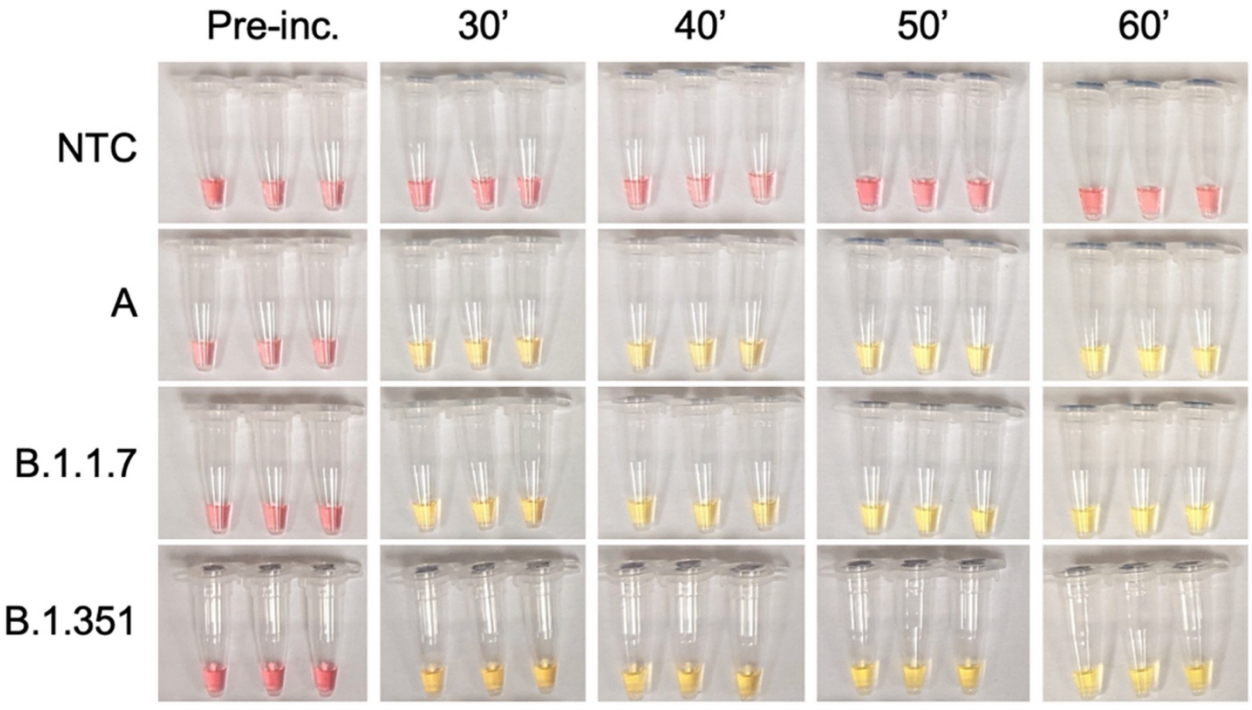

[Figure A2.3]

A2.3 Validation of the RT-LAMP home test on heat inactivated SARS-CoV-2 variants (calculated viral copy numbers per tube indicated):

A (WA-1/2020; 4.86 × 10^4), B.1.1.7 (1.51 × 10^5), and B.1.351 (4.79 × 10^5). Heat-inactivated virus was diluted in nuclease-free water. Viral copy numbers were calculated following quantification of stocks. Methods otherwise as described previously. NTC: non-template control (nuclease-free water).

Figure[A2.4]

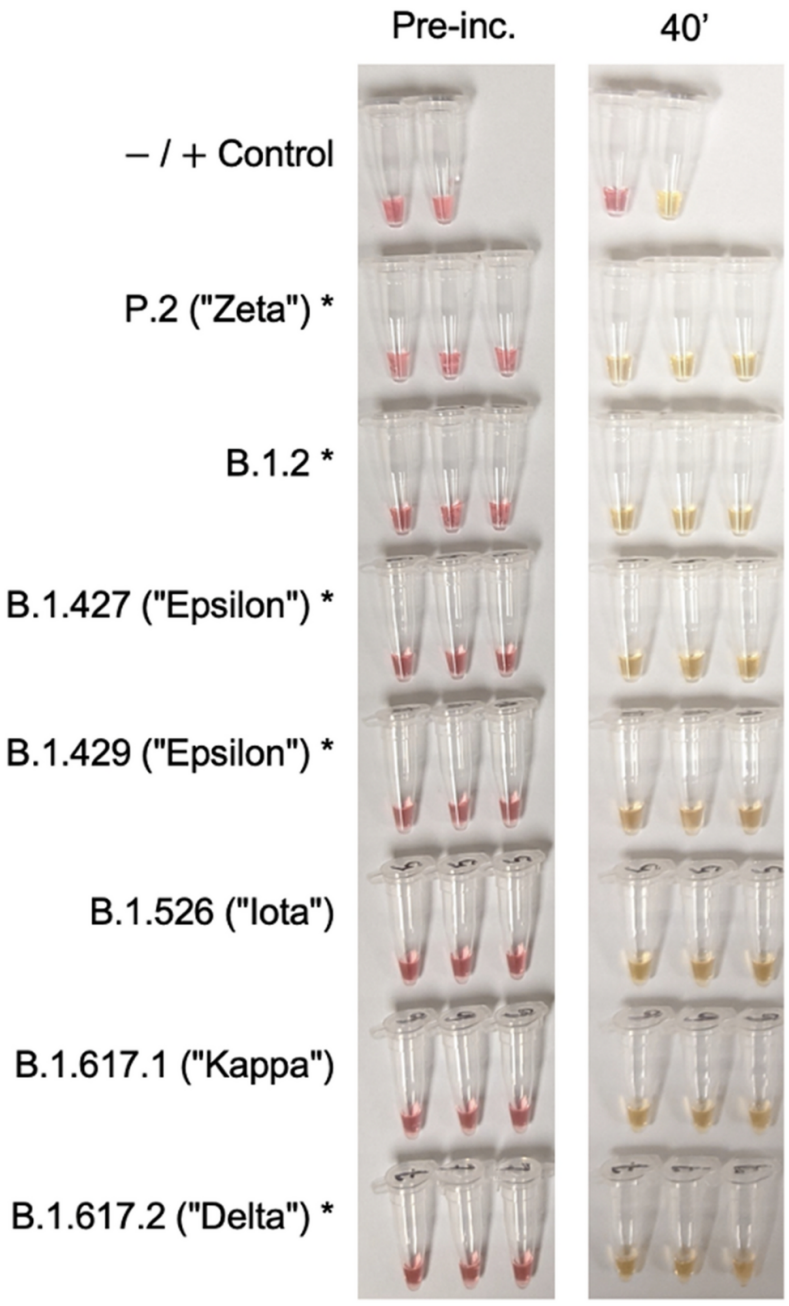

[Figure A2.4]

[A2.4] **Validation of the RT-LAMP home test on additional heat inactivated SARS-CoV-2 variants (calculated viral copy numbers per tube):**
P.2 (6.60 × 10^4), B.1.2 (2.69 × 10^5), B.1.427 (5.05 × 10^5), B.1.429 (4.12 × 10^4), B.1.526 (2.72 × 10^5), B.1.617.1 (1.65 × 10^5) and B.1.617.2 (4.05 × 10^4). Negative and positive controls were nuclease-free water and

commercially available genomic RNA (BEI), respectively. Asterisk indicates viruses originating from clinical samples, confirmed by sequencing.

Section A2.4: Discussion

In this work, we have demonstrated an inexpensive, one-pot lyophilized colorimetric RT-LAMP molecular test kit for self-administered COVID-19 diagnosis. In addition to its low cost and simplicity, the test kit features a user-friendly home testing workflow that can be easily completed in under 1 h with no specialized instrumentation or trained personnel (Table 3). Specifically, we developed a simple one-pot protocol for lyophilizing colorimetric RT-LAMP. All reagents needed for the isothermal amplification reaction can be quickly preserved in a single microtube, facilitating long-term storage, inexpensive distribution, and simple testing workflow without multiple liquid transfers. Unlike prior work of lyophilized LAMP/RT-LAMP that requires sophisticated lab procedures to separately lyophilize the enzymes from the reaction buffers, the simplicity and robustness of our one-pot lyophilization protocol makes it easy to inexpensively manufacture the molecular test kits at scale. We tested our RT-LAMP assay in regular thermoses and verified its tolerance to temperature deviations in different thermoses (Fig. 5). Notably, our test conveniently tolerates larger sample input volumes (i.e., as opposed to 1 µL to 5 µL sample volume commonly used in standard RT-LAMP assays, our test directly accepts 20 µL swab media sample to rehydrate the lyophilized reagents for a 20 µL RT-LAMP reaction). Furthermore, in contrast to conventional molecular diagnostics that usually involve multiple precise volume liquid transfers, our test requires only a single pipetting step (using a low-cost disposable transfer pipette) during the entire testing workflow.

Table[A2.3]

Low cost	Total cost per all-in-one kit ~ 2 USD (detailed cost breakdown in Table S1)
Simple, noninvasive, reliable workflow	No need for standard/specialized lab equipment or trained personnel Self-sample collection with minimal discomfort (anterior nasal swab or gingival swab) Simple and reproducible testing workflow with minimal liquid transfer steps Tolerant of temperature deviations in regular thermoses
Rapid and visual result	Sample-to-result in under 1 h Simple visual inspection of colorimetric test readout
Sensitive and accurate RT-LAMP assay	Tolerant to large sample input volume: 20 µL sample directly reconstitutes RT-LAMP Excellent analytical limit of detection: 100 RNA copies per reaction (i.e., 5 copies/µL) Excellent analytical sensitivity: ≥ 95% Excellent analytical specificity: > 99% Detects all SARS-CoV-2 variants that were tested in this paper
Long-term stability	Stable for ≥ 30 days at typical home-refrigeration temperature (4 °C) Stable for ≥ 10 days at room temperature (~ 20–22 °C)
Easy to manufacture	Fast (2 h) one-pot lyophilization preserves all test regents in a single microtube Extraction-free RNA preparation with inexpensive shelf-stable reagents
Easy to distribute	Compact all-in-one home test kit Minimal accessories required (thermos, thermometer, ice)* Good stability for potential over-the-counter distribution without cold chain

*The thermos/thermometer can be replaced by other low-cost solutions depending on use case.

[Table A2.3]

Table A2.3 Features and advantages of the COVID-19 molecular home test kit.

Figure[A2.5]

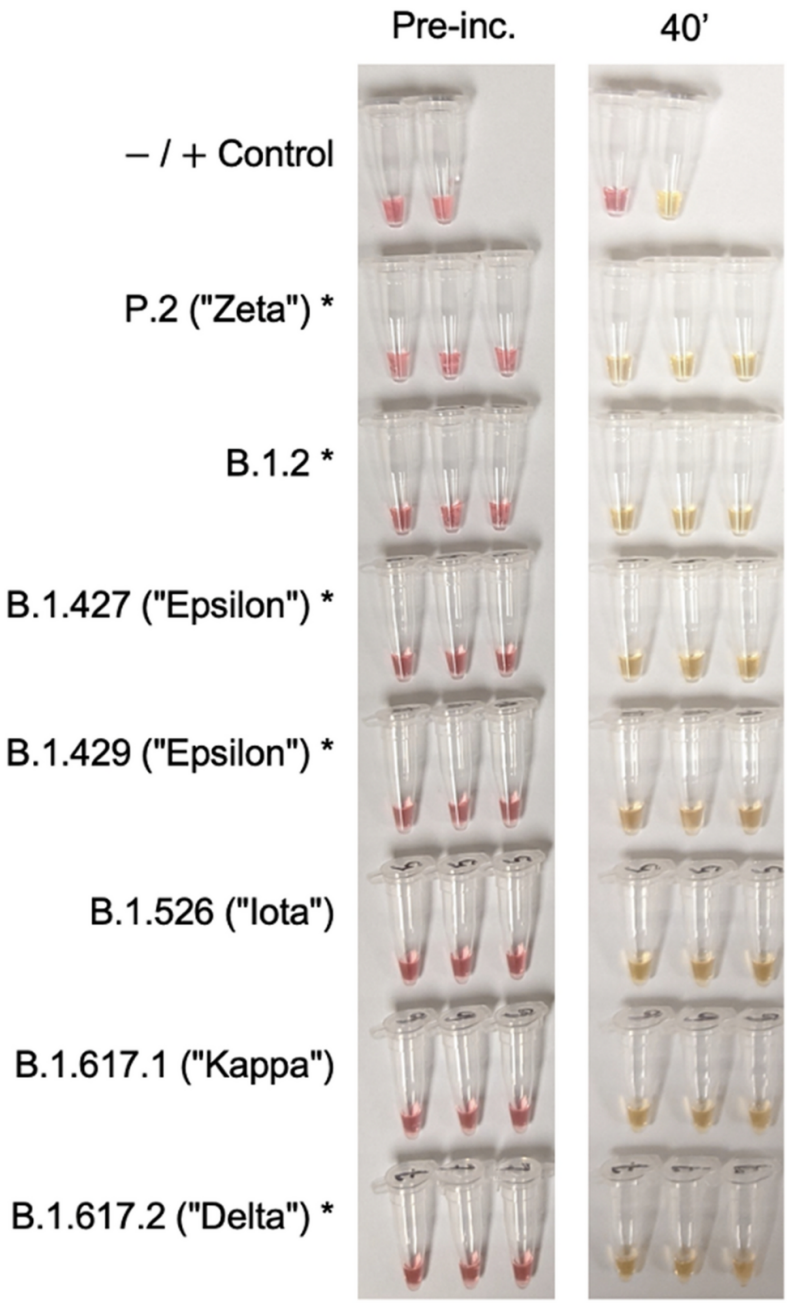

[Figure A2.5]

Figure A2.5 Validation of the RT-LAMP home test in different commercially available thermoses (see Methods for thermos details.)

Viral strain: Inactivated SARS-CoV-2 A (WA-1/2020) in gingival swab media. One non-template control (gingival swab media only) and triplicate virus, (−) and (+) respectively, per thermos experiment.

Nevertheless, the present work has several limitations. First, the RT-LAMP assay is qualitative and relies on visual interpretation of the colorimetric test result. Besides potential user errors, extended storage of the current test kit under elevated temperatures may reduce the color contrast between the positive and negative readouts, thus increasing the likelihood of misinterpretation. The continuing development of the test kit requires thorough characterization and rigorous testing of the assay performance under uncontrolled environments, for example, by conducting shipping and storage simulations under a wider range of temperature and humidity conditions. Second, while we have demonstrated excellent analytical performance of the underlying lyophilized RT-LAMP assay, further optimizations of the RNA isolation protocol are needed to achieve better sensitivity on clinical samples. However, for perspective, we compared the results of our dose–response evaluation of the RT-LAMP platform in its current configuration with the real-world CT values from the OHSU clinical diagnostic laboratory, we predict a real-world sensitivity of approximately 72% for all SARS-CoV-2 infections. While this value is below the performance of some other RT-LAMP platforms, it is well above the predicted sensitivity for symptomatic individuals of the widely used BinaxNOW for symptomatic individuals of 64.2%[40]. Third, the off-the-shelf RT-LAMP master mix used in the present assay contains glycerol, which may cause insufficient removal of water during lyophilization[41]. While our real-time stability experiments suggested that the simple one-pot lyophilization could readily preserve the colorimetric RT-LAMP reactivity for > 4 months (data not shown), the long-term stability of our assay could be substantially improved by using glycerol-free enzymes. Fourth, the present study evaluated an extraction-free RNA preparation protocol (i.e., heating for 10 min at 95 °C in 0.0025X TBE) but did not assess its efficacy for SARS-CoV-2 inactivation. While recent studies[19·42] have suggested the use of similar heating protocols for effective inactivation of SARS-CoV-2, thorough validations must be conducted before pursuing other applications beyond home testing.

Compared to other COVID-19 testing platforms available at the time of this writing, our rapid molecular test kit shows good potential to enable affordable and frequent at-home testing. Due to its low cost and simplicity, our test can allow mass manufacturing in a short timeframe to potentially address the pressing need for global population-scale surveillance, especially in resource-limited regions where COVID-19 is still raging and vaccinations are lagging. For users

who cannot conveniently perform the test at home, our test kits can also be readily used at point-of-care settings such as local pharmacies or mobile laboratories, where batch testing of samples can be easily conducted on site using a dedicated dry or water bath or a similar heat source. The patient would still self-collect a sample using the provided swab with the collection tube and then return the sample to the pharmacy. Due to the fast turnaround of our RT-LAMP assay, the test result can be returned to the patient in under one hour. Advantages of using our tests for point-of-care/near-patient testing include the further simplified testing workflow and the improved quality control of the tests. However, this alternative configuration would require a technician to handle the patient samples, thus enhanced precautions must be carefully followed (e.g., use of PPE, hand hygiene, frequent instrument decontamination) and assure that all samples are fully inactivated upon receipt. Ideally, the sample handling protocol would be automated at the pharmacy to reduce the risk and improve the testing throughput. Furthermore, it is important to note that our all-in-one lyophilized colorimetric RT-LAMP test kit can be quickly adapted to detect different RNA or DNA targets by simply changing the primer set. This remarkable flexibility coupled with the simplicity and reliability of our test kit and testing workflow hold great promise to enable a robust model platform for low-cost decentralized surveillance of other pathogens (e.g., viruses, bacteria, fungi), including infectious diseases of global public health importance (e.g., dengue, tuberculosis, malaria).

Section A2.5: Methods

A2.5.1 RT-LAMP primers

Several published SARS-CoV-2 RT-LAMP primer sets[14,15,36,37,38] were carefully screened in terms of the detection sensitivity, false positive and false negative rates, reaction speed, and test reproducibility (Figs. S1–S6). The best performing primer set[38] (Table 2) was selected for further characterization and optimization in our lyophilized colorimetric RT-LAMP home test kit. This primer set targets the ORF1a gene of the SARS-CoV-2 viral genome and is minimally impacted

by mutations on recent SARS-CoV-2 variants of concern. An additional primer set23 (Table S2) was tested to confirm the reliable performance of the one-pot lyophilization protocol.

A2.5.2 RT-LAMP reagents

WarmStart Colorimetric LAMP 2X Master Mix (New England Biolabs, cat. M1800L) was used as the RT-LAMP master mix for the test kit. RT-LAMP primers were ordered from IDT as custom DNA oligos with standard desalting. The primers were resuspended in nuclease-free water (Sigma-Aldrich) and mixed to form a 10X primer mix consisting of 2 µM F3 primer, 2 µM B3 primer, 16 µM FIP primer, 16 µM BIP primer, 4 µM LoopF primer, and 4 µM LoopB primer. RT-LAMP reactions were run at 20 µL total reaction volume. Specifically, the lyophilized RT-LAMP reagents were reconstituted with 5 µL sample + 15 µL nuclease-free water in all analytical experiments conducted with synthetic SARS-CoV-2 RNA control (Twist Bioscience, cat. 102024). Unless otherwise specified, 20 µL of sample (as opposed to 5 µL sample + 15 µL nuclease-free water) was directly added to the lyophilized RT-LAMP mix in validation experiments conducted with simulated SARS-CoV-2 infected samples.

A2.5.3 Fast one-pot lyophilization of colorimetric RT-LAMP reagents

The 3 M trehalose solution was prepared by dissolving 0.5 g D-(+)-trehalose dihydrate powder (Sigma-Aldrich, M.W. 378.33 g/mol) in 440.5 µL nuclease-free water, followed by vigorous vortexing and heating at 60 °C for 10 min to fully dissolve the trehalose to yield a supersaturated solution. This resulted in a solution with a total volume of approximately 760 µL, corresponding to an effective trehalose concentration of around 1.75 M. Because our assay prototyping needed only small amounts of the solutions, to keep the measuring simple and consistent, we refer to this resulting solution as the 3 M trehalose throughout the text unless otherwise specified. The trehalose solution was then sterilized by filtering through a 0.2 µm syringe filter (VWR), followed by brief vortex and centrifuge to remove air bubbles. For consistency, the 1 M GuHCl solution was prepared similarly by directly dissolving 0.1 g guanidine hydrochloride powder (VWR, M.W. 95.53 g/mol) in 1046.8 µL nuclease-free water without further adjustment of the final volume. The

tube containing the GuHCl solution was covered with aluminum foil to protect it from light. Components of the colorimetric RT-LAMP lyophilization formulation were mixed at the specified ratio (Table 1), aliquoted into 0.2 mL PCR tubes, and frozen at − 20 °C for 1 h. Finally, the tubes were quickly transferred with caps open into a vacuum concentrator (Savant Speedvac SVC-100H) connected to the lyophilizer (VirTis Freezemobile 12SL). Lyophilization was run for 1 h with the chamber pressure at ~ 10 milliTorr and the condenser temperature at ~ − 40 °C. Details of the RT-LAMP lyophilization protocol optimizations are shown in Fig. S7–S16.

A2.5.4 Viruses

SARS-CoV-2 Pango lineage A (WA-1/2020) was used in all whole virus assays for in-house test kit optimization. Other variants obtained through BEI Resources were B.1.1.7, B.1.351, B.1.526.2 and B.1.617.1. Other viruses were isolated from clinical samples, and lineage determined by next generation sequencing. These include P.2, B.1.2, B.1.427, B.1.429, B.1.526, and B.1.617.2. Further virus information including source are summarized in Table S3. Authentic SARS-CoV-2 were propagated and inactivated in a BSL-3 laboratory under a protocol approved by the OHSU Institutional Biosafety Committee under the supervision of Dr. Tafesse.

A2.5.5 Simulated SARS-CoV-2 infected samples

Anterior nasal swab (and alternatively gingival swab) samples were collected as described below from 10 uninfected individuals, into sample collection media (TBE (1X: 90 mM Tris–borate-2 mM EDTA, pH 8.0) at the specified concentration, in nuclease-free water) and pooled. Heat-inactivated SARS-CoV-2 virus was diluted in sample collection media to achieve the specified viral copy numbers, according to in-house qRT-PCR. Virus-spiked samples were heated at 95 °C for the specified duration and chilled on ice. Then, 20 µL of the resulting sample was added directly into the RT-LAMP microtube to reconstitute the lyophilized reagents. RT-LAMP microtubes were vortexed (spun down, if necessary) and briefly chilled on ice, before pre-incubation photos were

taken. Finally, RT-LAMP microtubes were incubated for 60 min at 65 °C, with photos taken at 30–60 min to assess color change. The best detection sensitivity was achieved by RNA isolation with 0.01X TBE (based on 5 µL sample input into a 20 µL reaction) and heating for 10 min at 95 °C (Figs. S17–18). Subsequent assays were performed using 20 µL direct sample input and 0.0025X TBE, to reduce pipetting steps.

A1.5.6 Colorimetric RT-LAMP in thermocycler

RT-LAMP microtubes containing samples or non-template control (NTC) were vortexed, spun down and briefly chilled on ice before pre-incubation photos were taken. RT-LAMP microtubes were incubated in a thermocycler for 60 min at the specified temperature, with photos taken at 30–60 min to assess color change. Tubes were briefly chilled on ice to allow color stabilization, before being photographed. The optimal RT-LAMP incubation temperature was identified by running the reactions with a temperature gradient (T = 65 °C, G = 5 °C) set in a gradient thermal cycler (Eppendorf MasterCycler). To avoid contamination, the RT-LAMP tubes should never be reopened after the incubation reaction.

A2.5.7 Colorimetric RT-LAMP in thermos

Both the viral RNA preparation and the RT-LAMP incubation were conducted in a thermos. Freshly boiled water was added to pre-warm the thermos for 2 min and then dumped out. Next, boiling water was re-added into the thermos and chilled to ~ 97 °C, after which the virus-spiked samples and NTC (swab media without virus) were incubated for 10 min in the thermos (with lid on) and then chilled on ice for 5 min to allow cell debris to settle. Next, 20 µL of the heat-inactivated sample “supernatant” (i.e., no cell debris) or NTC were transferred to the RT-LAMP microtube using a disposable transfer pipette. The microtubes were recapped and flicked gently (being careful not to introduce bubbles) to resuspend the lyophilized RT-LAMP reagents and then

chilled on ice before pre-incubation photos were taken. Meanwhile, a mug was filled with boiling water, and allowed to chill to ~ 70 °C before pouring into the thermos. The water was allowed to further chill to ~ 67 °C before samples were added. Next, the RT-LAMP microtubes were incubated in the thermos with the lid tightly closed for 60 min, with photos taken at 30–60 min. During incubation, the microtubes were secured on a foam floater to ensure that they were vertically and sufficiently submerged in water to activate the RT-LAMP reaction. Finally, the tubes were removed from thermos and briefly chilled on ice to allow color stabilization, before being photographed for test result readout.

A2.5.8 Quantitative RT-PCR (OHSU)

Heat-inactivated SARS-CoV-2 RNA was isolated using the Zymo Directzol RNA purification kit according to the manufacturer's protocol and eluted in 50 µL elution buffer. SARS-CoV2 RNA levels were measured by a one-step quantitative real time reverse transcription polymerase chain reaction assay (qRT-PCR) using TaqMan One-Step RT-PCR Master Mix (Applied Biosystems) with 4 µL per reaction. Primers and probes were as follows: Forward: 5'-TTTGGCTTTGTGTGCTGACTCT; Reverse: 5'-CCCTTTGAGTGCGTGACAAAT and TaqMan probe: 5' FAM-ATTGGTGGAGCTAAAC-MGB. Forward and reverse primers were used at 250 nM in the reaction, and the probe at 200 nM. For RNA standards, a ten-fold dilution series of 10^6 to 10^1 of a synthetic RNA control (Twist Biosciences: MN908947.3) was used.

A2.5.9 Statistical analysis

To estimate the analytic sensitivity of the RT-LAMP platform with human samples, simulated NP swab samples were spiked with serial dilutions of inactivated WA-1 strain of SARS CoV-2 starting at a calculated 17,473 copies, twofold to 8737 copies and then every 1.6-fold to a final dilution of 227 viral copies. Three independent replicates four-reactions per dilution were performed for each dilution. The average percent-positive for each dilution was calculated and fitted to a dose–

response curve with log RNA copy as the dose and percent positive samples as the response and subjected to Find ECanything least squares dose–response curve fitting with lower and upper limits of 0 and 100 respectively (GraphPad Prism V9.3). Fifty and ninety-five percent sensitivity estimates were estimated by setting the F parameter to 50 and 95 respectively.

A2.5.10 Thermoses

Three different types of thermoses were used in these assays, available from Amazon (ASINs B00IR77HMW (#1), B08LPZZGCT (#2), B07MJR3P1H (#3)). Temperature drift experiments were conducted—thermoses were pre-warmed and filled with 67 °C water, lids were secured, and final temperatures taken after 40 min, on 3 separate days. Final temperatures were 61.5 °C, 62.5 °C and 62.5 °C for thermos #1, 61 °C, 65 °C and 65 °C for thermos #2, and 61 °C, 62 °C and 62 °C for thermos #3.

A2.5.11 Instruction for sample self-collection using anterior nasal swab

No food or drink other than water 30 min prior to sample collection. Wash hands prior to sample collection. Insert swab into nostril just enough so the cotton tip is no longer visible. Swipe the inside of nostril in a circular motion, 5 times. Repeat for the other nostril, using the same swab. Dunk the swab into the labeled tube, plunging it into the liquid about 10 times. Discard the swab and replace the lid on the tube.

A2.5.12 Instruction for sample self-collection using gingival swab

No food or drink other than water 30 min prior to sample collection. Wash hands prior to sample collection. Insert bristled swab into mouth and position the swab so that it covers the gingival line

(line between gum and teeth) of top teeth. Gently swipe back and forth several times along the gingival line (in a tooth-brushing motion) on the outside face of top teeth. Flip the swab over and repeat for the outside face of bottom teeth. Dunk the gingival swab into the labeled tube, plunging it into the liquid about 10 times. “Squeeze” out the remaining fluid in the swab by pressing it on the side of the tube like a sponge. Discard the swab and replace the lid on the tube.

A2.5.13 Human research ethics

This study has been reviewed and approved by the Oregon Health and Science University (OHSU) Institutional Review Board (IRB#20114). Informed consent was obtained from subjects upon enrolment.

A2.5.14 Data availability

All data associated with this study are available in the main text or the Supplementary Materials.

Section A2.6: References

1. Kojima,N.&Klausner,J.D.ProtectiveimmunityafterrecoveryfromSARS-CoV-2infection.LancetInfect.Dis.22,12–14.https:// doi.org/10.1016/S1473-3099(21)00676-9 (2022).
2. Wang,S.Y.etal.SeverebreakthroughCOVID-19casesintheSARS-CoV-2delta(B.1.617.2)variantera.LancetMicrob.3,e4–e5. https://doi.org/10.1016/S2666-5247(21)00306-2 (2022).
3. Kuhlmann, C., Ck, M. & Claassen, M. Breakthrough infections with SARS-CoV-2 omicron despite mRNA vaccine booster dose (vol 399, pg 625, 2022). Lancet 399, 628–628. https://doi.org/10.1016/S0140-6736(22)00090-3 (2022).

4. Larremore,D.B.etal.Testsensitivityissecondarytofrequencyandturnaroundtimeforcovid-19screening.Sci.Adv.https:// doi.org/10.1126/sciadv.abd5393 (2021).
5. He, X. *et al.* Temporal dynamics in viral shedding and transmissibility of COVID-19 (vol 53, pg 751, 2020). Nat. Med. 26, 1491– 1493. https://doi.org/10.1038/s41591-020-1016-z (2020).
6. Peeling,R.W.,Olliaro,P.L.,Boeras,D.I.&Fongwen,N.ScalingupCOVID-19rapidantigentests:promisesandchallenges.Lancet Infect. Dis. 21, E290–E295. https://doi.org/10.1016/S1473-3099(21)00048-7 (2021).
7. Scohy,A.etal.Lowperformanceofrapidantigendetectiontestasfrontlinetestingforcovid-19diagnosis.J.Clin.Virol.https:// doi.org/10.1016/j.jcv.2020.104455 (2020).
8. Eshghifar, N., Busheri, A., Shrestha, R. & Beqaj, S. Evaluation of analytical performance of seven rapid antigen detection kits for detection of SARS-CoV-2 virus. Int J Gen Med 14, 435–440. https://doi.org/10.2147/Ijgm.S297762 (2021).
9. Udugama,B.etal.DiagnosingCOVID-19:thediseaseandtoolsfordetection.ACSNano14,3822–3835.https://doi.org/10.1021/acsnano.0c02624 (2020).
10. Zhao, Y. X., Chen, F., Li, Q., Wang, L. H. & Fan, C. H. Isothermal amplification of nucleic acids. Chem. Rev. 115, 12491–12545. https://doi.org/10.1021/acs.chemrev.5b00428 (2015).
11. Notomi,T.etal.Loop-mediatedisothermalamplificationofDNA.Nucl.AcidsRes.https://doi.org/10.1093/nar/28.12.e63(2000).
12. Tanner, N. A., Zhang, Y. H. & Evans, T. C. Visual detection of isothermal nucleic acid amplification using pH-sensitive dyes. Biotechniques 58, 59–68. https://doi.org/10.2144/000114253 (2015).
13. Huang, W. E. *et al.* RT-LAMP for rapid diagnosis of coronavirus SARS-CoV-2. Microb. Biotechnol. 13, 950–961. https://doi.org/10.1111/1751-7915.13586 (2020).
14. Butler, D. *et al.* Shotgun transcriptome, spatial omics, and isothermal profiling of SARS-CoV-2 infection reveals unique host responses, viral diversification, and drug interactions. Nat. Commun. https://doi.org/10.1038/s41467-021-21361-7 (2021).

15. Lamb, L. E., Bartolone,S.N.,Ward,E.&Chancellor,M.B. Rapiddetectionofnovelcoronavirus/severeacuterespiratorysyndrome coronavirus 2 (SARS-CoV-2) by reverse transcription-loop-mediated isothermal amplification. PLoS ONE https://doi.org/10.1371/ journal.pone.0234682 (2020).
16. Anahtar, M. N. *et al.* Clinical assessment and validation of a rapid and sensitive SARS-CoV-2 test using reverse transcription loop-mediated isothermal amplification without the need for RNA extraction. Open Forum Infect. Dis. https://doi.org/10.1093/ ofid/ofaa631 (2021).
17. Mohon, A. *et al.* Optimizationandclinicalvalidationofdual-targetRT-LAMPforSARS-CoV-2.J.Virol.Methodshttps://doi.org/ 10.1016/j.jviromet.2020.113972 (2020).
18. Thi, V.L.D. *et al.* AcolorimetricRT-LAMPassayandLAMP-sequencingfordetectingSARS-CoV-2RNAinclinicalsamples.Sci. Trans. Med. https://doi.org/10.1126/scitranslmed.abc7075 (2020).
19. Ranoa, D. R. E. *et al.* Saliva-based molecular testing for SARS-CoV-2 that bypasses RNA extraction. bioRxiv https://doi.org/10. 1101/2020.06.18.159434 (2020).
20. Lalli, M. A. *et al.* Rapid and extraction-free detection of SARS-CoV-2 from saliva by colorimetric reverse-transcription loop- mediated isothermal amplification. Clin. Chem. 67, 415–424. https://doi.org/10.1093/clinchem/hvaa267 (2021).
21. Ben-Assa, N. *et al.*SARS-CoV-2on-the-spotvirusdetectiondirectlyfrompatients.medRxivhttps://doi.org/10.1101/2020.04.22. 20072389 (2020).
22. L'Helgouach, N. *et al.* EasyCOV: LAMP based rapid detection of SARS-CoV-2 in saliva. medRxiv https://doi.org/10.1101/2020. 05.30.20117291 (2020).
23. FDA.EmergencyUseAuthorizationforColorSARS-CoV-2RT-LAMP DiagnosticAssay,<https://www.fda.gov/media/138249/downl oad> (2020).
24. FDA. Emergency Use Authorization for AQ-TOP COVID-19 Rapid Detection Kit, <https://www.fda.gov/media/138300/download> (2020).
25. FDA.EmergencyUseAuthorizationforMobileDetectBioBCC19(MD-BioBCC19)TestKit,<https://www.fda.gov/media/141788/ download> (2020).

26. Leung, V., Brooks, M., Emerson, S., Ali, M. & Filipe, C. D. M. Ready-to-use thermally stable mastermix pills for molecular biology applications. Biotechnol. Prog. https://doi.org/10.1002/btpr.2764 (2019).
27. Tang, X. L.&Pikal, M.J.Designoffreeze-dryingprocessesforpharmaceuticals:practicaladvice.Pharm.Res.21,191–200.https:// doi.org/10.1023/B:Pham.0000016234.73023.75 (2004).
28. Chang, B. S.&Fischer, N.L. Development of an efficient single-step freeze-drying cycle forproteinformulations.Pharm.Res.12, 831–837. https://doi.org/10.1023/A:1016200818343 (1995).
29. Diego, J.G.B. *et al.* Progress in loop-mediated isothermal amplification assay for detection of Schistosoma mansoni DNA: towards a ready-to-use test. Sci. Rep. https://doi.org/10.1038/s41598-019-51342-2 (2019).
30. Jain, N. K. & Roy, I. Trehalose and protein stability.Curr.Protoc.ProteinSci.https://doi.org/10.1002/0471140864.ps0409s59(2010).
31. Sun, W. Q. & Davidson, P. Protein inactivation in amorphous sucrose and trehalose matrices: effects of phase separation and crystallization. Biochim. Biophys. Acta 1425, 235–244. https://doi.org/10.1016/s0304-4165(98)00076-2 (1998).
32. Karig,D.K.,Bessling,S.,Thielen,P.,Zhang,S.&Wolfe,J.Preservation of protein expression systems at elevated temperatures for portable therapeutic production. J. R. Soc. Interface https://doi.org/10.1098/rsif.2016.1039 (2017).
33. Sun,W.Q.&Davidson,P.Effectofdextranmolecularweightonproteinstabilizationduringfreeze-dryingandstorage.CryoLetters 22, 285–292 (2001).
34. Baheti,A.,Kumar,L.&Bansal,A.K.Excipientsusedinlyophilizationofsmallmolecules.J.Excip.FoodChem.1(1),1135(2010).
35. Zhang, Y. *et al.* Enhancing colorimetric loop-mediated isothermal amplification speed and sensitivity with guanidine chloride.Biotechniques 69, 178–185. https://doi.org/10.2144/btn-2020-0078 (2020).
36. Yu, L. *et al.* Rapid detection of COVID-19 coronavirus using a reverse transcriptional loop-mediated isothermal amplification (RT-LAMP) diagnostic platform. Clin. Chem. 66, 975–977. https://doi.org/10.1093/clinchem/hvaa102 (2020).

37. Zhang, Y. *et al.* Rapid molecular detection of SARS-CoV-2 (COVID-19) virus RNA using colorimetric LAMP. medRxiv https://doi.org/10.1101/2020.02.26.20028373 (2020).
38. Rabe, B. A. & Cepko, C. SARS-CoV-2 detection using isothermal amplification and a rapid, inexpensive protocol for sample inactivation and purification. Proc. Natl. Acad. Sci. U.S.A. 117, 24450–24458. https://doi.org/10.1073/pnas.2011221117 (2020).
39. Ozay, B. & McCalla, S. E. A review of reaction enhancement strategies for isothermal nucleic acid amplification reactions. Sens. Actuators Rep. https://doi.org/10.1016/j.snr.2021.100033 (2021).
40. Prince-Guerra,J.L.etal.EvaluationofabbottBinaxNOWrapidantigentestforSARS-CoV-2infectionattwocommunity-based testing sites - Pima County, Arizona, November 3–17, 2020. MMWR Morb. Mortal Wkly. Rep. 70, 100–105.https://doi.org/10.15585/mmwr.mm7003e3 (2021).
41. Bircher, L., Geirnaert, A., Hammes, F., Lacroix, C. & Schwab, C. Effect of cryopreservation and lyophilization on viability and growth of strict anaerobic human gut microbes. Microb. Biotechnol. 11, 721–733. https://doi.org/10.1111/1751-7915.13265 (2018).
42. Pastorino, B. *et al.* Evaluation of chemical protocols for inactivating SARS-CoV-2 infectious samples. Viruses https://doi.org/10.3390/v12060624 (2020).

Section A2.7: Acknowledgements

We are thankful to Prof. Rytas Vilgalys for offering us immediate training and access to the lyophilizer used in this study. We also thank Prof. Randy Smith, Dr. Peter Silinski, Dr. Liang Jiang, Prof. Katherine Franz, Prof. Paul Manos, Prof. Amanda Hargrove, Zhengguo Cai, Misty Roland, Samuel Kamau, and Melanie Eberhart for their assistance in coordinating facilities needed for this work during the campus lockdown. We also thank Prof. Xuan Qin in the OHSU Department of Pathology for providing CT values for our samples and the distribution of CT values for SARS-CoV-2 clinical tests performed at OHSU. We wish to thank all the frontline essential personnel for supporting our work during this challenging time. This work was supported by NSF grants CCF-1813805 and CCF-1909848 (J.H.R.).

Section A2.8: Author information

These authors contributed equally: Felicity J. Coulter and Ming Yang.

A2.8.1 Authors and Affiliations

Department of Electrical and Computer Engineering, Duke University, Durham, NC, 27708, USA
Xin Song & John H. Reif

Department of Biomedical Engineering, Duke University, Durham, NC, 27708, USA
Xin Song

Department of Computer Science, Duke University, Durham, NC, 27708, USA
Xin Song, Ming Yang & John H. Reif

Department of Molecular Microbiology and Immunology, Oregon Health and Science University, Portland, OR, 97239, USA
Felicity J. Coulter, Fikadu G. Tafesse & William B. Messer

Vaccine and Gene Therapy Institute, Oregon Health and Science University, Beaverton, OR, 97006, USA
Jessica L. Smith

Department of Medicine, Division of Infectious Diseases, Oregon Health and Science University, Portland, OR, 97239, USA
William B. Messer

Program in Epidemiology, OHSU-PSU School of Public Health, Oregon Health and Science University, Portland, OR, 97239, USA
William B. Messer

A2.8.2 Contributions

X.S. and J.H.R. conceived and designed the study. X.S. designed, analyzed, and optimized the RT-LAMP test kit, the one-pot lyophilization protocol, and the testing workflow. J.H.R. supervised the design and implementation of the test kit and the testing workflow. X.S. and M.Y. prepared the lyophilized test kits, performed optimization experiments and analytical validation of the test kit with synthetic SARS-CoV-2 RNA and collected data. W.B.M. supervised and coordinated the clinical evaluation of the test kit and the testing workflow. F.J.C. performed validation of the test using simulated SARS-CoV-2 infected samples, conducted optimization experiments for the sample collection and RNA isolation protocol, collected data and analyzed results with W.B.M., X.S., and J.H.R.. J.L.S. conducted the RT-qPCR. F.G.T. assisted the coordination of the clinical study and provided the lab-cultured SARS-CoV-2 virus for experiments. X.S., F.J.C., and W.B.M. wrote the manuscript with input from all authors.

A2.8.3 Corresponding authors

Correspondence to Xin Song, William B. Messer or John H. Reif.

Section A2.9: Ethics declarations

A2.9.1 Competing interests

Duke University has filed a provisional patent covering aspects of this work. J.H.R and X.S. are co-founders of Domus Diagnostics, Inc. Other authors declare no potential conflict of interest.

Section A2.10: Additional information

A2.10.1 Publisher's note

Springer Nature remains neutral with regard to jurisdictional claims in published maps and institutional affiliations.

Section A2.11: Supplementary information

Available online at https://static-content.springer.com/esm/art%3A10.1038%2Fs41598-022-11144-5/MediaObjects/41598_2022_11144_MOESM1_ESM.pdf